COMPARISON OF SEDIMENT TRANSPORT MODELS FOR THE LOWER HASSAYAMPA RIVER

Prepared for

THE FLOOD CONTROL DISTRICT OF MARICIPA COUNTY

2801 W Durango St

Phoenix, AZ 85009

Prepared by

R2D

River Research & Design, Inc.

4359 N Pine Featherville Rd

Featherville, ID 83647

www.r2d-eng.com

Registered Professional Engineer (Civil)
CERTIFICATE NO.
36225
GARY E.
FREEMAN
Date Signed 11/21/11
ARIZONA, U.S.A.

Expires 6/30/2013

November 21, 2011

TABLE OF CONTENTS

A. EXECUTIVE SUMMARY **1**

A.1 SUMMARY OF FINDINGS 2

B. INTRODUCTION **5**

B.1 PURPOSE AND NEED FOR THE STUDY 5
B.2 STUDY REACH, TOPOGRAPHY, AND EVENTS 9
B.2.1 Study Reach *9*
B.2.2 Topography *11*
B.2.3 Incorporation of Pits *12*
B.2.4 Events Modeled *14*
B.2.5 Bank Stations, Flood Extents and Erosion Limits *15*
B.2.6 Transport Equations Used and other Technical Input Data *19*
B.3 OBSERVED HEADCUTS AND TAILCUTS 20

C. COMPARISON OF THE MODELS **24**

C.1 OVERVIEW OF MODEL COMPARISON METHODS 24
C.2 COMPARISON OF MODEL FEATURES AND ASSUMPTIONS 25
C.3 SEDIMENT MODEL COMPARISON FOR THE 100 YEAR EVENT 30
C.4 2010 SINGLE EVENT MODELING 34
C.4.1 Model Inputs *35*
C.4.2 Model Results for 2010 Event *35*
C.4.2.3 Impact of Pit Depth. *40*
C4.2.4 Use of Additional Transport Equations *41*
C.4.5 Absolute Performance Index *46*
C.5 COMPARISON OF THE MODELS FOR THE 2005 EVENT PLUS THE 2010 EVENT 52
C.5.1 Results for the 2005+2010 Simulation *55*
C.6 TWO-DIMENSIONAL MODELS 64
C.6.1 FLO-2D Sediment Model Results *64*
C.6.2 RiverFLO-2D Model Results *65*
C.6.3 RMA-2/SED2D Results *65*
C.6.4 2D Modeling Recommendations *65*

D. CONCLUSIONS **66**

D.1 RECOMMENDATIONS 68
D.2 AREAS FOR FUTURE STUDY 68

E. REFERENCES **69**

Registered Professional Engineer (Civil)
CERTIFICATE NO.
36225
GARY E.
FREEMAN
Date Signed 11/21/11
ARIZONA, U.S.A.

Expires 6/30/2013

LIST OF FIGURES

Figure 1. Project Location. 10
Figure 2. Location of Mining Pits in Hassayampa River. Blue lines show extent of January 2010 flood event. 11
Figure 3. Flow Data for Hassayampa River at I-10 Gage with Zero Flow Readings Removed. 15
Figure 4. Flood Extents/Bank Stations for 2005 and 2010 Events 18
Figure 5. Comparison of Hassayampa River Thalweg for 2010 Pre-flood (Ignoring Small Pits) with Estimated 2009 Mining Pits and 2010 Post Flood Showing Impacts of Mining on Channel Elevation. 21
Figure 6. Hassayampa River above Hanson Pit showing Old Channel with Approximate 3 feet of Channel Lowering. 22
Figure 7. Approximate 9-10 Foot Channel Lowering above Pioneer Pit along West Bank of Hassayampa River. 22
Figure 8. Tailcut Erosion Immediately Downstream from Pioneer Pit. Tailcut depth is approximately 7 feet. 23
Figure 9. East Braid Headcut above Pioneer Pit Looking Downstream Towards pit. 23
Figure 10. Initial Thalweg Elevations for FLUVIAL-12, HEC-6 and HEC-RAS 31
Figure 11. Results for 100 Year Simulation. The HEC-6 model does not have flow through the overbank pits but HEC-RAS and FLUVIAL-12 both include flow through the pits. 32
Figure 12. Model Data at Hanson and CEMEX pits for 100 Year Event. The HEC-6 model did not allow flow through pits. 34
Figure 13. Results for HEC-6T Model using Engelund-Hansen Transport Equation for the 2010 Event... 36
Figure 14. HEC-RAS and HEC-6T Model Results at the Pioneer Pit for the 2010 Event. 37
Figure 15. HEC-RAS and HEC-6T Model Results at the CEMEX and Hanson Pits for 2010 Event. 38
Figure 16. FLUVIAL-12 Results for 2010 Event Only Compared with 2010 Observed Data. Only headcut and tailcut values are shown. 39
Figure 17. Comparison of HEC-RAS Model Results with Modified Pit Configuration and Original Pit Estimate for Engelund Hansen Transport Equation. 41
Figure 18. HEC-6T Results using Toffaleti Equation Combined with the Meyer-Peter & Muller Equation for 2010 Event. 43
Figure 19. Comparison of Equations used in HEC-6T Modeling Effort. 44
Figure 20. Comparison of HEC-RAS Model Results for the Various Equations Available in HEC-RAS. 45
Figure 21. HEC-RAS Model Results Compared with the Observed Thalweg for 2005 Event Followed by 2010 Event (Engelund Hansen Equation). 56
Figure 22. Comparison of Modeling of 2010 Event only with Modeling of 2005 Event followed by 2010 Event for HEC-RAS with Engelund Hansen Equation. 57
Figure 23. HEC-6T Model Results for the Mined Reach showing Results for 2005+2010 Model Results Compared with Observed Results. 59
Figure 24. HEC-6T Model Results for the Hanson and CEMEX Pit Reach Compared with Observed Values (T+MPM). 60
Figure 25. Comparison of 2005 Model Results for Fuller (Post 2005 T+MPM) and Lowered n Values (2005 Lowered n T+MPM) for Hanson and CEMEX Reach. 61

Figure 26. FLUVIAL-12 Results for the 2005+2010 Event Model. Results are shown only for pit Impacted reaches. 62

LIST OF TABLES

Table 1. Estimated Mine Depths and Areal Extents. 13
Table 2. Comparison of Features in HEC-6/6T, HEC-RAS, and FLUVIAL-12 Sediment Transport Models.. 27
Table 3. Differences Between HEC-6 and HEC-6T (Partial List). 28
Table 4. Comparison of 2D Model Features. 29
Table 5. Sediment Transport Equations used in the Various Models for this Study. 42
Table 6. Cross Sections Determined to be Scoured due to Headcuts and Tailcuts. 47
Table 7. API Values for the FLUVIAL-12 Model for 2010 Event. 48
Table 8. HEC-RAS Sediment Transport Equations, Results and Recommendations for Sand Bed Rivers.. 49
Table 9. Individual Results for API by pit for Headcuts and Tailcuts for HEC-RAS and HEC-6T. 50
Table 10. API for differences between HEC-RAS and HEC-6T Results with 25 ft Bed Sediment Reservoir. 51
Table 11. Comparison of API and RMS values for FLUVIAL-12, HEC-RAS and HEC-6T results 63

COMPARISON OF SEDIMENT TRANSPORT MODELS FOR THE LOWER HASSAYAMPA RIVER

A. EXECUTIVE SUMMARY

A number of sediment transport models were reviewed for formulation and applicability to the Hassayampa River. Most of these models were then applied to the Hassayampa River in an attempt to reproduce data obtained after the January 20-21, 2010 flood. The return period for this flood was estimated to be approximately 20 years. These models that were applied to reproduce the 2010 data included HEC-RAS, HEC-6T, FLUVIAL-12 and a number of two-dimensional models. HEC-RAS, HEC-6 and FLUVIAL-12 were also run for the 100 year flood for comparison purposes.

The one-dimensional models (HEC-RAS, HEC-6T, and FLUVIAL-12) were applied to the 2010 event as well as to a combination of the largest hydrograph from 2005 plus the 2010 event. The model results were compared with the post 2010 flood topography. Based on this study it was found that the HEC-6T model using the combination of the Toffaleti and Meyer-Peter & Muller equation and the FLUVIAL-12 model using the Engelund Hansen equation produced the most accurate results. The HEC-RAS results, using the Engelund Hansen equation, over predicts headcut depth but gives good results for the headcut length. The other equations available in HEC-RAS did not satisfactorily model the headcut from the Pioneer pit. We recommend that the Flood Control District of Maricopa County coordinate with HEC staff and perform additional analysis in the future to investigate the findings of this study.

The results also indicated that the 2010 event was large enough that the 2005 and smaller events could be ignored in the prediction of headcuts and tailcuts from pits in the Hassayampa River. The smaller events may, however; be important in predicting pit deposition. The wash load was not modeled in this effort but also may be important in modeling pit deposition. Future analysis may be needed to incorporate the wash load.

The two-dimensional models applied either did not produce acceptable results or were so complex that their use would require extensive experience in the application of the models. Further analysis with additional models and flood events is needed to evaluate two-dimensional sediment transport models.

A.1 Summary of Findings

Input Data and General Findings

- The modeling of headcuts by the use of one-dimensional sediment transport appears to give reasonable results if the correct combination of models and transport equations are used.
- Once flow has been established in a sand bed channel such as the Hassayampa, the bed roughness (Manning's n value) is reduced to either grain roughness or bed form roughness. Exactly when this transformation occurs is not known but is likely early, during the rising limb of the hydrograph.
- From the modeling and other tasks associated with this study it appears that the elevation of the downstream pit brink is significant in the calculation of the ultimate headcut depth and length.
- Away from the pits the one-dimensional models all gave close agreement regarding the stability of the river.
- Based on the review of data it appears that the 2010 event was large enough to overcome erosion caused by the 2005 and other smaller events. Pit deposition modeling may be dependent on these smaller events and it appears that pit deposition is significantly impacted by the more frequent small events that were not modeled in this study.
- The use of multiple events does not appear necessary to obtain good headcut/tailcut results if large events (50 to 100 year or greater) are used in the modeling.

HEC-6T and HEC-RAS

- The Engelund Hansen equation as implemented in HEC-6T and HEC-RAS over predicts thalweg depths when compared to observed values.
- Results indicate that the various sediment transport equations in HEC-RAS are not producing results that are as accurate as those produced by the HEC-6T model and the FLUVIAL-12 model when compared to one another and the observed data. This is based on a limited analysis and further analysis is recommended.
- The HEC-RAS model has the best user interface with the ability to more easily view the inputs and results, however; results are not as accurate as those obtained from HEC-6T and FLUVIAL-12. The best HEC-RAS results were obtained with the Engelund Hansen transport equation but the Engelund Hansen equation significantly over predicts erosion. Based on this limited study on the Lower Hassayampa River, we found that HEC-RAS using the Engelund Hansen transport equation over predicts headcut depth on

the order of 2 to 4 feet immediately upstream from the pit but the headcut length is reasonable. HEC-RAS with the Meyer-Peter & Muller, Yang, Ackers White, Wilcock, Toffaleti, and Laurson Copeland transport equations does not give as accurate of results.

- It is not necessary to combine empirical methods such as the ADOT method with the numerical modeling to obtain good headcut results. Based on other work (reported in R2D 2011) the ADOT and other methods are likely good to estimate maximum headcut lengths/depths for pits that drown out but not for estimating the maximum headcut/tailcut lengths for large pits that do not drown out during high flows.
- Smaller events may result in more serious headcut depths nearer the pit but maximum headcut lengths should be obtained from the larger events (i.e. 50 to 100 year events).
- Pit depths were likely over estimated in this study and the pit configuration may not have been as accurate as desired.
- HEC-6T and FLUVIAL-12 models provided the best results of the models evaluated.
- The equations recommended for use on the Hassayampa River with the HEC-6T Model are (in order of preference) 1) the combination Toffaleti and Meyer-Peter & Muller Equation, 2) Yang Equation, 3) the Toffaleti equation, and 4) the Ackers White Equation.
- The only HEC-RAS transport equation giving reasonable results was the Engelund Hansen equation.

FLUVIAL-12

- The FLUVIAL-12 model gave very good results and was as accurate as the HEC-6T model.
- The FLUVIAL-12 model provided good estimates of headcut depth and distance.
- FLUVIAL-12 is recommended for use on the Hassayampa River with the Engelund Hansen equation based on the results of this study. Only the Engelund Hansen and Yang equations were used in this modeling of the Lower Hassayampa River. Other equations available in the model may also be applicable but were not tested in the work done by Dr. Howard Chang (Chang 2011).

Two-dimensional Models

- **FLO-2D** scoured to the limits established by the maximum depth of scour input parameter. The results looked reasonable when the limit was set to be close to the maximum scour. When the scour limits were set to infinity the model did not complete calculations and was terminated after 862 hours of computer time.
- **RiverFLO-2D** gave reasonable hydraulic results but when the sediment was turned on the sediment calculations created hydraulic instabilities. No simulation could be run to completion and the model was unusable for this study.

- The combination of **RMA-2 and SED2D** was attempted and the hydraulics were run for all of the hydrograph steps. One hydrograph step was run in the SED2D model before 2D modeling was terminated. The RMA-2/SED2D model could be run but is complex and relatively difficult to run. It is not recommended for the faint of heart.

B. INTRODUCTION

The Hassayampa River is located in the western portion of Maricopa County. The Flood Control District of Maricopa County (District) currently has a number of mining permits and applications for mining permits on the Hassayampa River. The river has not been extensively mined but, as development has moved closer to the river, mining has increased.

The 2008 housing crash delayed additional mining and curtailed existing mining along the river. Based on the history of the other rivers in the area, mining is expected to increase when development resumes in the areas near the river. When mining resumes along the river it will be extremely important to understand the impacts of mining on the stability of the river. The stability of the river will be of major importance to the design of bridges and infrastructure crossing the river. The design of river encroachments will also need to be based on the reaction of the river to mining operations.

This study was designed to gain a better understanding of how to predict the impacts on river erosion and stability that occur due to mining. This better understanding will allow the District to better evaluate the impacts from both existing and proposed mining operations on the Hassayampa River. The knowledge and understanding gained from this study should also allow the District to better understand mining impacts on other rivers in the County.

B.1 Purpose and Need for the Study

The Hassayampa River is a sand bed river and is very susceptible to erosion. This is especially true when the river is impacted by mining operations. Under the right circumstances headcuts started at mining pits could propagate up the river and tributaries until hard layers or bedrock stop the progression of the headcuts. These headcuts can produce substantial sediment loads that will deposit downstream and increase flood heights and risks. The river does have a large sediment load during flood events but significant headcuts occurred during the 2010 flood event even with a large sediment inflow. This indicates a significant risk for headcutting.

The Hassayampa River is expected to be crossed by a number of bridges, pipelines, utilities and other infrastructure as the area develops. The importance of this future infrastructure coupled with the erosive nature of the sand bed river brings into focus the importance of understanding the impacts of sand and gravel mining in the river channel. Given the amount of infrastructure planed for the river between the Gila River Confluence and the nearest bedrock control near Morristown, it is important to understand how mining operations impact the stability of the river.

An earlier report, developed by River Research & Design, Inc. (R2D), reviewed the methodologies used to calculate headcuts and tailcuts that result from mining operations (R2D 2011). The review indicated that current technology used in the calculation of headcuts and tailcuts is based on research performed in the 1980's or earlier. The methods developed in the 1980's assumed; among other things that the pits would be small enough that they would drown out during high flows (i.e. flow into the pit would be subcritical or controlled by the downstream water surface). Since the 1980's the size of pits has increased such that many pits do not drown out even during 100 year flood flows. This change in the size of pits and the assumptions necessary when modeling them has led to the conclusion that the methodology needs to be updated to better reflect current mining configurations.

After the January 2010 flood event on the Hassayampa River the headcut methodology review task described above was extended to apply the available empirical methodologies to the 2010 Hassayampa River data. The results indicated that most of the available empirical methodologies were not accurately predicting the headcut lengths observed at the Hassayampa River pits. When the review was completed it was apparent that additional work would be necessary to determine if current computer models could accurately predict the length and depth of headcuts and tailcuts. The sediment models in use today were either not available in the 1980's when the original headcut/tailcut studies were performed or were in the early stages of their development. As results it was desired to know how accurately the current sediment transport models could model the observed headcuts and tailcuts along the Hassayampa River. These headcuts and tailcuts occurred as a direct result of sand and gravel mining operations and provide a good data set for model comparison.

Sediment transport modeling has been required by the District to determine river stability for mining permits for at least five years. Modeling is also used to predict the headcuts and tailcuts associated with mining operations. A demonstration of how accurate the various models can predict headcuts and tailcuts on the Hassayampa River would allow the District to more confidently help applicants avoid adverse off-site impacts due to mining operations. The data from this study would also allow the District to develop guidelines for sand and gravel mining along the Hassayampa River.

As a part of this study it was also desired to compare differing transport models and equations to see if one model or equation performed significantly better than the others. One of the desired results of the study was to determine if one sediment transport model significantly outperformed the others and should be selected to be a "living model" of the river. This "living" model would be updated on a continuous basis. This model could then be made

available to consultants for use in permitting mining operations or the design of bank protection and other infrastructure. The recommendations from this study would be a partial basis for determining if a living model was desirable and, if so, which model would be the best to use.

This study reviewed both one-dimensional (1D) and two-dimensional (2D) models that could be used to model headcutting and tailcutting from sand and gravel pits on the Hassayampa River. Two 2D models were run by the District and R2D started modeling using the RMA-2/SED2D model package. The RMA-2/SED2D modeling was suspended when more critical modeling was taking longer than expected and the complexity of the RMA2/SED2D modeling made it less desirable for general use. Results from the District's 2D modeling are reported later in this document but the results were not encouraging for the models used.

Sediment transport modeling has traditionally been done using HEC-6, HEC-6T, FLUVIAL-12 and a few other models. The Corps' HEC-RAS model now has a sediment transport modeling capability (version 4.0 and higher) and a part of this study was designed to see if the HEC-RAS model would be acceptable for the modeling of sediment transport on the Hassayampa River. The HEC-RAS model results are compared with the observed headcuts and tailcuts for three pits that were impacted by the 2010 flood event as well as the results from the other models used.

This study comprised two main tasks. The first task was a comparison of three models (HEC-6, HEC-RAS, and FLUVIAL-12) for the 100 year flood event for the Hassayampa River. This task was designed to allow the direct comparison of the models for a large flood event using the 2002 topography that was available. The HEC-6 model had previously been run by J.E. Fuller & Associates (Fuller) in 2006 and both the model and results were available. FLUVIAL-12 had been run by Howard Chang as part of another study and was being rerun in a companion task for this study. The FLUVIAL-12 results are incorporated into this report and the report is contained in the Appendix. R2D was tasked to run the HEC-RAS model to see how it would compare with FLUVIAL-12 and HEC-6 for the 100 year event.

The second task was to compare HEC-6T (an updated version of HEC-6), HEC-RAS, FLUVIAL-12, FLO-2D, RiverFLO-2D, and RMA-2/SED2D results with the observed data from the 2010 event. If the models could accurately predict erosion associated with the pits between the two most recent topographic sets (2002 and 2010) then the models would be recommended for use in permit applications.

A subtask was to determine if smaller flow events could be ignored in headcut/tailcut modeling of the Hassayampa River. Since the topography included the results of a series of small events

and two relatively large events it was also desired to know if the smaller events could be ignored and just the larger 2010 event modeled to determine headcut lengths. The events included the 20 year event in 2010, a 10 year event in 2005, and series of small (mostly < 1,000 cfs) events.

The available topography and data provided a test case to see if the 2005 event as well as the smaller events could be ignored in the modeling of the river. The Pioneer pit (most upstream) had only experienced the 2010 event while the more downstream CEMEX and Hanson pits had experienced both the 2005 and 2010 events but intermediate topography was not available.

The results of this analysis could have large impacts on the District's modeling requirements for sand and gravel applicants. If the large events can mask the small events only a single large event would need to be modeled rather than a series of events with differing flow rates. This would greatly simplify the modeling to determine headcut lengths and depths.

There were a number of questions to be answered by this study, including:

1. What are the differences in the various models?
2. Can numerical models (i.e. HEC-RAS, HEC-6/6T, FLUVIAL-12, etc) adequately model headcutting and tailcutting such that other methods can be neglected in determination of headcut and tailcut lengths?
3. Is one model better than another for the modeling of sediment transport associated with sand and gravel pits on the Hassayampa River
4. Is there a sediment transport equation (or several) that can be recommended for use on the Hassayampa River with the various models?
5. Are there 2D models that can be used for sedimentation on the Hassayampa River and do they give better results than the 1D models?
6. Can the smaller events be ignored in the modeling and not impact the resulting headcut/tailcut lengths or depths?

B.2 Study Reach, Topography, and Events

B.2.1 Study Reach

The study reach for the Lower Hassayampa Watercourse Masterplan (Phase 2) reaches from the Gila River to the CAP crossing. The reach used in this study is smaller and covers a sub reach from about 1.5 miles downstream from I-10 to about 8.2 miles north of I-10 (See Figure 1). The full reach modeled is from about 600 feet north of the Buckeye Road alignment to a point approximately one-quarter mile north of the Olive Avenue alignment. The model coverage in terms of river miles was from RM 9.64 to RM 19.22 which is about 9.6 miles of river.

The study reach was impacted by two large flood events between a topographic data set obtained in 2002 and the next topographic data set developed in May 2010. One event occurred in February of 2005 and one in January of 2010 with flows (as measured at the I-10 gage) of approximately 5,600 cfs and 11,800 cfs respectively. Based on data available on the District's website for the I-10 gage (using the Bulletin 17B data) these correspond to about a 10 year and 20 year event respectively.

Three sand mines are located in this reach of the river. All three pits were actively mining material from the main channel of the river between 2005 and 2010. The pits (Figure 2) are located just south of the Tonopah-Salome Highway crossing (Hanson Pit - about 1 mile north of I-10), just north of the Tonopah-Salome Highway crossing (CEMEX – about 2 miles north of I-10) and about 4 miles north of I-10 (Pioneer Pit). The CEMEX and Hanson mines existed prior to the 2005 event and portions of the pits could be found in the 2002 topography. Mining in the CEMEX and Hanson pits continued from 2002 until the 2010 event. The Pioneer pit was not mined until after the 2005 flood. The depths and aerial extents of the pits were estimated from District inspection records and from annual aerial photos taken in November or December of each year. The determination of the area and depth of the pits for conditions just prior to the 2005 and 2010 events is shown in Appendix I.

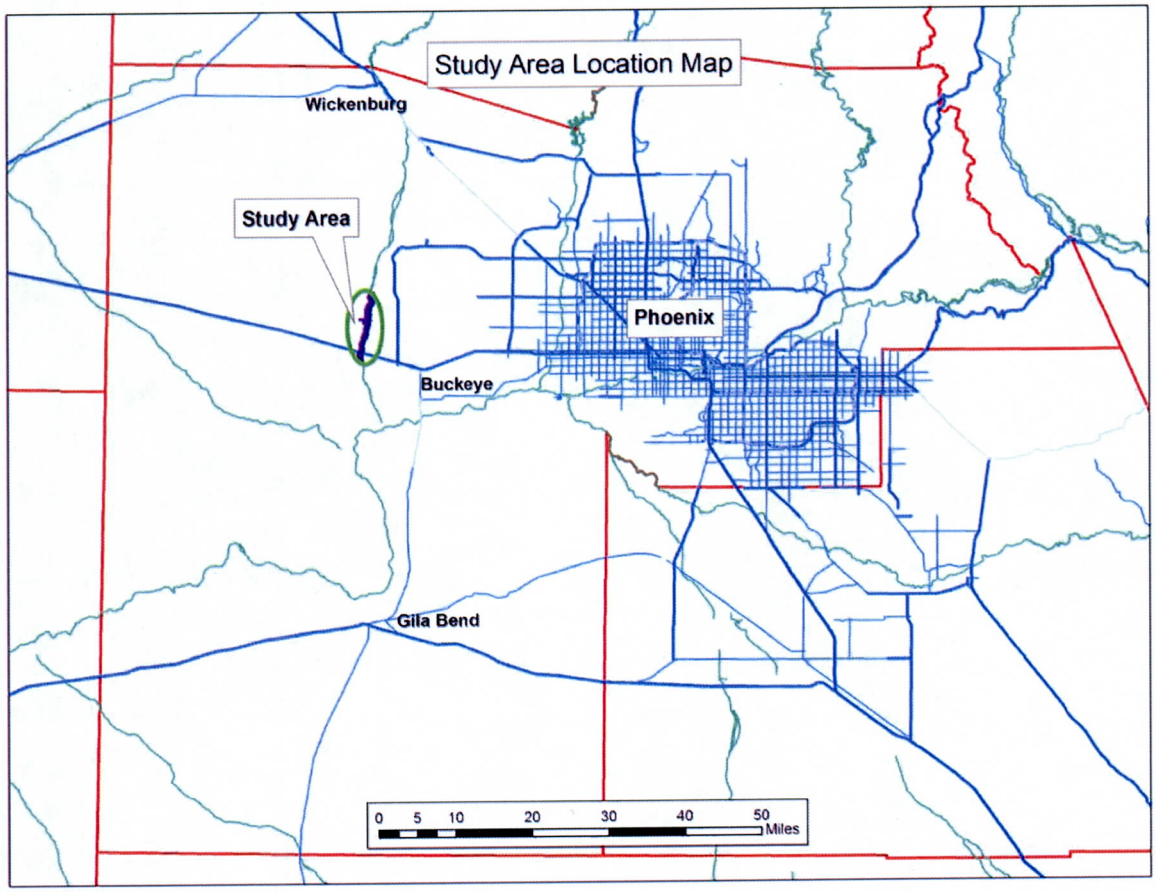

Figure 1. Project Location.

This reach was selected for modeling because the erosion resulting from the flood events provided an excellent data set to evaluate headcut/tailcut methodology and to test and compare sediment transport models. This reach provided enough data to see if the models evaluated could accurately predict the erosion and deposition due to mining activities. The analysis was primarily focused on predicting the impacts of headcuts and tailcuts from mining operations rather than the deposition into the pits. This focus was necessary since the actual depths of the pits were being estimated from aerial photos and ground observations with no surveyed data being available.

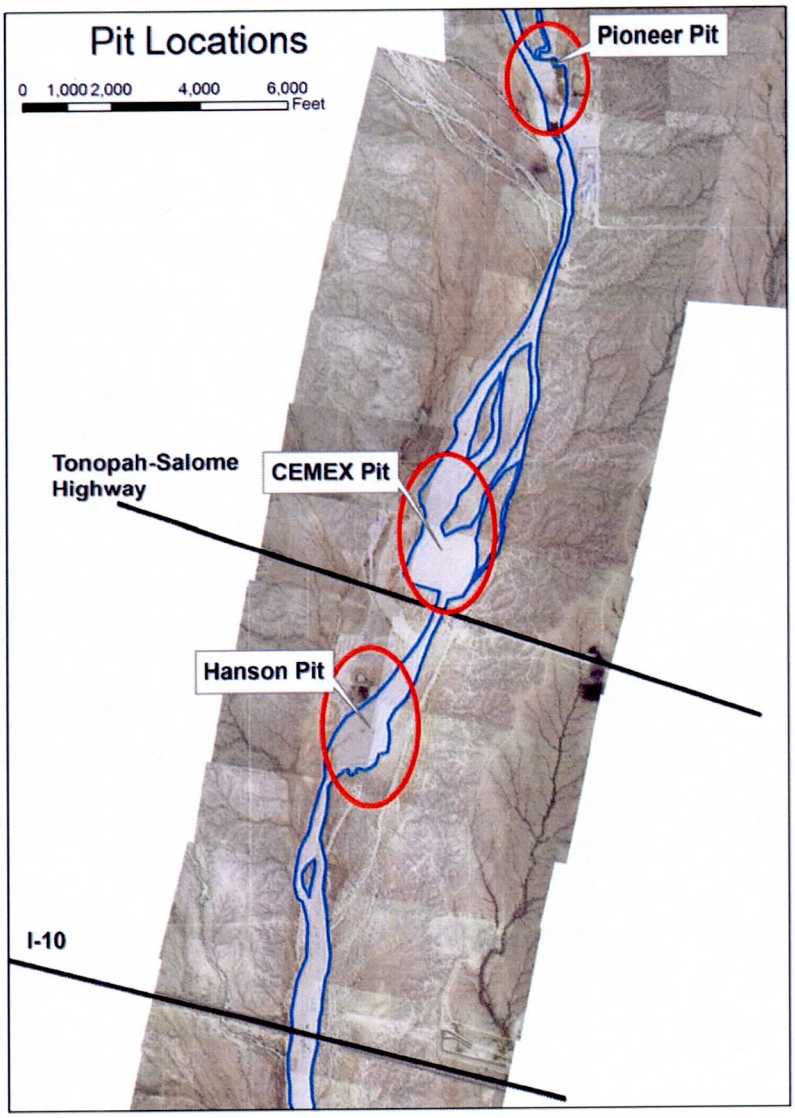

Figure 2. Location of Mining Pits in Hassayampa River. Blue lines show extent of January 2010 flood event.

B.2.2 Topography

The most recent pre-flood topographic data were obtained for most of the area in 2002 with some areas having been updated in 2004 as a part of the Phase I effort of the Hassayampa Watercourse Masterplan. Sediment transport modeling of the reach had also been completed as a part of Phase 1 of the Hassayampa Watercourse Master Plan. Phase 1 of the work was completed in 2006. The combined topography from prior to the 2005 flood event is referred to as the 2002 topography.

Since an excellent data set could be available for model testing and review, the District obtained new topographic data for approximately 10 miles of the river in May 2010. The data collected had a contour interval of 2 feet and covered the entire width of the river that experienced flow during the events (i.e. the full width of the 2010 flows).

The new topography data were obtained several months after the January 2010 flood event but during this period no new flows occurred in the river to cause changes in the river bed or scour depths. There was some activity around the mines (primarily the Pioneer pit) where some berms were rebuilt and other maintenance activities performed that did not obscure the changes in the river bed. There was, however; still water in the lower pit elevations in the Pioneer pit and a road/berm had been constructed across a shallow area of the pit to allow equipment access to the area west of the pit.

The new (2010) topographic data allowed the comparison of the river bed elevations to show the impacts of mining from 2002 to 2010. The comparison revealed significant down cutting in the river upstream and downstream from the mine operations as a result of the various flow events. Field observations indicated that most of the changes resulted from the 2010 flood event although a review of aerial photography indicated that significant changes had occurred in the river at the CEMEX and Hanson pits after the 2005 event.

The use of the topography to determine pit depths was not possible since the pits had filled enough to cover the original pit bottom or had water remaining in the pit. The 2010 topography did provide ample data to allow the comparison of models and transport equations to determine which could best predict the headcut/tailcut results of the 2010 flood event.

B.2.3 Incorporation of Pits

Pit depths and configurations were estimated based on annual aerial photos, information from District inspection records, and portions of the pits that existed in the 2002 topography. District personnel who inspected the pits were also interviewed regarding pit depths and their observations were incorporated into the data. The pit data was then incorporated into the 2002 topographic data. This was done for two differing pit scenarios - once for the pre-2005 event (2004) pits and once for the pre-2010 event (2009) pits.

The pit extent data (i.e. planform) was determined based on the most recent aerial photos available before the event – i.e. the November 2004 photos for the February 2005 event and the October 2009 photos for the January 2010 event. Since the flood events occurred in either January or February the difference between the area of the pits in the photos and the actual shape was probably not too large.

The depth of the pits is much more uncertain since some areas had filled during small events and pit depths are not normally equal across the entire areal extent. The depth was estimated based on the analysis of aerial photos and relied heavily on observations by District inspectors who visited the pits on at least a semi-annual basis. The pit depths and extents estimated by collaboration between the District and R2D are shown in Appendix I. The data is summarized in Table 1.

Table 1. Estimated Mine Depths and Areal Extents.

	Hanson		**Cemex***		**Pioneer**	
	Depth (ft)	Area (acres)	Depth (ft)	Area (acres)	Depth (ft)	Area (acres)
2002 (information only)	4	0.5	12, 20	4.3	N/A	N/A
2004 (before '05 events)	5-9	15	10-15, 10-15, 15-20	1.1, 1.1, 14	N/A	N/A
2005 (after '05 events)	5-9	10	mine filled	mine filled	8-10	3.3
2009 (before Jan. 2010 event)	10	22	10	45	28-30	23

*There are separate pits for this owner. See the photograph in Appendix I for estimate limits

Headcutting and channel lowering at the CEMEX pit from the 2005 event is evident in the subsequent aerial photos and estimates were made based on the aerial photos and observations. The permitted depths were also reviewed to see if the data matched the permitted depths for all of the pits. Some of the CEMEX pit area was already mined in the 2002 topography and this data was used to ground truth estimates of pit depth for some of the areas. Based on this evidence there was significant impact from the 2005 event but no topography was available to quantify the results.

The pits were specified as horizontal-bottom (single bottom elevation) pits to facilitate their incorporation into ARCMap and the digital terrain models. After the pits were inserted into the topography, digital terrain models were regenerated in ARCMap and the 1D model cross

sections were cut from the digital terrain model. The same cross section data was used for all of the 1D models evaluated.

Changes were necessary to the bottom elevation of the Hanson pit since it was longer than the other pits. When modeled as a single elevation, horizontal-bottom pit the downstream end of the pit was above the bed of the river. The elevation of the Hanson pit was broken into several sub-pits and each sub-pit was modeled with a differing bottom elevation. The elevation of each sub-pit was determined by viewing the aerial photos and estimating depths based on differing shadow lengths and other indicators. This made the Hanson pit elevations more realistic and kept the pit below the grade of the riverbed at the downstream end of the pit.

B.2.4 Events Modeled

The full hydrologic record was reviewed for the I-10 gage on the Hassayampa River from September 2002 to May 2010. The days with zero flows were removed from the record and the days showing flows reviewed. In Figure 3 it can be noted that there are a number of small flow events that are mostly well below 1,000 cfs. The events less than 1,000 cfs at the I-10 gage were ignored for this study. The total time water was flowing in the river is 385 hours (16 days) out of 7 years and 8 months (approx. 2800 days).

Relatively large flow events occurred on the Hassayampa River (as measured at the I-10 gage) on February 12, 2005 (approximately 5,600 cfs or about a 10 year event) and January 21, 2010 (approximately 11,800 cfs or about a 20 year event). One additional event of approximately 2,000 cfs also occurred on February of 2005 (< 5 year event) but, after discussions with the District, this smaller flow was also ignored to simplify the modeling. It was anticipated that the amount of sediment transport in the larger one or two large events would mask these smaller events.

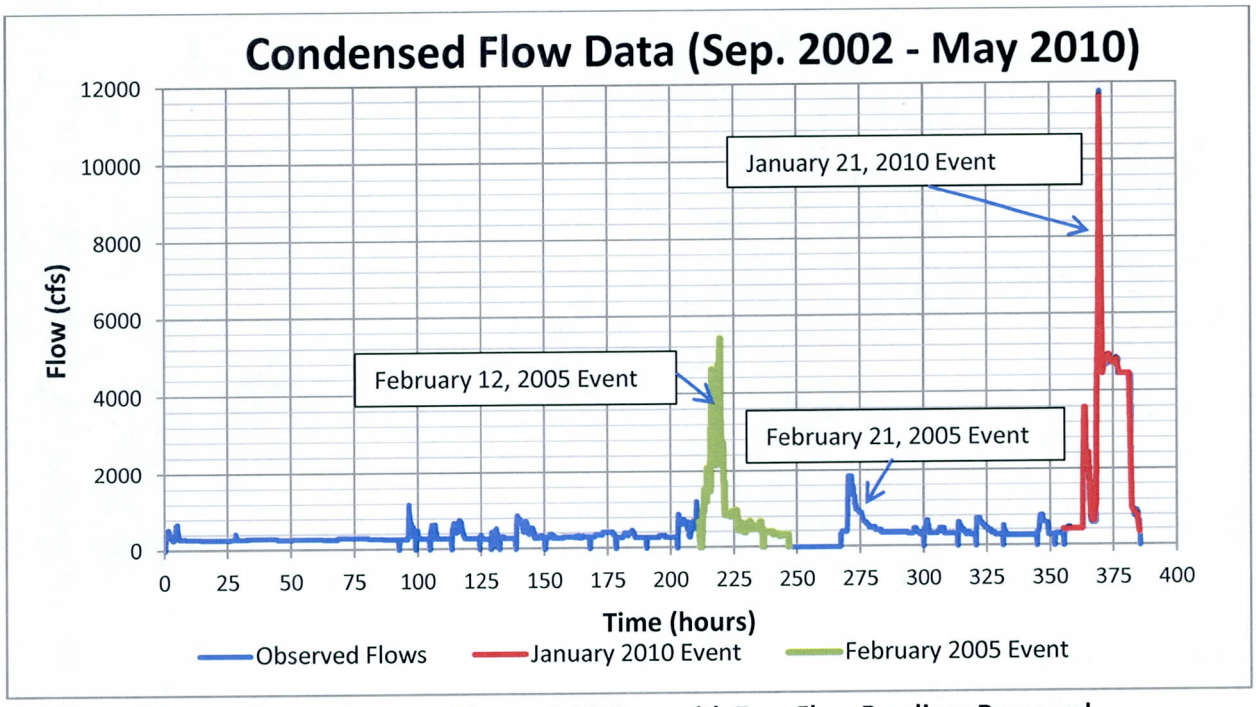

Figure 3. Flow Data for Hassayampa River at I-10 Gage with Zero Flow Readings Removed.

B.2.5 Bank Stations, Flood Extents and Erosion Limits

Bank stations were developed based on visual inspection of the post flood photos (i.e. the next available set of aerial photos). The photos allowed the delineation of the active channel areas from the overbank areas (areas that didn't have flow). The bank stations in the HEC-RAS and HEC-6T models were set equal to the observed flood extents for the respective floods. This delineation was performed for both the 2005 event and the 2010 event. The use of the cleared (scoured) areas was thought to be a reasonable estimate of the active channel limits and bank stations since vegetation was removed from these areas by scour during the events.

The 2005 flood extents (used as bank stations and erosion limits) were taken from the November 2005 aerial photos. Even though 8-10 months had passed between the flood and the new aerial photos the limits of the flood were still apparent in the aerial photos. Since erosion was evident to very near the flood limits, the flood extents were used as both the bank stations and limits of the active channel in HEC-RAS and HEC-6T.

The 2010 flood extents (channel width or active erosion limits) were taken from the May 2010 aerial photos. These photos were taken in conjunction with the new topographic mapping. These photos clearly showed the extent of the flooding and erosion in most areas. There were only a few very minor areas where flood extents could not be clearly determined from the photos but these were very small areas (primarily on the eastern boundary of the CEMEX pit)

where the photos were too light to view the differences between the flooded and non-flooded areas. The 2010 flood extent is shown as blue lines in Figure 4 while the 2005 flood extent is green. It can be seen that most of the floodplain was not inundated during these floods.

The banks stations / erosion limits in the models varied from those used in the effective floodplain delineation (Cella Bar 1988) and from those used by Fuller for the 100 year modeling efforts.

Perched Channels In a number of cross sections (primarily in the upper portion of the model) the areas inundated during the 2005 and 2010 floods were at a higher elevation than areas that were not flooded. The result was that flow in the various models would be routed through the lower areas rather than in the channels where flow actually occurred. This created messages that the channel had filled with sediment and other errors. This was not a problem for the 100 year model as flow would occur in all of the low areas during a 100 year event.

In order to prevent flow in the inactive channels that were lower than the 2005 and 2010 active channels these areas were initially marked as ineffective. At times one or more of the models would still give errors that the channel had dried up. As a result the areas where flow did not occur were blocked to the extent possible. In some areas and in some models the cross sections were simply cut off to remove the areas from the model. This simplified modeling and changes to the models. Changes to the cross sections for individual models are described below.

HEC-6T Areas to be blocked in HEC-6T were either removed from the cross section (i.e. the cross section shortened to eliminate no flow areas) or an elevation higher than the expected flow was input as the bed elevation. In the HEC-6T model the larger areas (i.e. the Hansen off-channel pit) were removed from the cross section (i.e. the cross section was shortened to eliminate the pits). This insured that the flow was in the channel rather than through the deep pits that were not flooded in either event. X3 cards were also used to confine flow to the channel.

HEC-RAS The low areas that were not impacted by the 2005 or 2010 events were blocked in HEC-RAS to the extent possible to prevent flow from occurring in these low areas. If one side of the overbank was blocked it was necessary to mark the other side as ineffective in HEC-RAS. Any attempt to have two blocked sections would cause the HEC-RAS interface to crash. This would lose any unsaved changes to the model. Thus the areas with the largest ineffective / inactive flow areas were blocked and more minor areas were marked as ineffective flow areas.

Problems were noted in the HEC-RAS model with the use of ineffective areas. The initial approach to keeping flow in the perched channels was to simply mark the lower dry areas as

being ineffective. This resulted in scour and deposition in some of the ineffective areas and it was decided the areas need to be blocked. The end result was that the low areas where flow did not occur for the 2005 and 2010 events were either blocked or eliminated from the modeled cross sections.

Since the use of ineffective areas was a problem it was decided to block the cross sections in the 2005 model. Applying this solution to the problem of the ineffective flow areas created problems later when the 2010 model was being prepared. The blocked elevations were then the only elevations that were available in the HEC-RAS output file that was now the input file for the next model. This meant that the original 2002 elevations to be used in the 2010 model (formerly overbanks areas in the 2005 model) had to be input manually into the 2005 output file.

Eastern Braid There was a small braid along the east side of the floodplain upstream from the Pioneer pit for the 2010 flood that was not modeled (See Figure 4). The braid was small in relation to the main channel and would have significantly complicated modeling efforts in the one-dimensional models. This braid was ignored in all of the 1D models. The data exists such that this braid could be modeled in the future if desired. There are no flow records for this braid but it could be estimated using high water marks from the channel upstream from the area where erosion occurred. This braid entered the Pioneer pit during the 2010 event and caused significant bank erosion in addition to head cutting up the braid channel (See Figure 9 later in this document).

Manning's n Values The Manning's n values used in the model were taken directly from the 2006 Fuller model for consistency. Based on the post flood assessment it appears that the channel n values drop to something very close to the grain roughness (or bed form roughness) after flow has started in the channel. Almost the entire area where flow occurred was cleared of vegetation by the flows. This resulted in a lower Manning's n value than used for some areas in the Fuller models. The HEC-6T model would not produce the post flood geometry with the NX records that were used in the original files for the 2005 + 2010 runs. It was necessary to comment out the NX records and use N records with fixed n values for the channel and overbanks. The values used were 0.025 for the channel and 0.045 for the overbanks (no flow areas). The values used by Howard Chang were 0.026 for the channel areas for all models he tested.

2005 and 2010 Flood Extents

Figure 4. Flood Extents/Bank Stations for 2005 and 2010 Events

B.2.6 Transport Equations Used and other Technical Input Data

The plan for the study was that a single sediment transport equation would be used in all of the models to allow direct comparisons. After the model review (prior to modeling) it was determined that the best option appeared to be the Engelund Hansen equation. This equation was utilized in all of the models initially. The results from the HEC-6T and HEC-RAS models indicated that the Engelund Hansen transport equation appeared to be scouring too much material from the channels. At that point it was determined that the inclusion of several other equations would be desirable to insure that the results would not be based on a single transport function – especially one that did not appear to be correctly modeling the behavior of the Hassayampa River. The other transport equations tested included the Yang equation, Toffaleti equation, Toffaleti combined with the Meyer-Peter & Muller equation, Laursen Copeland equation, Wilcock equation, and the Ackers White equation.

Inflowing Loads Model inputs included equilibrium loads that were calculated for the flow conditions at the upstream end of the models. Any errors in the inflowing loads were also far enough from the areas of interest that the models could come into equilibrium well before reaching the area of interest.

Temperature The temperature of the water used in the modeling effort can impact the sediment transport rate in some equations as well have an impact on the fall velocity of sediment particles. A temperature of 45 degrees was used in the HEC-RAS and HEC-6T modeling efforts since the events were winter storms and flow was coming from higher elevations.

Models Three models were prepared based on the data described above. Dr. Howard Chang was tasked with running his FLUVIAL-12 model for the 2010 event and then re-running the model for the 2005 event followed by the 2010 event. The second model that was prepared was a HEC-6T model based on the HEC-6 model prepared by Fuller as a part of the Hassayampa River Watercourse Master Plan (Phase I). This model was modified to include the pits for both the 2005 and 2010 events and run for both conditions.

The third model used was the HEC-RAS model that contained sediment transport (version 4.1.0). It was desired to use this model since it was available to be downloaded from the U.S. Army Corps of Engineers and is not proprietary. The graphical interface allowed the review of model input and output in a much more intuitive way and errors in input data could be much more readily determined. This model was also run for both the 2005 and 2010 pit configurations.

B.3 Observed Headcuts and Tailcuts

Headcuts and tailcuts from the various pits can be found in both the 2005-06 aerial photos and in the 2010 aerial photos. While the 2005 event created headcuts that were discernable in the photos of the river, the 2010 flood event created readily apparent headcuts and tailcuts from all three pits in the river channel. The thalweg elevations (lowest points in the channel cross sections) are shown in Figure 5 for the 2010 event.

It can be seen that a head cut on the order of 10-12 feet originated from the Pioneer pit (the pit furthest right in Figure 5 while a headcut on the order of a few feet moved upstream from the Hanson and CEMEX pits (furthest left and center respectively in Figure 5). Field observations indicate that the head cut upstream from the Hanson pit is on the order of 3 feet as can be seen in Figure 6. The channel lowering in the reach above the Pioneer pit can be seen in Figure 7. Tailcutting out of the Pioneer pit on the order of 6-7 feet can be seen in Figure 8. The result of headcutting upstream from the pit along an eastern braid (ignored in the modeling) can be seen in Figure 9. From Figure 5 it can be noted that the headcut from the Pioneer pit reached nearly a mile upstream before the pre- and post-flood lines merge together. The headcuts from the shallower pits downstream are much shorter – on the order of 1,200 to 2,000 feet.

In reviewing Figure 5 it should be noted that the pit elevations are estimated and were entered as a constant elevation for the CEMEX and Pioneer pits rather than sloped to match the river in the reach. This was done to facilitate the insertion of the pits into the topography and the cutting of new cross section in HEC-GeoRAS and in the 2D models. It is possible that the pit volumes in the models are significantly different than the actual pit volumes but since the primary interest was on the calculation of headcuts and tailcuts the amount of deposition in the pits was not as important. Later discussion will examine whether a change in pit depth produced a significant change in headcut depth or length for a fixed pit layout.

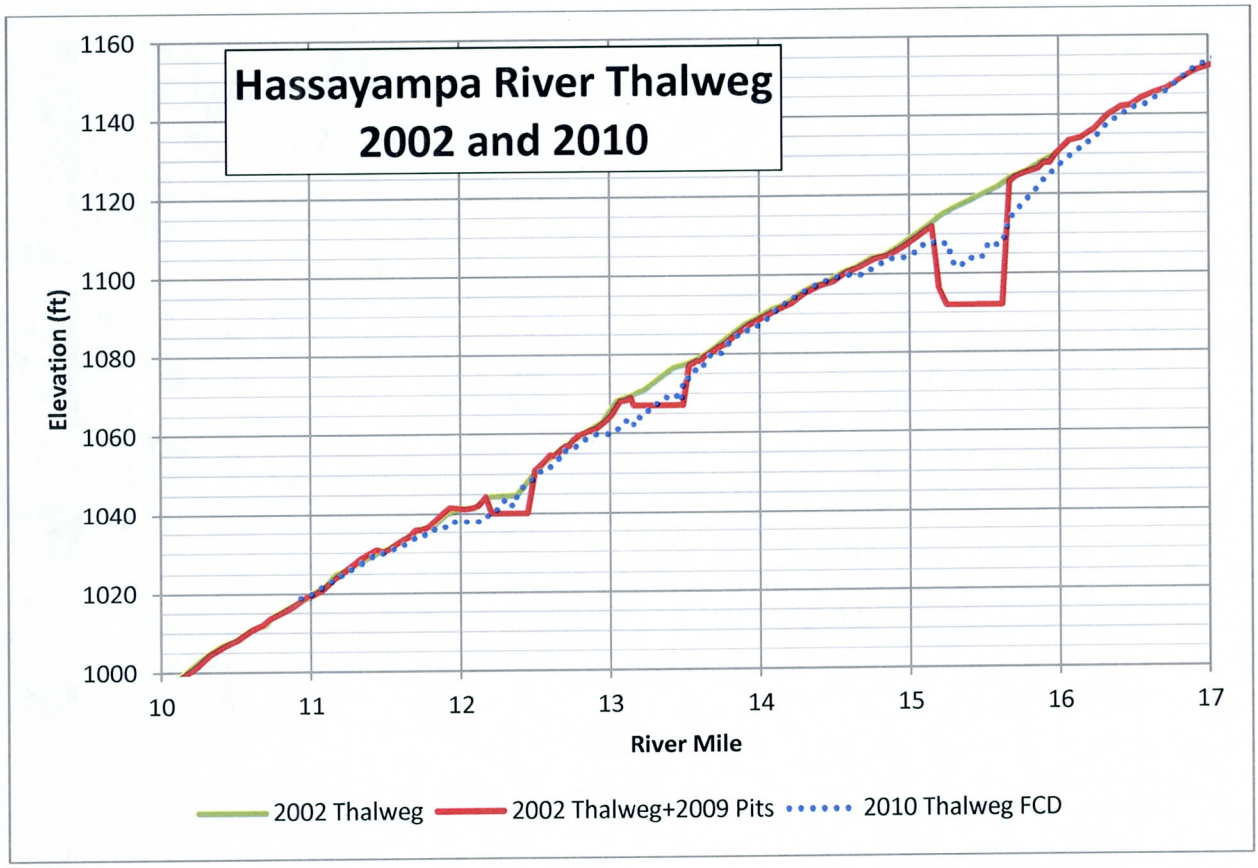

Figure 5. Comparison of Hassayampa River Thalweg for 2010 Pre-flood (Ignoring Small Pits) with Estimated 2009 Mining Pits and 2010 Post Flood Showing Impacts of Mining on Channel Elevation.

Figure 6. Hassayampa River above Hanson Pit showing Old Channel with Approximate 3 feet of Channel Lowering.

Figure 7. Approximate 9-10 Foot Channel Lowering above Pioneer Pit along West Bank of Hassayampa River.

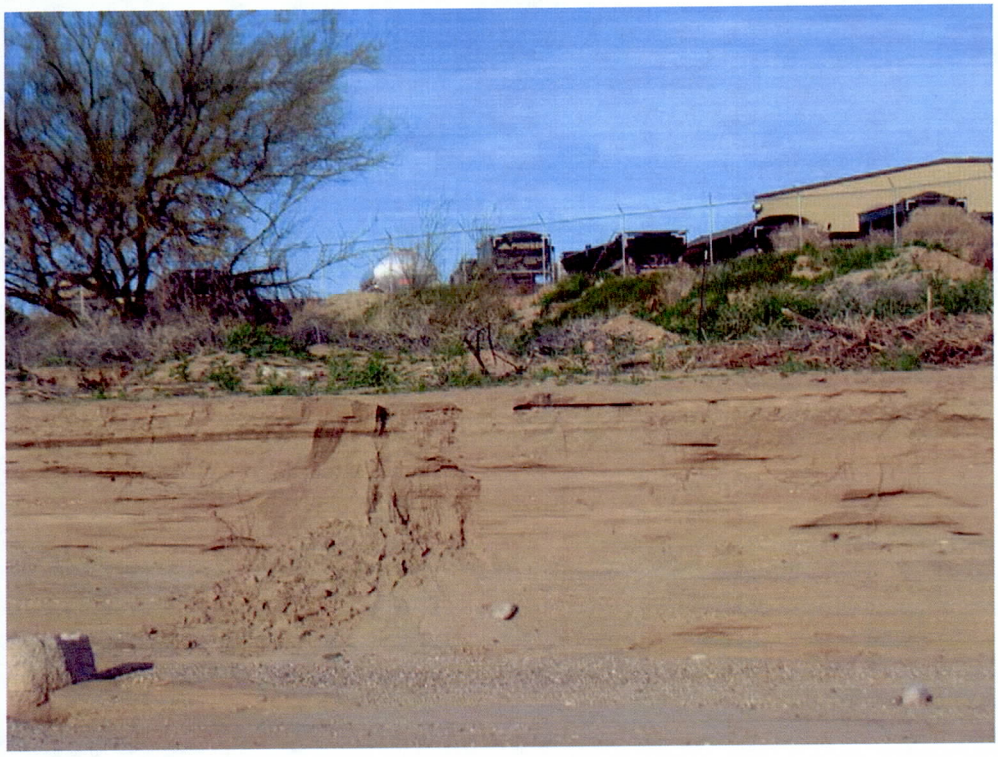

Figure 8. Tailcut Erosion Immediately Downstream from Pioneer Pit. Tailcut depth is approximately 7 feet.

Figure 9. East Braid Headcut above Pioneer Pit Looking Downstream Towards pit.

C. COMPARISON OF THE MODELS

C.1 Overview of Model Comparison Methods

The model comparison consisted of two main tasks. One task was to use previously developed models to model the 100 year flow event. The models represented the 2002 topography and the goal was to compare model results. The models used for this task were FLUVIAL-12, HEC-6, and the latest version of HEC-RAS with sediment transport capabilities (version 4.1.0). The original task called for converting the HEC-6 model to the more updated HEC-6T model but after discussions with the District it was determined that the existing HEC-6 model would be adequate for the level of comparison desired for the 100 year event. The primary difference between the models was that HEC-6T has more options available but none of the updated options were required for the 100 year model of the Hassayampa River. The basic calculation engine is the same in both models.

The goal for this task was to see how the models compared for a large event and to see if there were significant differences in the models due to their formulation or application. This would allow comparison of the models under existing conditions to see what they would predict for a 100 year event and allow a direct comparison of model output. Since no field data was available for a 100 year flood they could not be compared to the observed data but were simply compared to each other. This task also included a comparison of the model assumptions and available options.

The second main task was to model the observed flow events and see if the 2010 topography could be reproduced by the models. This task consisted of two sub-tasks. One was to model only the 2010 event and one was to model the 2005 event followed by the 2010 event.

The first event to be modeled was the 2010 event by itself starting from the 2002 topography. This was done to see how stable the models were and to obtain data to determine if the 2010 event was large enough to mask all of the other events that occurred from September 2002 until the January 2010 flood event. The pits that were used for this model were representations of those that existed at the end of 2009 when the last aerial photos were taken prior to the January 2010 event.

The second part of this task was to model both the 2005 event and the 2010 event starting with the 2002 topography. This involved incorporating the 2004 pits as observed from aerial photos taken at the end of 2004 and then running the 2005 event. The pit data was augmented with

information from District site visits that occurred prior to the 2005 event. The model output from the 2005 event was then used as input to the models for the 2010 event. The 2005 model output was updated by incorporating the 2009 pits before the 2010 event model was run. The results of the 2005 event followed by the 2010 event were then compared with the results from the model of only the 2010 event to see if the model using both large flows would predict the 2010 results more accurately than the model using only the 2010 event. The two sets of models provided data on which to base decisions regarding modeling requirements.

C.2 Comparison of Model Features and Assumptions

The models used in the study were reviewed for similarities and differences in formulation and application. The one-dimensional models compared were FLUVIAL-12, HEC-6/6T, and HEC-RAS. A number of two-dimensional models were also either compared or used in modeling. Models used in an attempt to obtain two-dimensional results included FLO-2D, RiverFLO-2D and RMA-2/SED2D. Two addition models were evaluated but not actually used for modeling - the Corp's ADH and the USBR's SRH-2D. The results of the comparison are shown in Table 2 (1D models) and Table 4 (2D models). The FLO-2D and RiverFLO-2D run by the District were not included in the tables since they were not evaluated for features by R2D. Table 3 shows a partial list of differences between the HEC-6 model and the more updated HEC-6T model.

The results of the model review and comparison of model features indicated that the FLUVIAL-12, HEC-RAS and HEC-6/6T models are similar although each has its features that make it more applicable to given applications. For example the FLUVIAL-12 model estimates the erodible channel width based on the flow while the erodible bed limits are fixed in HEC-6, HEC-6T, and HEC-RAS (referred to as the HEC models). This difference has some significant ramifications in model results. The FLUVIAL-12 model can model headcuts that form during varying flows but the outside extent of the erodible area is not limited except by the end of the cross section. The HEC-6, HEC-6T and HEC-RAS models do have fixed scour limits but only scour in areas where the channel is wet. This means that during low flows the lowest part of the channel will scour – similar to the FLUVIAL-12 model but the HEC-6T and HEC-RAS (HEC models) also provides limits on the maximum width that can scour. The approaches are different and both have their benefits and limitations. For example if scour is only expected in an area that is away from the lowest portion of a cross section (next to a gravel pit for example) the HEC models can accommodate this constraint more readily than the FLUVIAL-12 model.

The models have a wide variation in the availability of transport equations with HEC-6T having the widest selection of equations at 18 with HEC-RAS and FLUVIAL-12 having significantly fewer with only 6 equations each. This may limit the applicability of the models in some situations. It

is expected that additional equations may be added to the HEC-RAS model since it is under active development.

The HEC-6/6T and HEC-RAS models used Manning's n values that are estimated at discrete locations across the cross section. HEC-6/6T and HEC-RAS average the n values into 3 separate values – two overbanks (left and right) and the channel which allows better definition of the channel but this formulation of the models also limits the ability of the channel to adjust in width during an event. The FLUVIAL-12 model utilizes a single cross section n value and thus has no need for bank stations to differentiate between channel and overbank flows/roughness values.

Among the 2D models reviewed in Table 4 it is apparent that they all have significant differences. Only the RMA-2/SED2D use was funded in this study and the model was difficult to use at best. The newer ADH and SRH-2D, which are both being actively updated, appear to have significant advantages over the RMA-2/SED2D combination. SED2D is no longer being updated by the Corps and has been dropped from newer versions of the Surface water Modeling System (SMS) interface (versions higher than version 9.2). Both of the other models operate inside the SMS interface which allows the standardization of the interface. The use of the interface greatly simplifies operation of the models.

The ADH model utilizes an adaptive grid which allows the model to automatically increase grid density in areas where rapid changes in hydraulics are taking place – for example at the brink of a gravel pit. This allows more accurate calculations and better stability for the model. The SRH-2D was also highly recommended by USBR staff although neither model was run for this study.

Table 2. Comparison of Features in HEC-6/6T, HEC-RAS, and FLUVIAL-12 Sediment Transport Models

Model	HEC-RAS	HEC-6 / HEC-6T	FLUVIAL-12
Item			
Version Used in Modeling	Version 4.1.0 (Jan 2010)	Version 5.13.22_06 (7 February 2006)	
Flow	Quasi-Unsteady	Quasi-Unsteady*	Steady Unsteady-No Tribs Dynamic Wave
Reverse Flows		Yes (6T)	
Solution			
Hydraulics	Standard Step Backwater	Standard Step Backwater	Standard Step Backwater Dynamic Wave (unsteady) Stream Power Minimization
Sediment	Downstream Unsteady - Implicit	Downstream Explicit	Downstream Implicit Central Diff
Bendway Calculations	No	No	Yes
Sediment Continuity	Exner Equation 0.002-2048 mm Clay to Boulders	Exner Equation Models fines (0.002 mm- 80"+	Exner Equation 5 size fractions max <0.0625 normally excluded
Sediment Transport Equations	Ackers White Engelund Hansen Laursen-Copeland Meyer-Peter & Muller Toffaleti Yang Wilcock	Ackers White Engelund Hansen Laursen-Copeland Meyer-Peter & Muller Toffaleti Yang Duboys Einstein Laursen-Madden Colby Toffaleti and Schokhtlisch Parker – Gravel Proffitt and Sutherland Brownlie D50 Brownlie (Individ. Grain) Yang – High Concentration User Specified	Ackers White Engelund Hansen Meyer-Peter & Muller Yang Graf's Formula Parker - Gravel
Active Layer Calculations	Thomas (1982)	Thomas (1982)	Borah et al. (1982)
Armor Layer	Yes	Yes	Not Specifically Calculated
# Layers	Exner5- 3 layers Active Layer – 2 layers	Exner5 – 3 layers Active Layer – 2 layers	

Sediment Diffusion		Immediate	Zhang, et. al. (1983)
Clay / Silt	Yes Standard Transport Eqns Krone & Partheniades	Yes Standard Transport Eqns Krone & Partheniades	Normally Excluded
Item	**HEC-RAS**	**HEC-6 / HEC-6T**	**FLUVIAL-12**
Erosion	Limited to Active Channel	Active Channel	Active Channel
Deposition	Active Channel or Entire Wet X-section	Active Channel or Entire Wet X-section	
Channel Width Adjustment	None	If Bank Slope > Input Angle bank fails	Yes – Energy Gradient Factors are: Rock 0.0 Cohesive 0.2 Erodible 0.5 Sand 1.0
Dredging	No	Yes	
Imports HEC-6	Yes	Yes	Yes

*HEC-6T has been previously coupled with a fully dynamic hydraulic model (UNET) and was run as a fully dynamic transport model.

Table References:

Borah, D. K., Alonso, C. V., and Prasad, S. N., 1982, "Routing Graded Sediments in Streams: Formulations," *Journal of the Hydraulics Division*, ASCE, 108(HY12), 1486-1503

Thomas, William A., 1982, "Mathematical modeling of sediment movement," Chapter 18 of Gravel Bed Rivers, Edited by R.D. Hey, J.C. Bathurst, and C.R. Thorn, John Wiley & Sons, Ltd.

Zhang, Q, Zhang, Z., Yue, J., Duan, Z., and Dai, M., 1983, "A Mathematical Model for the Prediction of the Sedimentation Process in Rivers," *Proceedings* of the 2nd Intern. Sympo. on River Sedimentation, Nanjing, China.

Table 3. Differences Between HEC-6 and HEC-6T (Partial List).

Item	HEC-6	HEC-6T
Deposition & Erosion Limits	H/HD/HL/HI	Added HE Card
Hydrology Specifications	Reach Outflow Points	Reach Inflow Points
Rating Curve Override	Resumes standard curve at next event	Doesn't return to normal – must specify to return to standard
Mudflow Constraints	800,000 ppm	Concentrations must be < specific weight of bed

Table 4. Comparison of 2D Model Features.

Model	ADH (Corps)	SRH-2D (USBR)	RMA-2/SED2D (Corps)
Item			
Model Type	Finite Element	Finite Volume	Finite Element
Equations	St. Venant	St. Venant	St. Venant
Implicity/Explicit	Implicit	Implicit	Explicit
Time Step	Variable		Fixed
Adaptive Grid	Yes	No	No
Super/Subcritical Flow	Both	Both	Subcritical Only
Wetting Drying	Yes	Yes	Yes
Vorticity (Bends)	Yes		Yes
Quasi Unsteady	Yes	No	Yes
Sediment	Yes	Yes	Yes
Multiple Grain Size	Yes	Yes	No
Cohesive	Yes	Yes	Yes
Temperature		Yes	RMA-4
Vegetation		Yes	
Calculation Points	Nodes	Element Centers	Nodes
Interface	SMS v10.1+	SMA v10+	SMA 9.2 or less
FEMA			Yes
Former Names	None	GSTARS-W	Sediment – STUDH
Limitations/Notes			
All models use SI units for sediment transport		All calculations in SI but can input/output either units	
Comments:			Wetting Drying not stable

C.3 Sediment Model Comparison for the 100 Year Event

Three models were compared for the 100 year flood. The models were FLUVIAL-12 (modeled by Dr. Howard Chang), HEC-6 (developed by Fuller and adapted by River Research & Design, Inc. (R2D)) and HEC-RAS (developed by R2D). The FLUVIAL-12 and HEC-6 models were thought to have used the same hydrographs and topography but on closer inspection the HEC-6 hydrograph was significantly larger than the hydrograph used in the FLUVIAL-12 model. This required the detailed inspection of the hydrographs and models to insure they were modeling the same conditions. The hydrograph in the HEC-6 model was revised to match that used by Dr. Chang in the FLUVIAL-12 model since his 100 year modeling had been completed earlier under a separate task.

The models also had significant differences in how the channel was modeled. Pits that had been partially filled or were behind levees were found to be included in the channel in the Chang model but were blocked or marked as ineffective in the HEC-6 model. Part of this difference was in how the channel is represented in the two models. The difference in the thalweg elevation in the models can be seen in Figure 10. Away from the pits the differences (if any) are not significant for the 100 year event with the 2002 topography. The Chang model had been completed prior to this study and was not rerun as a part of this task.

The HEC-RAS sediment model was run both ways – with the pits either blocked or marked as ineffective and with the pits as effective flow areas. The Engelund Hansen equation was not particularly stable in the HEC-RAS model with the pits included in the channel area. The differences in the initial bed are shown in Figure 10 and final model results are shown in Figure 11 and Figure 12. It should be noted that the HEC-6 model did not allow flow through the overbank pits at the Hanson and CEMEX sites while the FLUVIAL-12 and HEC-RAS Models allowed flow through the pits. This accounts for the large difference in the final results upstream from the Hanson pits (RM 12.4-12.9).

The 2005 pit at the CEMEX site in the FLUVIAL-12 model is the remnant of a larger pit that was filled by low flows (<1,000 cfs at I-10) between the time the topography was flown and the 2005 event. Flows into the pit may have been higher than the 1,000 cfs noted at the bridge but no gages or references are available to estimate the flows at the CEMEX pit. It was apparent from the aerial photos that the pit had mostly filled due to low flow events prior to 2005. The results in Figure 11 show an inconsistency in the FLUVIAL-12 model at about RM 10.4 but this was not investigated since it was downstream of I-10 (RM 11.0) and beyond the area of interest.

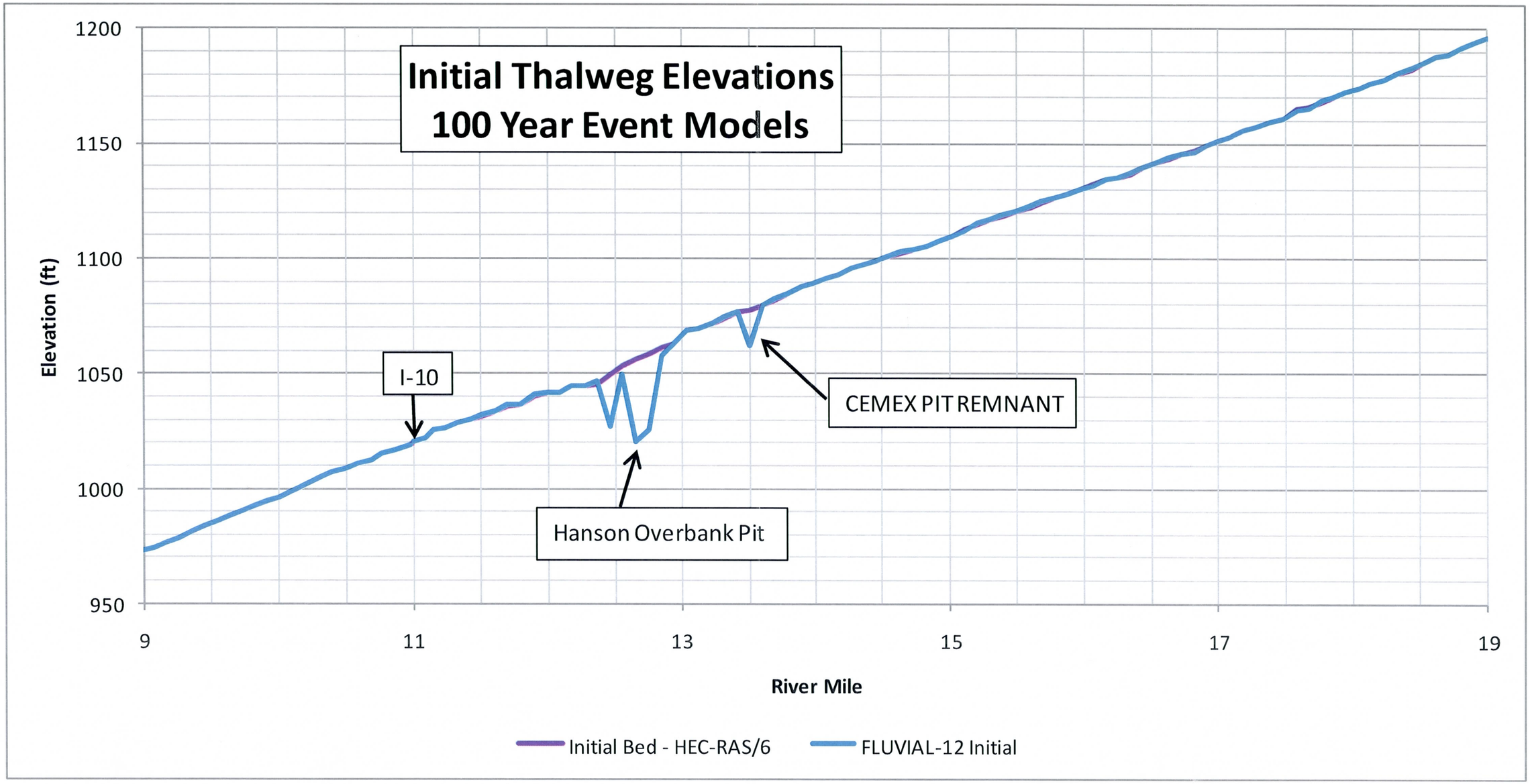

Figure 10. Initial Thalweg Elevations for FLUVIAL-12, HEC-6 and HEC-RAS

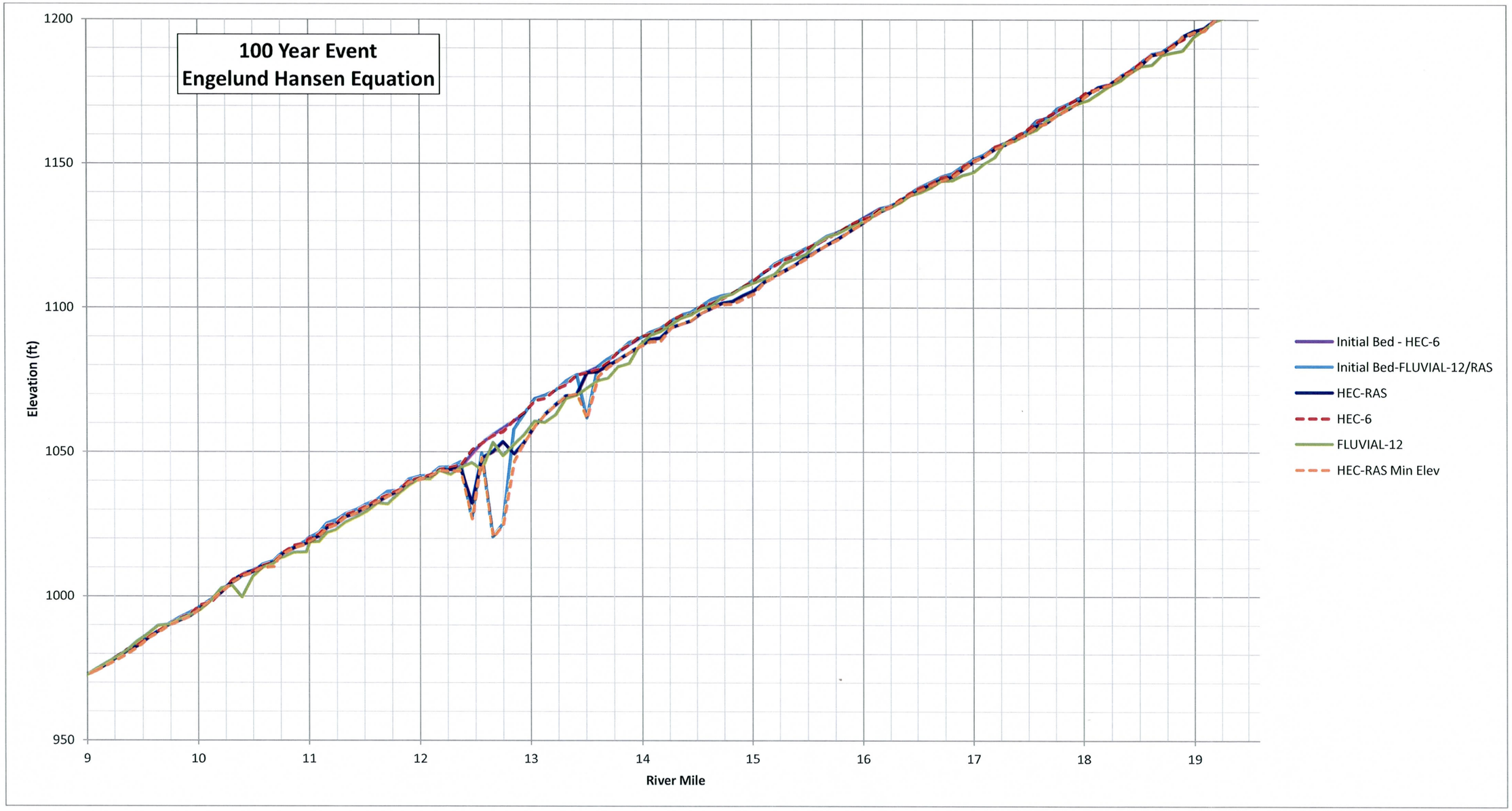

Figure 11. Results for 100 Year Simulation. The HEC-6 model does not have flow through the overbank pits but HEC-RAS and FLUVIAL-12 both include flow through the pits.

The results in Figure 11 show that the HEC-RAS and FLUVIAL-12 results are reasonably close in the area where the pits influenced the simulation. Both models show the impact of headcutting upstream from the Hanson Pits. It should be noted that both of the overbank pits have protective berms and neither was breached in either the 2005 or 2010 events. The HEC-RAS and FLUVIAL-12 models produce somewhat similar results and no tuning of the HEC-RAS model was used to obtain the results. A few minor adjustments were necessary to get HEC-RAS model to run since it was somewhat unstable with the pits in place. The adjustments were minor and consisted of shortening the time steps or a change in the location of one of the erodible bed limits to narrow the channel in the immediate area of the pit. The transport equations in HEC-RAS often resulted in an error that the channel had over filled with sediment at one location or another. Adjustment to the erodible limits on the side of the river away from the pit was thought to be reasonable since the water would tend to concentrate in the path of least resistance – i.e. through the mine pit – leaving the high portion of the channel dry.

The HEC-6 results do not contain the pits in the flow area as they are outside the erosion zone in HEC-6. Away from the influence of the pit the models are normally in close agreement regarding the stability of the river. In the areas where conditions were influenced by the pits the HEC-6 model produced different results based on the overbank pits not being included in the channel. Based on these data the FLUVIAL-12 and HEC-6 models predicted similar results for the 100 year flood event away from the pits and both of the models appear to give reasonable results for this simulation.

The HEC-RAS model shows less scour for about one quarter mile upstream from the CEMEX pit than the FLUVIAL-12 model but the HEC-RAS model then predicts more scour than the FLUVIAL-12 model for a long reach above the CEMEX pit remnant. The difference is on the order of 4 feet at a distance of a mile and a half above the CEMEX pit remnant. The average difference between the HEC-RAS results and the FLUVIAL-12 results was 3 feet between RM 13.7 (the upstream brink of the CEMEX pit) and 16.16 where the difference between the predicted and original elevations reduced to less than 1.0 ft.

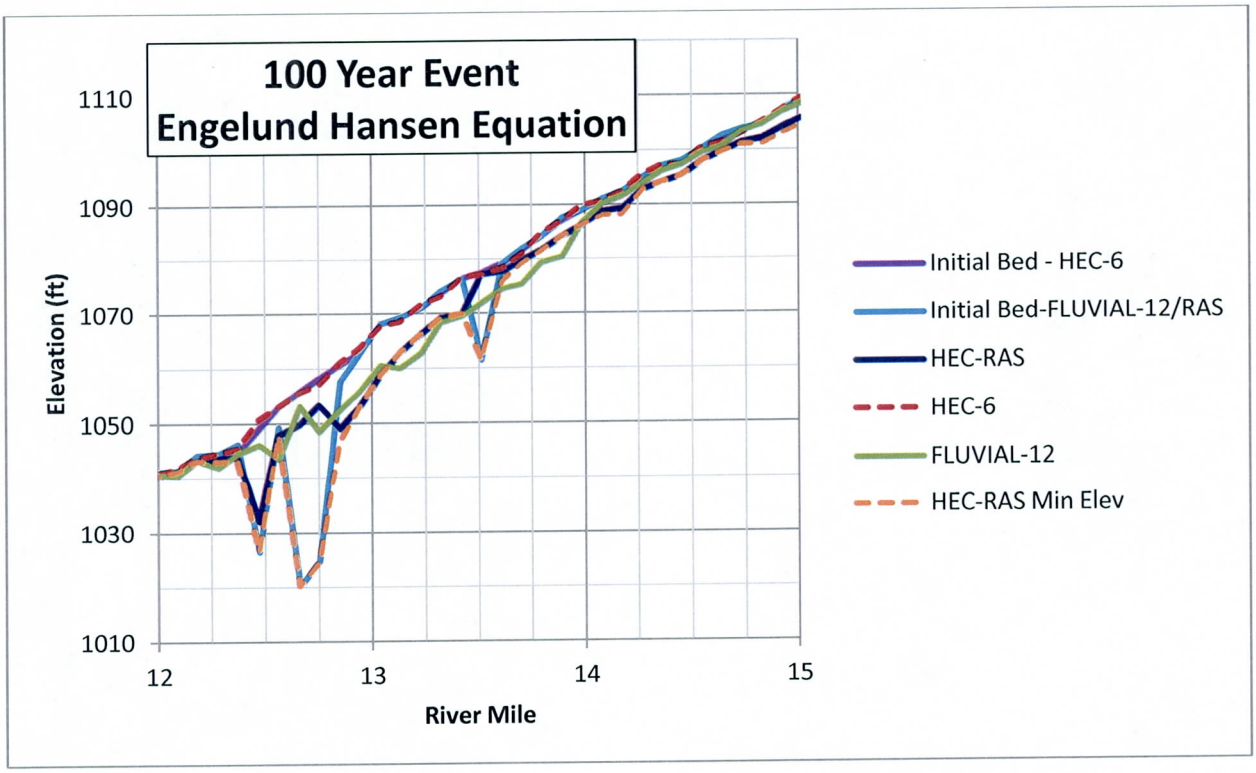

Figure 12. Model Data at Hanson and CEMEX pits for 100 Year Event. The HEC-6 model did not allow flow through pits.

C.4 2010 Single Event Modeling

Initial modeling for the 2002 to 2010 period focused on the 2010 event rather than on the modeling of the combined 2005 event followed by the 2010 event. This was done to simplify the initial modeling. By focusing only on one event the models could be more easily evaluated and compared and any problems determined before attempting to run the more complex multiple event models. The primary focus of the modeling effort was to compare models to see how the various models performed under the same model conditions.

The question of whether the 2010 event was large enough so that the 2005 and smaller events could be ignored was answered by comparing the results from the 2010 single event model with the results from the two event model which used the 2005 event followed by the 2010 event (2005+2010). This project task focused on the modeling of the 2010 event by itself to see how the models performed for the single event. The 2005 + 2010 event modeling will be described later in this report. The initial modeling again used the Engelund Hansen transport equation.

C.4.1 Model Inputs

The FLUVIAL-12, HEC-6T and HEC-RAS models used the cross sections developed for this study as described earlier. The models used the Phase 1 HEC-6 model (Fuller) n values and bank stations and erosion limits (in the HEC models) were taken from the observed limits of flow for the 2010 event. The inputs are described in detail earlier in this report.

C.4.2 Model Results for 2010 Event

HEC-6T and HEC-RAS. The HEC models (HEC-6T and HEC-RAS) were run with the 2010 event as the input flow. The initial results for the HEC-6T and HEC-RAS 2010 event models are shown in Figure 13. It can be seen that the models when used with the Engelund Hansen equation over predicted the end of event scour 1) upstream from the Pioneer pit, 2) upstream from the CEMEX pit and 3) between the CEMEX and Hanson pits. The models seem to do a good job downstream of the Pioneer and Hanson pits. It can be noted that both models do a good job of predicting the overall length of the headcut upstream from the Pioneer pit and the length of the tailcut downstream.

The results shown in Figure 13 indicate that the HEC-6T and HEC-RAS formulations of the Engelund Hansen equation give similar results although both models exhibit some instabilities (sharp peaks and dips). The instabilities are not, interestingly enough, always at the same locations with one model showing an instability and the other model being stable (or more so) at the same location. This can be seen more clearly in Figure 14 and Figure 15 where the differences between the models are more apparent. In some locations the instabilities are located at the same cross section but the magnitudes are significantly different. Whether these differences in magnitude could be due to internal computer calculations or model formulations cannot be determined from the results.

Some of the model instabilities may be due to cross section spacing or sudden changes in channel geometry. In areas at the upstream and downstream end of the pits the cross sections are very close together and may be too close in some cases. The downstream most cross section in the Pioneer pit (15.20) contains a very narrow section of the pit. This cross section has a tendency to scour since it is immediately downstream of the pit. This section probably should have been modified to remove the very narrow pit from the cross section prior to modeling but the problem was not discovered until other modeling efforts were completed. In order to keep the models identical to the extent possible the cross section was left as originally cut even though it was causing what appeared to be model instabilities in the HEC-6T and HEC-RAS models. In reviewing the cross section the thalweg lowered due to the lowering of the

entire wetted portion of the cross section rather than scour at the node giving the appearance of a model instability when one was not present.

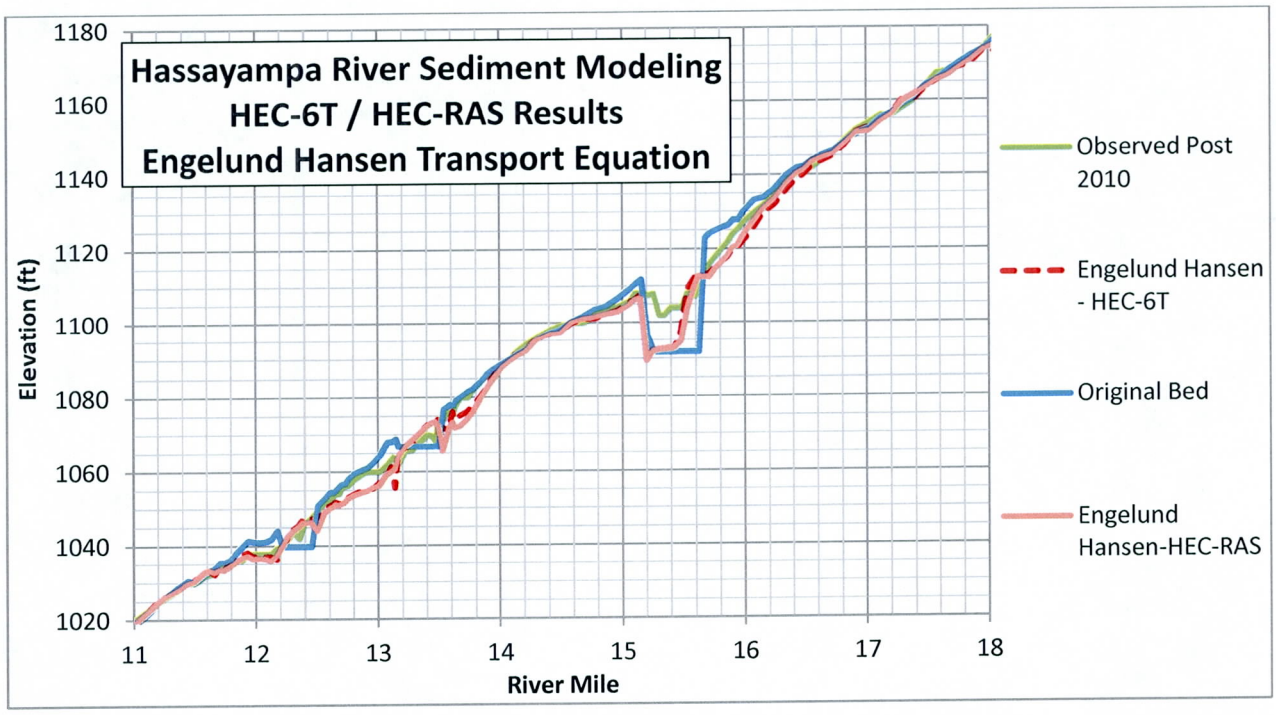

Figure 13. Results for HEC-6T Model using Engelund-Hansen Transport Equation for the 2010 Event.

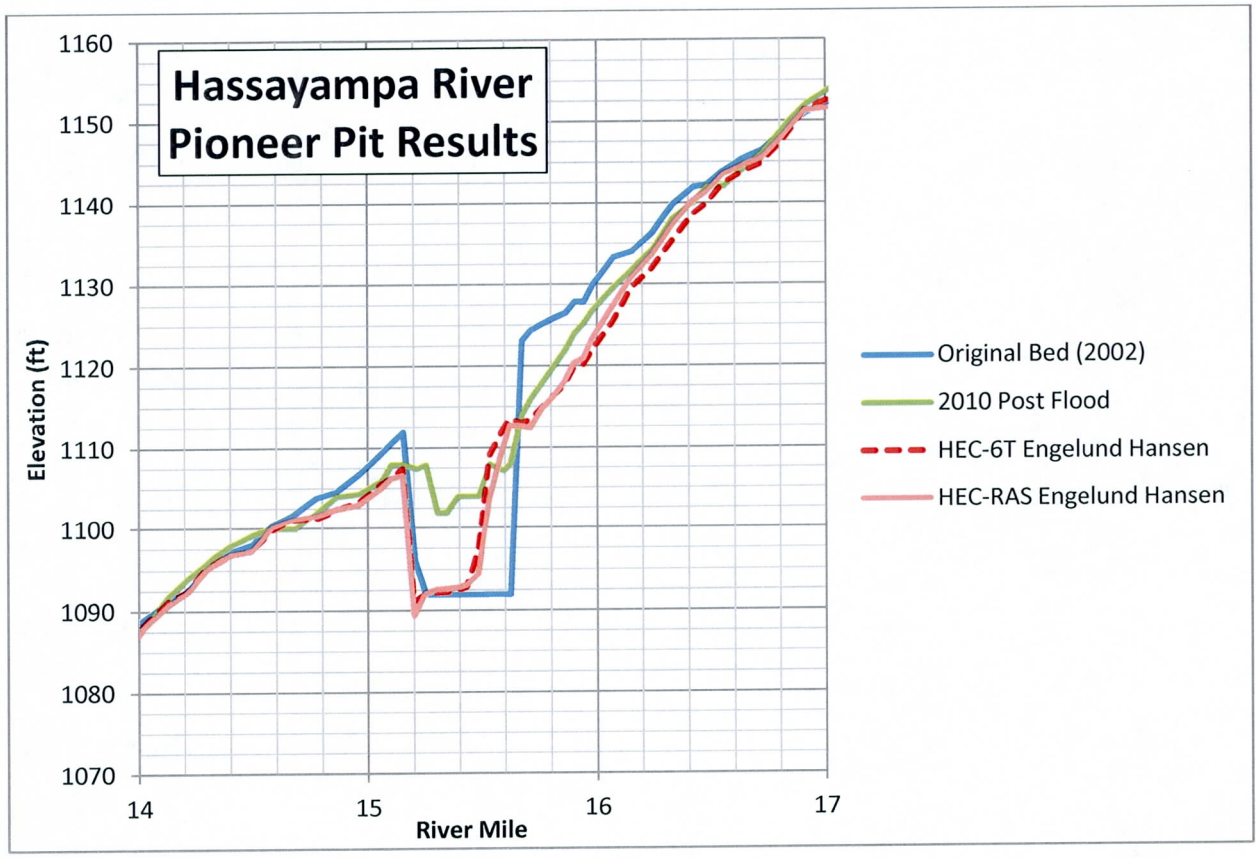

Figure 14. HEC-RAS and HEC-6T Model Results at the Pioneer Pit for the 2010 Event.

The change from a wide channel to an even wider pit also causes model instabilities. It is probable that with more time and latitude for model adjustment some of the instabilities could be removed from the models. The idea, however, was not to have models that were adjusted to the maximum extent but to have reasonable models that could be compared without expending extensive time adjusting the model. The goal was to have all the models using the same inputs for cross sections and other variables. This allowed the direct comparison of models.

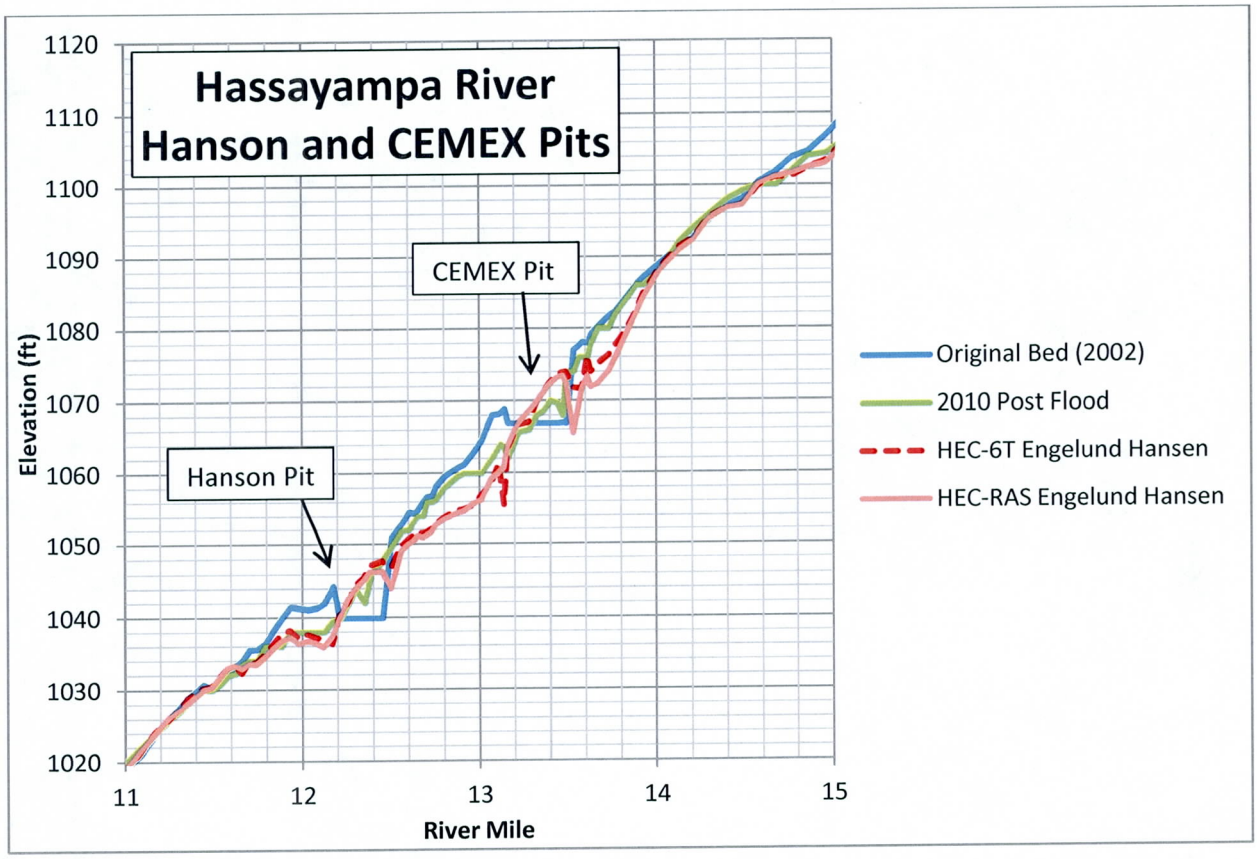

Figure 15. HEC-RAS and HEC-6T Model Results at the CEMEX and Hanson Pits for 2010 Event.

The use of ineffective areas in HEC-RAS was found to be problematic as previously mentioned in Section B.2.5. This was overcome by either blocking or removing the portions of the cross section from the model. Most of these results (other than in areas with off channel pits) were in areas that did not directly impact the results in the area of interest for this modeling.

FLUVIAL-12 Model Results. The FLUVIAL-12 model was run by Dr. Howard Chang who is the developer of the model. The model used the same conditions and inputs as the HEC-6T and HEC-RAS models. FLUVIAL-12 modeling was being done by Dr. Chang at the same time that modeling was being performed by R2D and required significant coordination between R2D, Chang and the District.

The FLUVIAL-12 model has six transport equations that are available but only two were used by Dr. Chang. The two equations that were used were the Yang equation and the Engelund Hansen equation. Only the Engelund Hansen equation was recommended by Dr. Chang.

The results of the FLUVIAL-12 as contained in Dr. Chang's report were only presented for the Pioneer pit and the model output did not contain a summary of the thalweg elevations. This required the determination of the thalweg elevation from the cross sectional output tables.

The data was reduced for the areas where headcuts and tailcuts were located in the observed data (See Table 6 later in this document).

The results for FLUVIAL-12 are shown in Figure 16 and show a good correlation between the observed data and the model results. There is one deviation from the observed results at RM 12 but this is relatively minor in comparison with the other models tested. This is likely due to a change in the channel location in this area that FLUVIAL-12 may have had more trouble modeling. The channel for the 2010 event avulsed from the main channel through the lower end of the Hanson pit. The FLUVIAL-12 model predicted the final bed elevations more accurately than either HEC-6T or HEC-RAS when compared for only the Engelund Hansen sediment transport equation. All of the models accurately predicted the length of the headcut and tailcut from the Pioneer pit.

The results will be compared using an absolute performance index later in this report.

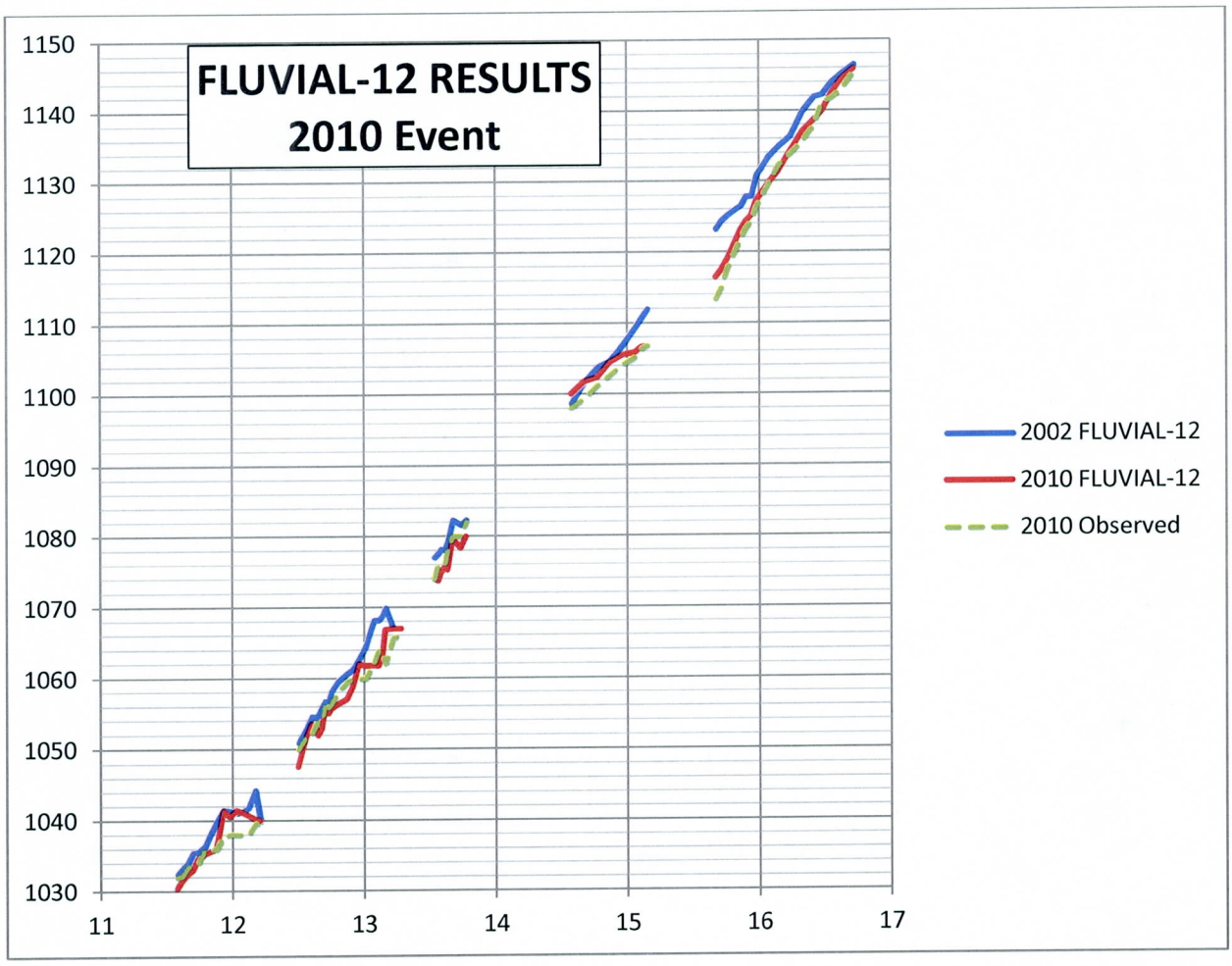

Figure 16. FLUVIAL-12 Results for 2010 Event Only Compared with 2010 Observed Data. Only headcut and tailcut values are shown.

C.4.2.3 Impact of Pit Depth.

None of the model results accurately predicted the deposition that was observed in the pits at the end of the 2010 flood event. The depth of the Pioneer pit used in the modeling was estimated from site visits and aerial photos. Since no measured data was available to verify the pit depths, the depth of the pit was varied to see how this impacted headcut, tailcut and pit deposition in the HEC-RAS model. The impact of an error in pit depth was investigated by reducing the pit depth to 20 ft maximum (rather than the originally estimated 30 ft). The pit was also given a bed slope that approximates the river slope in the vicinity. The changes in the pit configuration can be seen in Figure 17. The pit as originally configured had a horizontal bottom with the upstream depth (at the headwall) being 34 feet and 30 feet at the downstream end). The addition of the bed slope and lowering the elevation of the pit resulted in a 20 ft deep pit along most of the pit with the headwall being 22 ft in height.

This new geometry was then modeled with the Engelund Hansen equation in HEC-RAS to see if the influence of the pit depth was severely impacting the headcut and tailcut calculations. The results of this investigation are shown in Figure 17. It is apparent from Figure 17 that the pit depth is not controlling the headcut depth or length in the HEC-RAS model. This is apparent since a reduction in pit depth of 10 ft (from 34 ft to 22 ft at the upstream end of the pit) had only a minor impact on the headcut elevation and no impact of headcut length. The impact is more pronounced on the filling of the pit by deposition but the model still under predicts the deposition in the pit. Observations of the pit indicate that it is unlikely that the pit depth was less than 20 ft. One cause for the difference in deposition may be that pit deposition is impacted much more by small events than expected.

There is also what appears to be an instability in the model at the outlet of the pit. This is not an instability (as discussed earlier) but is due to a very narrow pit section in that cross section. The high portions of this cross section scour and even though the single point in the bottom of the pit would not scour it is lowered by the same amount calculated for the rest of the cross section. A better representation of the downstream end of the pit would eliminate the deep thalweg scour shown at the end of the pit. Overall the HEC-RAS model using the Engelund Hansen transport equation with the shallower pit depth does a fair job of representing scour in the vicinity of the Pioneer pit but over estimates the scour depth and continues to under estimate pit deposition. The under estimate of pit deposition may be due, in part, to the impact of wash load. Wash load is the portion of the sediment load that is suspended under normal flow conditions but which may deposit under the lower flow regime in the mining pits. The wash load is normally ignored and is more difficult to estimate than the bed load.

These data indicate that for the Engelund Hansen equation the depth of the pit is not the controlling factor for the headcut length for an event on the order of the 20 year event on the Hassayampa River. Based on the data in Figure 14 as well as other observations in associated projects and tasks it is likely that the elevation at the downstream end of the pit may be the controlling factor for the elevation of the headcut leaving the pit.

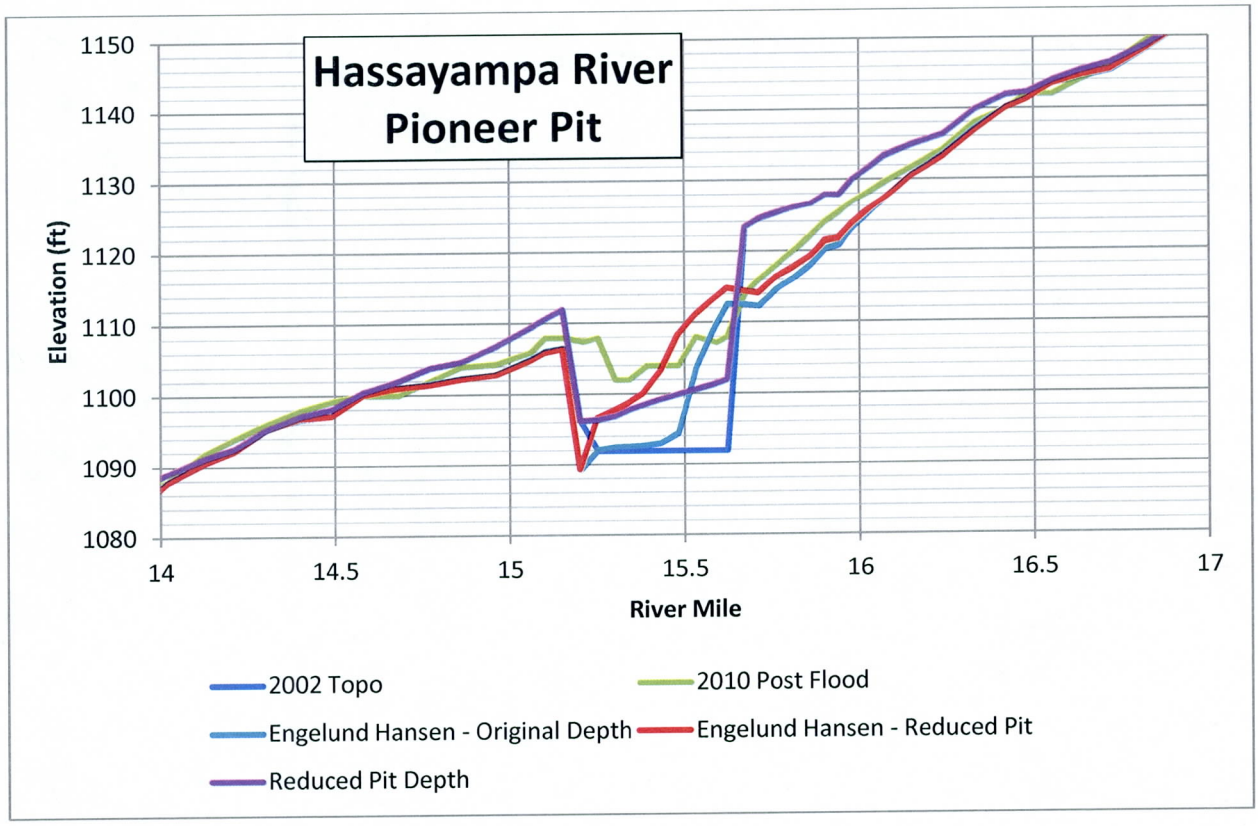

Figure 17. Comparison of HEC-RAS Model Results with Modified Pit Configuration and Original Pit Estimate for Engelund Hansen Transport Equation

C4.2.4 Use of Additional Transport Equations

As a result of the data obtained from the HEC-6T and HEC-RAS models using the Engelund Hansen equation it was determined that the Engelund Hansen equation appeared to be calculating too much scour[1]. As a result it was decided to evaluate additional sediment

[1] The Flood Control District Staff indicated that the maximum channel depth might be used to compute the bed shear stress for Engelund Hansen equation inside HEC-RAS instead of using the hydraulic depth. The HEC-RAS Reference Manual shows an example where the maximum channel depth is used to compute the bed shear stress for Engelund Hansen sediment transport rate. Hydraulic depth was used to compute the bed shear stress in the original Engelund Hansen equation (Frank Engelund and Eggert Hansen, A Monograph on Sediment Transport in

transport equations in the HEC-RAS and HEC-6T models. The additional equations tested included some of the equations commonly used in Maricopa County such as combined Toffaleti and Meyer-Peter & Muller equations, Yang's Equation and several others. The complete list is given in Table 5.

HEC-6T The first equation to be tested in the HEC-6T model was the combination of Toffaleti's Equation and the Meyer-Peter & Muller equation. This is an equation that has been used successfully in other studies in Maricopa County and was expected to do a good job on the river. This combination of equations is not available in the HEC-RAS model and was utilized only in the HEC-6T model. The results of the modeling using this equation are much closer to the observed data as shown in Figure 18. The deposition in the Pioneer pit is again seriously under estimated but otherwise the results generally match the observed data.

Table 5. Sediment Transport Equations used in the Various Models for this Study.

HEC-RAS	HEC-6T	Fluvial-12
Engelund Hansen	Engelund Hansen	Engelund Hansen
Laursen Copeland		
Toffaleti	Toffaleti	
Ackers White	Ackers White	
Wilcock		
Yang	Yang	Yang
Meyer-Peter & Muller	Meyer-Peter & Muller	
	Brownlie	
	Toffaleti+Meyer-Peter & Muller	

Additional equations available in HEC-6T were selected for use based on those available in HEC-RAS and those commonly used in other modeling in Maricopa County. These additional equations included the Yang, Meyer-Peter & Muller, Toffaleti, and Ackers White equations (See Table 5 for complete list). These equations all predicted values much closer to the observed values than the Engelund Hansen equation as can be seen in Figure 19. Individual plots can be seen in Appendix II-A since the individual results are hard to discern in Figure 19.

None of the equations predicted significant deposition in the pits so some problem exists in the modeling. Potential problems include: 1) the pit depth is significantly deeper than the actual pit depth 2) the sediment gradation / transport rate is off 3) small events may be important in this process, or 4) the wash load is an important factor in pit deposition. It may also be that the

---

Alluvial Streams, Teknisk Forlag, Copenhagen, 1967). The Engelund Hansen equation by Vito Vanoni (Sedimentation Engineering, ASCE, 2006) uses channel depth instead of hydraulic depth. FLUVIAL-12 appears to use hydraulic radius which is close to hydraulic depth.

concentration of fines in the flow is increasing the transport capacity of the river for the sand sizes. The deposition into the pits from smaller events may be much more important to final results than expected. This problem may warrant further investigation.

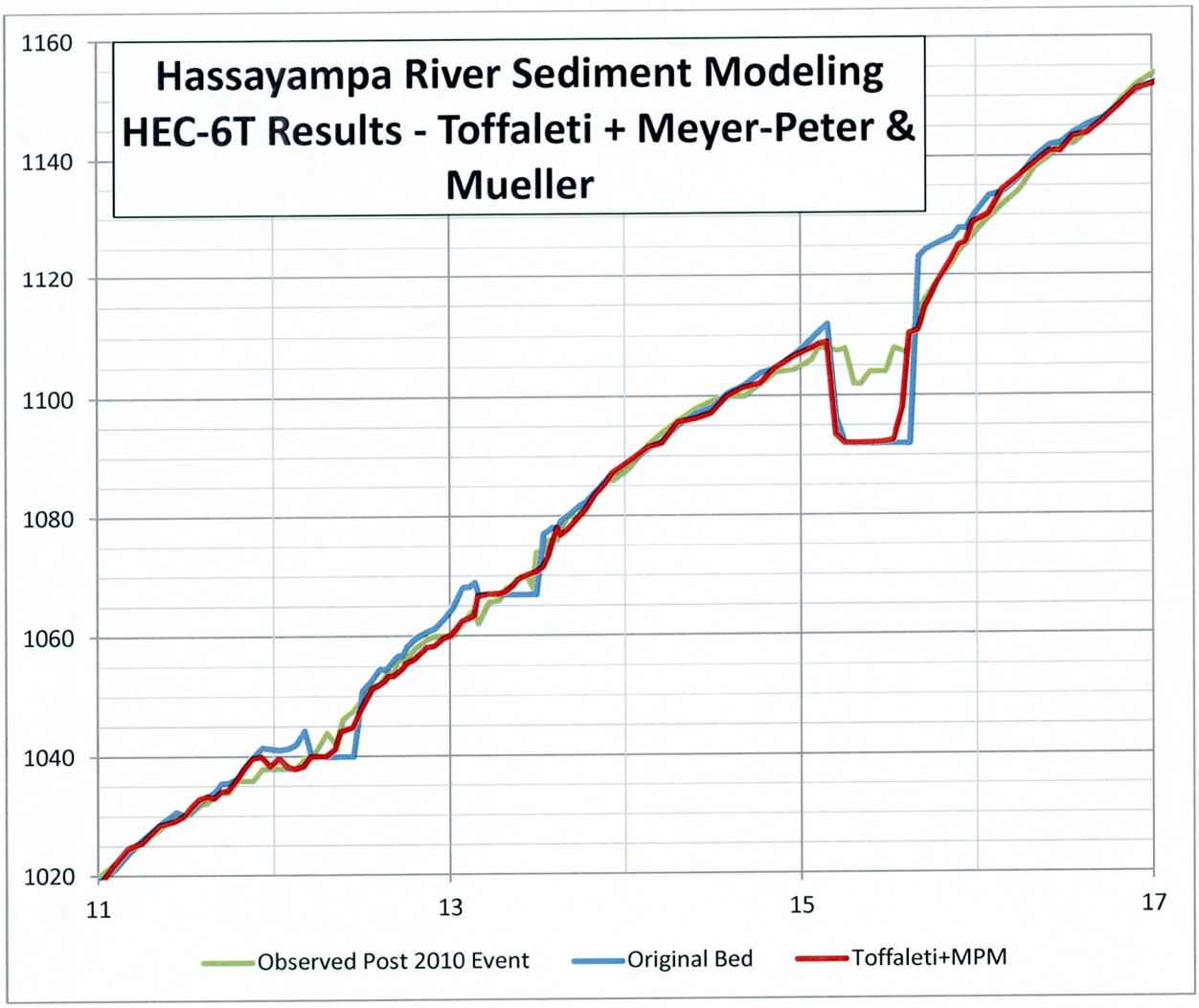

Figure 18. HEC-6T Results using Toffaleti Equation Combined with the Meyer-Peter & Muller Equation for 2010 Event.

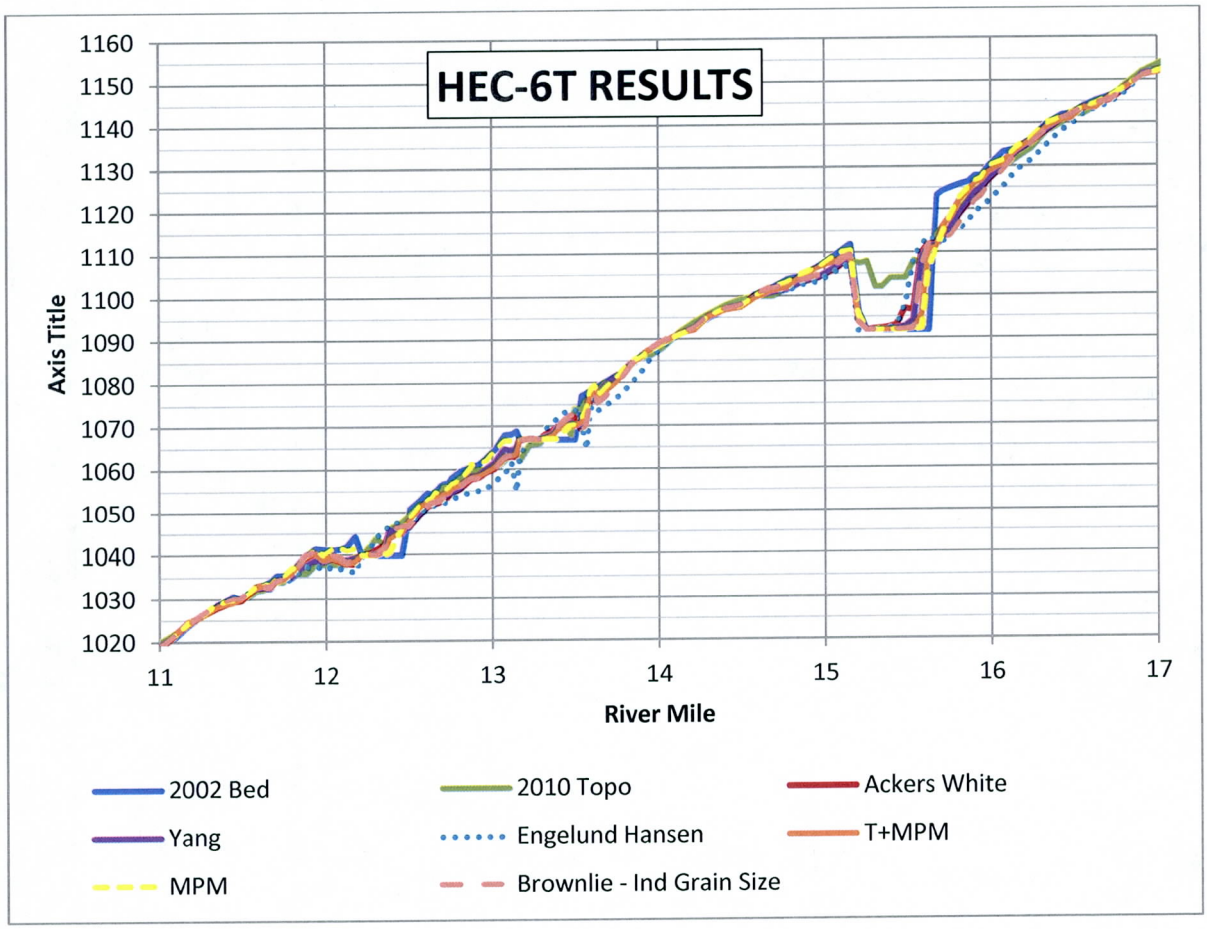

Figure 19. Comparison of Equations used in HEC-6T Modeling Effort.

HEC-RAS The modeling next turned to other equations available in HEC-RAS. Since only a limited number of equations are available and all of them are purportedly applicable to sand and gravel transport all of them were used in the modeling effort.

The various equations available in HEC-RAS predicted the observed erosion with varying degrees of success. The Engelund Hansen equation did the best at modeling the observed scour depths in HEC-RAS but over predicts scour and misses most of the deposition in the Pioneer pit. This latter concern may be due, however; to an error in the estimation of pit depth as discussed earlier since the actual excavation depths were not available. The combined results are plotted in Figure 20. It is apparent that the equations vary widely but none of them gave particularly good results. The individual results are shown in Appendix II-B.

The results indicate that the transport equations used in the HEC-RAS model do not accurately predict the headcut from the Pioneer pit. The Engelund Hansen does the best of the group but over predicts final scour depths. The results for the other pits were very hard to compare visually and since the results were mixed a comparison using the differences from the observed

values was utilized to compare the results. This comparison will be discussed later in this report. From Figure 20 it is apparent that none of the equations accurately predicted the headcut from the Pioneer pit. Most of the equations seriously under predicted the erosion depth and headcut length. Only the Engelund Hansen equation predicted headcut length while over predicting headcut depth.

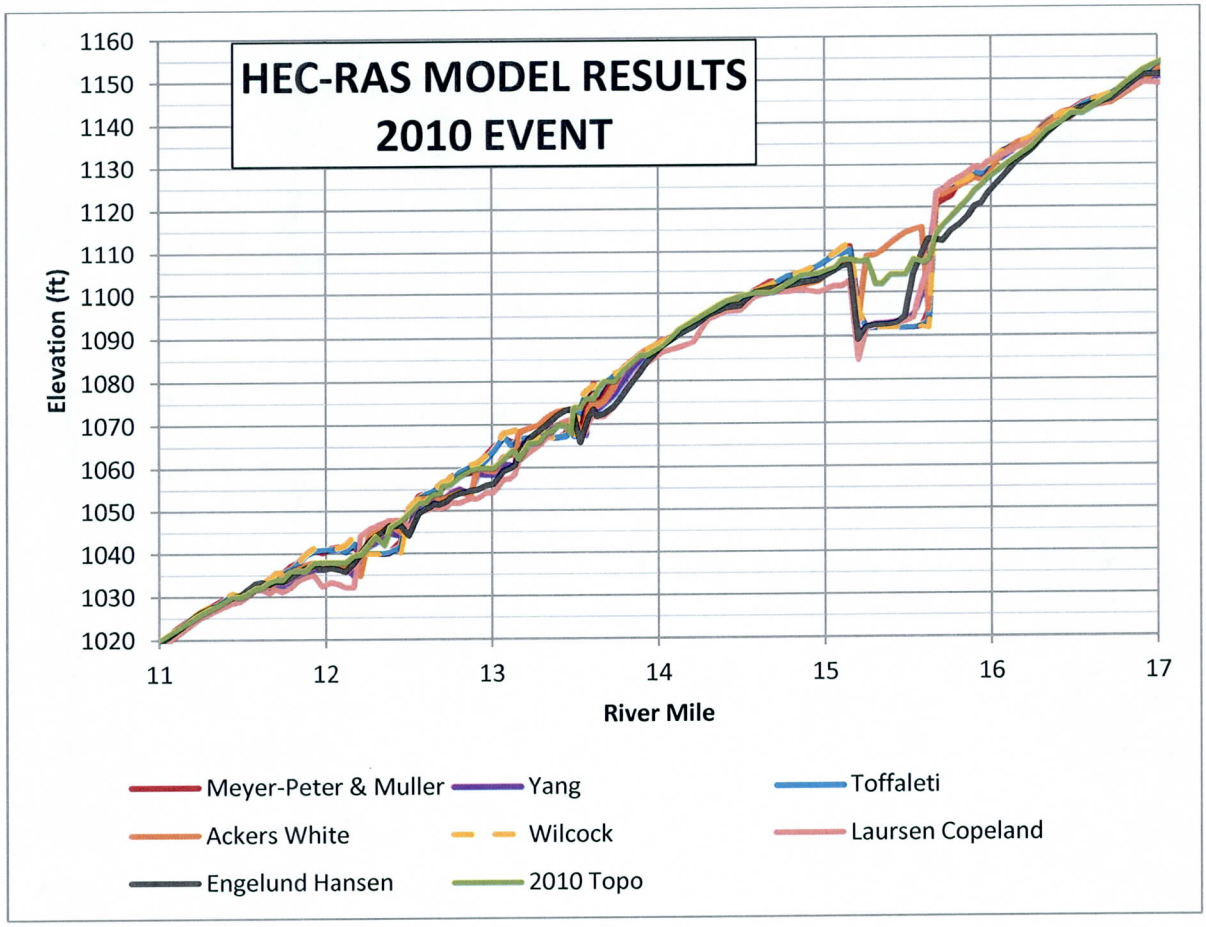

Figure 20. Comparison of HEC-RAS Model Results for the Various Equations Available in HEC-RAS.

Since all of the equations were giving less than encouraging results in HEC-RAS, the various transport equations were reviewed using a spreadsheet developed by PBS&J (2006). The spreadsheet requires to the user to input the D_{50}, temperature, depth of flow, mean flow velocity and energy slope. With this data the spreadsheet calculates a code that helps the user select the most appropriate equation for the river being modeled. The spreadsheet is based on a paper by Williams and Julien (1996). This methodology showed the Engelund Hansen equation as most applicable (rated excellent) followed by the Yang (1973) Equation (good), the Brownlie Equation (good), and the Ackers White Equation (good). This confirmed that at least some of the equations should work if implemented correctly in the HEC-RAS model.

C.4.5 Absolute Performance Index

An absolute performance index (API) was developed by the District to facilitate model comparison. The District requested that this method be applied to the model results to aid in comparison across the various models. This index is based on the following equation:

$$\text{API} = \frac{\sum_{i=1}^{n} |M_i - C_i|}{n}$$

Where:

M_i is the measured headcut / tailcut depth (positive) or deposition (negative values)

C_i is the computed headcut / tailcut depth, and

n is the number of cross sections included

The District used erosion as a positive value and deposition as a negative value for these calculations. The pit areas were excluded from the normal API calculations since the focus was on predicting headcuts and tailcuts rather than on pit filling.

The RMS values for the headcut and tailcut areas were also calculated as a comparison since they are widely used and understood. A second RMS calculation was performed for the HEC-6T model. This calculation, noted as "Total RMS", includes the entire reach including pits, headcuts, tailcuts and areas between pits – i.e. all areas of the model except where the models were adjusting to reach equilibrium at the very upstream end of the model.

The comparison of models required the determination of the length of the headcuts and tailcuts from the various pits. The length of headcuts and tailcuts from the pits was determined by comparing the 2002 topography and the 2010 post event topography. The length of the headcuts and tailcuts were taken to be the distance from the brink of the pit to the first cross section where the difference was less than one foot for two consecutive cross sections. The requirement to use two consecutive cross sections was utilized after it became apparent that, even though the difference may be less than one foot at a particular cross section, there were areas where the upstream cross sections again showed scour of 2-3 feet prior to the difference being consistently less than one foot. The one foot criterion was used to be consistent with current District policy that allows scour of less than one foot to be ignored when computing headcut and tailcut scour. The cross sections showing changes due to mining between the 2002 and 2010 topography and their description are shown in Table 6.

Table 6. Cross Sections Determined to be Scoured due to Headcuts and Tailcuts.

Cross Section Range	Description	Comments
16.72 - 15.67	Pioneer Pit Headcut	
15.62 - 15.2	Pioneer Pit	
15.15 - 14.58	Pioneer Pit Tailcut	
13.63 – 13.53	CEMEX Headcut	
13.49 – 13.32	CEMEX Pit	
13.28 – 12.73	CEMEX Pit Tailcut	Hanson headcut and CEMEX tailcut merged together
12.7 – 12.5	Hanson Pit Headcut	
12.45 – 12.26	Hanson Pit	
12.21 – 11.58	Hanson Pit Tailcut	

The differences between the model results and the observed data for only the cross sections contained in the headcuts and tailcuts from Table 6 were then used to calculate the absolute performance index (API) for the various runs. The API values for the FLUVIAL-12 model using the Engelund Hansen model for only the headcuts and tailcuts are shown in Table 7. The API and other model results for HEC-RAS can be seen in Table 8. None of the equations performed particularly well in HEC-RAS as can be seen when the data is compared with the FLUVIAL-12 results shown in Table 7. The average root mean squared (Ave RMS) values for the HEC-6T and the HEC-RAS model and the total RMS values for the HEC-6T model are given for comparison in Table 9.

The API data were broken out by headcut and tailcut for the pits. These data are shown in Table 7 for the FLUVIAL-12 model and in Table 9 for the HEC-RAS and HEC-6T models. In reviewing the data for the HEC-RAS model it was noted that the Toffaleti equation produced the best overall results with an API of 1.99 ft error for all the pits. Second in the HEC-RAS model was the Meyer-Peter & Muller equation with an API of 2.05 and third was the Ackers White with an API of 2.15 overall. In reviewing the plots of the results at the Pioneer pit it is obvious that while these equations give the best API the modeling of the headcut is not accurate. The HEC-RAS results compare with an API of 1.44 for the FLUVIAL-12 model using the Engelund Hansen equation (Table 7). The FLUVIAL-12 model performs significantly better than the current version of the HEC-RAS model. It should be noted that the Engelund Hansen equation in the HEC-RAS and HEC-6T models predicted headcut length reasonably well although the headcut depth was over predicted.

The shading in Table 9 is used to identify the best (green), second best (yellow) and third best (orange) results from the models both overall and for each headcut /tailcut. This was done to

help the reader quickly pick out the best results and to easily see how the results varied based on the transport equation and model used.

Table 7. API Values for the FLUVIAL-12 Model for 2010 Event.

Model/Transport Equation	Pioneer Pit		CEMEX Pit		Hanson Pit		Average API Values			RMS Values
FLUVIAL-12	HC	TC	HC	TC	HC	TC	HC	TC	Ave	
Engelund Hansen 2010 Only	1.16	1.24	1.32	1.57	1.11	1.50	1.32	1.20	1.44	1.66

The HEC-6T results indicate that all of equations performed much better with all equations producing average API values less than 2.0 with the exception of the Engelund Hansen equation. The Engelund Hansen equation was reported for an active bed scour depth of both 20 and 25 ft to show the impact of a shallow active bed. The deeper active bed (to eliminate warnings about the active bed layer depth) gave an API of 2.45 ft while the 20 ft bed depth resulted in an API of 2.36 in the HEC-6T model.

This data shows that if the active bed is set too shallow the erosion depth can be limited and the model results in error. This is an important consideration in reviewing model results. As a result of this trial the active bed was set to a depth of 25 ft after numerous warnings that the bed depth was not deep enough at the 20 ft value. There were a few cross sections that continued to give a warning and the bed sediment reservoir was deepened slightly to test the results but no significant changes were noted in the results when the bed was lowered to 28 ft in order to eliminate the warnings. A 25 ft bed depth was used for nearly all cross sections in all other modeling with the HEC models. Some of the sections may have retained a bed sediment reservoir depth of 28 ft to eliminate the bed depth warnings.

The data for HEC-6T indicates that the best equation of those tested was the combined Toffaleti and Meyer-Peter & Muller equations resulting in an API of 1.22 with the Yang equation producing a 1.24 API value. The results for the various models are shown in Table 7, Table 8, and Table 9. The FLUVIAL-12 results are shown in Table 7 and the results for the HEC models are in Table 9. The tables will be combined later with the 2005 + 2010 event results for easier comparison but the data show that HEC-6T and FLUVIAL 12 do a good job of accurately predicting future conditions. Recommendations for the use of equations in HEC-RAS for the Hassayampa River are given in Table 8.

Table 8. HEC-RAS Sediment Transport Equations, Results and Recommendations for Sand Bed Rivers.

Transport Equation	Normal Application (See RAS Hydraulic Manual)	Results	Max/Min	Absolute Performance Index (API)	Suggested for Pits in the Hassayampa River?*
Engelund Hansen	Sand Bed River/Streams 0.19 to .93 mm sands used in derivation	OK but Possibly Over Predicts Headcuts – May be due to errors in pit depth estimation	21.2 Deposit-Pioneer Pit 17.5 Scour-CEMEX HC	2.74 Ave 3.62 HC 1.86 TC	Yes but over predicts RMS = 3.0 ft
Laurson Copeland	Silt to Gravel Sized Silts not currently supported in RAS	Over predicted tail cuts and showed deposition in headcut areas	13.0 Deposit-Pioneer Pit 17.0 Scour-CEMEX HC	4.04 Ave 4.25 HC 3.83 TC	No RMS = 4.5 ft
Toffaleti	Sand Bed Rivers – usually considered "large river" function	Minor erosion in headcut areas and minor amounts of deposition and minor tailcuts	1.7 Deposit-Hanson Pit 3.0 Scour-CEMEX TC	1.99 Ave 2.08 HC 1.90 TC	1st Tier RMS = 2.4 ft
Wilcock	Graded Beds with both Sand & Gravel	No significant erosion or deposition	0.5 Deposit – CEMEX Pit 0.9 Erosion – CEMEX HC	2.39 Ave 2.31 HC 2.47 TC	No 2nd Tier RMS = 2.78 ft
Ackers White	Uniform Gradations of Sand to Fine Gravels Applicable to Ripple, Dune and Plane Bed Surfaces	Major deposits in pits (mostly over deposits) but headcut not modeled correctly. Under predicted Pioneer, over predicted CEMEX and OK for Hanson pit. Tailcuts good at Hanson OK at CEMEX, and good at Pioneer. Good results away from pits. Relatively unstable – may be better with fewer cross sections?	25.1 Deposit-Pioneer Pit 15.7 Scour-CEMEX HC	2.05 Ave 2.60 HC 1.49 TC	1st Tier RMS = 2.6 ft
Yang (1973, 1984)	Separate Equations for Sand & Gravel Transport – Sensitive to fall velocity	Under predicted Pioneer and CEMEX pit headcuts. OK Downstream of Hanson Pit and Overpredicted CEMEX to Hanson pit erosion for most part	15.2 Deposit-Pioneer Pit 12.0 Scour-CEMEX HC	2.38 Ave 3.14 HC 1.61 TC	1st Tier RMS = 2.8 ft
Meyer-Peter & Muller (MPM)	Sand and Gravels under plane bed conditions – Most successfully applied over gravel ranges	Under estimated headcuts, tailcuts and deposition by large amounts.	4.6 Deposit-CEMEX Pit 10.6 Scour CEMEX HC	2.15 Ave 2.31 HC 2.00 TC	1st Tier RMS = 2.5 ft

*All 1st Tier equations performed equally bad – RMS > 2.5 ft. Only the Engelund Hansen is suggested for modeling pits with HEC-RAS pending further review.

Table 9. Individual Results for API by pit for Headcuts and Tailcuts for HEC-RAS and HEC-6T.

HEC-RAS - Final API Values

	Pioneer Pit		CEMEX Pit		Hansen Pit		Average API Values				RMS Values[2]	
	HC	TC	HC	TC	HC	TC	Ave	HC	TC	Rank[1]	RMS	Rank
Engelund Hansen	2.21	1.14	5.58	3.37	3.01	1.06	2.73	3.62	1.86		3.00	
Laursen Copeland	3.60	3.36	5.96	4.70	3.19	3.44	4.04	4.25	3.83		4.54	
Wilcock	3.60	2.21	1.93	2.88	1.39	2.32	2.39	2.31	2.47		2.78	
Ackers White	2.92	0.98	3.75	2.46	1.13	1.04	2.05	2.60	1.50	2	2.57	3
Toffaleti	3.55	1.75	1.56	2.05	1.13	1.91	1.99	2.08	1.90	1	2.38	1
Yang	3.16	1.11	4.96	2.47	1.30	1.27	2.38	3.14	1.62		2.79	
Meyer-Peter & Muller	3.16	1.85	2.63	2.26	1.13	1.90	2.16	2.31	2.00	3	2.52	2
Engelund Hansen - Reduced Pioneer Pit Depth*	1.57	1.12	5.73	3.38	3.08	1.05	2.65	3.45	1.85		2.88	

Best Fit
2nd Best
3rd Best

TC = Tailcut
HC = Headcut

[1] Rank and shading are determined from data for all HC and TC calculations (Ave).
[2] RMS values are the average of individual headcut (HC)/tailcut (TC) RMS values
* The pit depth was reduced to 20 ft and sloped to match pre-mining bed slope.

HEC-6T – Final API Values

	Pioneer Pit		CEMEX Pit		Hanson Pit		Average API Values				RMS Values		
	HC	TC	HC	TC	HC	TC	Ave	HC	TC	Rank[1]	RMS[2]	Rank[2]	Total**
Engelund Hansen 20 ft Bed	2.73	0.95	3.51	3.56	2.52	0.90	2.36	2.92	1.81		2.64		2.89
Toffaleti + MPMuller 20 Ft Bed	1.15	0.95	1.61	1.27	0.97	0.95	1.15	1.24	1.06		1.45	1	1.47
Engelund Hansen - 25 ft Bed	2.94	0.92	4.32	3.39	2.26	0.89	2.45	3.18	1.73		2.85		2.45
Toffaleti + MPMuller 25 Ft Bed	1.35	1.04	1.77	1.27	0.78	1.09	1.22	1.30	1.13	1	1.49	1	1.54
Yang Equation (25 ft)	0.91	0.46	1.68	1.69	1.88	0.80	1.24	1.49	0.98	2	1.47	2	1.52
Meyer-Peter & Muller (25 ft)	1.86	1.89	1.62	2.24	0.64	1.96	1.70	1.38	2.03		1.97		2.16
Toffaleti (25 ft)	1.71	1.18	1.50	1.31	0.82	1.54	1.34	1.34	1.34	3	1.64	3	1.75
Ackers White (25 ft)	0.99	0.51	2.19	1.65	2.19	0.93	1.41	1.79	1.03		1.71		1.73
Brownlie - Indiv. Grain Size	1.64	0.80	2.77	1.53	1.84	1.26	1.64	2.08	1.19		1.96		2.01

Best Fit
2nd Best
3rd Best

**Total RMS were calculated using all headcut/tailcut data in one calculation
[1] Rank and shading was determined by the average API value for all conditions
[2] RMS values are the average of individual headcut (HC)/tailcut (TC) RMS values

The comparison of the results for all three models indicates that the HEC-6T and FLUVIAL-12 models had the best results based on the API data. The HEC-6T produced API values of 1.22 for the Toffaleti+Meyer-Peter & Muller, 1.24 for the Yang equation, and 1.34 for the Toffaleti equation followed by the FLUVIAL-12 model (1.44) using the Engelund Hansen equation. The HEC-RAS results were the worst of the one-dimensional models with the best equation (Engelund Hansen) producing and API of 1.99 for the Toffaleti equation, 2.05 for the Ackers White equation and, 2.16 for the Meyer-Peter & Muller equation.

The results of the equations implemented in HEC-RAS and HEC-6T were also compared to see if they were implemented the same in HEC-RAS and in HEC-6T. Plots of the results for the two models are shown in Appendix II-C. The API in this case was calculated based on the difference between the results for the two models for the thalweg at each cross section (i.e. HEC-6T thalweg – HEC-RAS thalweg). These results are shown in Table 10.

The Engelund Hansen results vary by about 0.9 ft between the two models and the Meyer-Peter & Muller equation results by about 0.7 ft. The Toffaleti equation is also similar with an API of about 1.1. The Yang and Laursen Copeland are less similar with API's of 2.2 to 2.6.

Table 10. API for differences between HEC-RAS and HEC-6T Results with 25 ft Bed Sediment Reservoir.

Equation	Average API	Total API	Comments
Engelund Hansen	1.10	0.92	Good match but both over predict scour
Ackers White	1.53	2.24	Major differences in pit deposition and Hanson-CEMEX reach
Toffaleti	0.92	1.05	OK match except Pioneer headcut
Yang	2.13	1.53	OK near Hanson - bad match at CEMEX and Pioneer headcut
Meyer-Peter & Muller	0.87	0.66	Good match except Pioneer headcut
Laursen Copeland	2.60	2.62	Poor match at Hanson pit, between Pioneer & CEMEX and at Pioneer Pit

The results in Table 10 and Appendix II-C indicate that the HEC-RAS and HEC-6T models are not giving the same results for identical situations – especially at the pits. The results in Appendix II-C clearly indicate that with the exception of the Engelund Hansen equation none of the transport equations are providing reasonable results for the headcut above the Pioneer pit. Based on the HEC-6T results matching the observed data it would appear that some problem

may exist in the HEC-RAS scour calculations for all of the sediment transport formulas. This is especially apparent in the sediment transport modeling for headcut and tailcut conditions. This was discussed earlier in regards to the Engelund Hansen transport equation but appears to be more widespread than just the single transport equation. This is unfortunate since the graphical user interface associated with HEC-RAS is so much easier to use and allows better visualization of the input and results. Based on this study with limited data on the Lower Hassayampa River, we found that HEC-RAS with the Engelund Hansen transport equation over-predicts headcut depth on an order of 2 to 4 feet at the immediate upstream brink of the pit but the predicted headcut length is reasonable. HEC-RAS with the Meyer-Peter & Muller, Yang, Ackers White, Wilcock, Toffaleti, and Laurson Copeland equations does not give reasonable results. Further analysis on more data is needed prior to making firm recommendations.

Based on the review of just the 2010 data it appears that the 2010 event was large enough to overcome erosion caused by the 2005 event but perhaps not pit deposition. It may be that pit deposition is impacted much more by the small events than the larger events based on the model results. It may also be that the pit depths were over estimated and the pit configuration may not have been as accurate as desired and the impact of wash load may be important.

C.5 Comparison of the Models for the 2005 Event plus the 2010 Event

Once the data from the 2010 modeling was completed for the Engelund Hansen equation with the various models work focused on modeling the 2005 event followed by the 2010 event. The modeling was performed by starting with the same 2002 topography used for all of the other modeling (100 year and 2010 models). The 2002 topography was used with the 2005 event and the model results from the 2005 event (ending bed configuration) was then used as the basis for the 2010 event.

The intention of this modeling was to determine how to best model the changes in the topography between 2002 and 2010. This modeling was done to confirm initial thoughts and impressions developed in the 2010 event modeling (described above) that the 2010 event was large enough that the 2005 event could be ignored in the calculation of headcuts and tailcuts. The modeling was based on the significant events that occurred in the period from September 2002 to January 2010. The selection of the hydrographs to use in the modeling was described earlier in this document. If the 2010 event was large enough to over shadow the smaller 2005 event then the 2005 and smaller events could be ignored in the modeling effort. This has large implications in future modeling efforts and District requirements for modeling.

All of the models were prepared with the new topography developed for the 2005 and 2010 events as described earlier and used identical hydrographs and input data to the extent possible (i.e. cross sections, sediment characteristics, transport equations, etc.)

The models all used bank stations/erosion limits that were set to match the limits of flow observed in the 2005 event for the 2005 model or those observed in the 2010 event for the 2010 model. The selection of the bank stations/erosion limits is discussed in an earlier section of the report but in summary the bank stations were set to the boundaries of the observed flows for the respective flood being modeled. The flood extents for both the 2005 and 2010 floods are shown in Figure 4.

Manning n values and cross section locations were based on previous work by Fuller. Some additional cross sections were added to the Fuller model layout near the pits to improve model stability and accuracy. As has been stated earlier care was taken to prepare only one set of cross sections and use them as the initial conditions in all three models. The cross section locations were coordinated between R2D, the District, and Howard Chang to insure all of the models used the same data. The pits locations, sizes, and depths were also coordinated between R2D and the District and then supplied to Howard Chang in HEC-RAS format to insure they were put into the models in the same manner.

The pit depths and areas prior to the two larger events were estimated from aerial photography, interviews with District staff and site visits after the flood events. There is some uncertainty in the pit depths as discussed earlier in this document.

A problem in using identical n values was noted in that the FLUVIAL-12 model used a fixed n value of 0.026 for the cross section and the HEC-6T model would not produce the post flood geometry file with the NX cards that were originally used. The channel values were set to 0.025 which was similar to the 0.026 used in FLUVIAL-12 and the most common channel value in the HEC-6T model. The impact of the change in n value was investigated and will be described later in this report.

After the sediment transport models were run for the 2005 event it was necessary to update the resulting bed to represent the pits that existed just prior to the 2010 event. The adding of the 2009 pits to the 2005 results turned out to be a much more involved process than anticipated. The HEC-RAS model using the Engelund Hansen transport equation had erosion depths after the 2005 event that were below the floor of the 2009 pit at the CEMEX and Hanson sites. Thus the pits could not be just directly inserted into the cross sections but each point had to be compared to see if the "new" 2009 pit elevation was higher than the bed of the channel that existed after the 2005 event was modeled. This problem existed at the downstream end of the CEMEX pit and for a couple of cross sections at the Hanson pit. This

area showed little, if any, scour in the aerial photos after the 2005 event and the model scour appears to be excessive. The result was that it was necessary to input the pits by hand into the post 2005 topography. Additionally the remnants of the 2004 pits that were not filled needed to be included in the 2009 geometry. The combination of the excess scour from the 2005 event and the 2004 pit remnants both added to the complication in the inclusion of the 2009 pits.

The original plan was to use only the Engelund Hansen transport equation since it was available in all of the models being compared. It was anticipated that this would allow a direct comparison of the models. In the initial stage of the modeling it became apparent that the Engelund Hansen equation was over predicting erosion – especially in the HEC-RAS and HEC-6T models. It appears to have worked well in the FLUVIAL-12 model based on Dr. Chang's work. The observed 2010 topography was not supplied to Dr. Chang until after modeling was complete and it appeared that little adjustment was required to obtain good results. The HEC-RAS and HEC-6T models were also run with no significant adjustments to obtain qualitative results rather than calibrated or adjusted results. Adjustments to the HEC-6T and HEC-RAS models consisted of time step adjustments or bed sediment reservoir depths and did not involved n values, erosion limits, or other factors normally used in model adjustment. The Engelund Hansen equation also appears to have worked satisfactorily in the 100 year model with no pits as described earlier in this report. No adjustment was made to get the HEC models to better match the data so comparisons with FLUVIAL-12 would be fair for all of the models.

As a result of this project and other attempts to apply the equation it is thought that the Engelund Hansen equation may not be calculating erosion correctly in the HEC-RAS model as well as possibly in the HEC-6T model. Investigations by the District indicate that the calculation may be using a depth that is too large in calculation of the sediment transport. The use of this larger depth in the calculations (i.e. maximum depth as opposed to hydraulic radius or hydraulic depth – see footnote 1) results in over calculation of sediment transport (and thus scour). There are several depths that can be used in determination of transport capacity. These include the hydraulic depth (area/top width), hydraulic radius (area/perimeter), maximum channel depth, and so forth. It appears that HEC-6T and HEC-RAS are using maximum channel depth rather than an averaged depth.

Since the HEC-6T and HEC-RAS models (HEC-models) appeared to not be correctly calculating scour using the Engelund Hansen transport equation (based on the limited data and analysis available) it was determined that other transport functions should be evaluated in the HEC models in addition to the Engelund Hansen equation. Additionally the Engelund Hansen equation is not as commonly used in modeling streams in Maricopa County as some other equations. Additional transport equations were then used in the HEC models to determine if

they could do a better job of modeling the Hassayampa River. Since the 2005+2010 process was complex only one additional equation was tested in the 2005 + 2010 event simulations. This equation was the combination of the Toffaleti plus the Meyer-Peter & Muller equation (TMPM) in HEC-6T. Only the Engelund Hansen transport equation was used in the HEC-RAS model. This decision was based in part on the behavior of the HEC-RAS model in the 2010 event modeling.

C.5.1 Results for the 2005+2010 Simulation

HEC-RAS The HEC-RAS model was run using the Engelund Hansen equation. This model produced scour from the 2005 event that extended below the bed of the 2009 CEMEX pit at the downstream end. This can be seen in Figure 21 just to the left of RM 13 and upstream of the 2004 CEMEX pit (about RM 13.6).

The 2009 pits were then incorporated into the HEC-RAS results from the 2005 event and the model run for the 2010 event. The HEC-RAS results for both events are shown in Figure 21 and Figure 22. It can be seen that the model continued to scour and that by the end of the 2010 event almost the entire area impacted by the mining shows scour depths below the thalweg elevations observed after the 2010 event.

The data from the 2005 + 2010 event model was then directly compared with that obtained using only the 2010 event (discussed earlier in the report). This is shown in Figure 22. It can be seen that in most areas the HEC-RAS model of the 2010 event by itself showed excessive scour. The addition of the 2005 event simply caused additional scour. The two sets of results are very similar with the exception of the area near the CEMEX pit (RM 13.5) where the 2005+2010 event scoured additional materials upstream and downstream of the 2009 pit. This is likely due to the additional pit excavation that was modeled in the 2005 event that was not contained in the 2009 pit data. Both HEC-RAS models continue to over predict scour in this reach.

The HEC-RAS data obtained from the area away from the CEMEX pit (i.e. excluding headcuts, pits, and tailcuts) indicate that the average thalweg difference between the model runs (2010 and 2005+2010) was 0.5 ft. The median value for differences through the pit influenced reach (i.e. headcuts, pits and tailcuts) was 2.2 ft.

In summary the data indicates that the running of the 2010 event in HEC-RAS is sufficient to model both events. The modeling of both events is not necessary (or desirable) for most of the area using the Engelund Hansen equation in the HEC-RAS model. The HEC-RAS produced results that were the least accurate in most of the areas impacted by the sand and gravel mining operations.

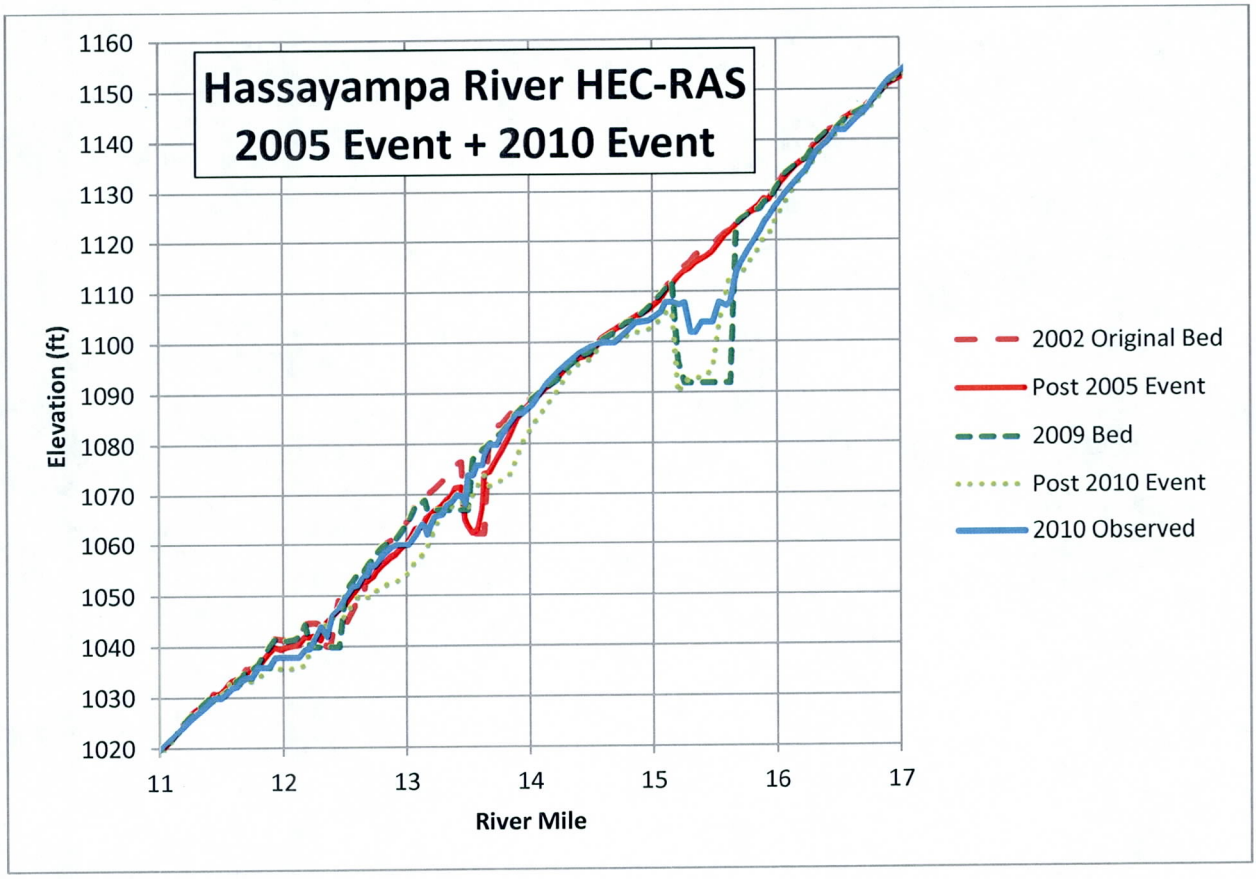

Figure 21. HEC-RAS Model Results Compared with the Observed Thalweg for 2005 Event Followed by 2010 Event (Engelund Hansen Equation).

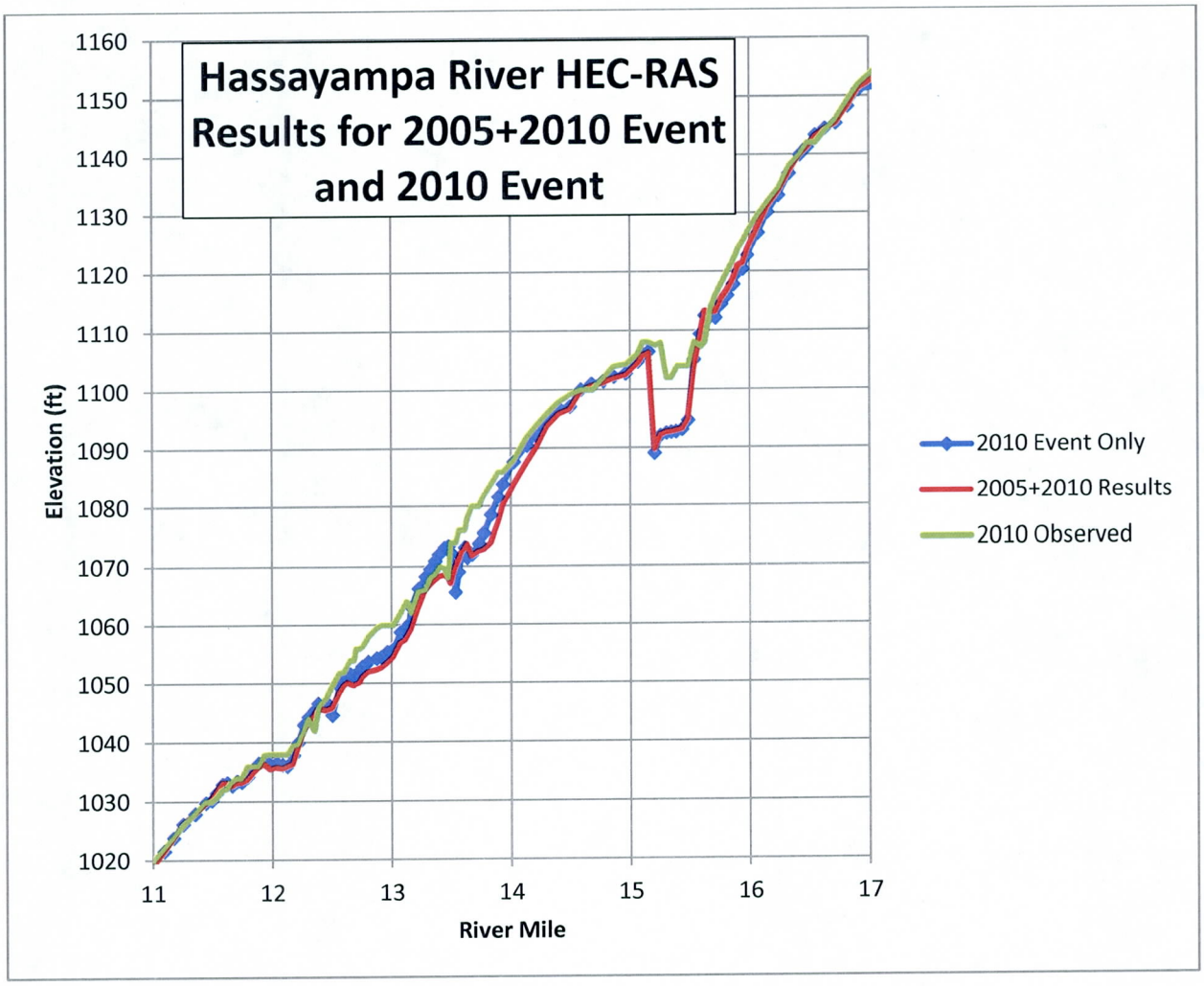

Figure 22. Comparison of Modeling of 2010 Event only with Modeling of 2005 Event followed by 2010 Event for HEC-RAS with Engelund Hansen Equation.

HEC-6T The HEC-6T model was run for the 2005 event with the 2004 pits. This was followed by the 2010 event after adding the 2009 pits to the 2005 output. The HEC-6T model results for the 2005+2010 events showed excess scour in most areas when using the Engelund Hansen transport equation as can be seen in Figure 23. The depth of scour in the downstream portion of the CEMEX pit, for example was below the bed of the 2009 CEMEX pit after only the 2005 event which is not supported by the aerial photos and field observations. The results for the HEC-6T modeling are shown in Figure 23 and Figure 24. The results show more scour than was observed through most of the reach when using the Engelund Hansen equation but good agreement for the Pioneer pit tailcut and the Hanson pit tailcut.

Since the HEC-6T model with the Engelund Hansen transport equation was showing more scour than was observed after the 2010 event in many locations the HEC-6T model was modified to use the combination of the Toffaleti and Meyer-Peter & Muller equations which gave the best

results for the 2010 event modeling. This equation has been used successfully in past HEC-6T simulations on the Hassayampa River as well as numerous other rivers in the County.

After the HEC-6T model was run for the 2005 event the bed was updated to include the 2010 pits. This was again a labor intensive exercise for both the HEC-RAS and HEC-6T models since the 2009 pits had to be compared with the post 2005 bed to insure that the inclusion of the 2009 pits was not filling scour that occurred during the 2005 event or filling pits that existed at the end of 2004 but that were not included in the 2009 pit scenario. The bank stations, erosion limits, and blocked areas also had to be changed to match the 2010 event values. The results of these runs are shown in Table 11.

The HEC-6T model results are shown in Figure 23 and Figure 24. In Figure 23 it can be noted that the results using the Toffaleti + Meyer-Peter & Muller transport equation are very similar to the observed results for the Pioneer Pit (RM 15.5) for both the headcut and tailcut. The results for the CEMEX and Hanson pits are more complex and are shown in more detail in Figure 24.

The results through the CEMEX and Hanson pit complex indicate that the modeling of both events with either the Engelund Hansen equation or Toffaleti + Meyer-Peter & Muller equations is unnecessary for most of the reach since the use of both events adds scour to results that are mostly more accurate after modeling only the 2010 event.

The lack of deposits in the 2009 CEMEX pit (RM 13.5) may account for some of the excess scour upstream of the pit although the scour at the pit outlet is close to the observed values. The 2004 pit did not fill during modeling although this filling was observed in the aerial photos. The results through the Hanson pit (RM 12) are closer to the observed results. The results in the Hanson/CEMEX reach are, for the most part, slight over estimates of the scour in the reach when using the Toffaleti + Meyer-Peter & Muller equation. Except for the CEMEX headcut the model results are good representations of the 2010 observed data. Based on the data it appears that the over estimate of scour in the CEMEX pit is due to the error in deposition in the 2004 CEMEX pit. This results in excessive headcutting above the remnant of the 2004 pit and almost no deposition in the 2009 pit. The 2004 pit was observed to fill during the small events and this may again indicate that the small events are important in the pit filling process and the calculation of accurate headcut / tailcut impacts for shallow existing pits. This limitation can be overcome by using current topography for modeling future excavations.

It should be noted that the CEMEX pit was long and mining had removed material to a depth of about 10 feet below the bed of the river in this reach. The 2004 CEMEX pit was located upstream from the 2010 pit and on the west side of the river while the 2010 pit was on the east side of the river. The combination of the 2004 CEMEX pit and the 2009 pit immediately

downstream likely accounted for the additional scour shown in the 2005 + 2010 combined event model. The lack of deposition in the 2010 model may be due to an underestimate of the impact on the 2004 pit on the resulting bed in the region of the CEMEX pit. Also there was a long narrow portion of the 2004 CEMEX pit downstream of the main pit that was not captured in the modeling. This long narrow portion appeared to be a drain constructed to keep the main pit dry in the event of small events.

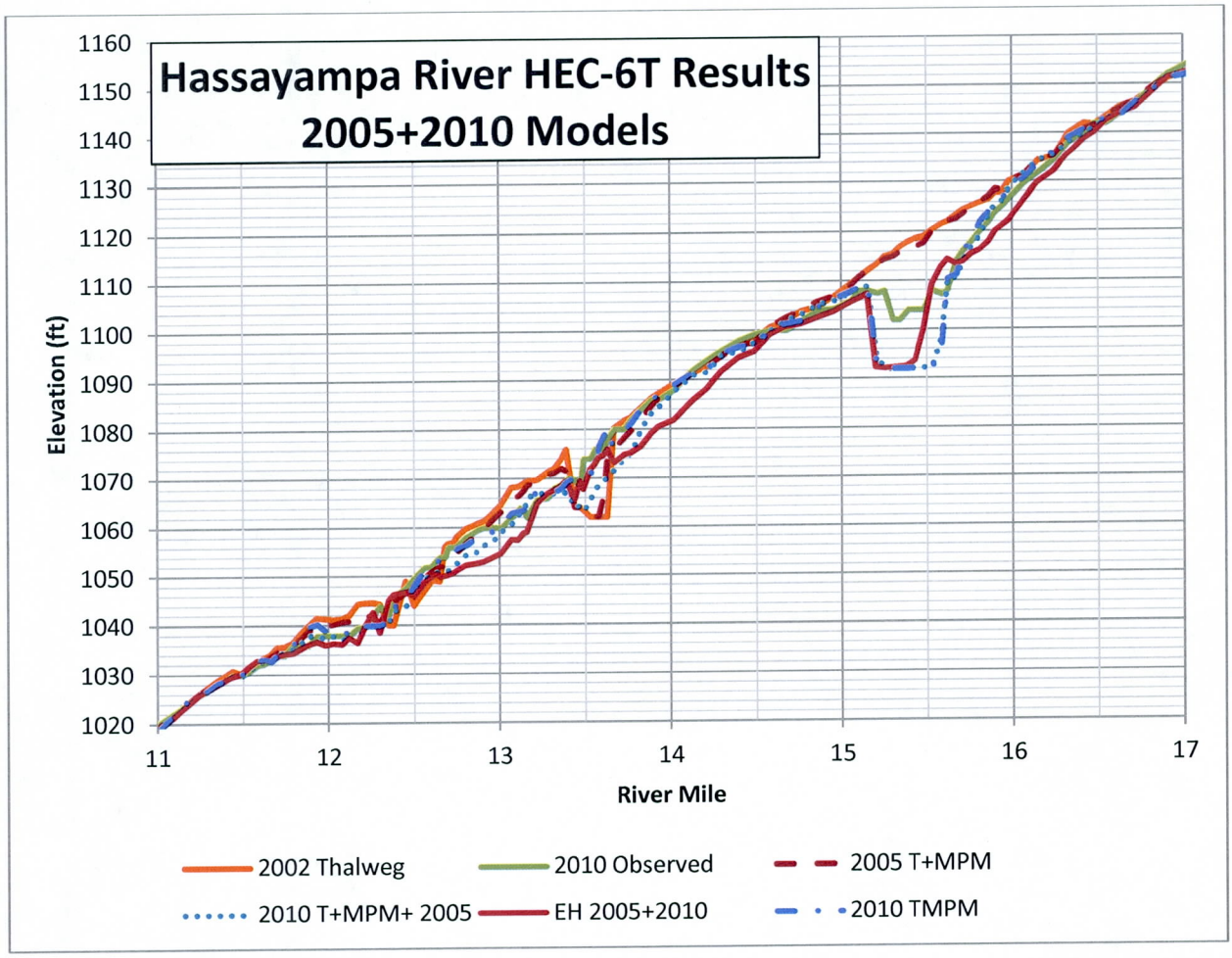

Figure 23. HEC-6T Model Results for the Mined Reach showing Results for 2005+2010 Model Results Compared with Observed Results.

Modification of N Values. It was desired to compare the impact of the lower n values used in some areas of the models for the 2005+2010 HEC-6T modeling (0.025) as well as to see the impacts of Chang's modification of the n values (using a constant 0.026 value). In order to test the impact of the observation that some channel n values appeared to be much lower than those used in some parts of the Fuller model a run was made using the 2005 event with n

values that were set to something closer to the estimated grain roughness (0.025) rather than the higher values used by Fuller(0.025 to 0.050). The majority of the cross sections developed by Fuller were 0.025 to 0.026 with numerous cross sections being in the 0.032 range.

The Fuller data (as supplied in the HEC-RAS format) was converted by Howard Chang to a single value for the FLUVIAL-12 model. He converted the multiple values in the Fuller model to 0.026 for use in FLUVIAL-12. This is not a large difference from the value tested in this exercise and the FLUVIAL-12 results should be comparable to the HEC models.

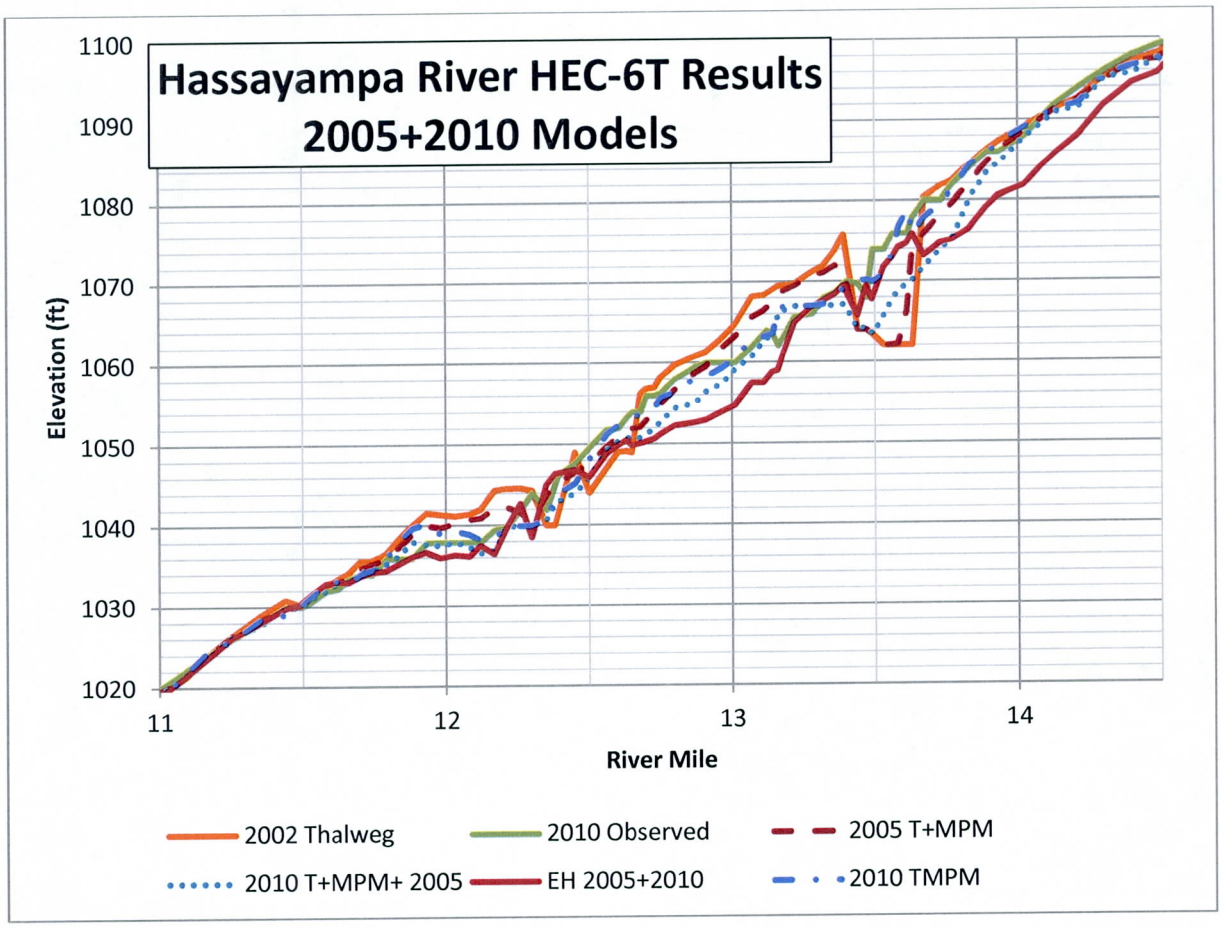

Figure 24. HEC-6T Model Results for the Hanson and CEMEX Pit Reach Compared with Observed Values (T+MPM).

The results produced when the Manning's n value was changed to a constant 0.025 for the entire model are shown in Figure 25. This indicates that the results are not extremely sensitive to the Manning's n value – at least for the 2005 event. The results show small changes in erosion between models using the two n values.

FLUVIAL-12. The results of the FLUVIAL-12 model also produced good results for the 2005+2010 events as shown in Figure 26. It can be seen that the results at the Pioneer pit

reproduce the observed data very well but there are some errors at the CEMEX and Hanson pits. The errors are not extreme and overall the model reproduces the observed data reasonably well. There continues to be problems with deposition in the pits as with the HEC-RAS and HEC-6T models but the pit values were not readily accessible in the Chang data and are not shown in Figure 26.

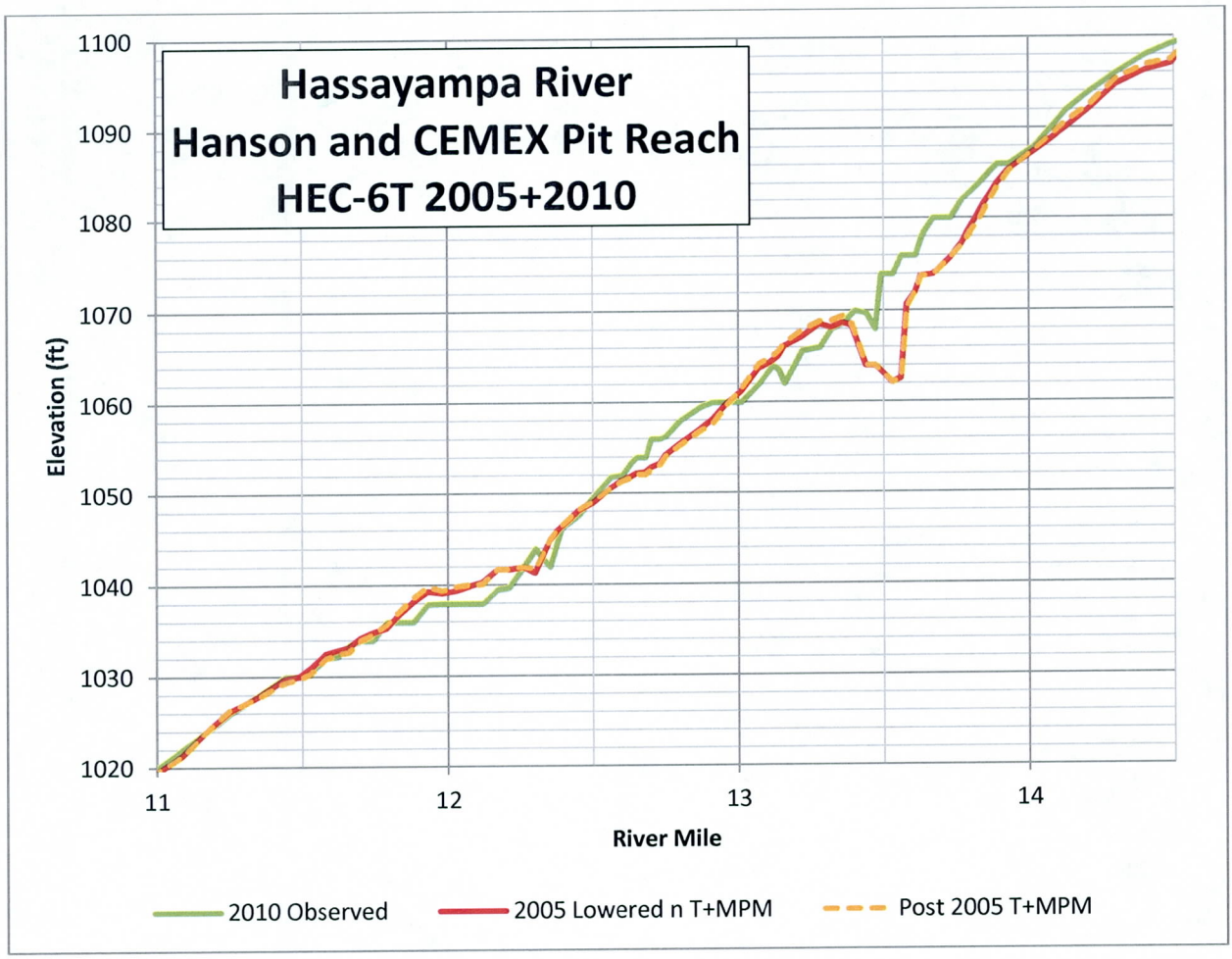

Figure 25. Comparison of 2005 Model Results for Fuller (Post 2005 T+MPM) and Lowered n Values (2005 Lowered n T+MPM) for Hanson and CEMEX Reach.

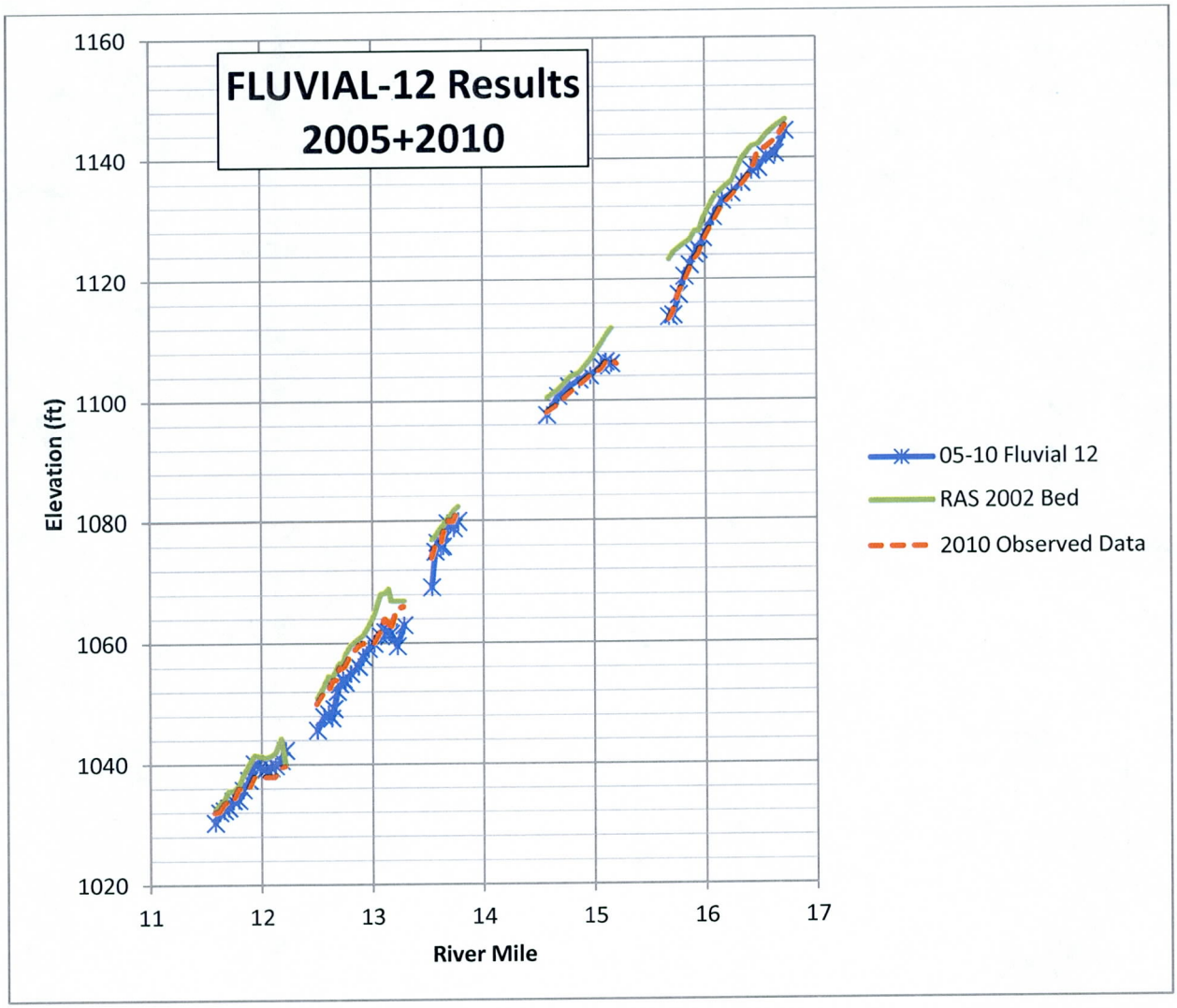

Figure 26. FLUVIAL-12 Results for the 2005+2010 Event Model. Results are shown only for pit Impacted reaches.

Performance Index Results. The results were evaluated using the API and RMS values as was done for the 2010 event model comparisons. The results of the 2005+2010 models are shown in Table 11. The results for the HEC-6T 2005 + 2010 event model using the Toffaleti + Meyer-Peter & Muller equations are better than the HEC-RAS results using the Engelund Hansen equation but still not great. The best results are obtained by the HEC-6T model when only the 2010 event was modeled. The FLUVIAL-12 model does show an improvement when the 2005 event was modeled prior to the 2010 event for the Pioneer pit but the improvement is small and is not worth the effort to model the additional event.

Table 11. Comparison of API and RMS values for FLUVIAL-12, HEC-RAS and HEC-6T results

Model/Transport Equation	Pioneer Pit		CEMEX Pit		Hanson Pit		Average API Values				RMS Values		
HEC-RAS	HC	TC	HC	TC	HC	TC	Ave	HC	TC	Rank[1]	RMS	Rank[2]	Total**
Engelund Hansen 2010 Only	2.21	1.14	5.58	3.37	3.01	1.06	2.73	3.62	1.86	5	3.30	5	3.94
Engelund Hansen 2005+2010	1.76	1.42	5.54	5.04	3.93	1.52	3.75	3.74	2.66		3.48		3.69
HEC-6T													
Engelund Hansen 2010 Only	2.94	0.92	4.32	3.39	2.26	0.89	2.45	3.18	1.73	4	2.85	4	2.45
Engelund Hansen 2005+2010	2.37	0.84	3.62*	4.77	3.70	1.01	2.72	3.23	2.21		2.59		3.19
T-MPM- 2010 Only	1.35	1.04	1.77	1.27	.78	1.09	1.22	1.30	1.13	1	1.49	1	1.54
Toffaleti + MPM 2005+2010	1.29	1.20	7.23*	2.38	3.08	0.71	2.65	3.86	1.43	3	2.86		4.34
FLUVIAL-12***													
Engelund Hansen 2010 Only	1.16	1.24	1.32	1.57	1.11	1.50	1.32	1.20	1.44	3	1.66	2	
Engelund Hansen 2005+2010	0.86	0.69	1.44	2.10	3.76	1.33	1.7	2.02	1.37	2	2.05	3	

* These numbers are impacted by the 2004 pit that did not fill during the 2005 event.

** Included pits, headcuts, tailcuts, and areas between pits but excluded upstream end of model where sediment load was coming into balance.

*** These numbers are different from those presented in the Chang report. They were recalculated from Chang's data based on the same cross sections used in the HEC-RAS and HEC-6T calculations.

[1] Based on Average API Value for both headcuts and tailcuts

[2] Based on RMS values for headcuts/tailcuts not on Total values

The over estimation of scour for both HEC-RAS and HEC-6T models using the Engelund Hansen equation could be due to the use of maximum channel depth instead of hydraulic depth in the Engelund Hansen equation as discussed earlier. The problem with Engelund Hansen equation became apparent when comparing results with the FLUVIAL-12 models results that use the hydraulic radius which is close to hydraulic depth. If the equations are applied with the same variables the results should be relatively similar for the same conditions even if applied in different models.

The API results show that the HEC-6T model produced more accurate results under both scenarios (2010 and 2005+2010) and with both equations than any scenario using the HEC-RAS model. The 2010 only HEC-6T models both produced more accurate results than the 2005+2010 models. A second comparison using the RMS values still shows the HEC-6T model outperforming the HEC-RAS model.

Based on the results from Table 11 for headcut estimation over the entire reach impacted by pits, the HEC-6T model (T+MPM) provided the best results with FLUVIAL-12 providing the 2nd and 3rd best results (2005+2010 2nd and 2010 only 3rd), HEC-6T Engelund Hansen 2010 only 4th and HEC-RAS being 5th. When considering results for only the Pioneer pit headcut the FLUVIAL-12 model performs best (Engelund Hansen 2005+2010), second best is the HEC-6T model (T+MPM 2005+2010), third best is FLUVIAL-12 Engelund Hansen (2010 only), fourth is HEC-RAS Engelund Hansen (2005+2010) and fifth is HEC-RAS Engelund Hansen (2010 only). The API differences between using the 2005 event followed by the 2010 event and the results from the models using only the 2010 events are small. This indicates that the headcutting and tailcutting at pits can be estimated using a model with a single large event rather than a model with a number of various sized events.

C.6 Two-dimensional Models

Several two-dimensional models were also evaluated as a part of the exercise. The District staff evaluated FLO-2D and RiverFLO-2D and R2D began evaluation of the RMA-2/SED2D model. The RMA-2/SED2D modeling was stopped during the SED2D effort after the RMA-2 modeling was nearly completed due to the complexity of the effort and the results of the District's two-dimensional modeling. The two-dimensional models evaluated by the District did not produce acceptable results and are not recommended for use at this time. The results are summarized below and the District's reports are included in Appendices.

C.6.1 FLO-2D Sediment Model Results

The FLO-2D results showed reasonable resemblance to the areas that were scoured in the 2010 event however the model scoured to the limit set as the maximum scour depth. When the

maximum scour depth was lowered the model scoured to the new limit. When the limit was set to infinity the model did not complete calculations and modeling was terminated after 862 hours of computer time. The model did not produce acceptable results. The District's report is contained in Appendix III

C.6.2 RiverFLO-2D Model Results

The hydraulic portion of the model ran and gave reasonable results. The sediment portion of the model never finished even though the model was run for dozens of hours. The sediment transport portion of the model caused instabilities in the hydraulic portion of the model. The model was not useable and did not produce any final results for the 2010 event. The 2005 event followed by the 2010 event was not attempted. The model was not useable for modeling of the erosion processes near a mining pit. The District's report on the model performance is contained in Appendix IV.

C.6.3 RMA-2/SED2D Results

The RMA-2 model was able to model all of the flows associated with the 2010 flood event. SED2D was run for only one of the flow events before modeling was terminated due to time and budget constraints. The complexity of running the model was high with the RMA-2 model needing to be run separately for each of the flow steps and then the SED2D model for that step. The new bed would then need to be used as input for the next time step. Normally this is modeled in dynamic mode but given the bed changes and the high velocities it is unlikely that the model would hold together for a dynamic run. This was the case for the attempts that were made prior to the 2D modeling being abandoned. It should be noted that the SED2D model has been dropped from current versions of SMS the user-interface for RMA-2. It may be useable but would be time consuming and complex to run.

C.6.4 2D Modeling Recommendations

There are a number of newer and currently supported two-dimensional sediment transport models. It is recommended that at least one, if not two current models be evaluated to see if they can accurately model the processes near sand and gravel pits. One of these is the Corps' ADH model which has been shown to be much more robust than the SED2D model and the other is USBR's SRH-2D model. These models are undergoing current, ongoing development and are available free of charge for use. The cost involved would be to obtain the current user interface. Both of the models are supported by the SMS interface.

D. CONCLUSIONS

The modeling of headcuts by the use of one-dimensional sediment transport appears to give reasonable results if the correct models and transport equations are used. The FLUVIAL-12 model gives excellent results when correctly applied as does the HEC-6T model. The HEC-RAS model has the best user interface with the ability to more easily view the inputs and results. The HEC-RAS model as currently available does not appear to be accurately modeling the transport processes associated with headcuts and tailcuts with any equation based on the limited analysis and data from this study. The majority of the equations under estimate scour on the Hassayampa while the Engelund Hansen transport equation over estimates scour for the most part. The Engelund Hansen equation over predicts sediment transport in both HEC-6T and in HEC-RAS but does an excellent job in FLUVIAL-12.

Based on this limited review the HEC-RAS model is currently recommended for the modeling of sand and gravel pits on the Hassayampa River only if the Engelund Hansen transport equation is selected.

HEC-6T is recommended for use with several equations. The equations recommended for use on the Hassayampa River with the HEC-6T Model are 1) the combined Toffaleti and Meyer-Peter & Muller Equation, 2) the Yang Equation, 3) the Toffaleti equation, and the 4) Ackers White Equation. The combined Toffaleti and Meyer-Peter & Muller equation produced the best results in the HEC-6T model.

FLUVIAL-12 is recommended for use with the Engelund Hansen equation based on the results of this study. Other equations may be useful in the FLUVIAL-12 model but the FLUVIAL-12 model could not be calibrated successfully using the Yang equation (or at least the results were not as accurate as the Engelund Hansen equation) (Chang 2011). The API values were not calculated for the Yang equation based on Chang's recommendation that the equation not be used for the Hassayampa River. Additional transport equations were not attempted in the FLUVIAL-12 modeling.

The series of questions raised at the beginning of this study can now be answered based on the results obtained:

1. *What are the differences in the various models?*

   The 1D models are very similar but do have some significant differences. The main difference is the FLUVIAL-12 calculation of active channel width as the flow rates change. This allows more flexibility in the model calculation of erosion widths. The

downside is the inability to limit where the model erodes (as can be done in HEC-6T and HEC-RAS with bank stations). The FLUVIAL-12 model automatically uses the minimum cross section location as the flow area. This complicated modeling in areas with off-channel pits that may not flood during the event being modeled. The use of ineffective flow areas in HEC-RAS may not prevent scour from occurring in the ineffective areas if they are lower than the main channel.

2. *Can numerical models (i.e. HEC-RAS, HEC-6/6T, FLUVIAL-12, etc) adequately model headcutting and tailcutting such that other methods can be neglected in determination of headcut and tailcut lengths?*

   Numerical Models have been shown to be capable of adequately modeling headcuts and tailcuts associated with sand and gravel mining on the Lower Hassayampa River. The models do not need to be used in conjunction with empirical methods.

3. *Is one model better than another for the modeling of sediment transport associated with sand and gravel pits on the Hassayampa River?*

   The HEC-6T and FLUVIAL-12 models did the best job of predicting headcutting and tailcutting from sand and gravel mining on the river. HEC-RAS using the Engelund Hansen transport equation predicted headcut lengths adequately but depths were overestimated. For other transport equations the erosion depths and headcut lengths were significantly under estimated.

4. *Is there a sediment transport equation (or several) that can be recommended for use on the Hassayampa River with the various models?*

   For the FLUVIAL-12 model the Engelund Hansen transport equation is recommended and for the HEC-6T model the combined Toffaleti and Meyer-Peter and Muller equation do the best job. Other equations that give good results in the HEC-6T model are Yang, Toffaleti, and Ackers White. For the HEC-RAS model the Engelund Hansen gives the best results although the results are not as accurate as the HEC-6T and the FLUVIAL-12 results. The other transport equations in the HEC-RAS model cannot be recommended based on the limited results of this study.

5. *Are there 2D models that can be used for sedimentation on the Hassayampa River and do they give better results than the 1D models?*

The two-dimensional models tested either did not perform acceptably (FLO-2D and RiverFLO-2D) or were so complex that modeling was not completed (RMA-2/SED2D).

6. *Can the smaller events be ignored in the modeling and not impact the resulting headcut/tailcut lengths or depths?*

   The smaller events can be ignored for scour but possibly not for predicting pit deposition. If larger events are used the headcut and tailcut length and depth can be predicted using a single event. If pit deposition is important the smaller events appear to contribute significant amounts of sediment. Hydrographs were only available downstream from the pits after some attenuation had already occurred in the pits which also may have been a factor in predicting pit deposition.

In summary the models provided good estimates of headcut distance if applied correctly and did not appear to be overly sensitive to pit depth errors. The use of multiple events does not appear necessary to obtain good results if large events are used in the modeling. Smaller events may result in more serious headcut depths nearer the pit but maximum headcut lengths should be obtained from the larger events (i.e. 50 to 100 year events). It does not appear to be necessary to combine empirical methods such as the ADOT method with the numerical modeling to obtain good headcut results. The ADOT and other methods are likely good to estimate maximum headcut depths for pits that drown out but not for estimating the maximum headcut/tailcut lengths for large pits that do not drown out during high flows. From the modeling and other tasks associated with this study it appears that the final elevation of the downstream pit brink may be significant in the calculation of final headcut depth and will impact headcut length.

D.1 Recommendations

It is recommended that the FLUVIAL-12 and HEC-6T models be used for estimating headcuts and tailcuts for pits on the Hassayampa River. The models should be applied using the acceptable sediment transport equations described earlier in the report – namely the Engelund Hansen equation for FLUVIAL-12 and for HEC-6T the combined Toffaleti + Meyer-Peter & Muller equation or (in order of preference) the Yang, Toffaleti or Ackers White equations. HEC-RAS is recommended to be used with caution pending further analysis and only with the Engelund Hansen equation for the modeling of pit impacts on the Hassayampa River.

D.2 Areas for Future Study

The results of this research indicate that the depth of the upstream headcut may be dependent on the elevation of the downstream pit brink for pits that do not drown out when filled with

water. This would be an important consideration in determination of the acceptable pit size on the Hassayampa River. This warrants further investigation. Modeling could also be performed to investigate the impact of pit size and shape on the river.

The impact of small events on pit deposition also warrants further investigation. From the modeling performed in this study it is apparent that either the pit deposition was not captured correctly or the depth of the pits was greatly over estimated. Part of this under estimate may be due to the influence of the wash load contained in the river flows that was not modeled.

E. References

Ackers, P., and W. R. White. (1973). "Sediment transport: new approach and analysis," Journal of the Hydraulics Division, American Society of Engineers, Vol 99, No HY11, pp 2041-2060.

Cella Bar, (1988). "Hydrologic Analysis of the Hassayampa River in Maricopa County, Arizona" Cella Barr and Assoc. for Federal Emergency Management Agency-FEMA, ID # CBA 04856-07-74, FCD Library Call Number A343.703S

Chang, Howard (2009). FLUVIAL-12 Modeling of the Sand Mining Impacts for Lower Hassayampa River, Chang Consultants, Rancho Santa Fe, CA (May 2009)

Chang, Howard (2011). "Mining Pit Headcut/Tailcut Modeling in Lower Hassayampa River for Major Recent Flooding Events, Chang Consultants, Rancho Santa Fe, CA (June 2011)

Engelund, Frank, and Eggert Hansen. (1967). "A Monograph on Sediment Transport in Alluvial Streams," Teknisk Forlag, Copenhagen, Denmark, pp. 1-62.

Engelund, F., and Hansen, E. (1967). A monograph on sediment transport in alluvial streams, Teknish Forlag, Technical Press, Copenhagen, Denmark.

Meyer-Peter, E., and R. Muller. (1948). "Formulas for bed-load transport," International Association of Hydraulic Research, 2nd Meeting, Stockholm, Sweden.

(R2D) River Research & Design, Inc. (2011). "Review of Headcut and Tailcut Methodologies", Funded by The Flood Control District of Maricopa County.

PBS&J (2006). PBS&J's Sediment Selection Spreadsheet, Version 1.1, Developed by David T. Williams, Compiled by Harshal Desai. Based on methods presented in Williams & Julien, 1996.

Thomas, William A. (1982). "Mathematical modeling of sediment movement," Chapter 18 of Gravel Bed Rivers, Edited by R.D. Hey, J.C. Bathurst, and C.R. Thorn, John Wiley & Sons, Ltd. Mr.

Thomas suggested that the 1993 HEC-6 manual discussion could also be used for a discussion of armor layers and active beds or a dissertation by Dr. Ron Copeland from the University of Iowa in 1993.

Toffaleti, F. B. (1968) (Nov). "A Procedure for Computation of Total River Sand Discharge and

Detailed Distribution, Bed to Surface," Committee on Channel Stabilization, U.S. Army Corps of Engineers.

Williams, David T. and Julien, Pierre Y. (1996). "Selection of Sediment Transport Relations: Part III, Numerical Ranking of Sediment Transport Relations," Proceedings, ASCE North American Water and Environmental Congress, Anaheim, California, June 22-28, 1996.

Yang, C. T. (1973) (Oct). "Incipient motion and sediment transport," Journal of the Hydraulics Division, American Society of Civil Engineers, Vol 99, No HY10, pp 1679-1704.

APPENDIX I

DETERMINATION OF INPUT PARAMENTERS AND VARIABLES FOR SEDIMENT TRANSPORT MODELING

OF THE 2005-2010 MINING OPERATIONS AND IMPACTS

Flood Control District
of Maricopa County

MEMORANDUM

Date: November 22, 2010

To: Theresa Pinto, CFM, Project Manager, Planning Branch, Planning and Project Management Division

From: Richard Waskowsky, Hydrologist, Engineering Application Development and River Mechanics Branch, Engineering Division

CC: Bing Zhao, PhD, PE, Engineering Application Development and River Mechanics Branch Manager, Engineering Division

Subject: Data Collection and Modeling Approach for Selected River Mechanics Tasks of Phase II of the Lower Hassayampa Watercourse Master Plan (WCMP)

This memorandum was prepared to document the data collection and the modeling approach for selected river mechanics tasks of Phase II of the Lower Hassayampa WCMP. There are two selected tasks. The first task is to compare three different sediment transport software packages (HEC-6T, Fluvial-12 and HEC-RAS) for the entire reach of the Lower Hassayampa River under the same conditions (i.e., same topography, hydrology, and other required parameters). The models developed using the three software packages should be based on the topographic data from the HEC-6 model of Phase I of the Lower Hassayampa WCMP. The sediment transport function should be the same for the three models. River Research & Design, Inc. (R2D) will convert the existing HEC-6 model to HEC-6T and HEC-RAS models. The Fluvial-12 model was already developed by Chang Consultants. If any changes are needed for the Fluvial-12 model, FCDMC will perform the changes.

The second task is to study the headcut/tailcut due to sand and gravel mines, in particular the Pioneer mine, for the major flows from 2002 to 2010 using HEC-6T, Fluvial-12, HEC-RAS, RMA-2/SED2D, RiverFLO-2D, and FLO-2D. This task is divided into two sub-tasks. The sub-tasks are 1) model the January 2010 event only and 2) model either the two or three largest events from 2002 to 2010, depending on the results from the January 2010 event. To model the topographic change from 2002 to 2010, it is very important to understand the mining history (i.e., the mining depth and surface area) between 2002 and 2010. Therefore, the depths and surface area were also estimated. R2D will develop the HEC-6T, HEC-RAS and RMA-2/SED2D models, while Chang Consultants will develop the Fluvial-12 model. FCDMC will develop both the RiverFLO-2D and FLO-2D models.

The discussion below documents the collection and source of the input data for the sediment transport models.

2801 West Durango Street Phoenix, Arizona 85009 Phone: 602-506-1501 Fax: 602-506-4601

1) The initial topography for all the models (for both tasks) is from Phase 1 of the Lower Hassayampa WCMP (WEST, 2006). The 2D models use the original Digital Terrain Model (DTM), while HEC-6T, Fluvial-12 and HEC-RAS use the cross-sections from the Phase 1 HEC-RAS and HEC-6 models (originally developed using the same DTM). As a note, the Phase 1 DTM was developed from multiple sources; however, the majority of the area was flown in 2002 or 2004. Older topography was only used for a very small portion of the river. The final vertical datum for the DTM was NAVD 88. The areal extent and vertical datum for the topography set are shown in Figure 1, while the flight dates and conversion (between NGVD 29 and NAVD 88) are shown in Table 1. This topography is known as the Phase I topography.

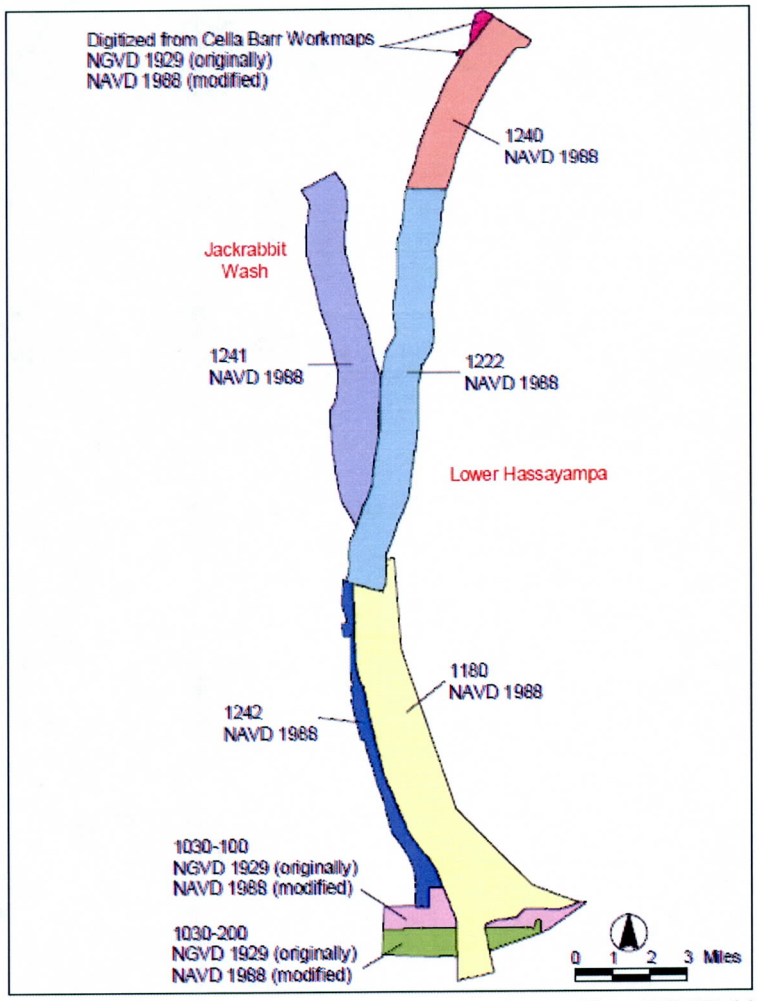

Figure 1. Extent and vertical datum of topography for Phase 1 (from WEST, 2006)

Table 1. Flight dates, vertical datum and conversion factor for the topography in Figure 1 (from WEST, 2006)

Topography ID	Flight Date	Vertical Datum of DTM	Adjustment to convert NGVD 1929 values to NAVD 1988
1030-100	12/14/1991	NGVD 1929	+2.08
1030-200	02/07/1993	NGVD 1929	+2.08
1180	04/08/2002	NAVD 1988	-
1222	11/02/2002	NAVD 1988	-
1240	04/21/2004	NAVD 1988	-
1241	04/21/2004	NAVD 1988	-
1242	04/22/2004	NAVD 1988	-
Digitized from Cella Barr work maps	03/18/1988	NGVD 1929	+1.98

2) The inflow hydrograph for the first task is the 100-year flood hydrograph, which was used in the original HEC-6 from Phase 1. However, because the input procedures between the sediment transport models are different, the 100-year hydrograph should be verified to ensure consistency between models.

3) In the second task, there are two sub-tasks. The first sub-task is to model the January 2010 event with the Phase I topography and mine configurations prior to the January 2010 event. This subtask is designed to view the impact of the larger 2010 event in relation to the earlier smaller events (see Figure 3). If the 2010 event is sufficient to yield the 2010 topography in the various models the two smaller events may be eliminated from consideration.

   The second sub-task is to model the major events from 2002 to January 2010 with the Phase I topography as the initial condition and mine configurations as the mines changed in time. The modeling results will be compared with the post-event topography obtained in the summer of 2010, but it should be noted that the post-event topography should only be used for comparison. The initial modeling should not be calibrated based on the new topography. If there is any need to calibrate the model, all changed parameters must be documented.

   There are three pits (the Hanson, Cemex and Pioneer mines) near the Tonopah-Salome Highway. The depths were estimated based on reports from the sand and gravel mining inspector at the Flood Control District (Wergen, 2010) and from aerial photographs. The areas of the mines were estimated from aerial photographs and the 2010 topography. The pit locations are labeled in Figure 2. The pit characteristics are summarized in Table 2. Aerial photographs of the mines for different years are included in the appendix.

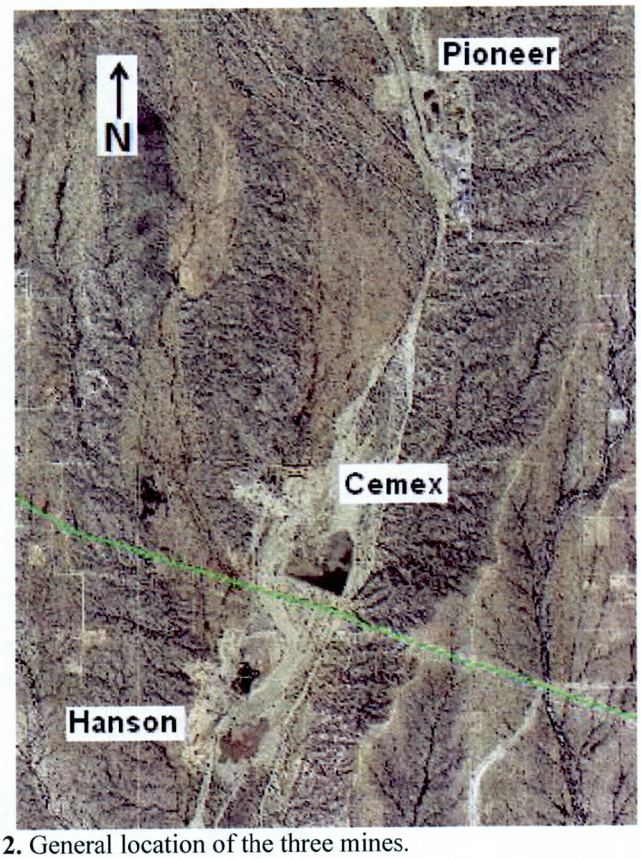

Figure 2. General location of the three mines.

Table 2. Estimated mine depths and areal extents

	Hanson		Cemex*		Pioneer	
	Depth (ft)	Area (acres)	Depth (ft)	Area (acres)	Depth (ft)	Area (acres)
2002 (information only)	4	0.5	12, 20	4.3	N/A	N/A
2004 (before '05 events)	5-9	15	10-15, 10-15, 15-20	1.1, 1.1, 14	N/A	N/A
2005 (after '05 events)	5-9	10	mine filled	mine filled	8-10	3.3
2009 (before Jan. 2010 event)	10	22	10	45	28-30	23

*There are separate pits for this owner. See the photograph in the Appendix for estimate limits

4) The inflow hydrographs for the second task are based on the two largest events that occurred on the Hassayampa River from September 2002 to January 2010. The third (smallest) event may be added if results do not match the 2010 topography. The events were recorded on the Flood Control District of Maricopa County (FCDMC) gage

(number 5283) at the I-10 Bridge. The events are circled (in red) in Figure 3. These three events will serve as the inflow hydrographs for Task 2 with priority given to the 2010 event (largest) and the 2005 (second largest event). The dates of the events are as follow (based on 15 minute data):

Largest:	2010: January 20-21, 2010	11,600 cfs peak
2nd Largest:	2005: February 11-12, 2005	5,500 cfs peak
Smallest:	2005: February 22-23, 2005	2,000 cfs peak

There are a number of small events in the intervening eight years but they are less than 1,000 cfs with most being below about 600 cfs. As such it is anticipated that they will not have major impacts on the river but may have had some local impacts in or very near the mine pits.

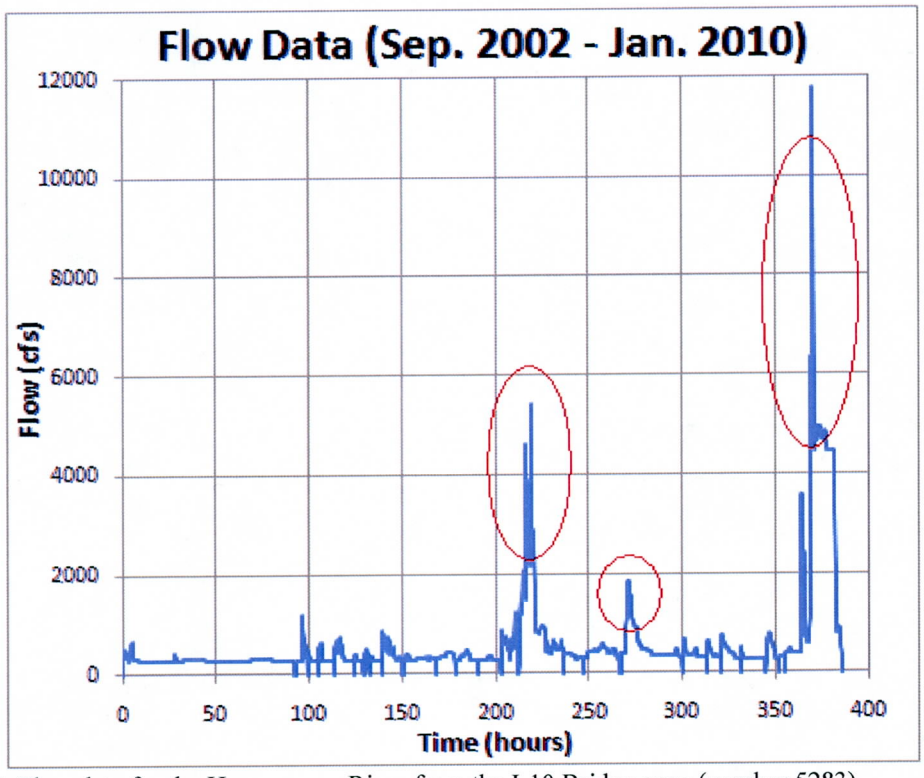

Figure 3. Flow data for the Hassayampa River from the I-10 Bridge gage (number 5283)

5) The attached CD contains the following data:

   a. original DTM for Phase I

   b. HEC-6 and HEC-RAS models for Phase I

   c. Fluvial-12 model and report by Chang Consultants (based on Phase I topography)

   d. Aerial photos that show the changes for mining surface area

   e. Topographic data that was obtained in summer of 2010 (after January 2010 event) for an approximately 11 mile reach

   f. Flow data from 2002 to 2010 in Excel format at I-10 (note: this will data will be used for the second task: pit headcut/tailcut)

   g. Phase I Report (River Behavior Report)

   h. Miscellaneous items

References

Wergen, Thomas. 2010. personal communication.

WEST Consultants, Inc. (WEST). 2006. Lower Hassayampa River Watercourse Master Plan, Final Hydraulics Report, Hassayampa River. Prepared for JE Fuller Hydrology & Geomorphology, Inc.

2801 West Durango Street Phoenix, Arizona 85009 Phone: 602-506-1501 Fax: 602-506-4601

Appendix

Pioneer Photographs

21 acres: 28-30 feet deep

3.3 acres: 8-10 feet deep

Hanson/Cemex Photographs

Hanson/Cemex 2009

22 acres: 10 feet deep

45 acres: 10 feet deep

Hanson/Cemex 2005

8.22 acres: 5-9 feet deep

1.22 acres: 5-9 feet deep

Cemex pits filled

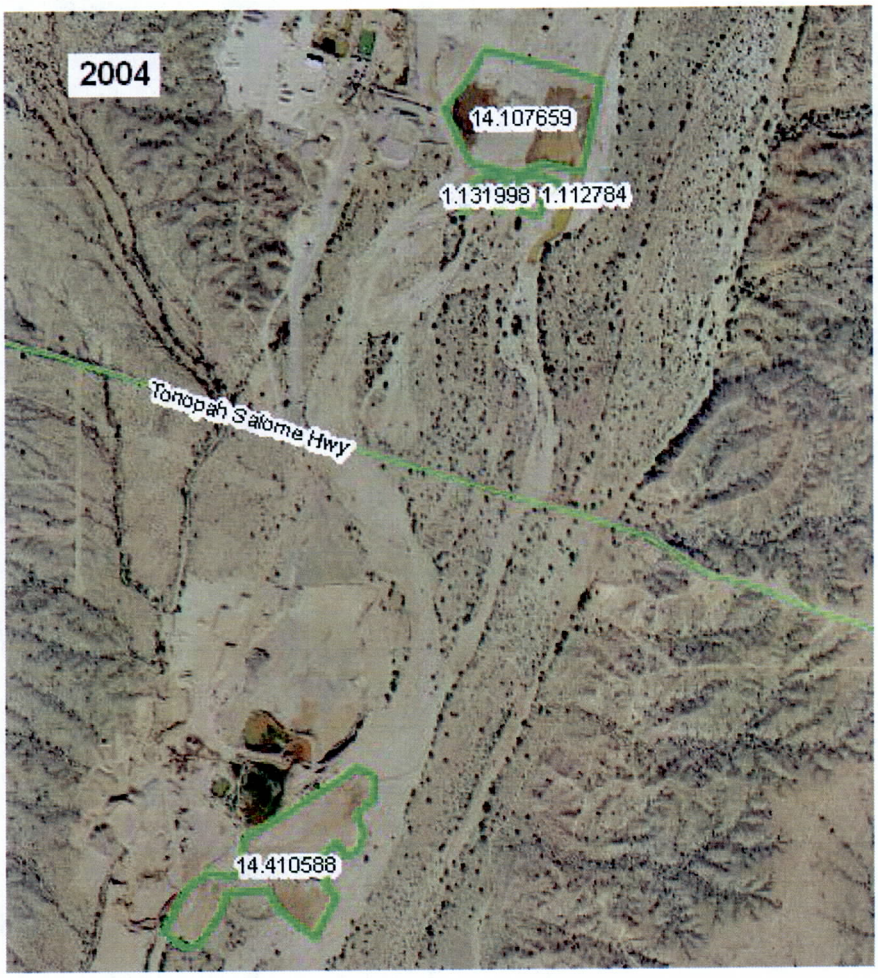

Hanson/Cemex 2004

14.41 acres: 5-9 feet deep

14.10 acres: 15-20 feet deep

1.13 acres: 10-15 feet deep

1.11 acres: 10-15 feet deep

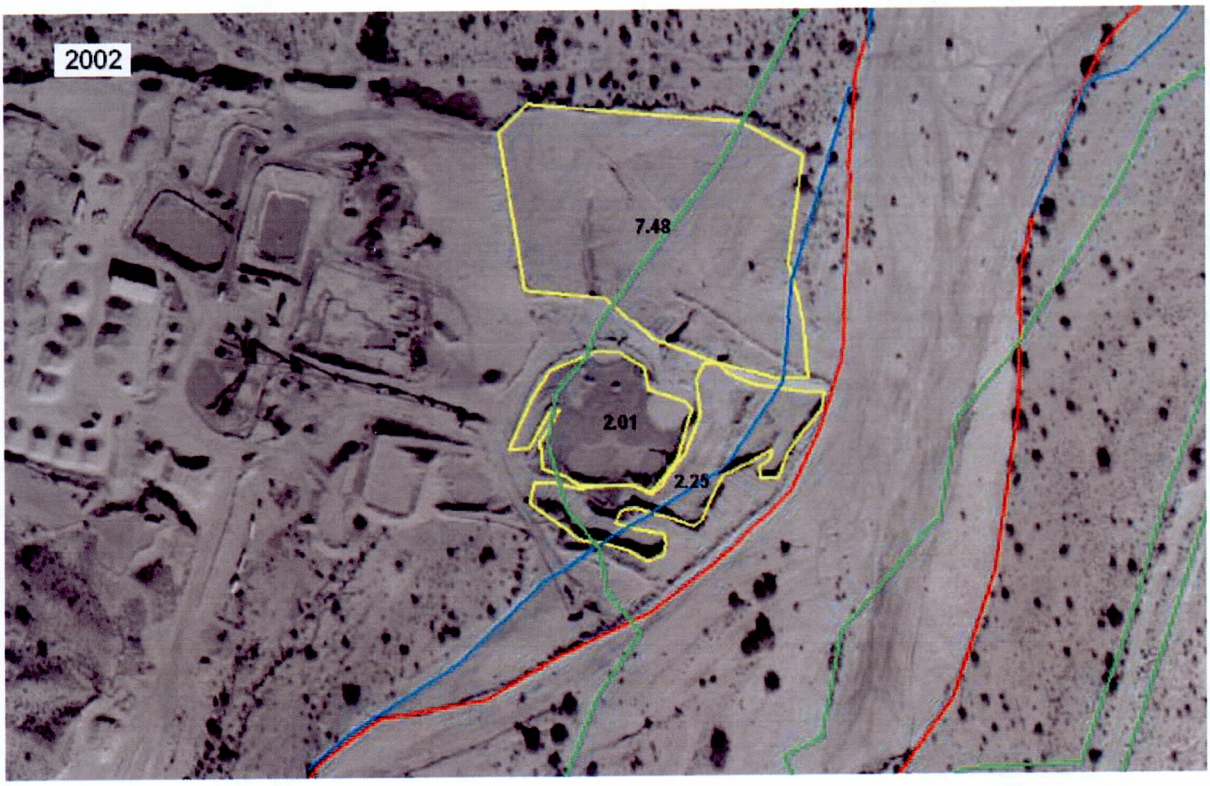

Cemex 2002 (information only)

11.7 total but 7.48 does not appear to have impacted the flow so the net impacted area is:
4.3 acres

2.0 acres – 20 ft deep (2002 topo)
2.25 acres – 12 ft deep (2002 topo)

The bank lines are also shown in this figure – green are 2010, red are 2002 and blue are 2004.

APPENDIX II

COMPARISON PLOTS

MODEL RESULTS FOR MINED REACH

APPENDIX II-A

COMPARISON PLOTS

MODEL RESULTS FOR MINED REACH

HEC-6T RESULTS

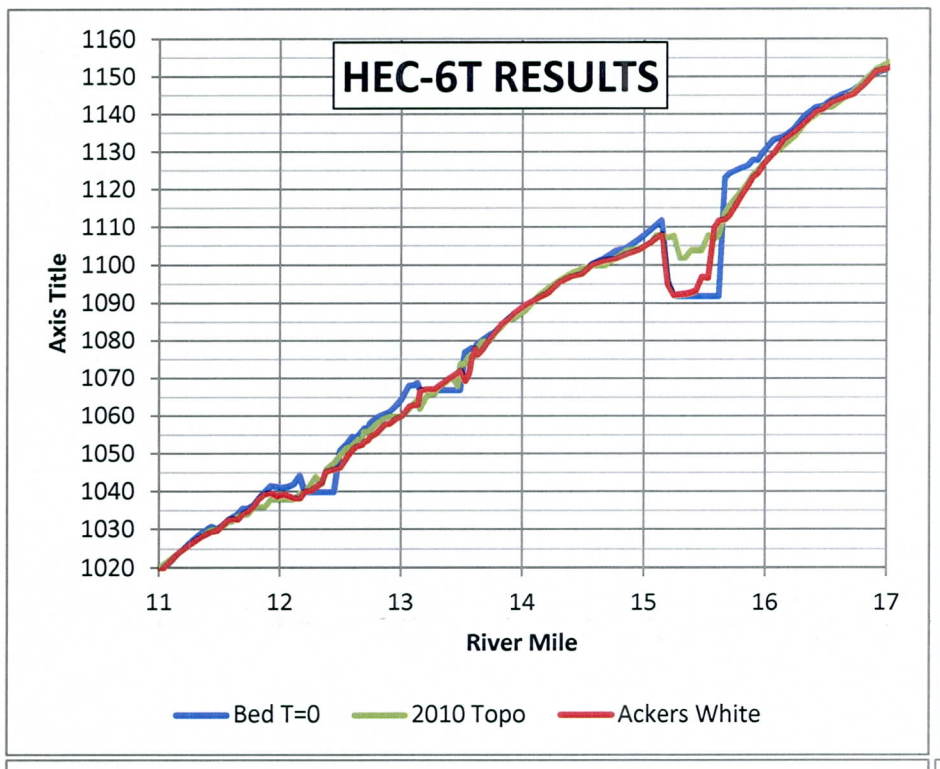

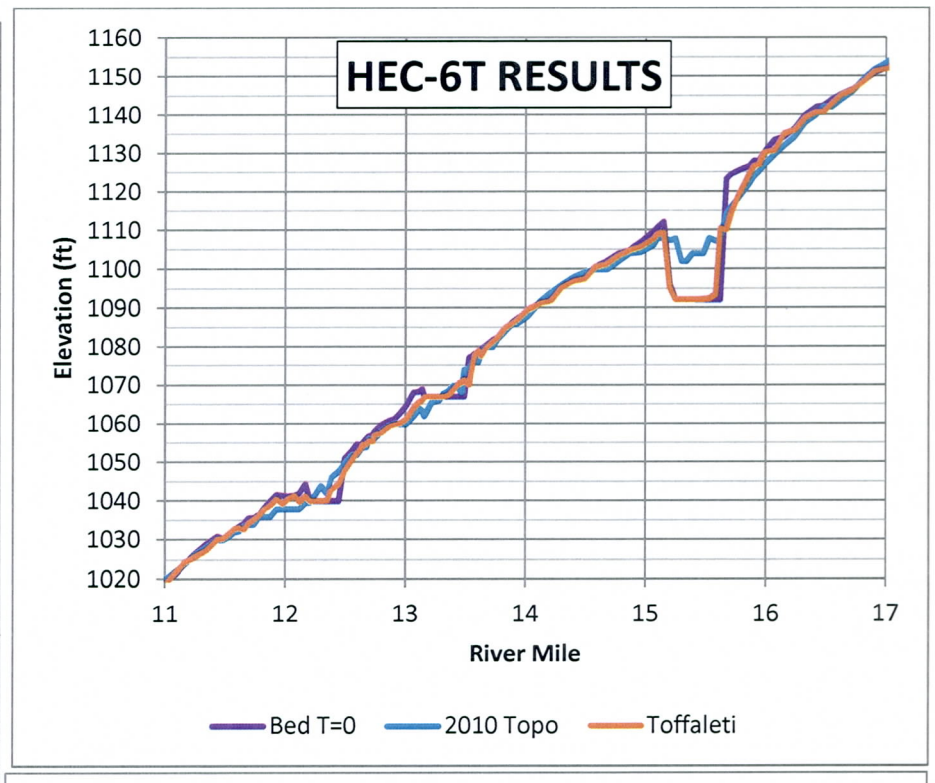

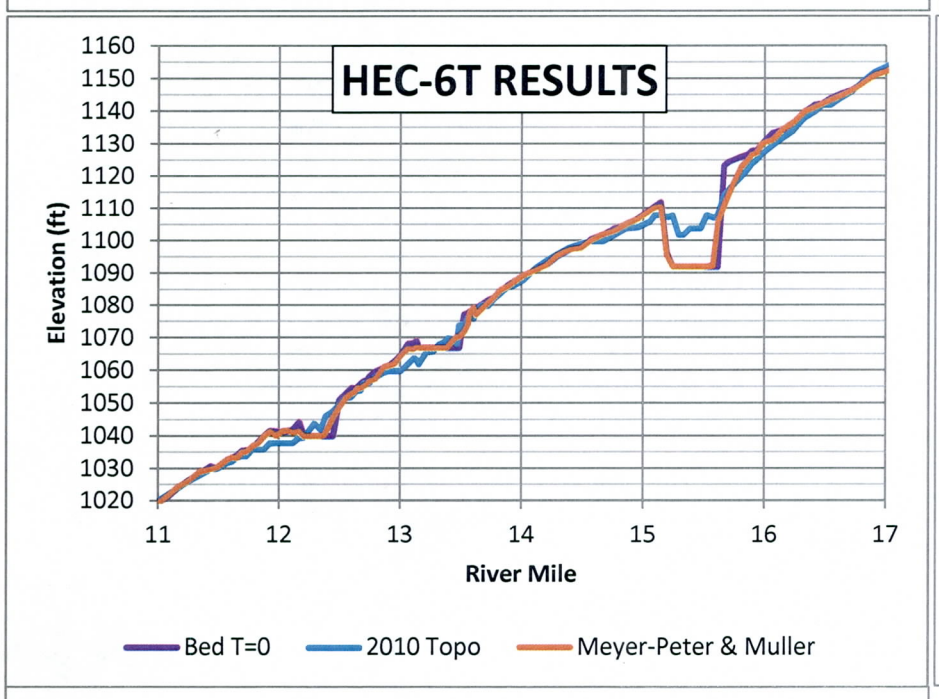

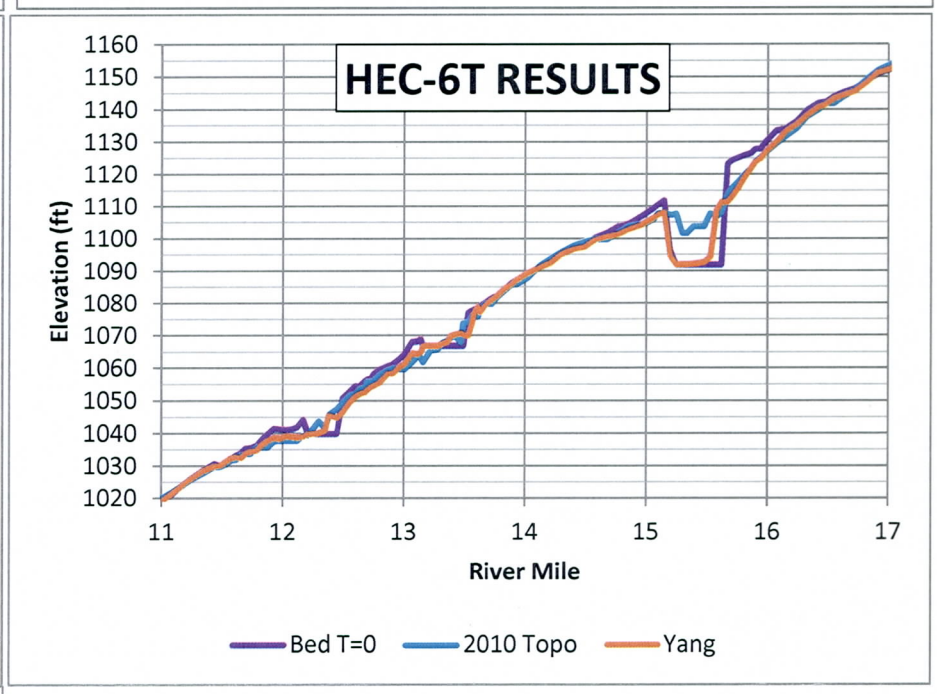

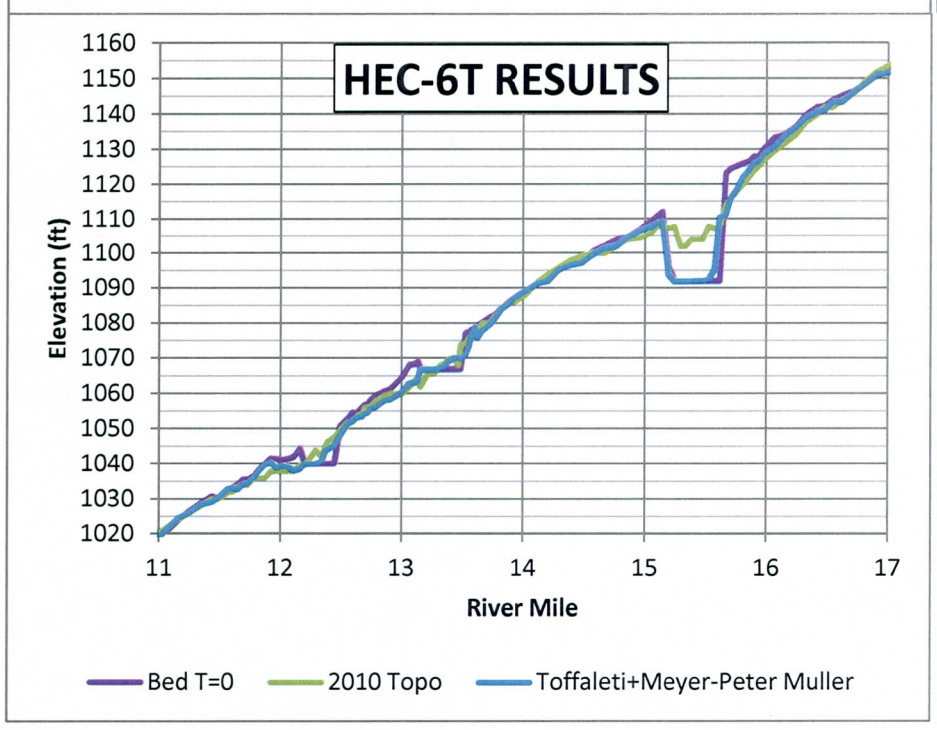

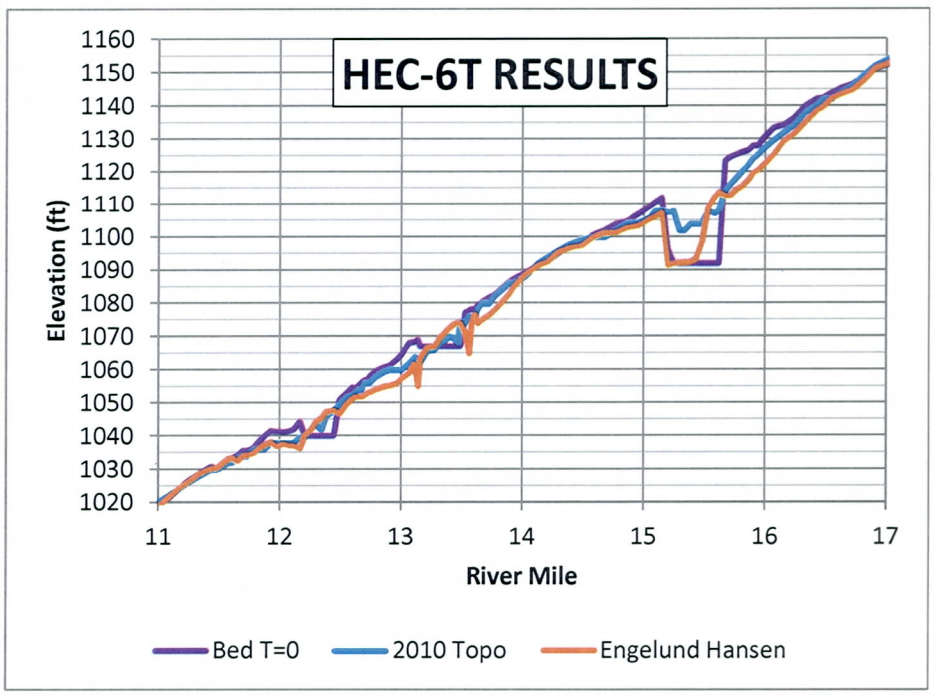

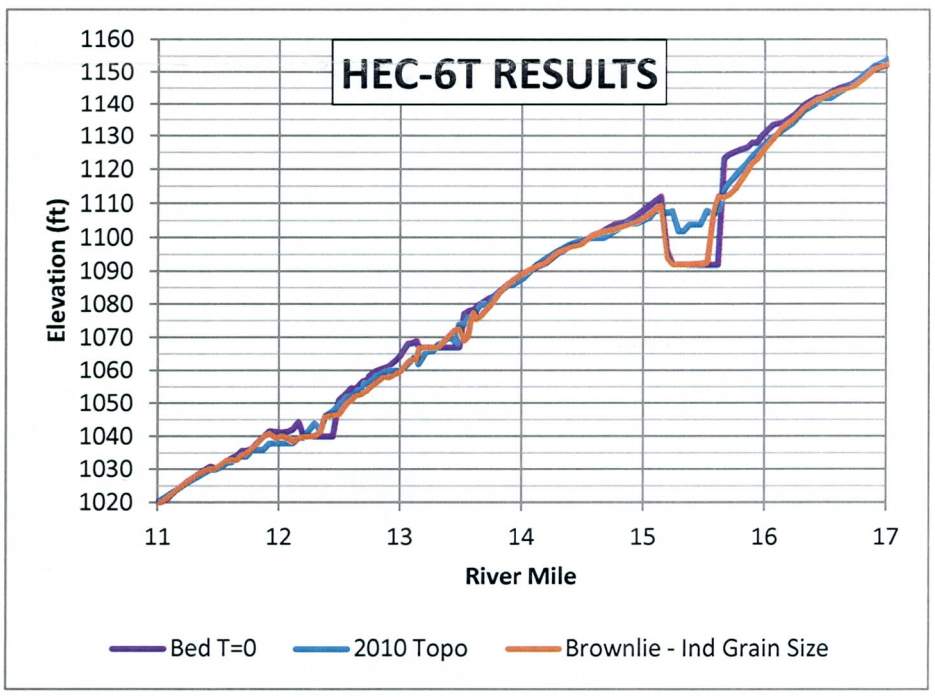

HEC-6T RESULTS

HASSAYAMPA RIVER 2010 FLOOD EVENT

APPENDIX II-B

MODEL RESULTS FOR MINED REACH

HEC-RAS RESULTS

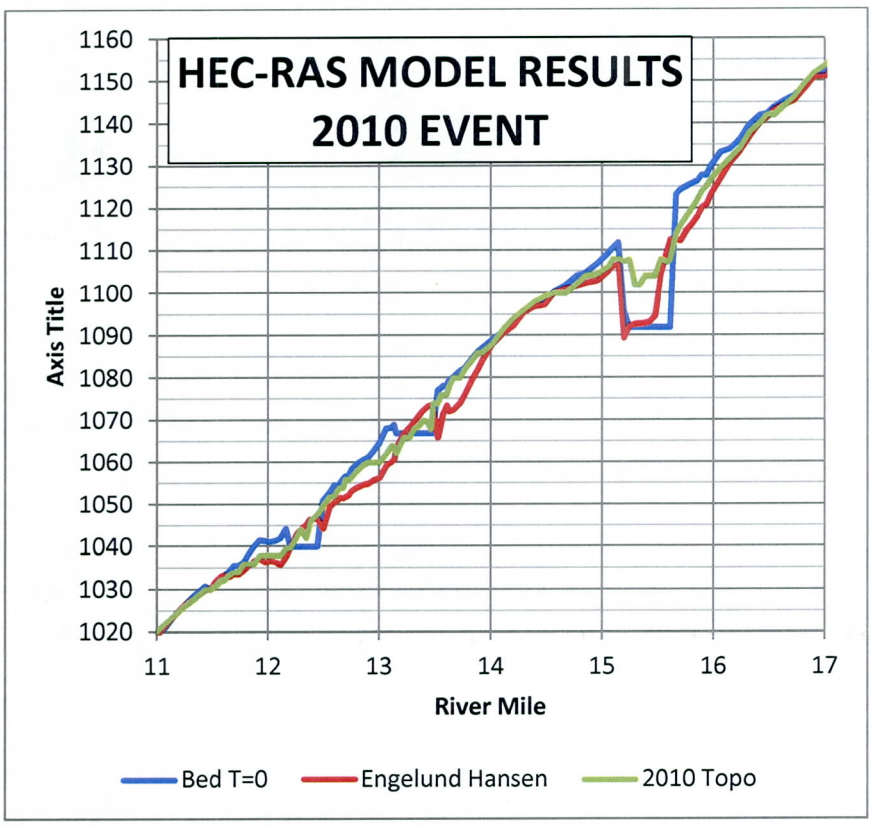
HEC-RAS MODEL RESULTS
2010 EVENT
Axis Title
River Mile
Bed T=0
Engelund Hansen
2010 Topo

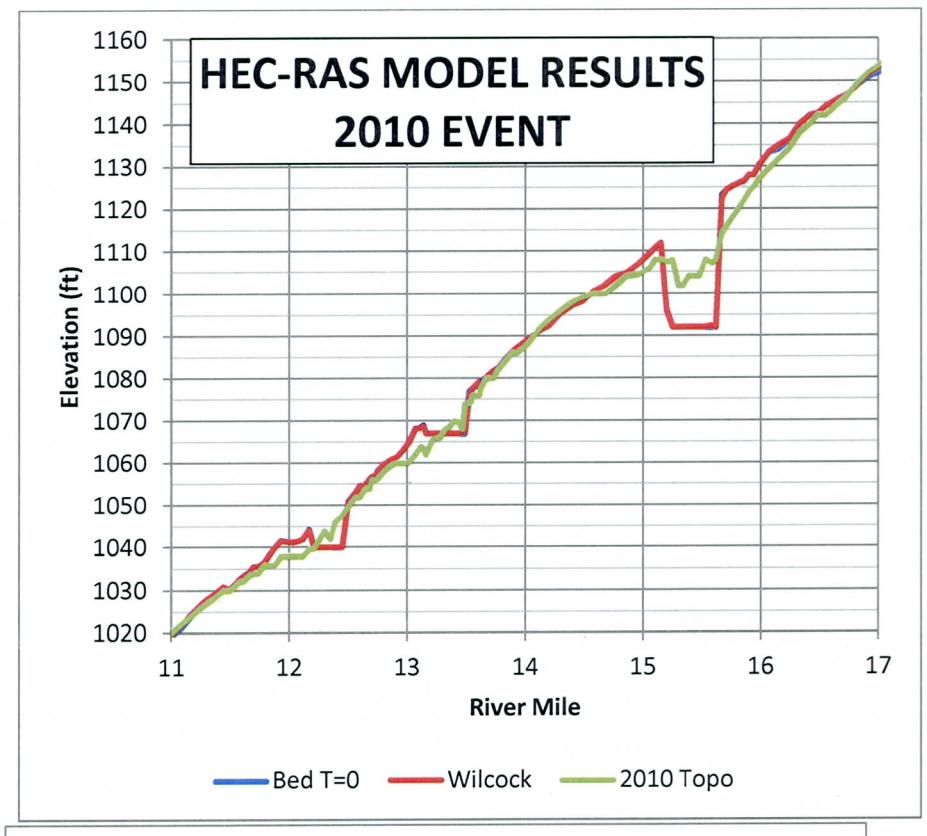
HEC-RAS MODEL RESULTS
2010 EVENT
Elevation (ft)
River Mile
Bed T=0
Wilcock
2010 Topo

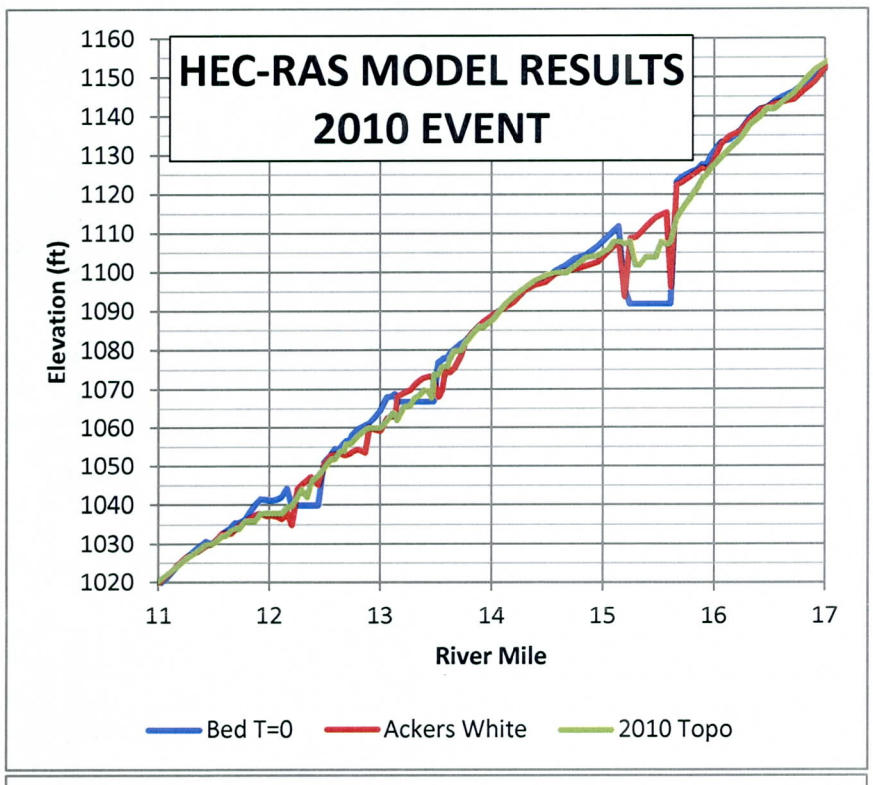
HEC-RAS MODEL RESULTS
2010 EVENT
Elevation (ft)
River Mile
Bed T=0
Ackers White
2010 Topo

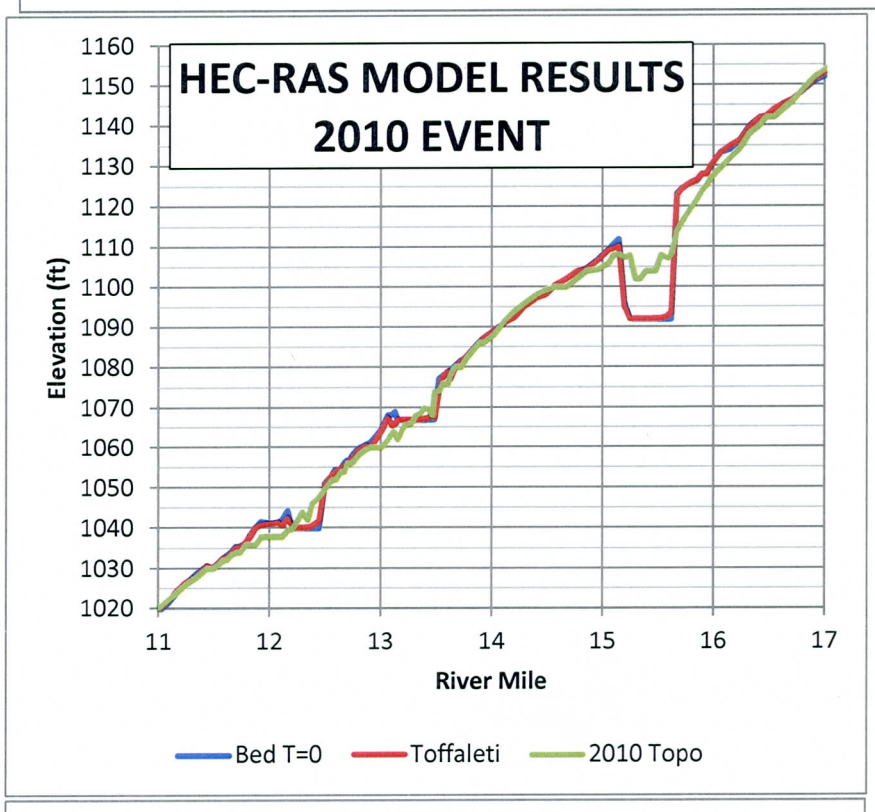
HEC-RAS MODEL RESULTS
2010 EVENT
Elevation (ft)
River Mile
Bed T=0
Toffaleti
2010 Topo

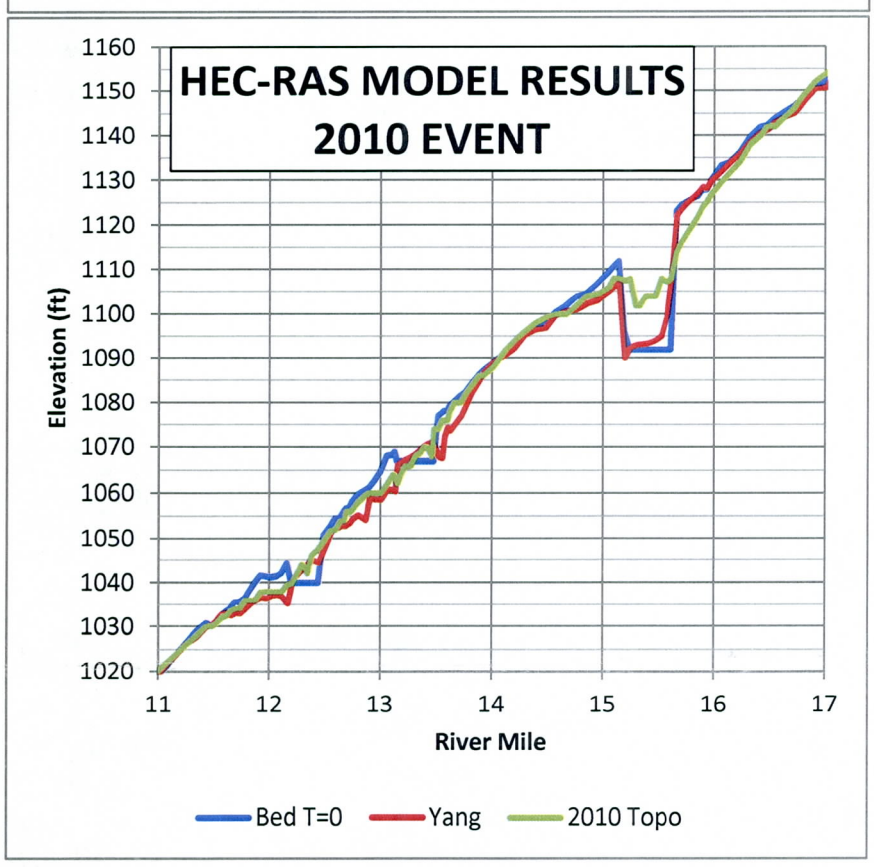
HEC-RAS MODEL RESULTS
2010 EVENT
Elevation (ft)
River Mile
Bed T=0
Yang
2010 Topo

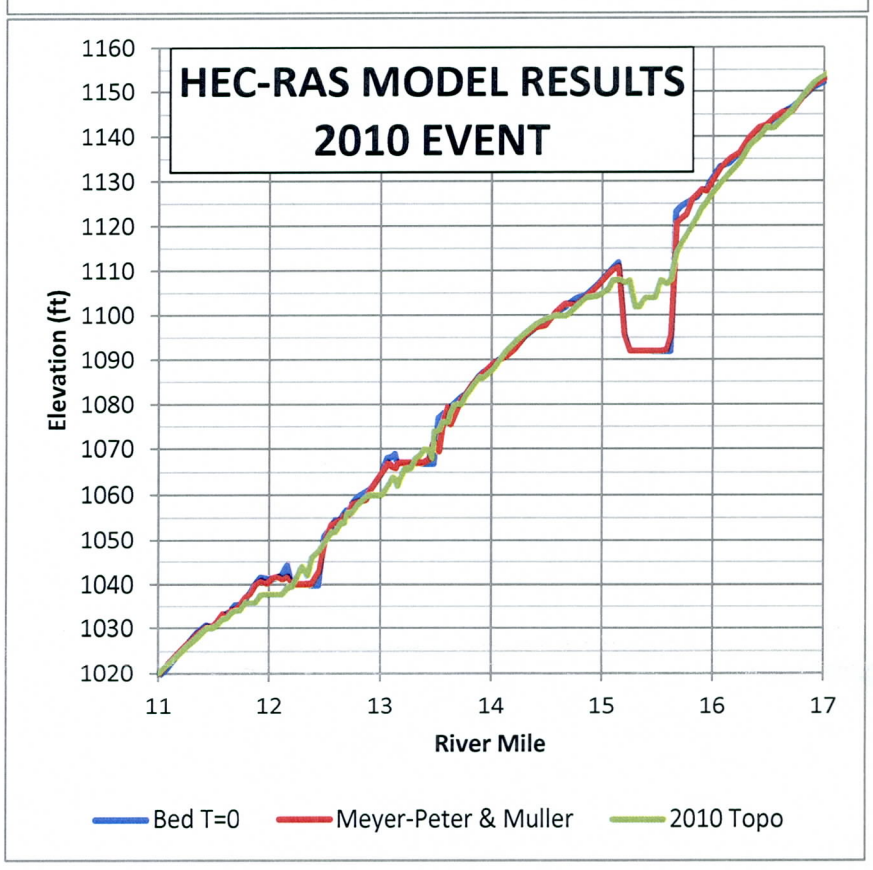
HEC-RAS MODEL RESULTS
2010 EVENT
Elevation (ft)
River Mile
Bed T=0
Meyer-Peter & Muller
2010 Topo

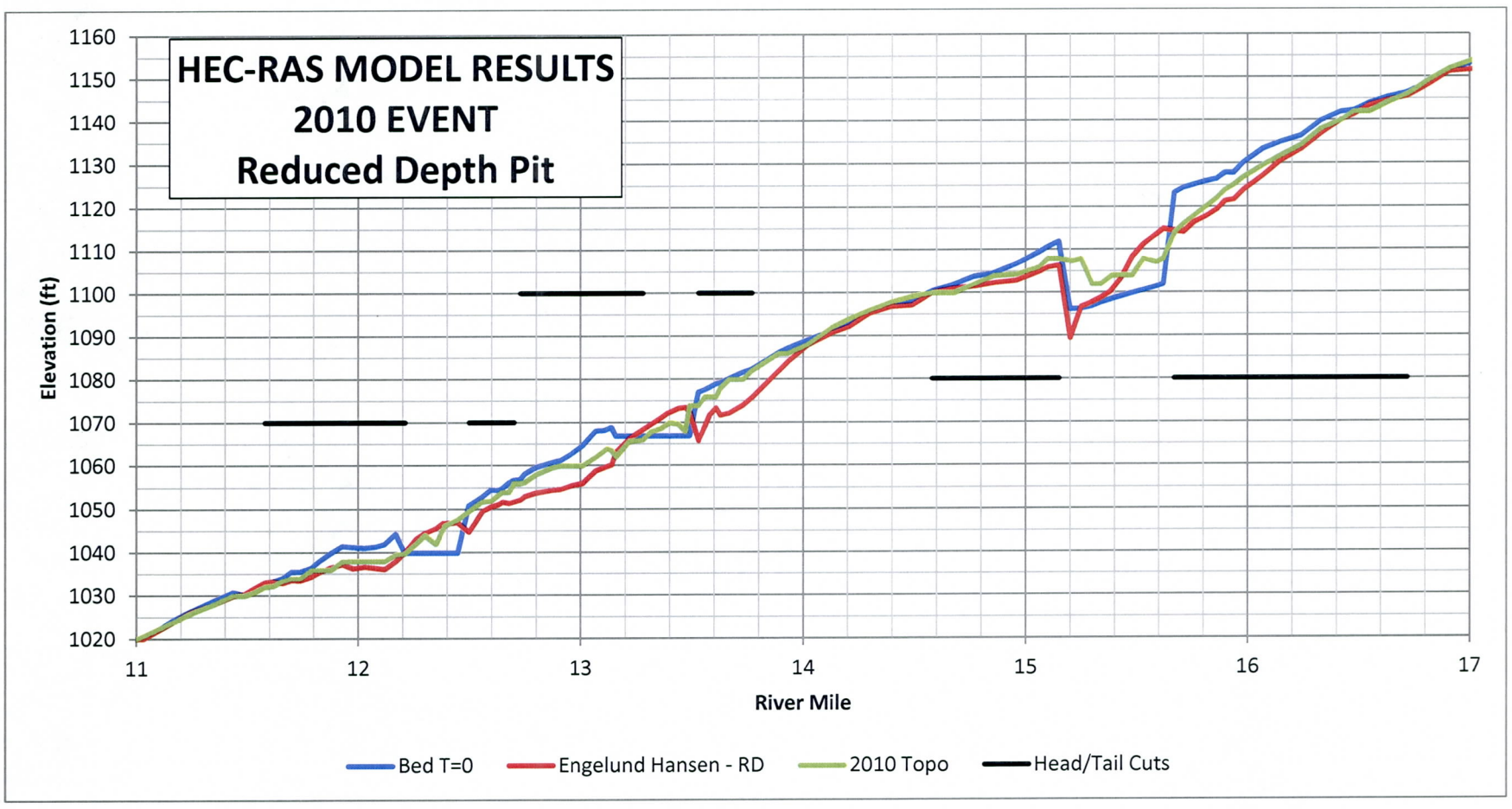

HEC-RAS Model Results based on reduced depth for Pioneer Pit using Engelund Hansen Transport Equation. Actual Headcut and Tailcut distances are shown as Black Lines.

APPENDIX II-C

COMPARISON PLOTS

MODEL RESULTS FOR MINED REACH

COMPARISON OF

HEC-6T AND HEC-RAS RESULTS

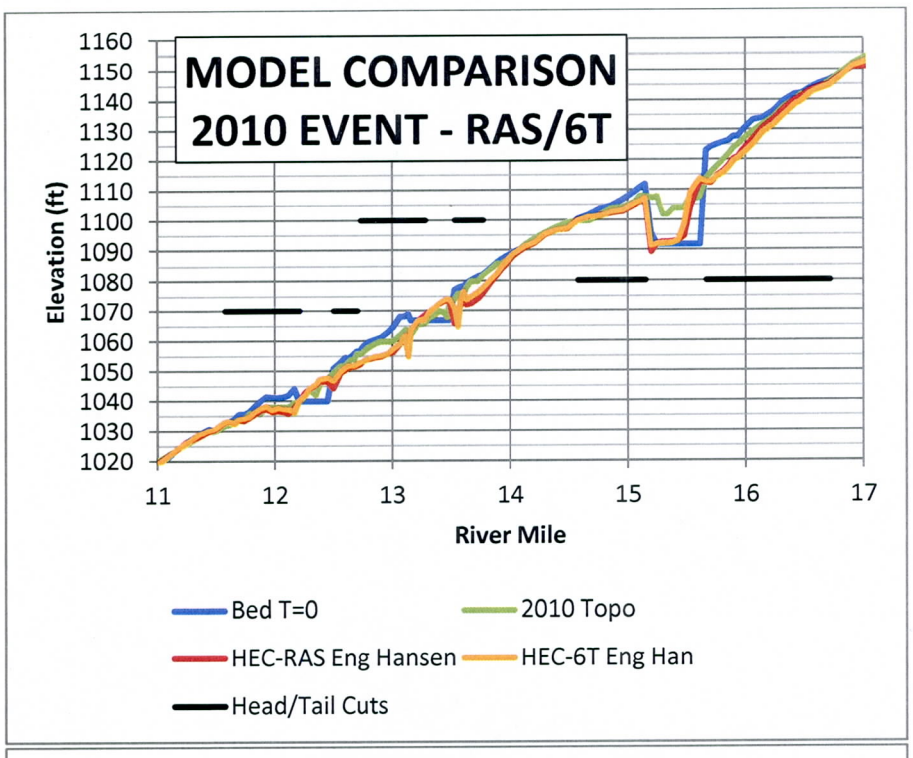

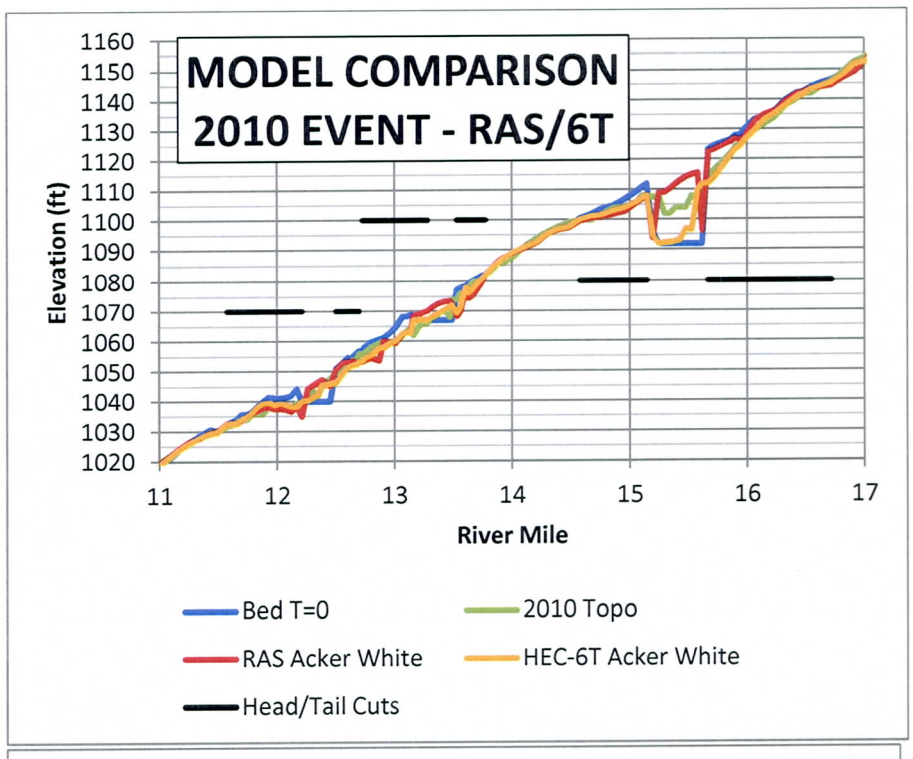

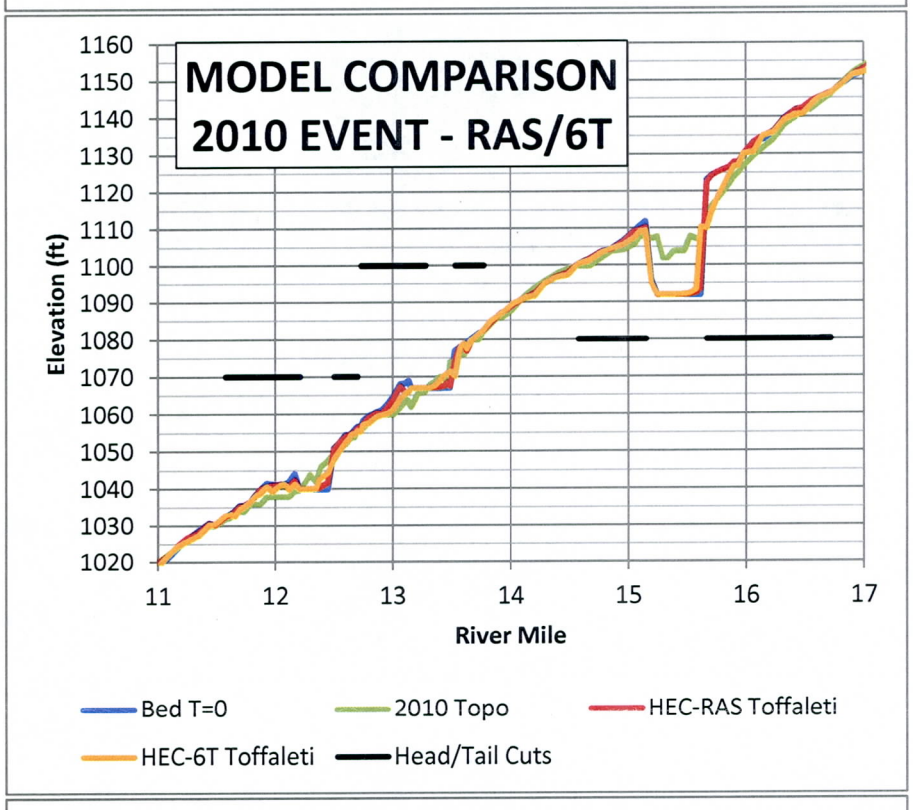

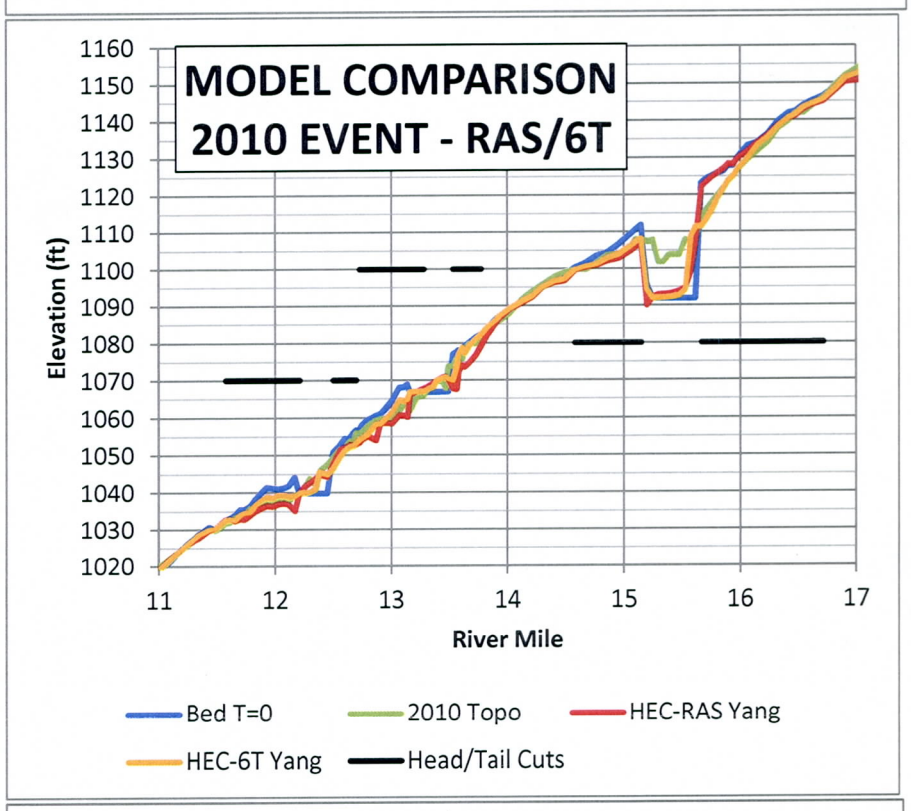

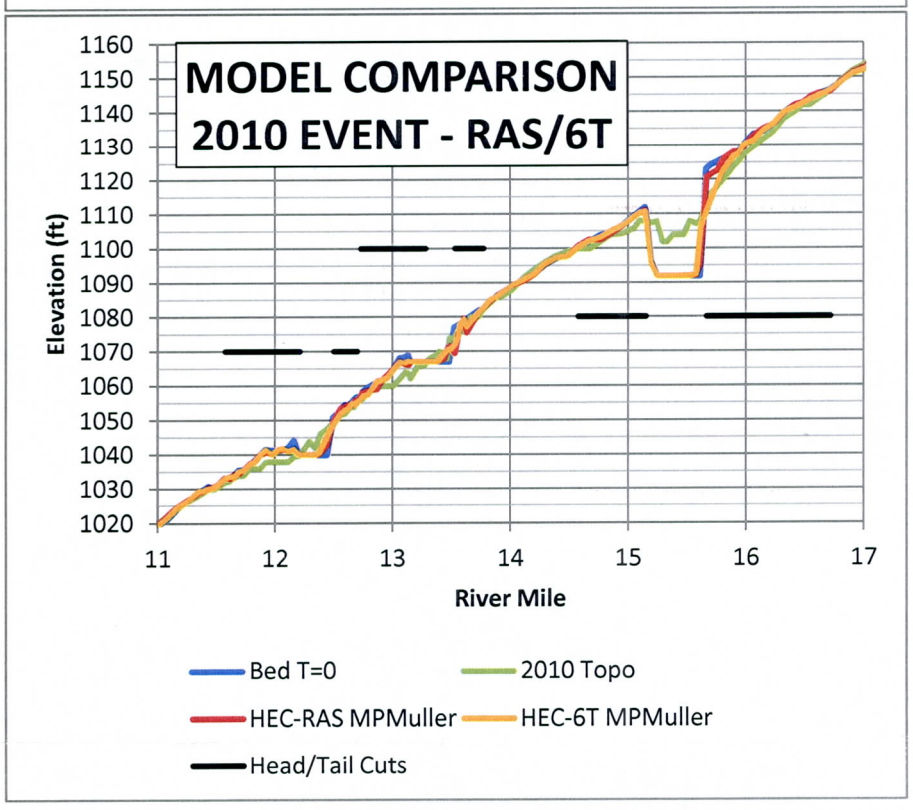

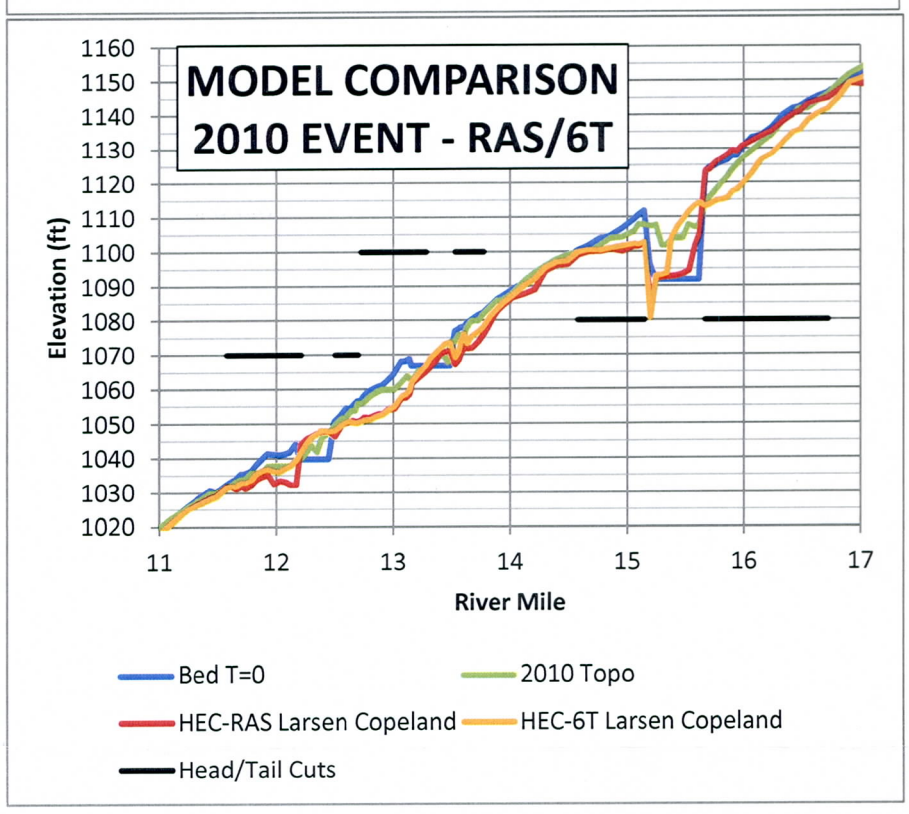

COMPARISON OF HEC-RAS AND HEC-6T SEDIMENT TRANSPORT EQUATION RESULTS FOR THE 2010 EVENT ON THE HASSAYAMPA RIVER, BUCKEYE, ARIZONA

APPENDIX III

DISTRICT REPORT ON USE OF FLO-2D TO MODEL HASSAYAMPA MINING REACH

Flood Control District
of Maricopa County

MEMORANDUM

Date: June 2, 2011

To: Theresa Pinto, CFM, Project Manager, Planning Branch, Planning and Project Management Division

From: Richard Waskowsky, Hydrologist, Engineering Application Development and River Mechanics Branch, Engineering Division

CC: Bing Zhao, PhD, PE, Engineering Application Development and River Mechanics Branch Manager, Engineering Division

Subject: Flo-2D Modeling for Phase II of the Lower Hassayampa Watercourse Master Plan (WCMP) – Model Development and Results

This memorandum was prepared to document the development of the Flo-2D models and the results from these models. The Flo-2D models were prepared as a part of the river mechanics portion of Phase II of the Lower Hassayampa Watercourse Master Plan. The data collection for the Flo-2D (and other software) models has been documented in the November 22, 2010 memorandum (Waskowsky, 2010).

The goal of the Flo-2D modeling is to study the headcut/tailcut due to sand and gravel mines, in particular the Pioneer mine, for the major flows from 2002 to 2010. The modeling is divided into two scenarios. The first one is to model the January 2010 event only, while the second is to model the two largest events from 2002 to 2010.

The discussion below documents both the development of the models and the results from these models.

1) **Model Reach Length:** The reach that was modeled was determined with two factors in mind. The first factor was to totally encompass the headcuts/tailcuts from the sand and gravel mines. The second one was to keep the total number of grid elements manageable. The final reach length that was selected was about six miles. The headcut/tailcut estimates and the final reach are shown in Figure 1.

2) **Flow Scenarios:** Two scenarios were run for the Flo-2D model. One for the 2010 event only, and the second for the 2005 and 2010 events. The 2010 hydrograph that was used in both Flo-2D models is shown in Figure 2, and the 2005 hydrograph that was used in the Flo-2D model for the second scenario is shown in Figure 3.

2801 West Durango Street Phoenix, Arizona 85009 Phone: 602-506-1501 Fax: 602-506-4601

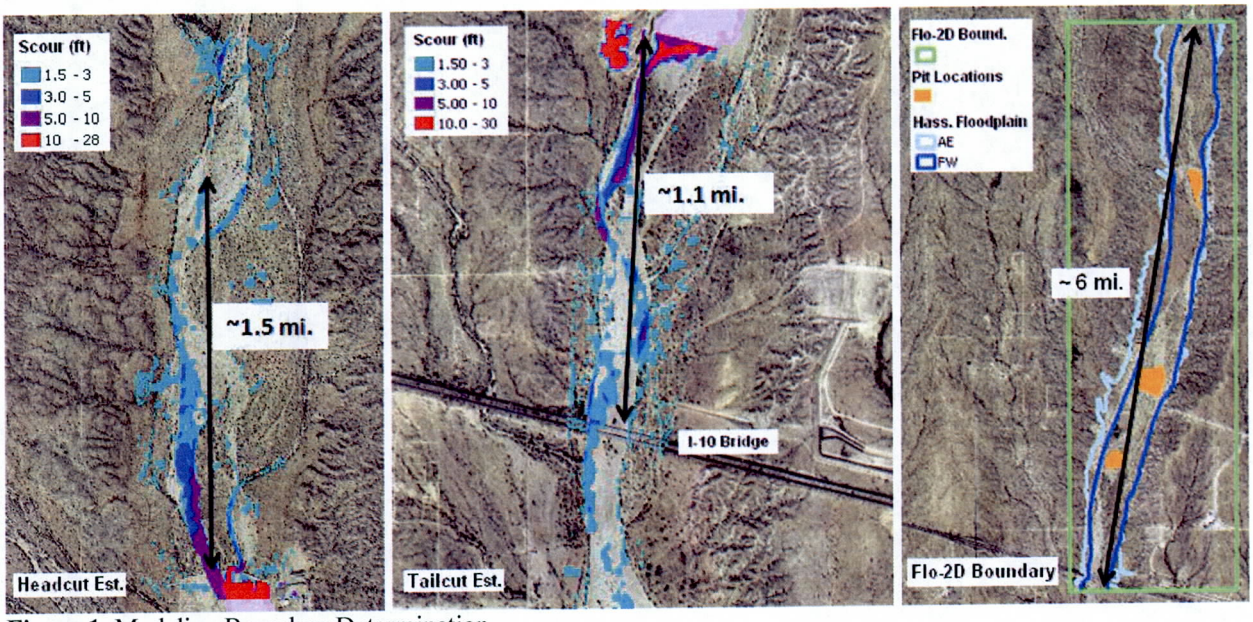

Figure 1. Modeling Boundary Determination.

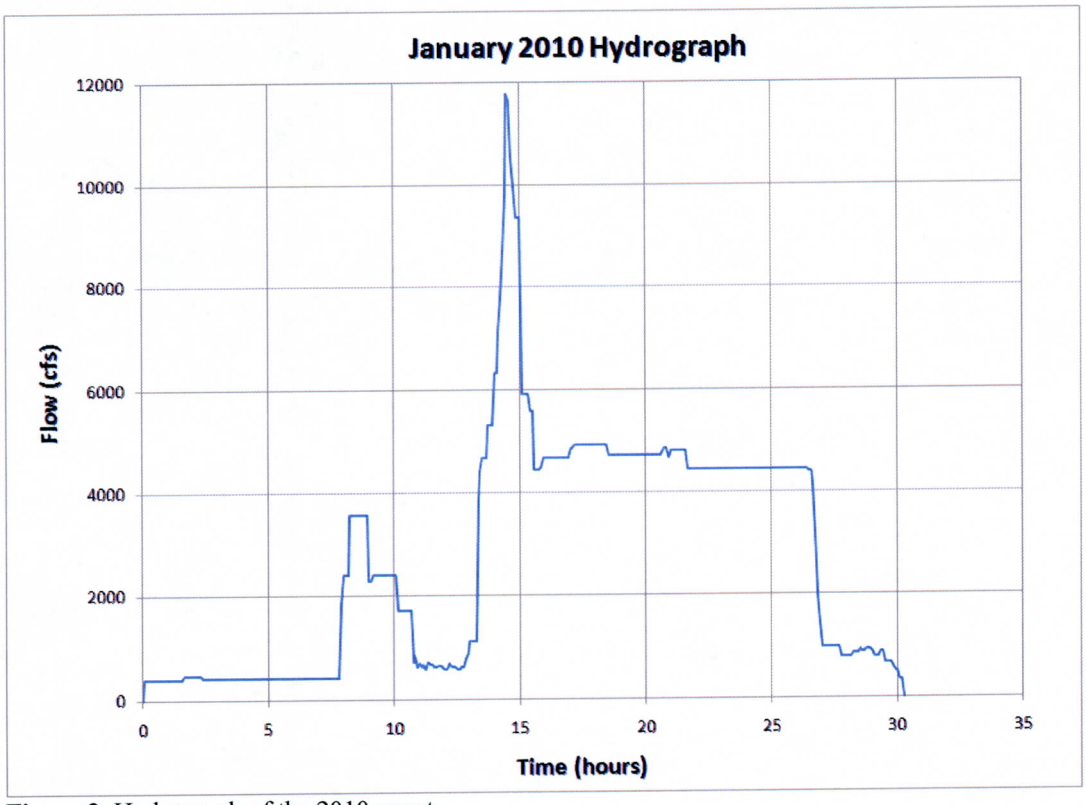

Figure 2. Hydrograph of the 2010 event.

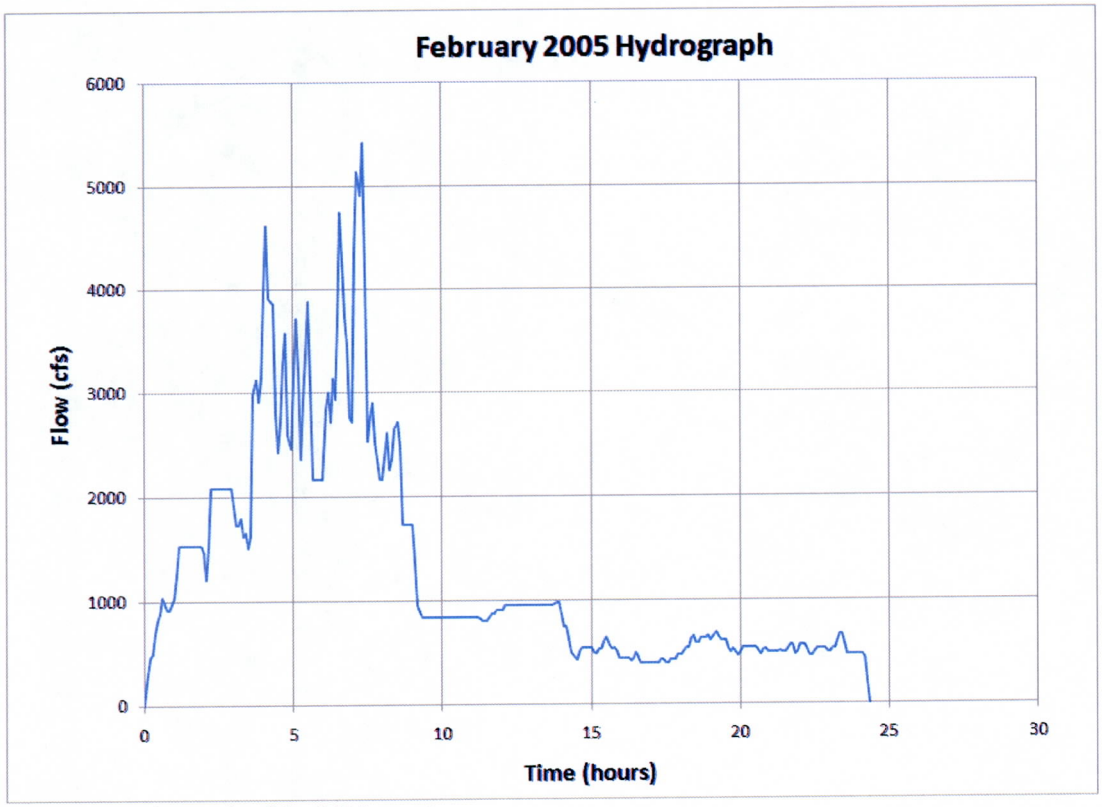

Figure 3. Hydrograph of the 2005 event.

3) **Grid Development:** To develop the Flo-2D grid, some steps needed to be followed. First, the Digital Terrain Model (DTM) from Phase I of the Lower Hassayampa Watercourse Master Plan was converted to a 5-foot grid ascii file. The date of the DTM was 2002. Next, the 5-foot ascii file was loaded into the Flo-2D Grid Development System (GDS), and GDS was used to interpolate a 50-foot grid, as well as a 20-foot grid. Finally, to obtain the initial grid elevations for both flow scenarios (2010 event only and 2005 plus 2010 events), the elevations of the grid elements were modified to include the mines. The estimated December 2009 locations and bottom elevations are shown in Figure 4, and the estimated December 2004 locations and bottom elevations are shown in Figure 5.

4) **Model Set-up and Procedure:** After the grids were developed, the Flo-2D models were run. The model with the 20-foot grid crashed, and no results were obtained. Therefore, the bulk of the effort focused on the models with a 50-foot grid. All simulations were performed with Flo-2D version 2007.06 with the FLO.EXE that was compiled on March 6, 2008.

   For the 50-foot grid, the Manning's n value was obtained by running flow simulations without sediment (hydraulics only). For scenario one (2010 event only), the 2010 event was run with a -1.00 dynamic wave number coefficient to obtain the FPLAIN.RGH file. The total simulated time was 35 hours and a limiting Froude number was not used. In scenario two (2005 and 2010 events), the 2005 event was run with a -1.00 dynamic wave number coefficient to obtain the FPLAIN.RGH file. The total simulated time was 30 hours and a

limiting Froude number was not used. The FPLAIN.RGH file was renamed FPLAIN.DAT, and the new FPLAIN.DAT was used as an input file for the sediment transport simulations.

Figure 4. Location of mines before the 2010 event. The elevations that were used in the Flo-2D grid are shown over the pit locations. The background aerial photograph is from May 2009.

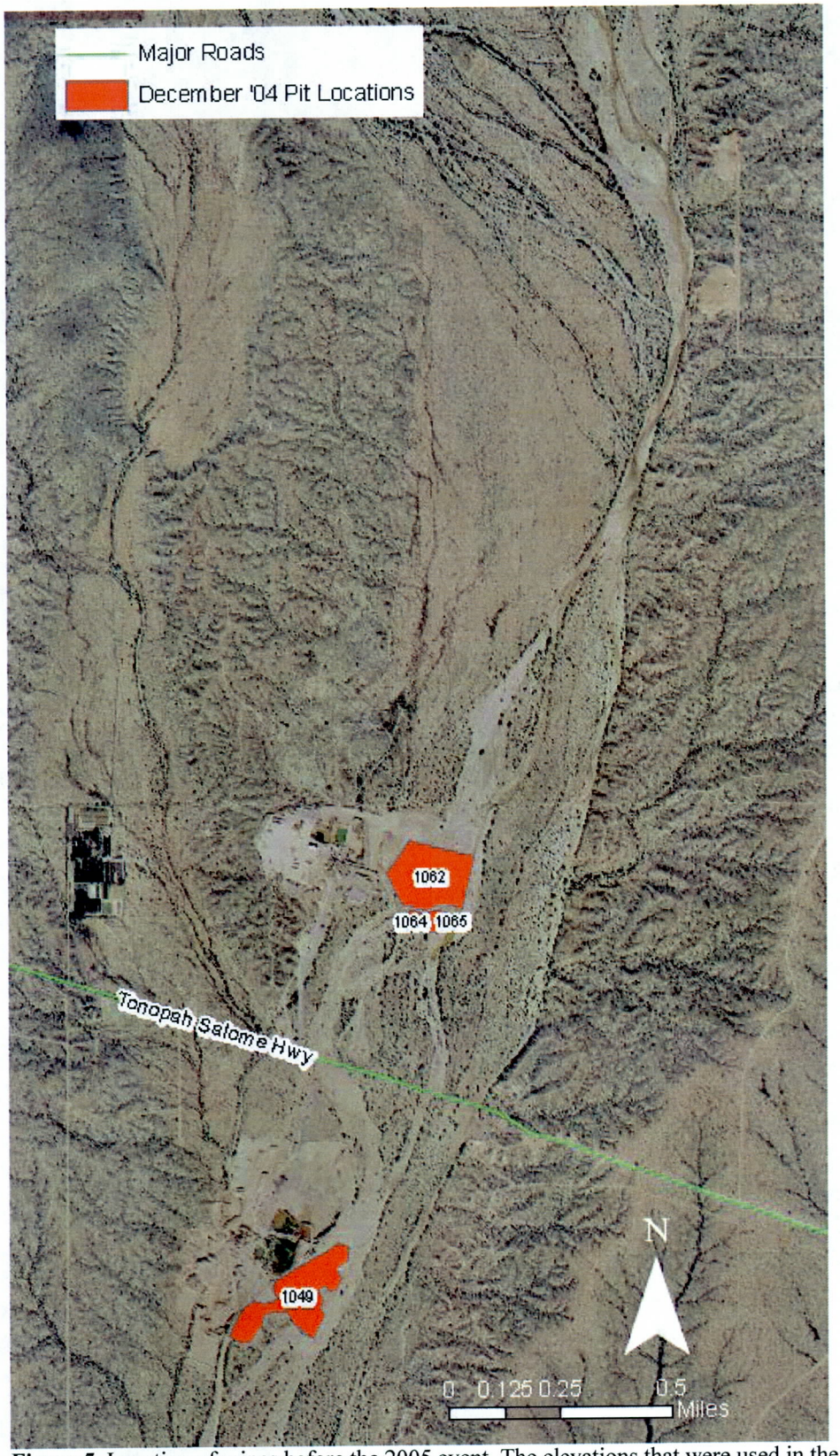

Figure 5. Location of mines before the 2005 event. The elevations that were used in the Flo-2D grid are shown over the pit locations. The background aerial photograph is from December 2004.

5) **Sediment Transport Simulations (Input Parameters):** With the revised FPLAIN.DAT file that was developed from the hydraulics-only simulations, multiple sediment transport simulations were run. To allow supercritical flow over the brinks of the mines, a limiting Froude number was not specified for the simulations. The dynamic wave number was set to 1.00, while other tolerance values were left as the default values.

   For the sediment parameters, both the average D50 value and the gradation coefficient were taken from the Phase I River Behavior Report (JEF, 2006). The D50 value was 0.45 mm, while the gradation coefficient was 5. The Engelund-Hansen sediment transport equation was chosen because good results were obtained on the Hassayampa River by Chang (2009). Reasonable values were chosen for other sediment input parameters, such as the dry specific weight, the specific gravity and the fine sediment volumetric concentration. The dry specific weight was specified as 110 pounds/ft^3, the specific gravity was 2.65 and the fine sediment volumetric concentration was 0.02. Finally, the maximum scour depth was initially set at 8 feet based on previous Flo-2D modeling experience for the H3 Fan study.

   For flow scenario one (2010 event only), the 2010 event was run for a total of 35 hours to include an extra 5 hours after the actual flow ceased. For flow scenario two (2005 and 2010 events), the 2005 and 2010 events were run for a total of 65 hours (30 hours for 2005 flood event, 35 hours for 2010 flood event) to include an extra 5 hours after the actual flow ceased for each flood event. In scenario two, the 2005 event was run with the mine configurations from Figure 5. The final bed elevations from the 2005 event simulation were modified to include the mine configurations from Figure 4, and the 2010 event was run. As a note, the hours mentioned above were for the flood hydrographs and not the computer run time.

6) **Sediment Transport Simulations (Results):** The actual topography difference between the topography from 2002 and the topography in 2010 for the area near the northern sand and gravel mine is shown in Figure 6. In this figure, not all the bed changes are caused by flooding. For example, the largest changes near the mine are caused by man-made mining activities. The full topography difference figure is included on the DVD with the name "ActualTopoDifference_2002minus2010topo.zip".

   The bed change for flow scenario one (2010 only) is shown in Figure 7, while the bed change for flow scenario two is shown in Figure 8. From a comparison of the three figures, it can be seen that Flo-2D spatially distributes the area of erosion reasonably well. For example, two headcuts different headcuts can be seen in all three figures, but the depth and length of the Flo-2D headcuts (Figures 7 and 8) are different than those that actually occurred in the January 2010 event (Figure 6). The east headcut is much longer for both of the Flo-2D results. Additionally, the depths are different from the actual depth and between the Flo-2D results. The results for the 2010 event indicate that the maximum scour was 8 feet, while the maximum scour for the 2005 and 2010 events was 16 feet. From these two maximum scour values, the results indicate that both simulations reached the specified value of maximum scour of 8 feet (8 feet for the 2010 event in flow scenario one, 8 feet for the 2005 event and 8 feet for the 2010 event for flow scenario two). Therefore, more simulations have been done to quantify if Flo-2D can predict the maximum scour.

   As one final check, the thalweg profiles between the two Flo-2D results were compared with the thalweg profile from the May 2010 topography. For flow scenario one, the bed change was added (in an Excel file) to the initial elevation to obtain the final elevation. The final

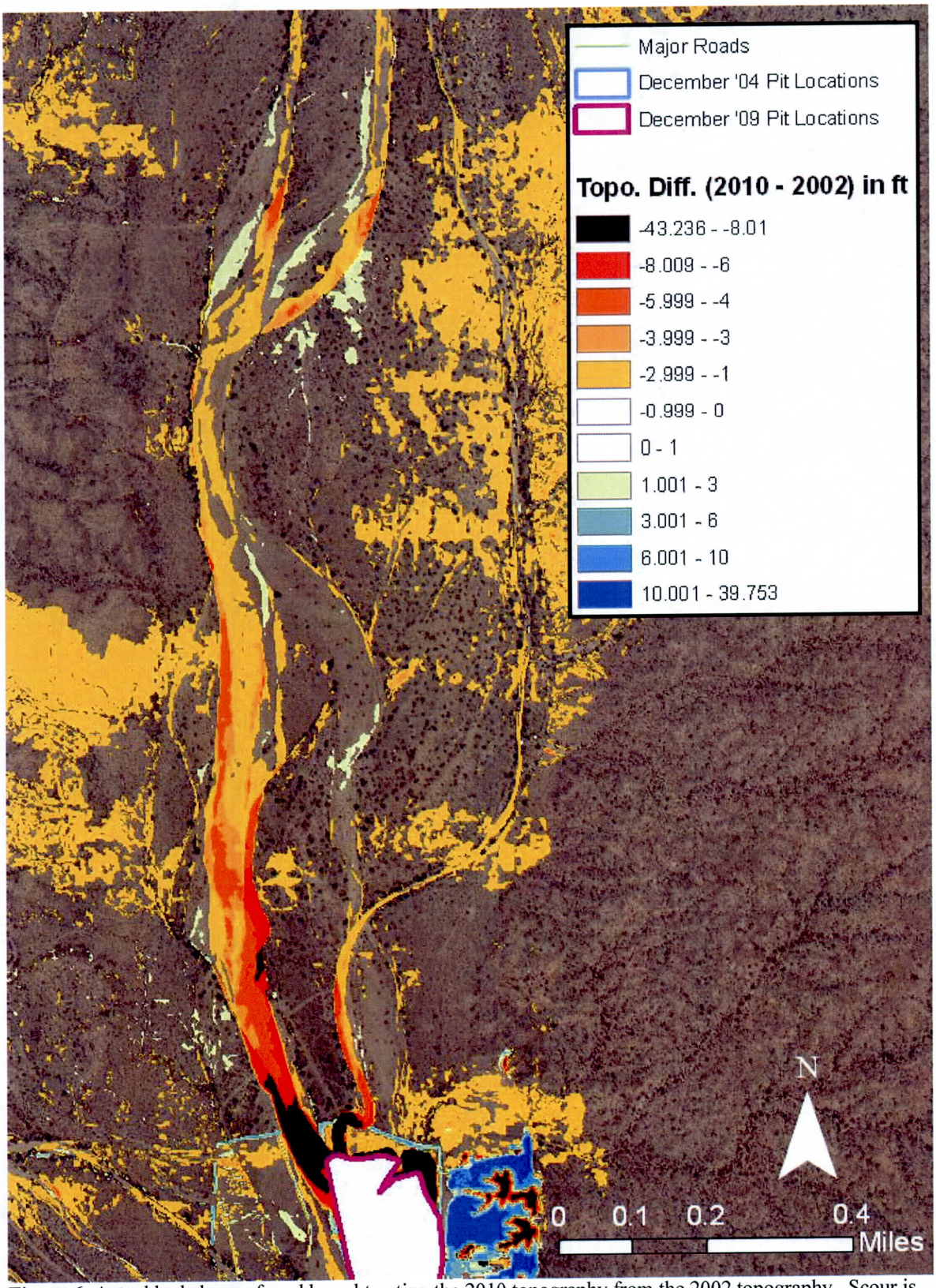

Figure 6. Actual bed change found by subtracting the 2010 topography from the 2002 topography. Scour is negative while aggradation is positive. The background aerial photograph is from May 2009.

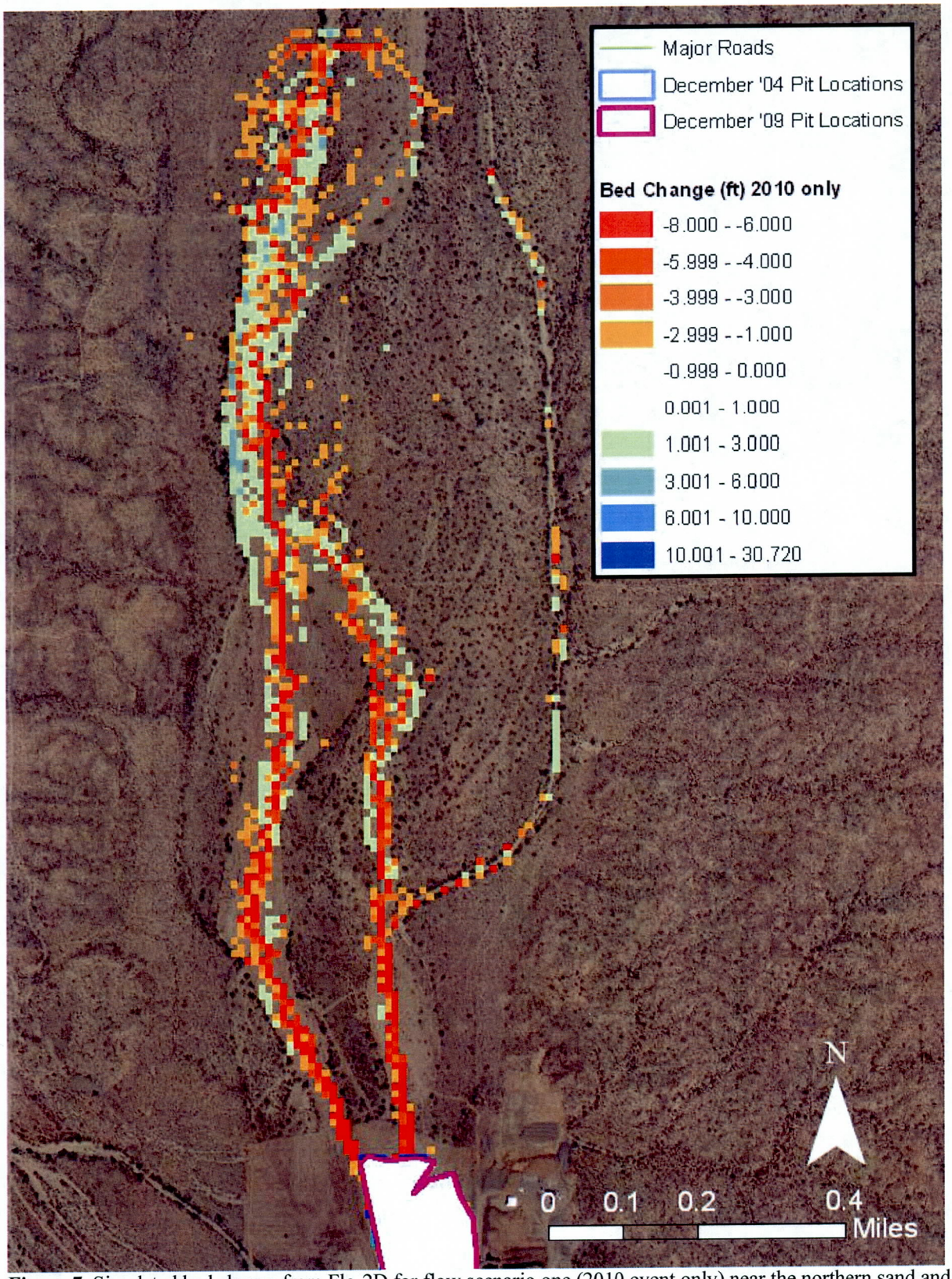

Figure 7. Simulated bed change from Flo-2D for flow scenario one (2010 event only) near the northern sand and gravel mine. Scour is negative while aggradation is positive. The background aerial photograph is from May 2009.

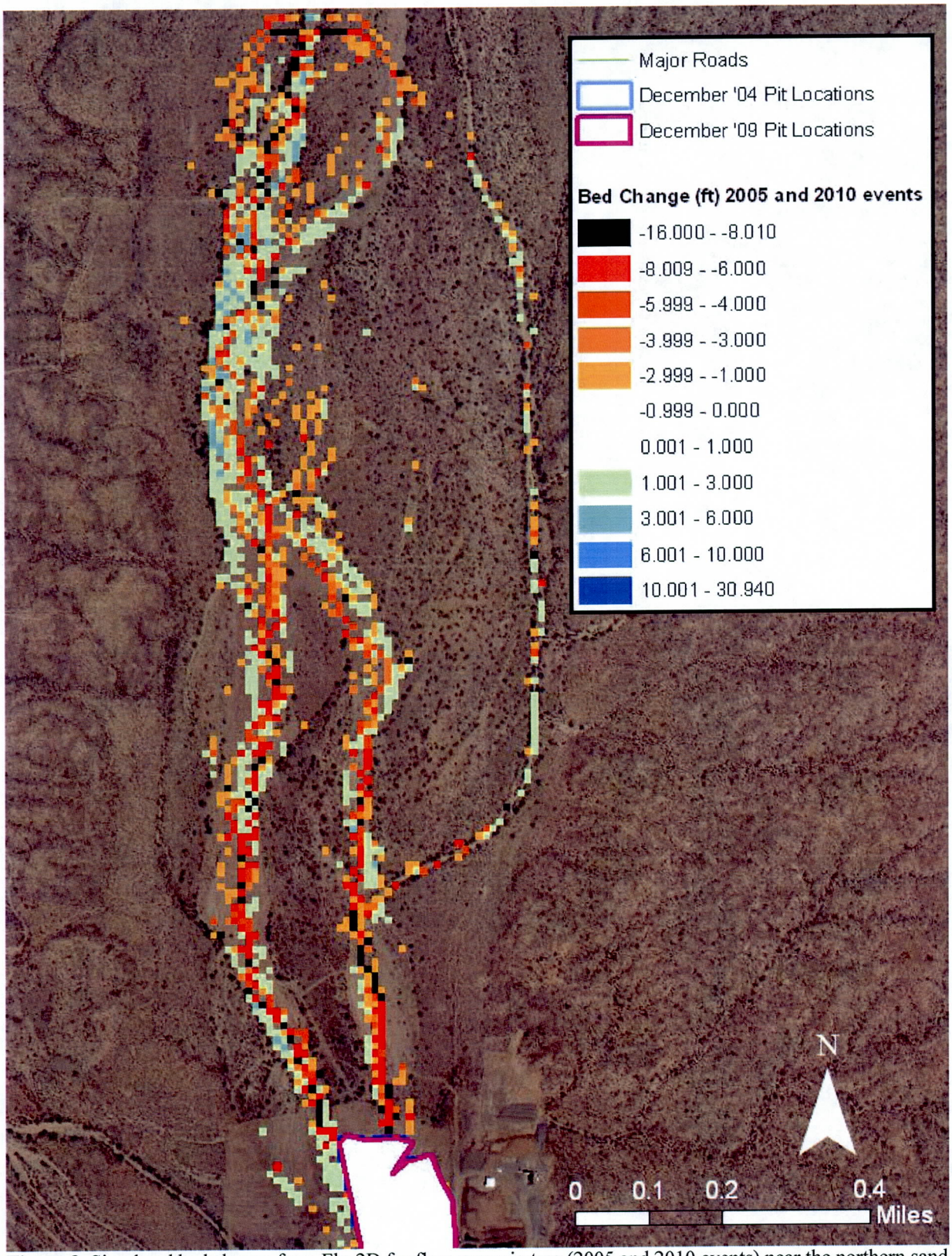

Figure 8. Simulated bed change from Flo-2D for flow scenario two (2005 and 2010 events) near the northern sand and gravel mine. Scour is negative while aggradation is positive. The background aerial photograph is from May 2009.

elevations were converted to a grid file, and that grid file was then converted to a triangulated irregular network (TIN). From the TIN, HEC-GeoRAS was used to extract the elevations at the same cross-section locations (that overlap the Flo-2D boundary) that were used in the HEC-6T and HEC-RAS modeling of the same two flow scenarios. For flow scenario two, the same basic procedure was followed. However, the bed change for the 2005 event was added to the initial elevations. Then, the 2009 mine elevations were added to the modified elevations, and finally, the bed change for the 2010 event was added to these modified elevations (with 2009 mines) to obtain the final elevations. The final elevations were the converted through the same process to a TIN. The same cross-section locations were then used to obtain the thalweg profile. The two Flo-2D profiles are compared with the 2010 profile and the initial profile, which is based on the 2002 topography with the 2009 estimate mine elevations. This comparison is shown in Figure 9. From this comparison, it appears that the depths were predicted reasonable well. However, there are two major issues with the results. First, the maximum scour is limited to 8 feet, and thus more simulations will be run to quantify if a maximum scour depth needs to be specified. The second major issue is that the bottoms of the mines are predicted to scour by Flo-2D. This result is not reasonable and needs further investigation. All digital files that are associated with the Flo-2D models are included on the attached DVD.

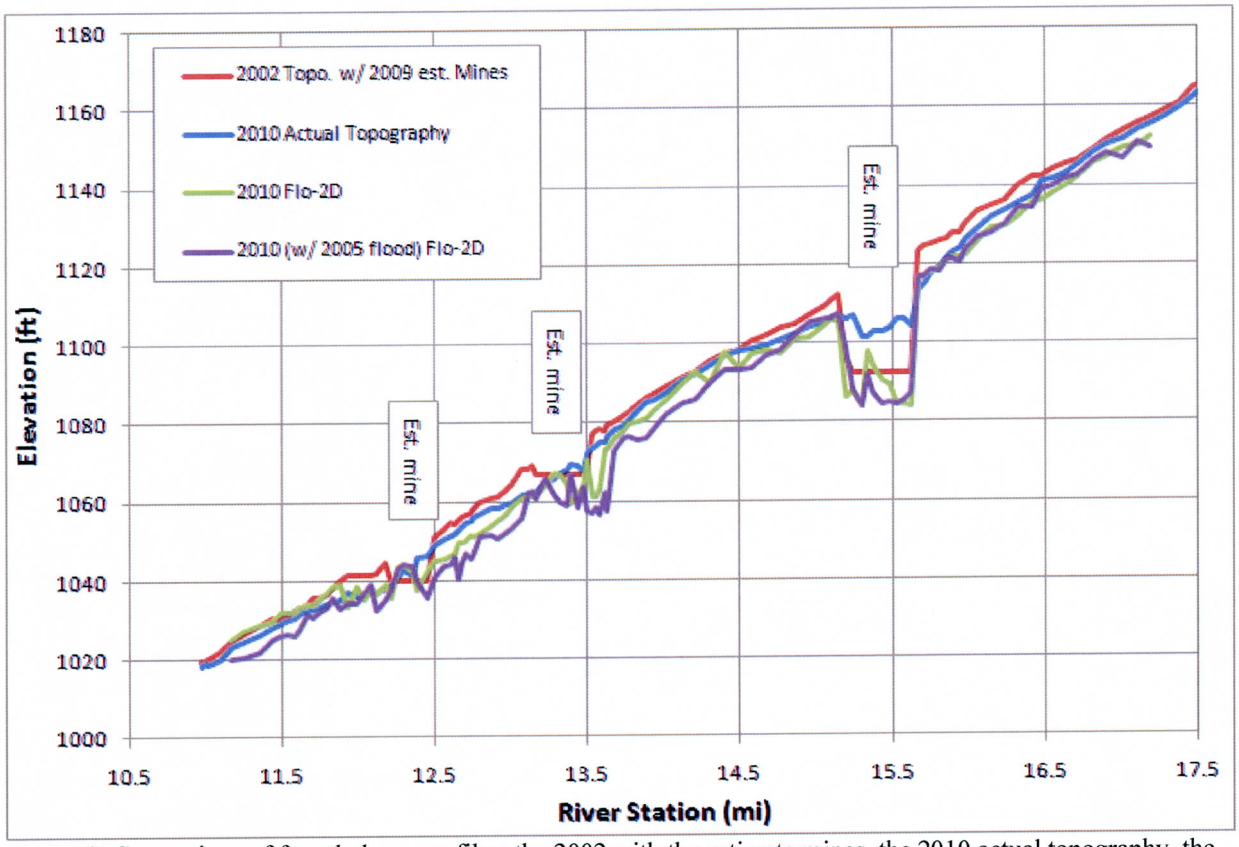

Figure 9. Comparison of four thalweg profiles: the 2002 with the estimate mines, the 2010 actual topography, the Flo-2D profile based on the 2010 event only and the Flo-2D profile based on the 2005 and 2010 events. The 2009 mine locations are noted on the chart.

7) **Sediment Transport Simulations (Verification):** In order to quantify the maximum scour, multiple simulations were run with different maximum scour depths. The first type of testing simulation that was done was with an unconfined (no maximum) scour depth and all other input variables the same as the previous simulations. For both flow scenarios, the computers were left to run over a month, but had only finished 25% of the simulation. Since this extreme run time indicated that the simulations would not finish, they were stopped, and the results were saved to the output files. From a review of the intermediate results, the maximum scour for the flow scenario one (2010 event only) was 267 feet, while the maximum scour for flow scenario two (2005 and 2010 events) was 268 feet. Both of these results are unreasonable and seem to indicate that a maximum scour depth needs to be defined. However, because of the extreme run time, flow scenario one was the only one used for subsequent simulations. A listing of all completed simulations and associated run times are listed in Table 1.

The next test used a maximum scour depth of 15 feet because the maximum scour of a headcut is generally half the mine depth. In this scenario, the deepest mine is about 25 feet deep, and 15 feet is just below half the depth. In theory, the maximum scour should not reach this depth. All other input variables remained the same. With the deeper depth, the simulation took longer to run than the 8 foot depth (Table 6), and the maximum scour again reached the specified maximum limit. For the next simulation, the maximum scour depth was limited to 30 feet, a depth just deeper than the deepest mine. Again, the maximum scour reached the specified limit.

When reviewing the results of all the simulations, the maximum velocities also appeared unreasonable (> 20 ft/s). Therefore, for the next simulation, a limiting Froude number of 2.0 was specified. This value was chosen to limit unreasonable velocities but still allow for supercritical flow at the mine brink. The maximum scour depth was limited to 30 feet, and

Table 1. Comparison of computer run times for the six different types of simulations. All simulations were run with detailed graphics. Without detailed graphics, the run times would be lower.

Simulation Number	Simulation Type	Flow Scenario One (hours)	Flow Scenario Two (hours)
1	Unconfined[1,2]	862.20386	862.5838
2	8 ft[3]	123.44585	407.97989
3	15 ft	307.69415	N/A
4	30 ft	315.43298	N/A
5	30 ft, 2.0 Fr Number	308.28940	N/A
6	30 ft, 2.0 Fr No., -1.0 Wave[4]	N/A	N/A

Notes:

[1]These simulations did not finish. They only completed about 25% of the hydrograph.

[2]For scenario two, the hydrograph that did not finish was the 2005 hydrograph.

[3]For scenario two, the hours are from the last simulation, which was the 2010 hydrograph.

[4]For scenario one, the simulation had 693 time step decrements and did not finish.

all other variables remained the same. The simulated maximum scour reached the limit of 30 feet, and the maximum velocity in the simulation was 34.93 ft/s. The final results with the limiting Froude number of 2.0 are very similar to previous simulations.

One final simulation was tested. This simulation limited the maximum scour to 30 feet. A limiting Froude number of 2.0 was used, but a value of -1.0 was used for the wave number. However, this simulation has over 600 time decrements and did not finish. Therefore, no meaningful results were obtained.

8) **Conclusions:** From the results of the various simulations, some conclusions can be made. The conclusions are

   a) Flo-2D spatially distributes the scour better than a one-dimensional model,

   b) the run times for a sediment transport model in Flo-2D are unreasonable to require Flo-2D sediment transport models for permit applications, and

   c) engineering judgment should be used to specify a maximum scour depth before Flo-2D is run.

9) **Attachment:** All digital files that are associated with the Flo-2D modeling have been included on the attached DVD.

References

Chang, H. H. 2009. Fluvial-12 Modeling of Sand Mining Impacts for Lower Hassayampa River. prepared for the Flood Control District of Maricopa County. August 2009.

JE Fuller Hydrology and Geomorphology, Inc. (JEF). 2006. Lower Hassayampa River Watercourse Master Plan, River Behavior Report.

Waskowsky, R. 2010. Data Collection and Modeling Approach for Selected River Mechanics Tasks of Phase II of the Lower Hassayampa Watercourse Master Plan (WCMP). Memorandum to Theresa Pinto. November 22, 2010.

APPENDIX IV

DISTRICT REPORT ON USE OF RIVERFLO-2D FOR MODELING OF HASSAYAMPA MINING REACH

Flood Control District
of Maricopa County

MEMORANDUM

Date: June 2nd, 2011

To: Theresa Pinto, CFM, Project Manager, Planning Branch, Planning and Project Management Division

From: Rafael Pacheco, Associate Engineer
Richard Waskowsky, Hydrologist
Engineering Application Development and River Mechanics Branch
Engineering Division

CC: Bing Zhao, PhD, PE, Engineering Application Development and River Mechanics Branch Manager, Engineering Division

Subject: RiverFlo-2D Modeling for Phase II of the Lower Hassayampa Watercourse Master Plan (WCMP) – Model Development and Results

This memorandum was prepared to document the development of the RiverFlo-2D models and the results from these models. The RiverFlo-2D models were prepared as a part of the river mechanics portion of Phase II of the Lower Hassayampa Watercourse Master Plan. The data collection for the RiverFlo-2D (and other software) models has been documented in the November 22, 2010 memorandum (Waskowsky, 2010).

The goal of the RiverFlo-2D modeling is to study the headcut/tailcut due to sand and gravel mines, in particular the Pioneer mine, for the major flows from 2002 to 2010. The modeling is divided into two scenarios. The first one is to model the January 2010 event only, while the second is to model the two largest events from 2002 to 2010.

The discussion below documents both the development of the models and the results from these models.

1) Data Collection: The documentation has been reported in the November 22, 2010 memorandum (Waskowsky, 2010). A copy of this memorandum is attached to the CD.
   1.1. Modeling Reach Determination (see Figure 1). The region was selected to encompass headcuts and tailcuts and to keep number of grid elements manageable, even for modern computer capabilities.
   1.2. Total reach length: approximately 6 miles
2) Input Data Development: in order to create the necessary data used by RiverFlo-2D it was necessary to create the bed elevation file. The creating of the required data was accomplished by creating the bed elevation in a Flo-2D format and transforming the data to a bed elevation file in the format

2801 West Durango Street Phoenix, Arizona 85009 Phone: 602-506-1501 Fax: 602-506-4601

required by RiverFlo-2D. The data development for RiverFlo-2D included some intermediate steps as outlined below. The Fortran file is located in the attached in a CD.

2.1. RiverFlo-2D

2.1.1. DTM (dated 2002) from Phase I of the Lower Hassayampa Watercourse Master Plan converted to a 5-foot grid ascii file.

2.1.2. The Flo-2D Grid Development System was used to develop a 50-foot grid, as well as a 20-foot grid.

2.1.3. Figures 2 and 3 below are schematics of hydrographs of two events measured in 2010 and 2005. These values were measured by the FCDMC gage at I-10. These hydrographs are used as an upstream boundary conditions for RiverFlo-2D.

2.1.4. The elevations of the grid elements were modified to include the pits (see Figures 4 and 5)

2.1.5. For the downstream boundary condition RiverFlo-2D does not allow currently allow for an open boundary condition. Therefore, a rating curve was developed from the HEC-RAS model of the Lower Hassayampa Master Course. The original and modified files are also attached in the CD.

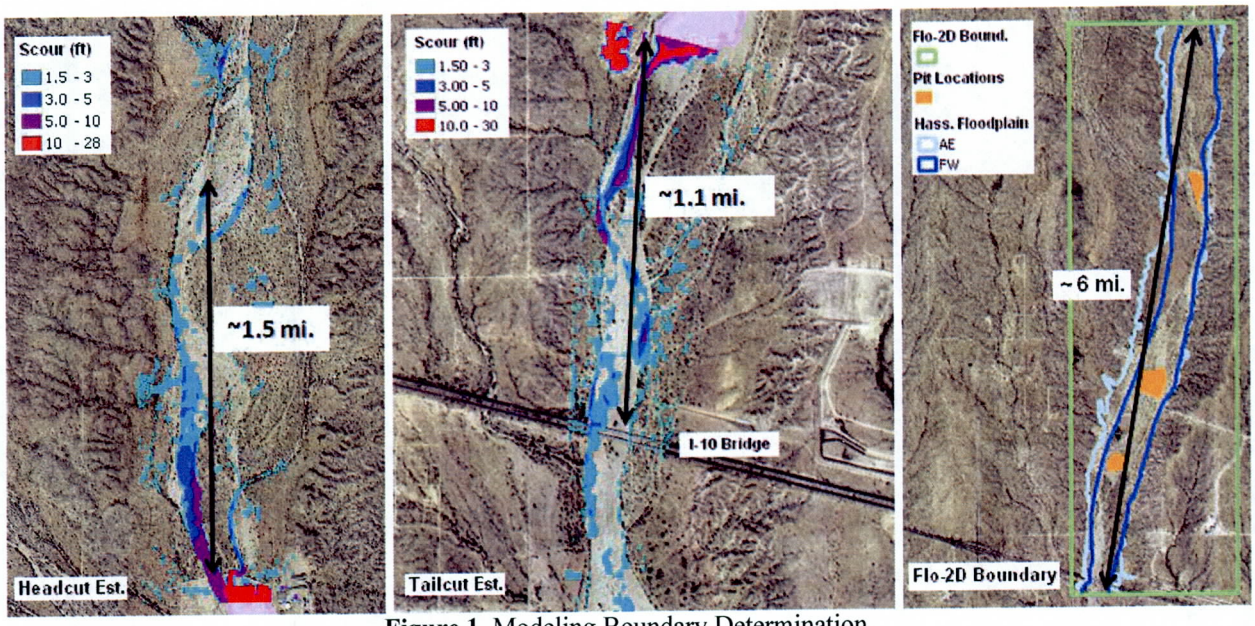

Figure 1. Modeling Boundary Determination.

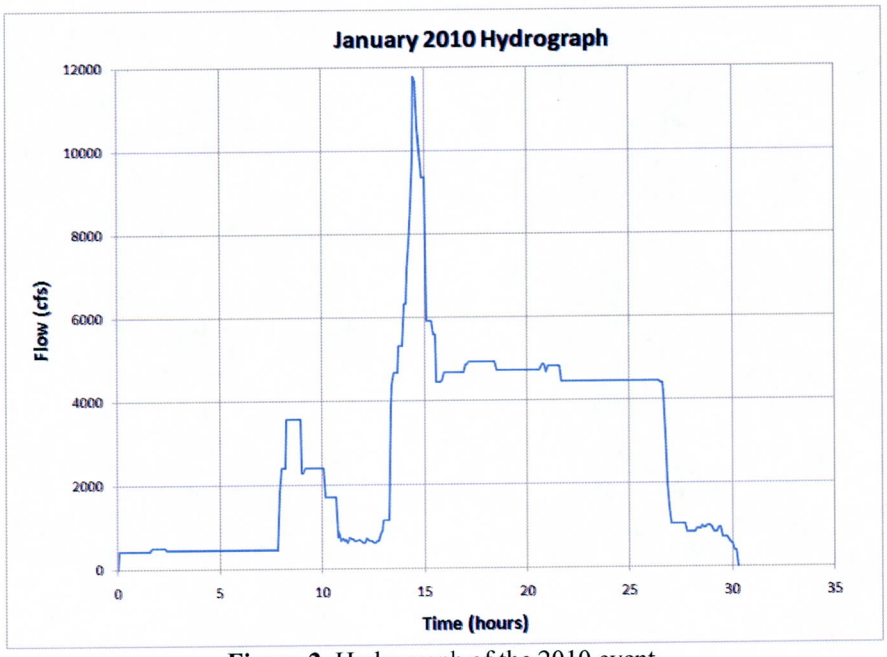

Figure 2. Hydrograph of the 2010 event.

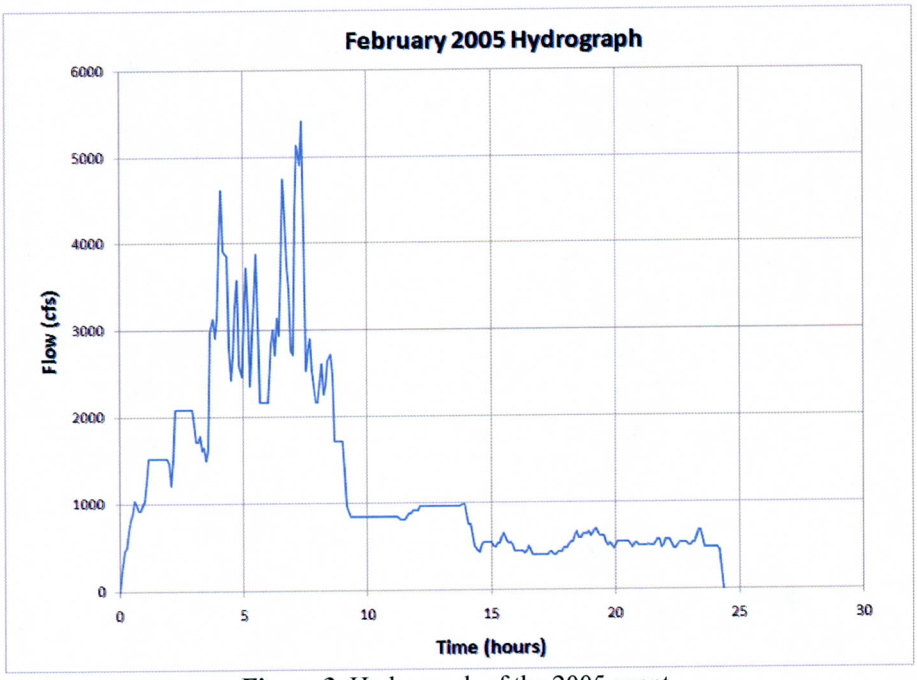

Figure 3. Hydrograph of the 2005 event.

2801 West Durango Street Phoenix, Arizona 85009 Phone: 602-506-1501 Fax: 602-506-4601

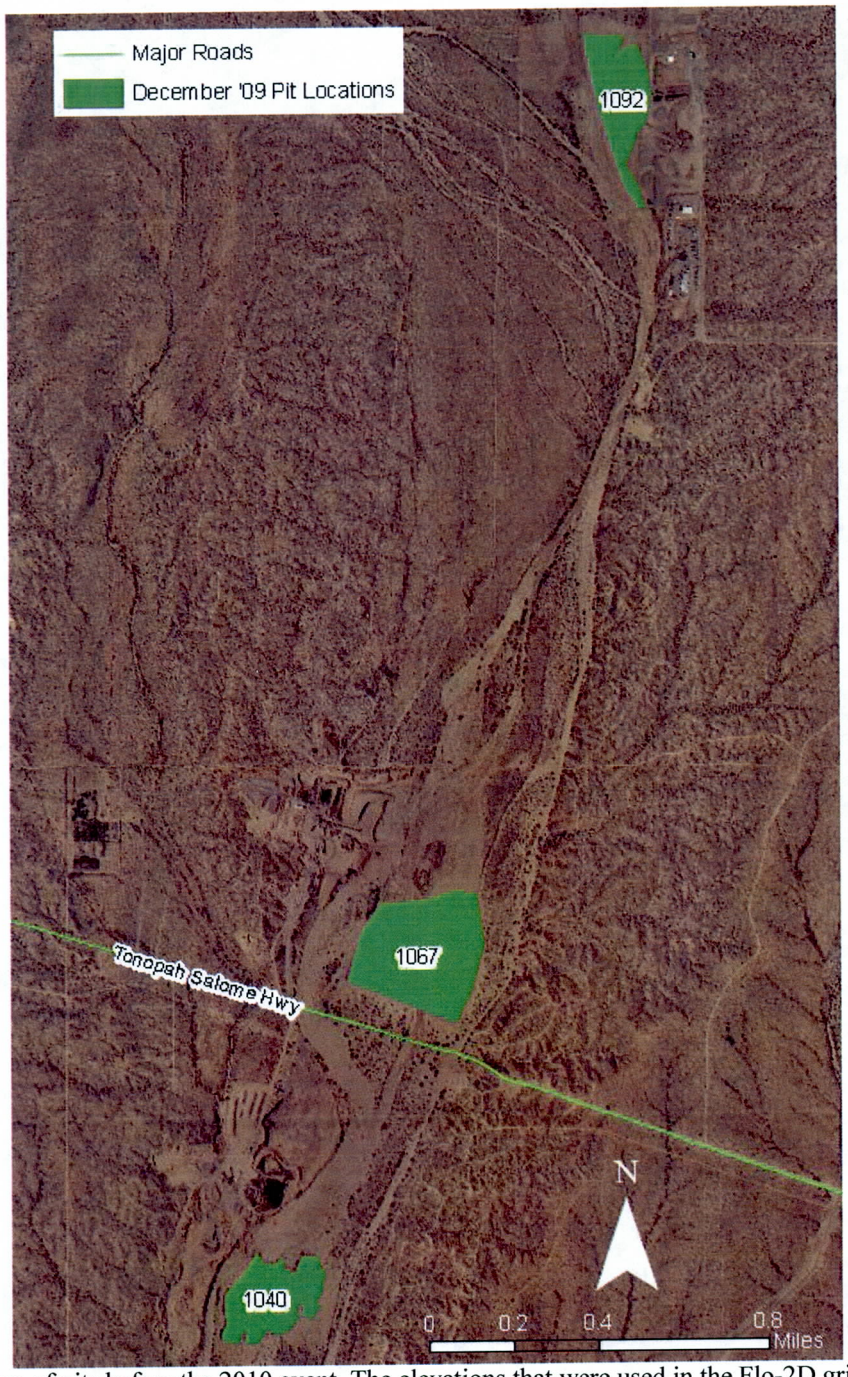

Figure 4. Location of pits before the 2010 event. The elevations that were used in the Flo-2D grid are shown over the pit locations.

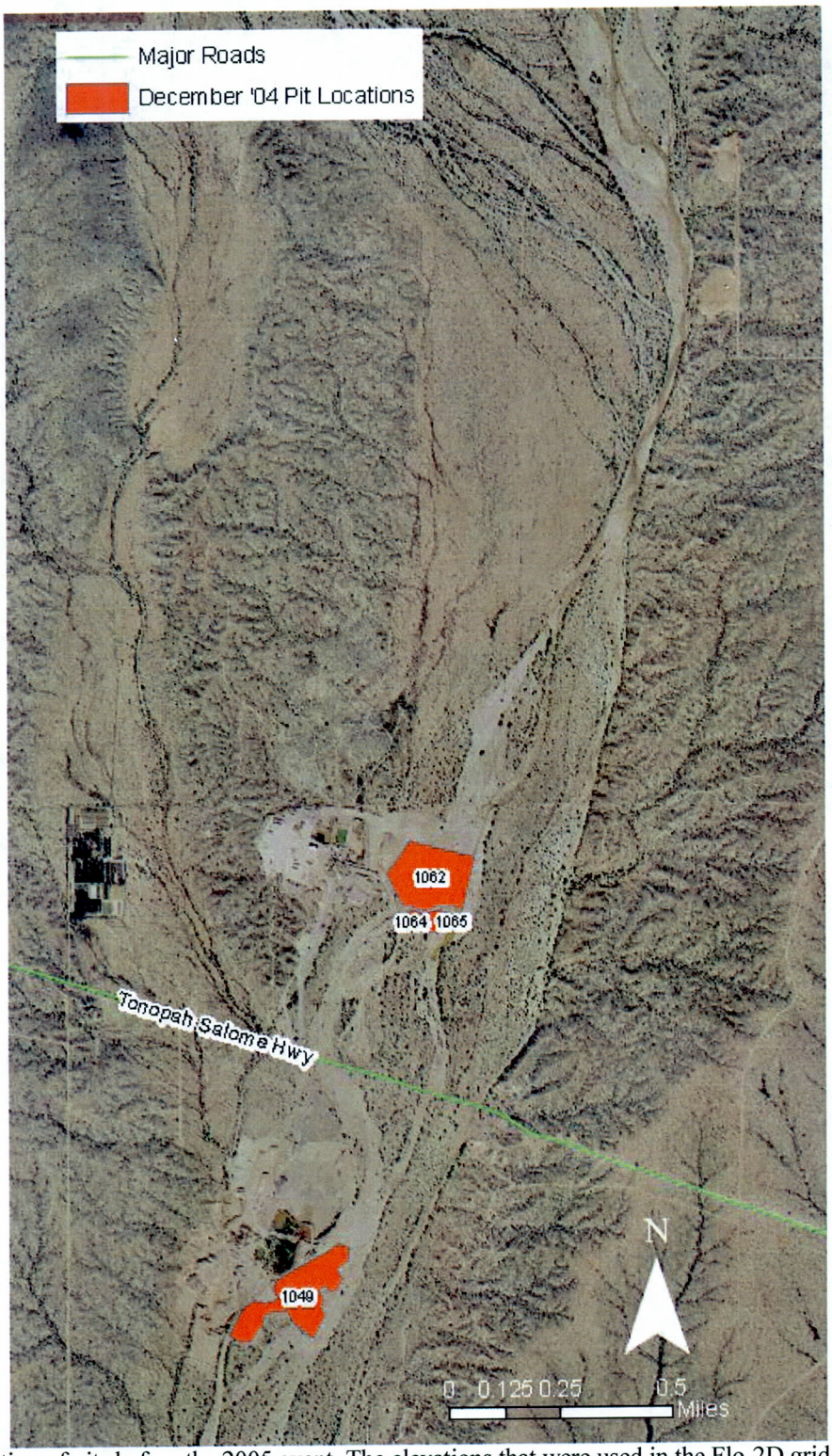

Figure 5. Location of pits before the 2005 event. The elevations that were used in the Flo-2D grid are shown over the pit locations.

3) RiverFlo-2D modeling

3.1. Finite element grids of different densities were generated from a large polygon of density 200 (ft), a polygon surrounding the floodplain of density 50 (ft) and smaller polygons of density 20 (ft) which correspond from north to south to the Pioneer pit, the CEMEX pit and the Hanson pit. Figure 6 shows the locations of the different densities of the elements.

3.2. 2010 event only simulation

3.2.1. Hydraulic modeling

3.2.1.1. Total simulated time was 20 hours.

3.2.1.2. Hydraulic results were reasonable. The program appeared to work well.

3.2.2. Sediment Transport Modeling

3.2.2.1. The Engelund-Hansen sediment transport equation was used.

3.2.2.2. The simulation did not finish and reasonable results were not obtained.

3.3. 2005 and 2010 Events simulation

3.3.1. Since the 2010 event only sediment transport simulation did not finish. The 2005 and 2010 events simulation was not run.

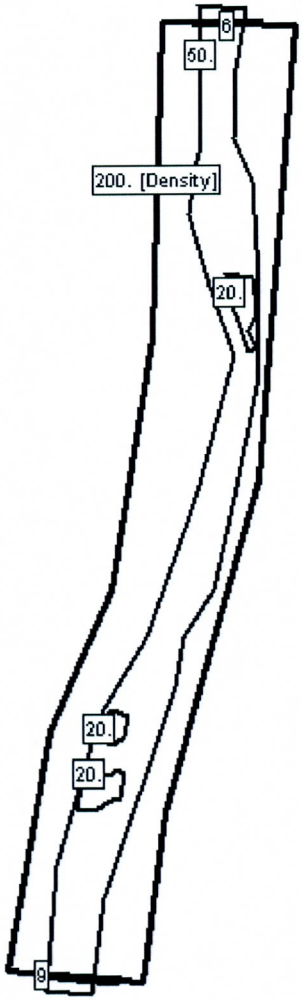

Figure 6. Polygons describing the density of the grid.

4) RiverFlo-2D Results: Results at t=6:45 (6 hours, 45 minutes) without and with sediment are shown in figures 7 and 8. Figure 7 shows velocities near the Pioneer pit in the neighborhood of 10 ft/s, while the velocities at the same location in the sediment transport simulation are unreasonably high. Figure 8 shows the velocity vectors from the sediment transport simulation. Both Figures 7 and 8 use the same scale and the input hydrographs were the same. Therefore, it was expected to see similar velocity vectors. However, from Figure 8, the velocity vectors are much longer, which indicates that the vectors are much larger than those in Figure 7.
   4.1. Two versions of the RiverFlo-2D model were used. The first version included the executables, riverflo-2dgr.exe and RiverFLO-2Dm.exe, which were compiled on January 18, 2011. The second version included the executables, riverflo-2dgr.exe and RiverFLO-2Dm.exe, which were compiled on March 9, 2011.
   4.2. No reasonable results were able to be obtained from the sediment transport simulation using the Engelund-Hansen sediment transport function.
   4.3. Some results were obtained using other sediment transport equations (i.e. the MPM formula), but these results did not correlate with the physical observations.
   4.4. The developer of the RiverFlo-2D was notified about the erroneous results from the sediment transport simulation.

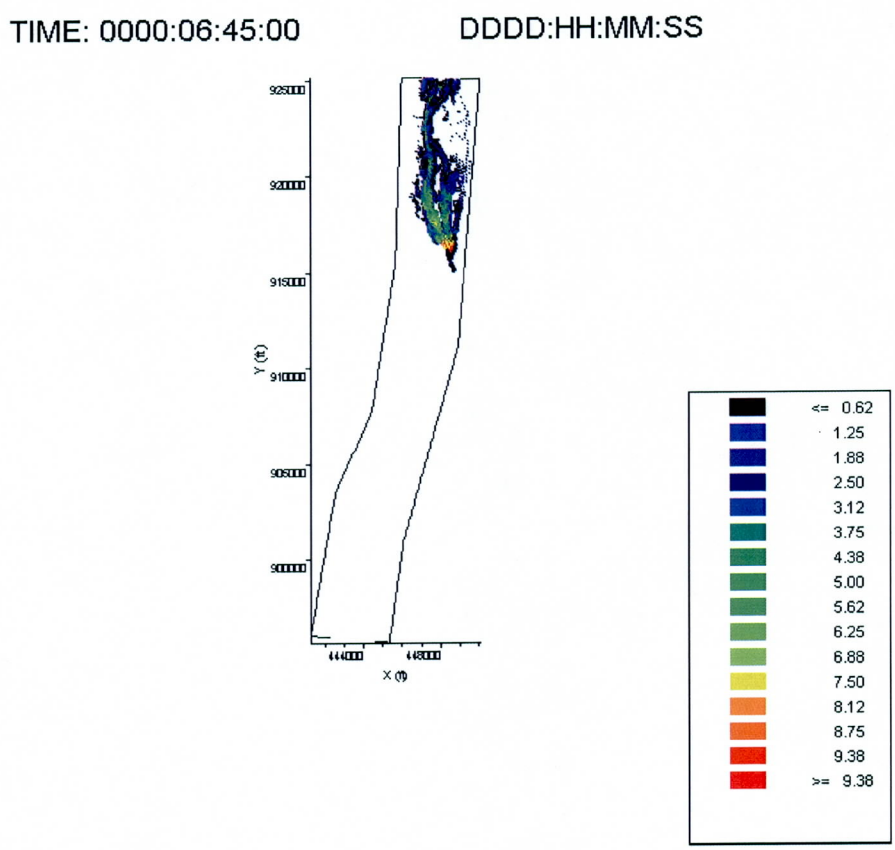

Figure 7. Velocity vectors for the 2010 event without sediment.

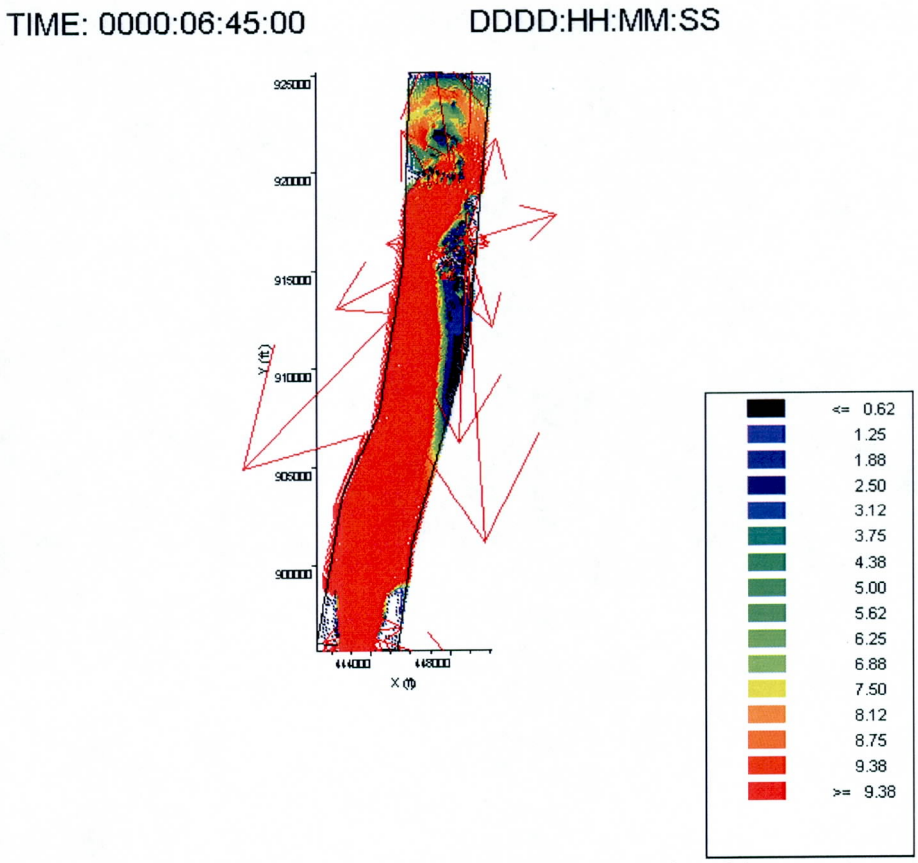

Figure 8. Velocity vectors for the 2010 event with sediment. Note the extreme size of the vectors.

References

Chang, H. H., 2009, *Fluvial-12 Modeling of Sand and Mining Impacts for Lower Hassayampa River*, prepared for the Flood Control District of Maricopa County, August 2009. FCD Call Number: A346.902S

JE Fuller Hydrology and Geomorphology, Inc. (JEF), 2006, *Lower Hassayampa River Watercourse Master Plan, River Behavior Report*, Final HEC-6 model dated May 2007

RiverFLO-2D, 2009a, Two-Dimensional Finite-Element River Dynamics Model - Input and Output Files Reference Manual, Release 2009.

RiverFLO-2D, 2009b, Tutorials, Release 2009.

Waskowsky, R., 2010, *Data Collection and Modeling Approach for Selected River Mechanics Tasks of Phase II of the Lower Hassayampa Watercourse Master Plan (WCMP)*, memorandum to Theresa Pinto, November 22, 2010.

WEST Consultants, Inc. (WEST), 2006, *Lower Hassayampa River Watercourse Master Plan, Final Hydraulics Report, Hassayampa River*, Prepared for JE Fuller Hydrology & Geomorphology, Inc.

APPENDIX V

HOWARD CHANG's REPORT:

MODELING PIT HEADCUT/TAILCUT IN LOWER HASSAYAMPA RIVER FOR MAJOR RECENT FLOODING EVENTS

JUNE 2011

Mining Pit Headcut/tailcut Modeling in Lower Hassayampa River for Major Recent Flooding Events

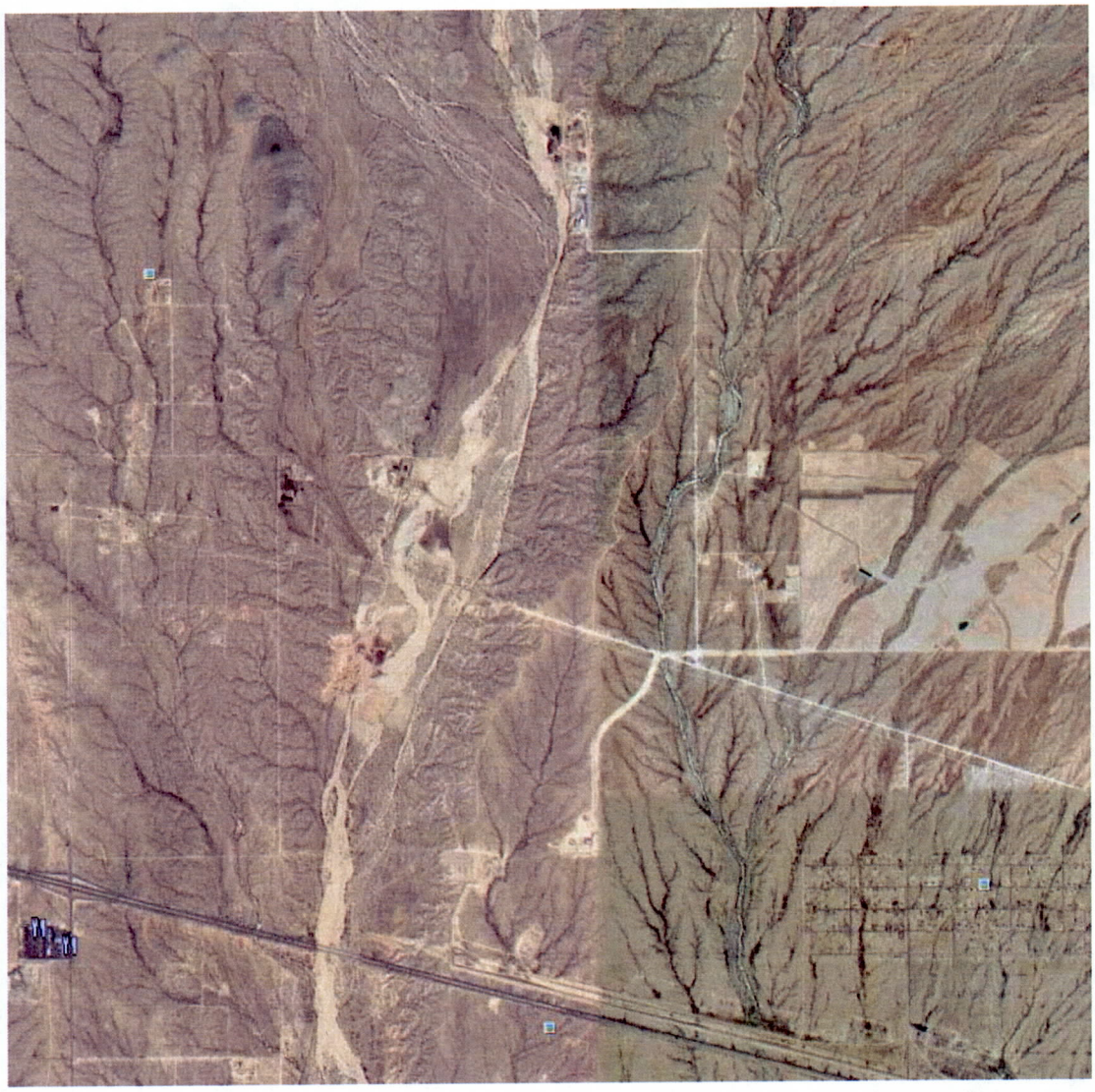

Prepared for
Engineering Application Development and
River Mechanics Branch
Engineering Division
Flood Control District of Maricopa County

Prepared by
Howard H. Chang
Chang Consultants
June 2011

CHANG Consultants Hydraulic and Hydrologic Engineering Erosion and Sedimentation	P.O. Box 9492 6001 Avenida Alteras Rancho Santa Fe, CA 92067-4492 TEL: (858) 756-9050, (858) 692-0761 FAX: (858) 756-9460

TABLE OF CONTENTS

EXECUTIVE SUMMARY 1

I. INTRODUCTION 5
River Data 5
Modeling Approach 11

II. PERFORMANCE INDEX 11

III. MODEL CALIBRATION 12
Selection of Sediment Transport Formula Based on Simulated River Channel Changes near Pioneer Site 12
Comparison of Modeled Results on Sediment Delivery 14
Selection of Channel Roughness Coefficient 15
Performance Index for Calibration Results 15

IV. CALIBRATION AND PERFORMANCE INDEX BASED ON 2010 FLOOD ONLY .. 18

V. FLUVIAL-12 MODELING OF BOTH 2005 AND 2010 FLOOD EVENTS 29
(for February 11-12, 2005 event and January 20-21, 2010 event modeling)
Simulation of Headcut/Tailcut 30

VI. HEADCUT AND TAILCUT NEAR THE PIONEER MINING SITE 31

VII. COMPARISON OF MODELING RESULTS FOR ONE FLOOD AND TWO FLOODS 41
Discussion of Study Results 42

VIII. SUMMARY OF COMPUTER FILES USED IN THE STUDY 43

REFERENCES 43

APPENDIX A. INPUT/OUTPUT DESCRIPTIONS FOR FLUVIAL-12 44

ATTACHMENTS

COMPUTER FILES FOR NON-CALIBRATED GROUP

HASSA-CUT.FLU: FLUVIAL-12 input file for 2010 flood only

HASSA-CUTEH.OUT: FLUVIAL-12 output file for 2010 flood only using Engelund-Hansen formula

HASSA-CUTY.OUT: FLUVIAL-12 output file for 2010 flood only using Yang formula

COMPUTER FILES FOR CALIBRATED GROUP

HASSA-CUTEH.FLU: FLUVIAL-12 input file for 2010 flood only using Engelund-Hansen formula

HASSA-CUTEH.OUT: FLUVIAL-12 output file for 2010 flood using Engelund-Hansen formula

HASSA-EH05.FLU: FLUVIAL-12 input file using 2005 channel data and Engelund-Hansen formula

HASSA-EH05.OUT: Output file produced by HASSA-EH05.FLU

HASSA-EH10.FLU: FLUVIAL-12 input file using the output channel data from HASSA-EH05.OUT plus the mining site data just before 2010 flood

HASSA-EH10.OUT: FLUVIAL-12 output file produced by HASSA-EH10.FLU using the Engelund-Hansen formula and the 2010 flood

HASSA-Y05.FLU: FLUVIAL-12 input file using 2005 channel data and Yang formula

HASSA-Y05.OUT: Output file produced by HASSA-Y05.FLU executed for 2005 flood

HASSA-Y10.FLU: FLUVIAL-12 input file using output channel data from HASSA-Y05.OUT plus mining site data just before 2010 flood

HASSA-Y10.OUT: FLUVIAL-12 output file produced by HASSA-Y10.FLU using Yang formula and 2010 flood.

EXECUTIVE SUMMARY

The sand and gravel mining operations in the lower Hassayampa River have created three pits: Pioneer Pit, Cemex Pit, and Hanson Pit. Significant flooding events on February 11-12, 2005 and January 20-21, 2010 have caused headcuts and tailcuts near the sand and gravel mining pits. The headcut and tailcut modeling study has been made following two approaches. The first approach is to model the January 20-21, 2010 event using 2002 topographic data as the basis and using the pit configuration to modify the topographic data. The pit configuration is estimated for the condition prior to the January 20-21, 2010 event.

For modeling the January 20-21, 2010 event, three pits were incorporated into the initial topographic data. Chang Consultants used these cross sections to develop a FLUVIAL-12 model with Engelund-Hansen transport equation. All other parameters are based on the same parameters from R2D's HEC-6T and HEC-RAS sediment transport models. The mathematical models of FLUVIAL-12 and HEC-RAS are developed to simulate the hydraulics of flow, sediment transport, and river channel changes. Calibration of the FLUVIAL-12 model was made in order to mach the modeled results with measurement.

Simulated Results on Sediment Delivery — Sediment delivery is defined as the cumulative amount of sediment that has been delivered passing a certain channel section for a specified period of time. The spatial variation of sediment delivery along the river channel is simulated by FLUVIAL-12. The simulated results show that sediment delivery increases as the flow approaches a mining site. This increase in sediment delivery indicates erosion of the river bed in the process of headcut. The sediment delivery increases as the flow leaves the mining site, indicating erosion in the process of tailcut. The sediment delivery decreases through the three mining sites, indicating deposition since there is more sediment inflow than outflow. Channel changes near the mining sites are simulated by the FLUVIAL-12. Such changes are characterized by headcut upstream of the mining site, sediment deposition in the pit, and tailcut downstream of the pit.

Calibration Study — Topographic survey of the river channel made after the 2010 flood was used to calibrate the modeling results for headcut/tailcut. The purpose of calibration is to match the simulated results for headcut/tailcut with the measurement. To accomplish this objective, the roughness coefficient, the sediment transport formula, and the bank erodibility factor were selected in modeling experiments. In the calibration study, the roughness coefficient that produces the best correlation of simulated and measured results was determined to be 0.026 through modeling experiments. The Engelund-Hansen formula and the Yang formula for sediment transport were used in the FLUVIAL-12 model. The results generated by these sediment transport formulas were compared with the survey. The post-flood channel bed generated by the Engelund-Hansen formula is in general agreement with the post-flood survey. However, the post-flood channel bed generated using the Yang formula correlates poorly with the survey. Model calibration using the Yang formula failed. All other results as presented in the report are based on the Engelund-Hansen formula.

In the FLUVIAL-12 model, the bank erodibility factor (BEF) is the parameter that governs the rate of bank erosion and width change. The width change also affects channel bed aggradation and degradation since these changes are inter-related. In the calibration study, the

BEF value that provides the best correlation of simulated and surveyed results was selected. This value was varied in modeling runs in order to select the value that provides the best correlation of modeling results with the measurement. The BEF value was determined to be 1.0 through this process. This BEF value means that the bank of the headcut/tailcut channel is as erodible as the channel bed for the Hassayampa River.

The simulated results with calibration are presented in two figures. The first figure shows the simulated changes in channel bed profile compared the post-flood survey based on the 2010 flood only. The second figure shows longitudinal bed profile changes simulated using both the 2005 and 2010 floods, also compared with the post-flood survey. The simulated post-flood channel bed profiles for both cases compare favorably with the post-flood survey.

Modeled Results Based on 2010 Flood Only — Channel changes due to headcut/tailcut near the Pioneer pit are shown in the first figure. Headcut developed along the channel reach upstream of the Pioneer site. The headcut zone is from the Pioneer pit at section 15.67 to section 16.72 for a total channel length of about 1 mile. For the channel reach downstream of the Pioneer site, the tailcut zone is from the downstream edge of the Pioneer pit at section 15.15 down to section 14.77 for a total channel length of about 0.5 mile.

River channel changes along reaches near the Cemex site and the Hanson site were caused by both river channel scour and sand mining. The effects of these two factors on channel changes can not be separated; therefore, no attempt is made to determine the scour depth due to headcut/tailcut.

Modeling Using 2005 and 2010 Floods — Two steps were taken in modeling the February 11-12, 2005 event and January 20-21, 2010 event. The first step is to use the LHWMP-Phase I topographic data that has incorporated the mining pits configuration into the topographic data provided to Chang Consultants as HEC-RAS cross-sections. After the Fluvial-12 modeling of the 2005 flood, the original cross-section data were changed by Fluvial-12 at the end of the simulation due to river channel changes. Chang Consultants converted the output simulated by FLUVIAL-12 for the 2005 event into the input data for the 2010 flood event.

After the Fluvial-12 modeling of the 2005 flood, the original cross-section data were changed by Fluvial-12 at the end of the simulation due to river channel changes. Chang Consultants converted the output simulated by FLUVIAL-12 for the 2005 event into the input data for the 2010 flood event. Chang Consultants modeled the January 20-21, 2010 event based on the end-of-simulation cross-section data after the 2005 event. The cross-section data were then revised by incorporating the pit configuration prior to the January 2010 event.

The simulated changes in channel geometry due to headcut/tailcut are compared with the surveyed results. Headcut developed along the channel reach upstream of Pioneer pit. The headcut reach from the simulated results is from section 15.67 at the upstream edge of the mining pit to section 16.82 for a total channel length of about 1.1 miles. Tailcut developed along the channel reach downstream of the Pioneer pit. The tailcut zone is from the downstream edge of the Pioneer pit at section 15.20 down to section 14.60 for a total channel length of about 0.6 mile.

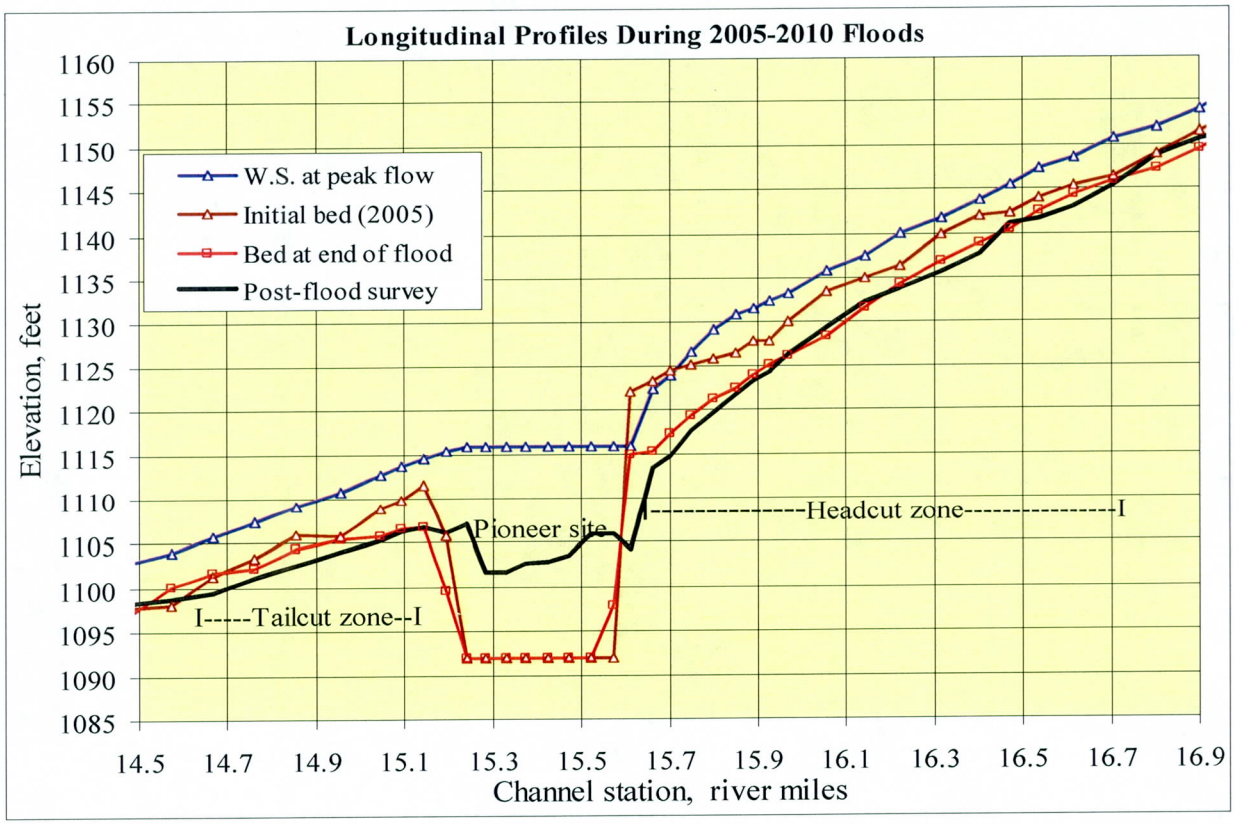

Simulated channel bed profile changes based on 2010 flood together with post-flood survey

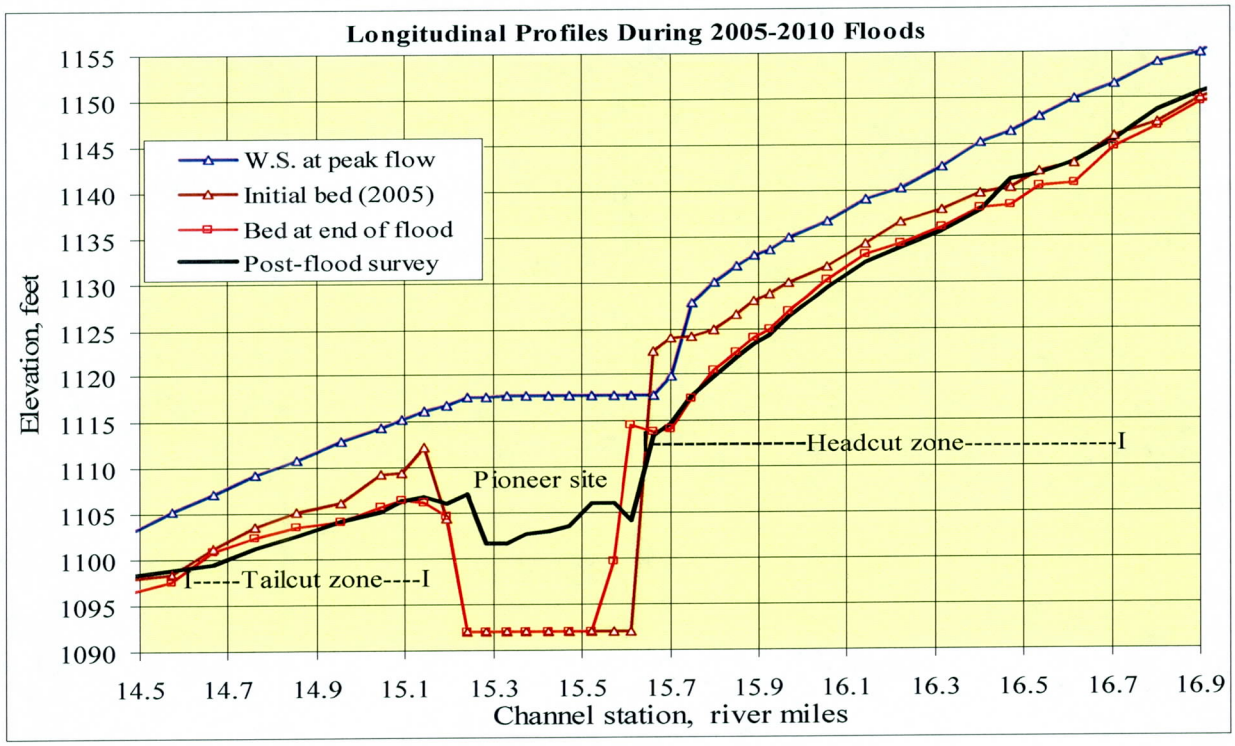

Simulated channel bed profile changes based on both 2005 and 2010 floods together with post-flood survey

Simulated changes in longitudinal profiles near the Cemex and Hanson mining sites were compared. The comparison of the surveyed post-flood channel bed profile with the simulated bed profile changes shows no clear pattern of headcut/tailcut. It is also easy to see that the channel bed was affected by sand and gravel mining during the period from 2005 to 2010, in addition to mining activities prior to 2005. The effects of mining and headcut/tailcut induced by the mining sites can not be separated along this river reach.

Performance Indices — A Performance Index is used to assess the correlation of the simulated and surveyed results for headcut and tailcut. The Absolute Performance Index, *API*, is defined by the following equation:

$$API = \Sigma_{i=1}^{n} \frac{|M_i - C_i|}{n}$$

where M_i is the measured headcut/tailcut depth (positive values) or deposition depth (negative values), C_i is the computed headcut/tailcut depth (positive values) or deposition depth (negative values), and n is the number of cross-sections. The performance index represents the deviation of the simulated value from the surveyed value for headcut/tailcut. To assess the modeling results for the two approaches, the computed API's for the scour depths are compared as summarized in the table below.

Comparison of Absolute Performance Indices with Calibration

Cases	Absolute Performance Index API	
	Based on 2010 flood only	Based on 2005 and 2010 events
Headcut depth above Pioneer pit	1.05 feet	0.85 foot
Tailcut depth below Pioneer pit	1.02 feet	0.56 foot

The API values indicate that the differences of simulated and measured scour depths for headcut/tailcut are approximately one foot based on the results from the 2010 flood. The differences of simulated and measured scour depths are less than one foot based on the results of both the 2005 and 2010 floods. For these reasons, the correlations of simulated and measured headcut/tailcut depths near the Pioneer pit are generally good. The modeling results from both flood events have better correlations with measurement than the case of one flood only. This is expected since the scour depths developed during both floods.

The performance indices presented in the report are based on channel bed scour. In addition to the scour depth, simulated changes in cross-sectional profiles for the two cases are also presented in the report. The simulated cross-sectional changed based on both the 2005 and 2010 floods are similar to the surveyed cross sectional profiles. However the cross-sectional profiles based on the 2010 flood only are not as well correlated with the surveyed results. In summary, model study using both the 2005 and 2010 floods has improved the correlation with measurement.

Discussion of Study Results — The comparisons show that the differences between simulated and measured headcut/tailcut depths induced by the mining pits are generally small. In other words, the correlations of simulated and measured scour depth are considered good. Such results were achieved through the calibration process.

Certain sources for the discrepancy between the simulated and measured results can be cited. Channel morphology associated with headcut/tailcut is normally characterized by the formation of narrow and deep gullies. However, the channels formed by headcut/tailcut for this case are generally wider and larger in cross-sectional area than a typical gulley. The discrepancies are attributed to several factors. An important factor is the fact that the Hassayampa River has a broad floodplain with a highly braided channel pattern. Because of multiple channel branches, headcut/tailcut changes induced by the mining pit are also affected by the presence of other channel branches. The tributary inflow from Jackrabbit Wash has significant effects on channel morphology downstream of the Pioneer pit, as the large width is closely related to the lateral inflow from Jackrabbit Wash. The effects of lateral inflow on channel morphology at this location were not simulated in modeling.

Mining Pit Headcut/tailcut modeling in Lower Hassayampa River for Major Recent Flooding Events

I. INTRODUCTION

Significant flooding events on February 11-12, 2005 and January 20-21, 2010 have caused headcuts and tailcuts for the sand and gravel mining pits in the Lower Hassayampa River shown in Figures 1, 2, and 3. After the January 20-21, 2010 flooding event, new topographic data were obtained for a reach of 13 miles in the river. The purpose of this study is to use Fluvial-12 to model these flooding events using pre-2005 flooding topographic data as the initial condition to predict the headcut and tailcut and then compare the results with the new 2010 topographic data. The sand and gravel pits will be included to revise the topographic data since there were sand and gravel operations during the period. Both the original modeling results (without calibration) and the calibrated modeling results will be reported as compared with the observed new 2010 topographic data. All the results will be compiled into another report by R2D for comparison with HEC-6T and HEC-RAS sediment transport modeling results.

River Data - According to the Flood Control District of Maricopa County (FCDMC), the initial topographic data for the sediment transport modeling is based on the Lower Hassayampa River Watercourse Master Plan (JE Fuller, 2006, 2007). The topographic dates for the initial topographic data range from 4/2002 to 4/2004. This topographic data may be called Lower Hassayampa River Watercourse Master Plan Phase I (LHWMP-Phase I) topographic data. The topographic date for the new 2010 topographic data is dated 5/1/2010. The two major flooding event dates are February 11-12, 2005 and January 20-21, 2010 with the peak flows of 5500 cfs and 11600 cfs, respectively. The peak flows and flow hydrographs are based on FCDMC's stream gage at I-10. FCDMC has provided Chang Consultants the flow hydrographs.

There have been sand and gravel pit operations. Figure 2 shows the locations of the Pioneer Pit, Cemex Pit, and Hanson Pit. Figure 3 shows the river bed topography near the Pioneer pit. The following table shows the activities for these three pits.

Table 1. Estimated mine depths and areal extents (Waskowsky, 2010)

	Hanson		Cemex*		Pioneer	
	Depth (ft)	Area (acres)	Depth (ft)	Area (acres)	Depth (ft)	Area (acres)
2002 (information only)	4	0.5	12, 20	4.3	N/A	N/A
2004 (before '05 events)	5-9	15	10-15, 10-15, 15-20	1.1, 1.1, 14	N/A	N/A
2005 (after '05 events)	5-9	10	mine filled	mine filled	8-10	3.3
2009 (before Jan. 2010 event)	10	22	10	45	28-30	23

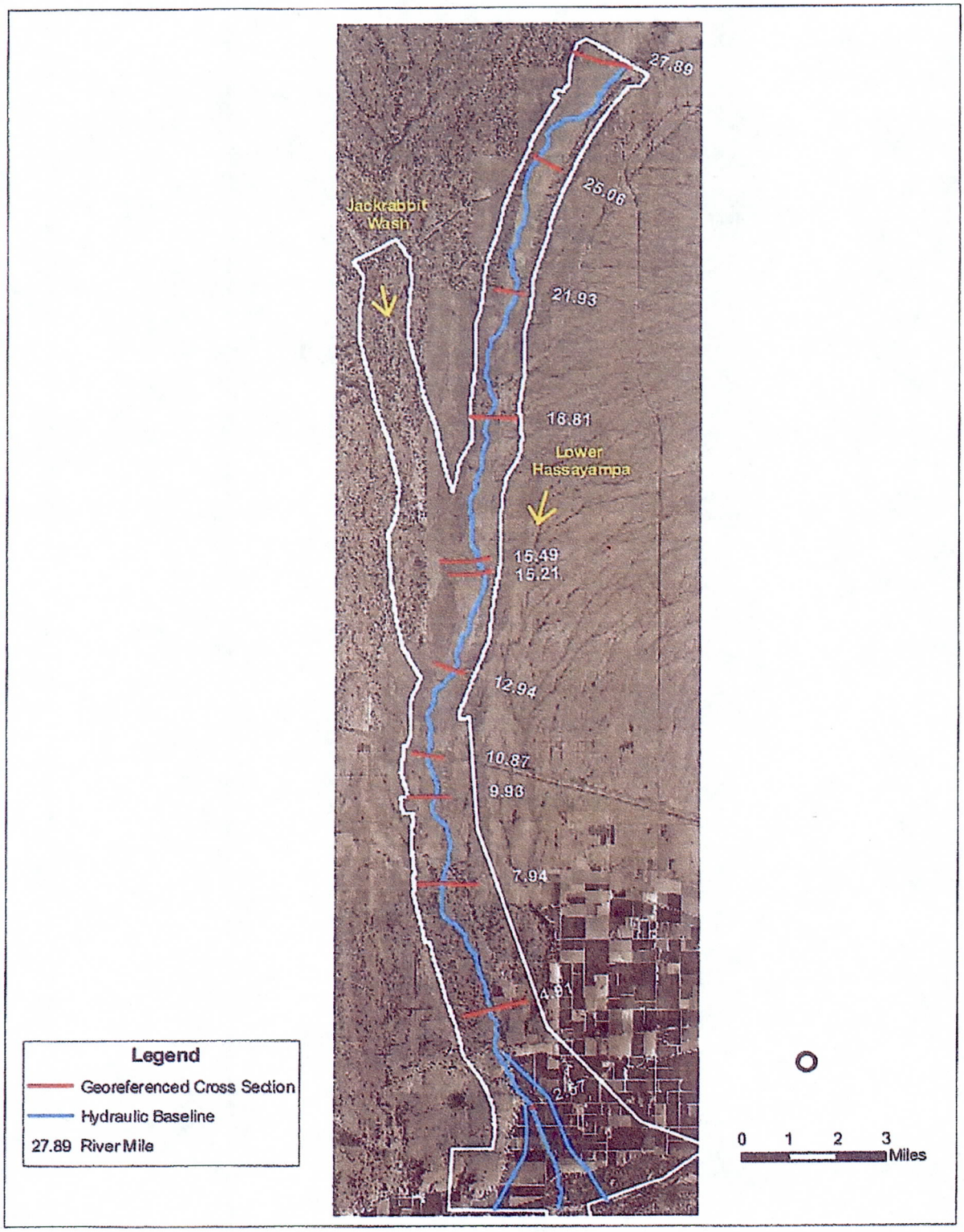

Figure 1. Lower Hassayampa River and its tributary Jackrabbit Wash

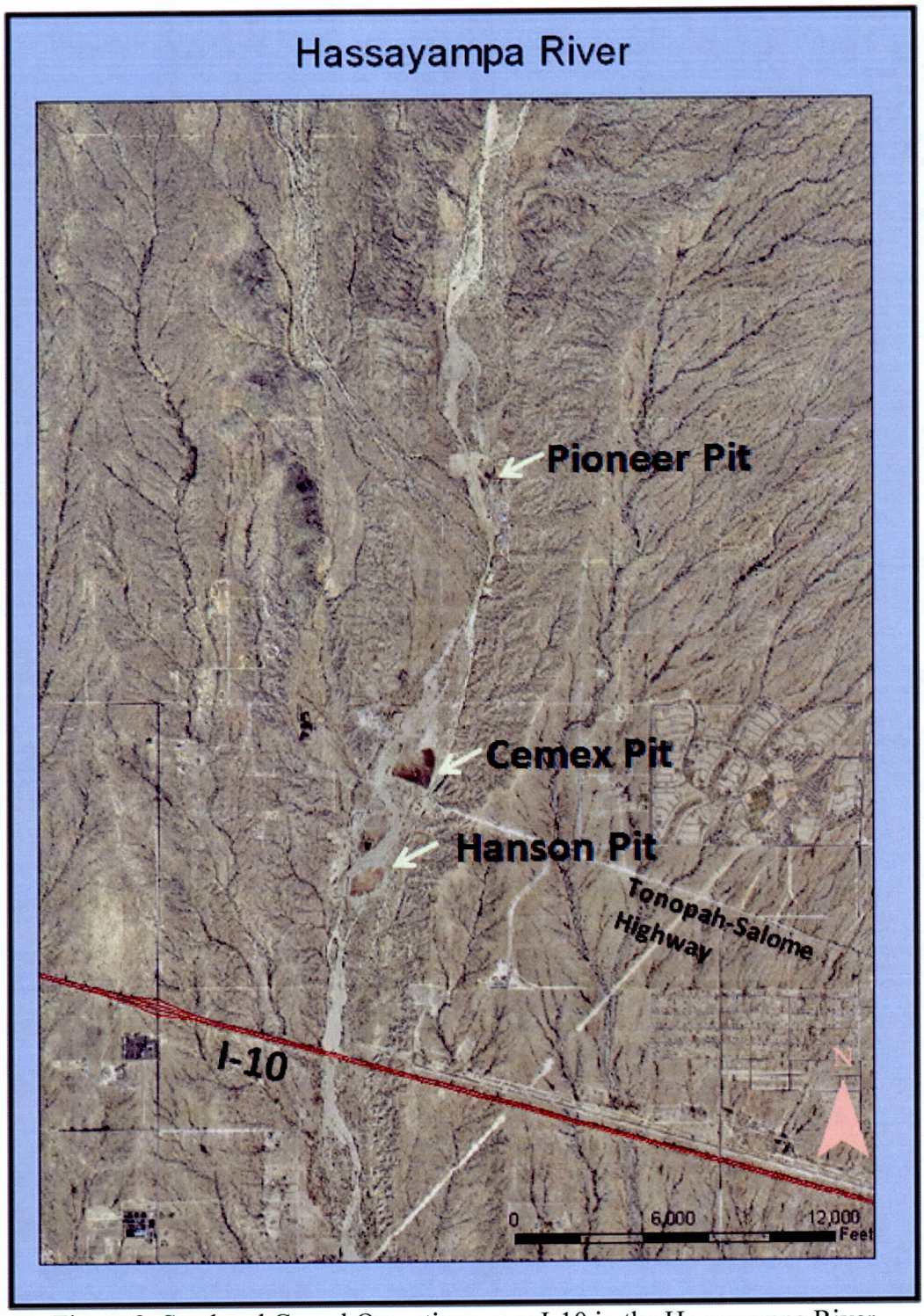

Figure 2. Sand and Gravel Operations near I-10 in the Hassayampa River

Figure 3. Topography of the Hassayampa River near the Pioneer mining site

Grain size distribution of the bed material for the study river reach is shown in Figure 4. The 2010 flood hydrograph is shown in Figure 5, and the hydrograph for the 2002 to 2010 flood series is shown in Figure 6.

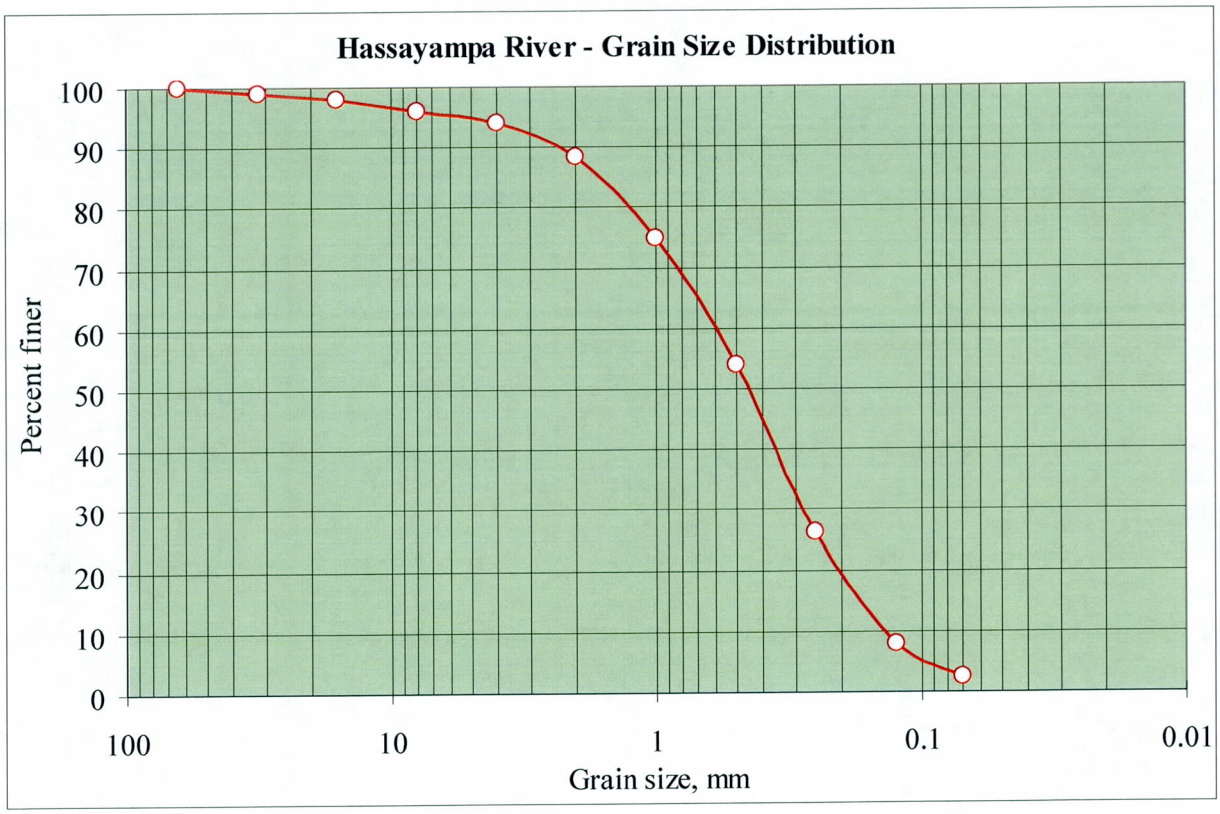

Figure 4. Grain size distribution of bed material for the study river reach

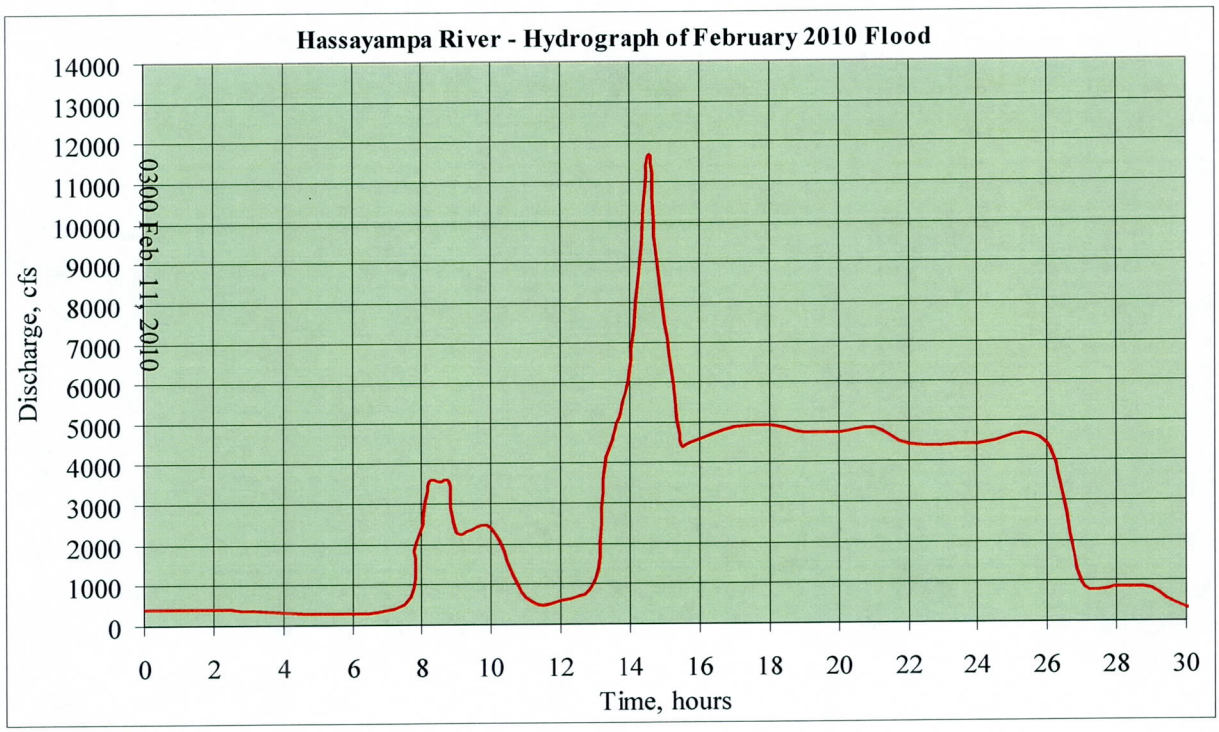

Figure 5. The 2010 flood hydrograph

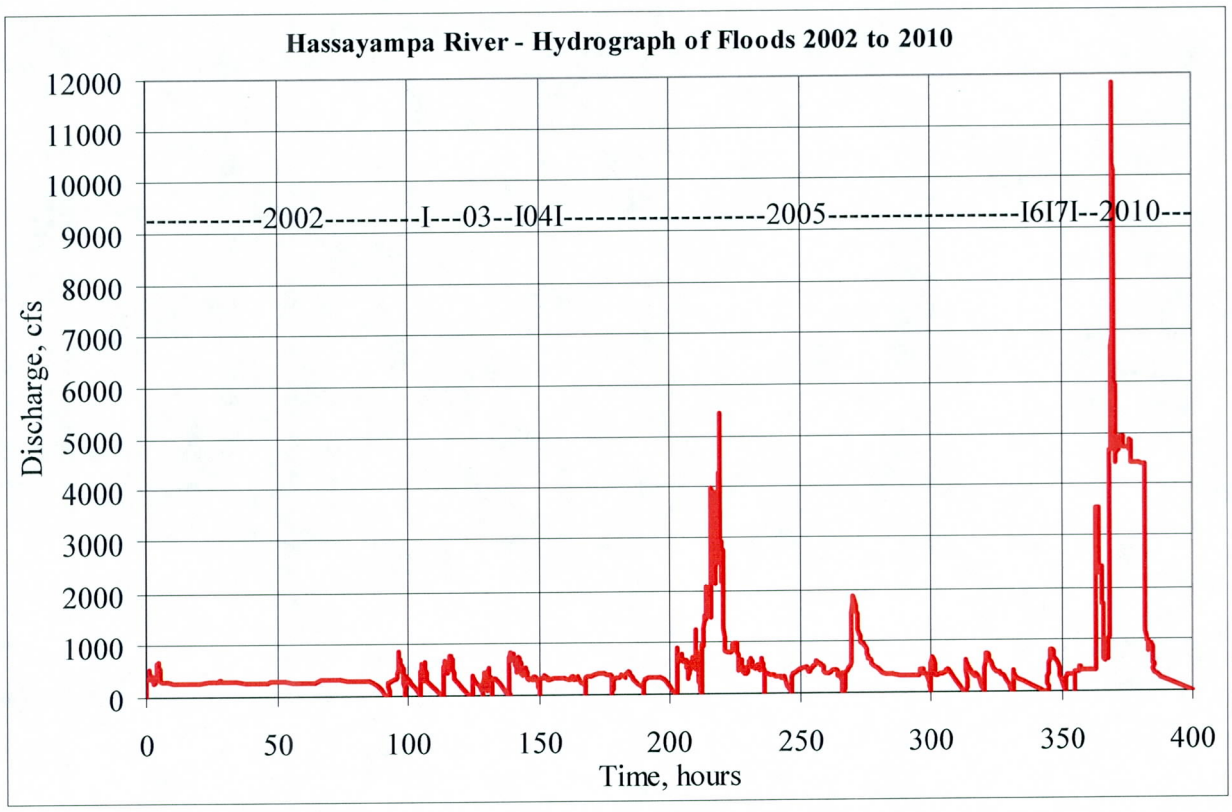

Figure 6. Hydrograph for the 2002 to 2010 flood series

Modeling Approach — There are two modeling approaches for the study. The first approach is simply to model January 20-21, 2010 event using 2002 topographic data as the basis and using the pit configuration to modify the topographic data. The pit configuration is estimated for the condition prior to the January 20-21, 2010 event. Both "without" and "with" calibration modeling will be performed.

The second approach is to model both 2005 and 2010 events using 2002 topographic data as the basis and using pit configuration to modify the topographic data. The modification of the topographic data has two steps. The first step is to modify the topographic data based on the pit configuration prior to February 11-12, 2005 event. The second step is to modify the end-of-Fluvial-12 February 11-12, 2005 event simulation cross-sections by adding the pit configurations observed prior to January 20-21, 2010 event. Both "without" and "with" calibration modeling will be performed.

II. PERFORMANCE INDEX

A Performance Index is used to assess the correlation of the simulated and surveyed results for headcut and tailcut. The Absolute Performance Index (API) is defined by Equation 1 below:

$$API = \Sigma_{i=1}^{n} \frac{|M_i - C_i|}{n} \quad (1)$$

where M_i is the measured headcut/tailcut depth (positive values) or deposition depth (negative values), C_i is the computed headcut/tailcut depth (positive values) or deposition depth (negative values), and n is the number of cross-sections.

III. MODEL CALIBRATION

The purpose of model calibration is to match the modeled results with measurement as closely as possible. In the process of calibration, certain parameters used in the study are selected. The modeled results using the selected parameters are compared with measurement. The selected parameters are then varied to improve the correlation of modeled results with measurement. For this study, model calibration includes the following steps:

(1) The selection of a computer model,
(2) The selection of sediment transport formula,
(3) The selection of channel roughness coefficients, and
(4) The selection of the Bank Erodibility Factor (for FLUVIAL-12 only).

The FLUVIAL-12 model was selected by Chang Consultants for the study. Model input is based on the initial topographic data called LHWMP-Phase I topographic data provided by R2D. As shown in Table 1, the Pioneer Pit has an area of 23 acres with a depth of 28-30 ft, Cemex Pit has an area of 45 acres with a depth of 10 ft, and Hanson Pit has an area of 22 acres with a depth of 10 ft. The outlines of the three pits are from the GIS Arcview shape file. R2D incorporated these pits into LHWMP-Phase I topographic data and develop HEC-RAS cross-sections. R2D provided Chang Consultants these HEC-RAS cross-sections. Before R2D cut cross-sections, R2D sent Chang Consultants the cross-sections layout for review and comments. Chang Consultants used these cross-sections to develop a Fluvial-12 model with Engelund-Hansen transport equation. All other parameters are based on the same parameters from R2D's HEC-6T and HEC-RAS sediment transport models (January 20-21, 2010 flow hydrograph, sediment inflow, time step for inflow hydrograph, sediment discharge rating curve, Manning's n, time step for computation, upstream and downstream boundary conditions…etc.). The maximum scour and scour at end of simulation will be reported. The results will be compared against the new 2010 topographic data.

Selection of Sediment Transport Formula Based on Simulated River Channel Changes near Pioneer Site — A sediment transport formula is employed in the computer model to simulate headcut/tailcut. The sediment transport formula for the study was selected based on the simulated results for headcut/tailcut induced by Pioneer pit. The Yang formula and the Engelund-Hansen formula were used separately in the study. Simulated changes in longitudinal profiles of channel reaches near the Pioneer site are shown in Figures 7 and 8, respectively. Such changes are characterized by headcut upstream of the mining site, sediment deposition in the pit, and tailcut downstream of the pit.

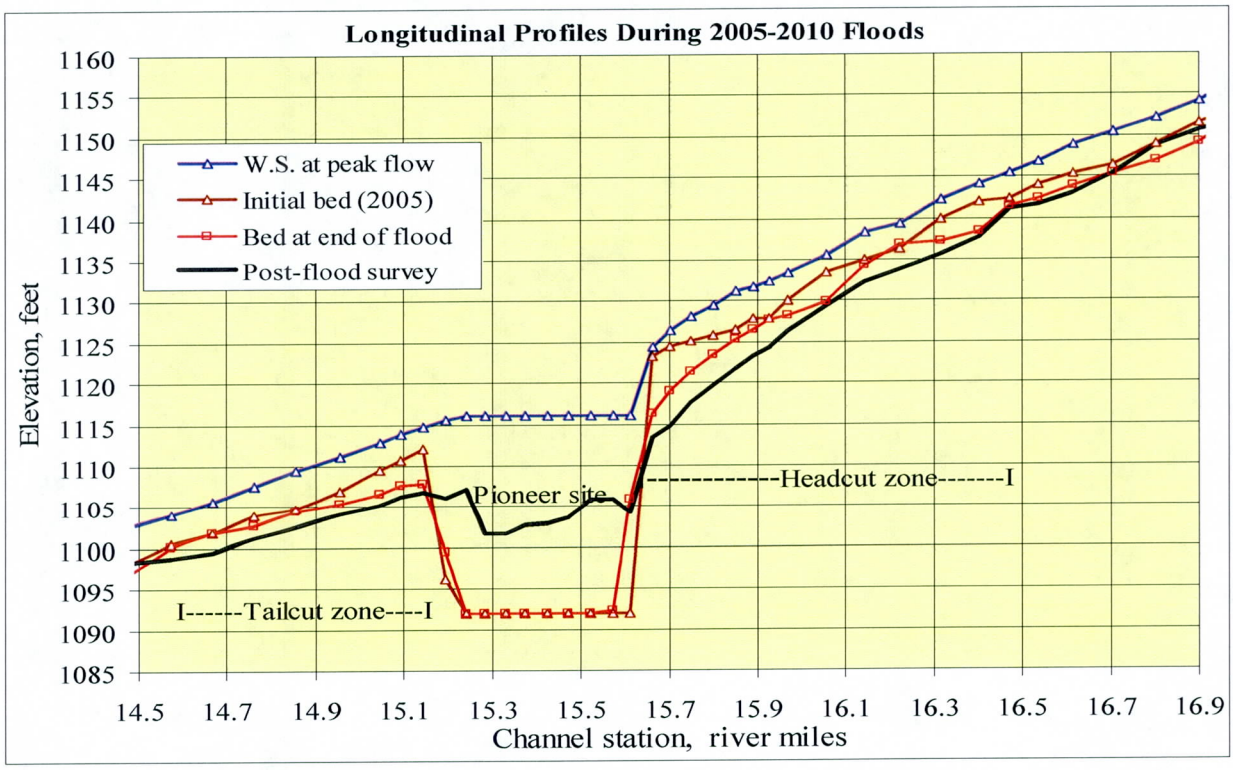

Figure 7. Simulated changes in longitudinal profiles using 2010 flood and Yang formula

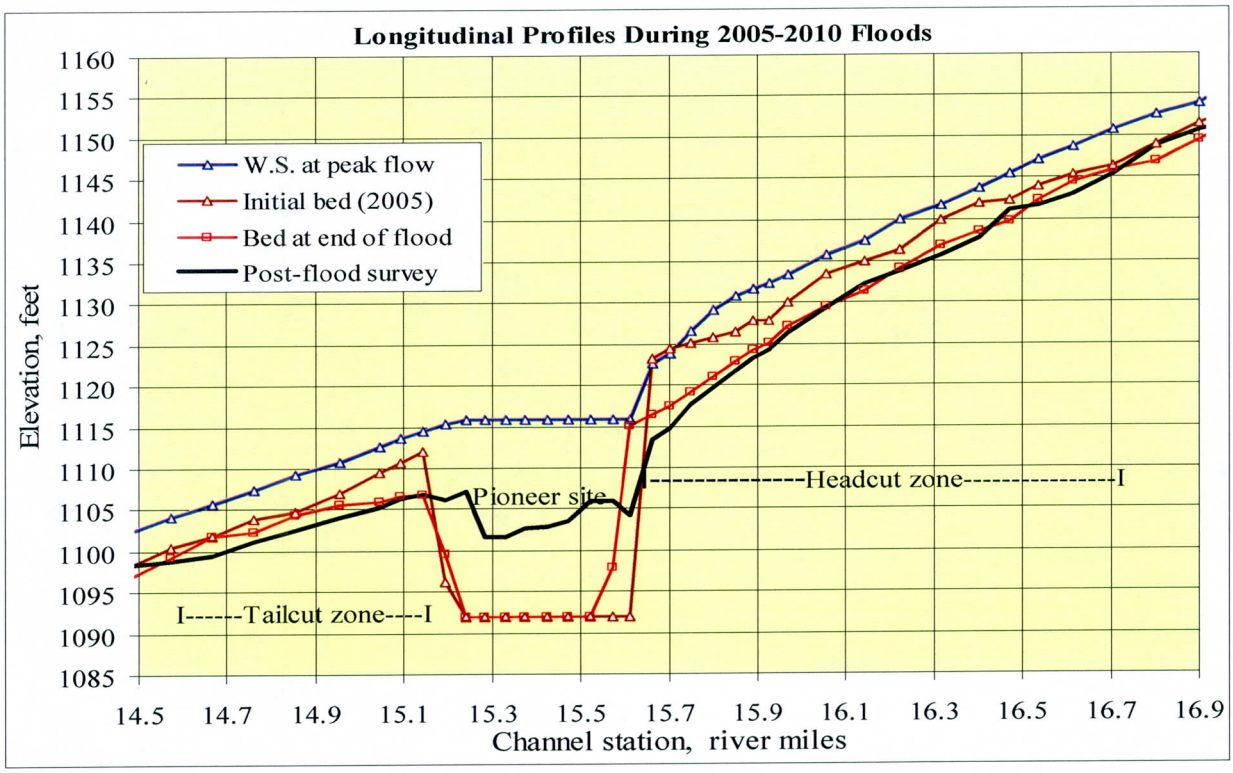

Figure 8. Simulated changes in longitudinal profiles using 2010 flood and Engelund-Hansen formula

The simulated results shown in Figures 7 and 8 are based on two different sediment transport formulas; they are used to select the sediment transport formula as a part of the calibration process. The simulated channel bed profile is now compared the post-flood survey in each figure. Since the simulated channel bed profile based on the Engelund-Hansen formula is well correlated with the survey, the Engelund-Hansen formula is therefore selected for the study.

It is clear that headcut developed along the upstream reach of Pioneer pit and tailcut developed along its downstream reach. Different scour depths due to headcut/tailcut are simulated by the Yang and Engelund-Hansen formulas. The scour depths simulated by the Yang formula are less than those by the Engelund-Hansen formula. This general trend suggests that the Yang formula calculates lower sediment transport rates than the Engelund-Hansen formula under the same conditions. The comparison for sediment transport rate prediction may also be verified by comparing sediment deliveries predicted by these two formulas as described below.

Comparison of Modeled Results on Sediment Delivery — Sediment delivery is defined as the cumulative amount of sediment that has been delivered passing a certain channel section for a specified period of time, that is,

$$Y = \int_{T} Q_s \, dt \tag{2}$$

Where Y is sediment delivery (yield); Q_s is sediment discharge for bed material load; t is time; and T is the duration. The sediment discharge Q_s pertains only to bed-material load of sand, gravel and cobble. Fine sediment of clay and silt constituting the wash load may not be computed by a sediment transport formula. Sediment delivery is widely employed by hydrologists for watershed management; it is used herein to keep track of sediment supply and removal along the channel reach.

Spatial variations in sediment delivery are manifested as channel storage or depletion of sediment associated stream channel changes since the sediment supply from upstream may be different from the removal. The spatial variation of sediment delivery depicts the erosion and deposition along a stream reach. A decreasing delivery in the downstream direction, i.e. downward gradient for the delivery-distance curve, signifies that sediment load is partially stored in the channel to result in a net deposition. On the other hand, an increasing delivery in the downstream direction (upward gradient for the delivery-distance curve) indicates sediment removal from the channel boundary or net scour. A uniform sediment delivery along the channel (horizontal curve) indicates that sediment inflow and outflow are in balance, i.e., no net erosion or deposition along the reach. Channel reaches with net sediment storage or depletion may thus be designated on the basis of the gradient. From the engineering viewpoint, it is best to achieve a uniform delivery, the non-silt and non-scour condition, for dynamic equilibrium.

Figure 9 shows the time and spatial variations of sediment delivery along the Hassayampa River during the 2010 flood using the Engelund-Hansen formula and the Yang formula. The simulated results of these two formulas show that the Engelund-Hansen formula predicts higher sediment transport rate than the Yang formula.

River reaches with distinct erosion and deposition are depicted in the figure. The sediment delivery increases as the flow approaches a mining site. This increase in sediment delivery indicates erosion of the river bed in the process of headcut. The sediment delivery increases as the flow leaves the mining site, indicating erosion in the process of tailcut. The sediment delivery decreases in the downstream direction through the three mining sites, indicating deposition since there is more sediment inflow than outflow. In fact, sediment delivery drops down to zero in a short distance into a mining site. This pattern indicates that sediment deposits as soon as the flow enters the mining site and it only advances for a certain distance inside the mining site. The amount of sediment deposition is a mining pit is the difference between the inflow and outflow. This figure shows that the Cemex site trapped more sediment than the other two sites. For example, the sediment inflow into the Cemex site, based on the Engelund-Hansen formula, is 184,000 tons and the outflow is zero; the net sediment deposition is 184,000 tons of bed material not including the wash load.

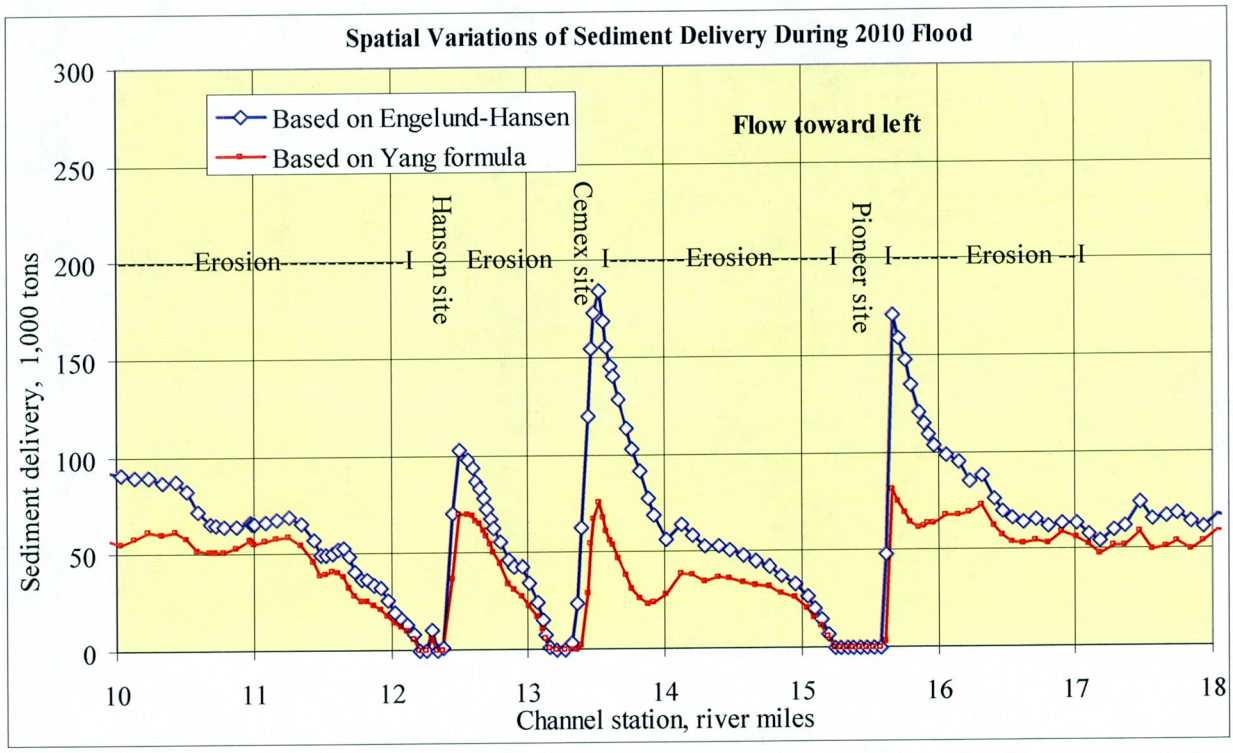

Figure 9. Time and spatial variations of sediment delivery in weight along the Hassayampa River during the 2010 flood – based on FLUVIAL-12

Selection of Channel Roughness Coefficient — The roughness coefficients provided in the HEC-RAS model by R2D were used in the initial modeling study. In the HEC-RAS file, different values of Manning's n are specified for different channel sections. The n values vary within a range and the average for the river channel is about 0.026. The simulated results shown in Figures 7 and 8 are based on n values provided by R2D. Since the simulated post-flood channel bed profile based on the Engelund-Hansen formula matches closely with the post-flood survey, the n value of 0.026 was selected as a part of the calibration process.

Performance Index for Modeled Results — The performance index, API, for the results shown in Figure 8 are computed as described below. Channel bed elevations for those cross

sections affected by headcut/tailcut shown in Figure 8 are listed in Table 2 below. In the table, the pre-flood thalweg elevation is the minimum bed elevation based on the pre-2005-flood topographic survey. The post-flood elevation from topographic survey is the minimum bed elevation from the topographic survey after the 2010 flood. The post-flood thalweg elevation from modeling is the simulated minimum bed elevation after the 2010 flood.

Table 2. Scour depths due to headcut/tailcut using 2010 flood and Engelund-Hansen formula

Location	Pre-flood thalweg elevation (feet)	Post-flood thalweg elevation from topographic mapping (feet)	Post-flood thalweg elevation from modeling (feet)	Minimum bed elevation from modeling (feet)	Scour depth from topographic mapping (feet)	Scour depth from modeling (at the end of flood simulation) (feet)
Headcut above Pioneer pit						
15.67	1123.3	1113.4	1116.4	1113.0	9.9	6.9
15.71	1124.4	1114.8	1117.4	1116.7	9.6	7.0
15.76	1125.2	1117.7	1119.1	1119.1	7.5	6.1
15.81	1125.9	1119.7	1121.0	1120.7	6.2	4.8
15.86	1126.5	1121.8	1123.0	1122.1	4.7	3.5
15.90	1127.9	T 1123.3	1124.3	1122.3	4.6	3.6
15.94	1127.9	1124.3	1125.1	1122.7	3.8	2.8
15.98	1130.9	1126.3	1127.2	1123.3	4.6	3.7
16.07	1133.4	1129.4	1129.6	1128.3	4.0	3.8
16.15	1135.0	1132.2	1131.4	1130.6	2.8	3.6
16.24	1136.4	1133.8	1134.2	1134.2	2.6	2.2
16.33	1139.9	1135.6	1136.9	1136.0	4.3	3.0
16.42	1142.0	1137.8	1138.6	1137.0	4.2	3.4
16.48	1142.3	1141.1	1139.8	1138.5	1.2	2.5
16.55	1144.0	1141.7	1142.3	1142.2	2.3	1.7

16.63	1145.3	1143.0	1144.5	1143.8	2.3	0.8
16.72	1146.5	1145.4	1145.9	1145.1	1.1	0.6
16.82	1148.9	1148.7	1147.0	1146.7	0.2	1.9
16.91	1151.5	1150.6	1149.4	1148.9	0.9	1.1
17.02	1155.5	1151.9	1152.0	1150.2	3.6	3.5
17.11	1155.6	1154.4	1154.0	1153.3	1.2	1.0
17.20	1156.8	1155.6	1156.1	1155.9	0.8	0.7
17.29	1159.0	1157.5	1159.6	1157.8	1.5	-0.6
17.38	1160.7	1159.8	1160.5	1159.9	0.9	0.2
Tailcut below Pioneer pit						
14.57	1098.8	1098.1	1100.1	1098.0	0.7	-1.3
14.67	1101.8	1099.4	1101.8	1100.9	2.4	0.0
14.77	1103.9	1101.2	1102.4	1102.1	2.7	1.5
14.86	1104.7	1102.6	1104.5	1103.7	2.1	0.2
14.96	1106.9	1104.1	1105.5	1105.4	2.8	1.4
15.06	1109.5	1105.2	1105.9	1105.8	4.3	3.6
15.10	1110.7	1106.3	1106.6	1106.5	4.3	4.1
15.15	1112.0	1106.8	1106.8	1106.7	5.2	5.2
15.20	1113.7	1106.1	1099.6	1096.2	3.6	14.1

Headcut developed along the channel reach upstream of the Pioneer site, the headcut zone may be estimated from Figure 8 and the calculated scour depths listed in Table 2. The headcut zone as estimated is from the Pioneer pit at section 15.67 to section 16.72 for a total channel length of about 1 mile. The API for the headcut scour depth is computed using the simulated and the surveyed scour depths in Table 2 as follows.

API = (3.0 + 2.6 + 0 + 1.4 + 1.2 + 1.0 + 1.0 + 0.9 + 0.2 + 0.2

$+ 0.4 + 1.3 + 0.8 + 1.3 + 0.6 + 1.5 + 0.5)/17$
$= 1.11$ feet

For the channel reach downstream of the Pioneer site, the tailcut zone may be estimated from Figure 8 and the scour depths listed in Table 2. The tailcut zone as estimated is from the downstream edge of the Pioneer pit at section 15.15 down to section 14.77 for a total channel length of about 0.6 mile. The API for tailcut scour depth is computed using the simulated and the surveyed scour depths in Table 2 as follows.

$$API = (1.2 + 1.9 + 1.4 + 0.7 + 0.2 + 0.0)/6 = 0.90 \text{ feet}$$

The computed Performance Indices for scour depths due to headcut/tailcut based on 2010 flood modeling are summarized in Table 3 below.

Table 3. Computed Performance Indices for scour depths due to headcut/tailcut using 2010 and Engelund-Hansen formula

Case	Absolute Performance Index
Headcut depth above Pioneer pit	1.11
Tailcut depth below Pioneer pit	0.90

IV. CALIBRATION AND PERFORMANCE INDEX BASED ON 2010 FLOOD ONLY

The calibration study presented in the previous section covers the selection of the sediment transport formula and the roughness coefficient. For the FLUVIAL-12 model, the Bank Erodibility Factor (BEF) is a parameter that governs the rate of bank erosion. Its value was selected in consideration of the geotechnical data for the bed material. For this calibration study, the BEF value that provides the best correlation of simulated and surveyed results was selected. The simulated cross-sectional profiles in the headcut/tailcut zones are generally smaller in width than the surveyed cross sections. The value of BEF was varied in modeling runs to select the value such that the cross sectional profiles match more closely with the measured cross-sectional profiles. Through this process, this value was determined to be 1.0 through several trial runs. This BEF value means that the bank of the headcut/tailcut channel is as erodible as the channel bed for the Hassayampa River. Input/output files for this case are as follows:

HASSA-CUTEH.FLU: FLUVIAL-12 input file for 2010 flood only using Engelund-Hansen formula

HASSA-CUTEH.OUT: FLUVIAL-12 output file for 2005 flood using Engelund-Hansen formula

Channel changes induced by mining pits during the 2010 flood was simulated. From the preliminary results, channel reaches with headcut and tailcut were first identified. The Pioneer pit has the largest depth, it induced headcut along the upstream channel reach and tailcut along the downstream reach. Headcut/tailcut also developed along channel reaches near the Cemex pit and Hanson pit. Because of instream sand/gravel mining in recent years, channel changes near the Cemex and Hanson pits were caused by headcut/tailcut as well as by mining. The effects of mining on channel changes can not be separated from the effects of headcut/tailcut.

Headcut/Tailcut near Pioneer Pit - The simulated water-surface profile and channel bed profile changes using the Engelund-Hansen formula are shown in Figures 10 and 11 for the reach upstream of the Pioneer site where headcut developed. These figures also have the following channel bed profiles:

1. Channel bed profile before the 2005 flood,
2. Simulated post-2010-flood channel bed profile, and
3. Channel bed profile from the post-2010-flood topographic survey.

Figure 12 is for the channel reach downstream of the Pioneer site with the same channel bed profiles. In addition, Figure 10 also has the simulated maximum scour profile during the 2010 flood.

Changes in channel cross-sections along the reach upstream of the Pioneer site are exemplified by those shown in Figure 13. Such changes illustrate the effects of headcut. Sample cross-sectional changes along the downstream reach of the Pioneer site are shown in Figure 14. These cross-sectional changes illustrate the effects of tailcut.

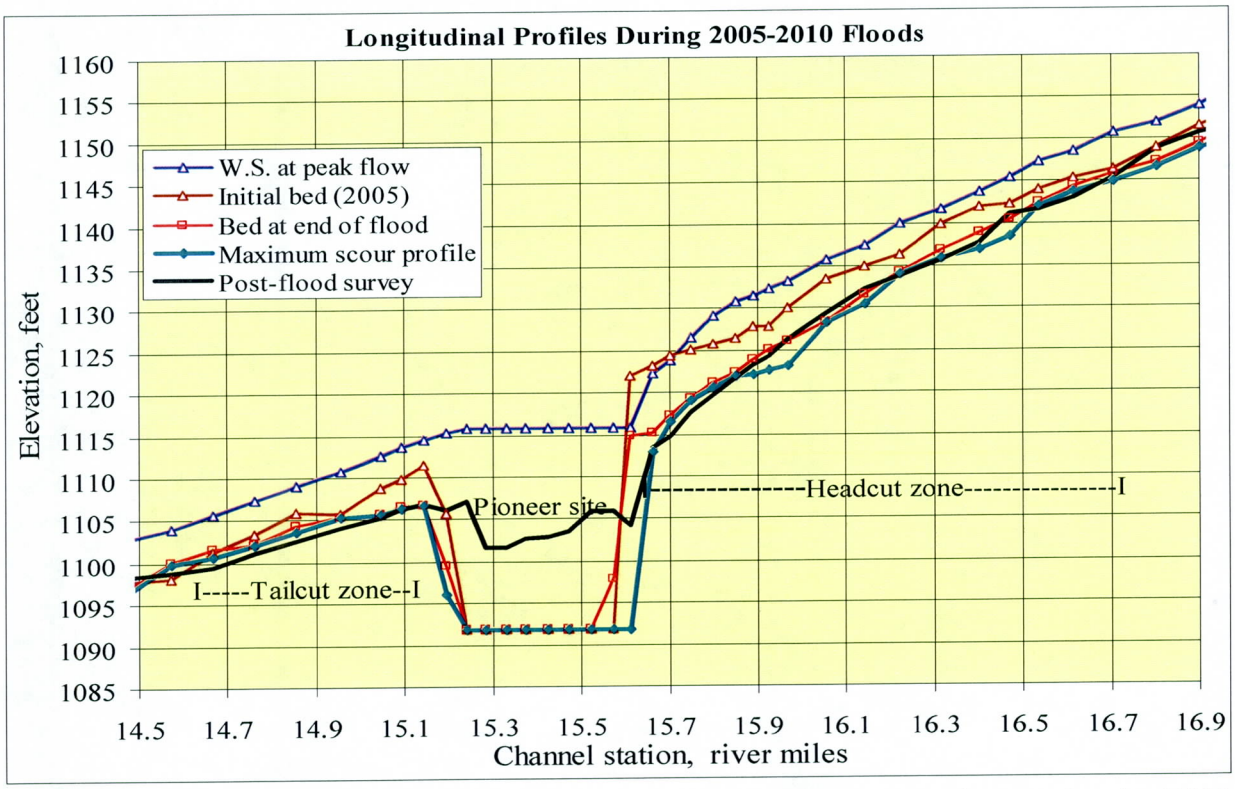

Figure 10. Simulated water-surface and channel bed profile changes near Pioneer pit using 2010 flood and Engelund-Hansen formula

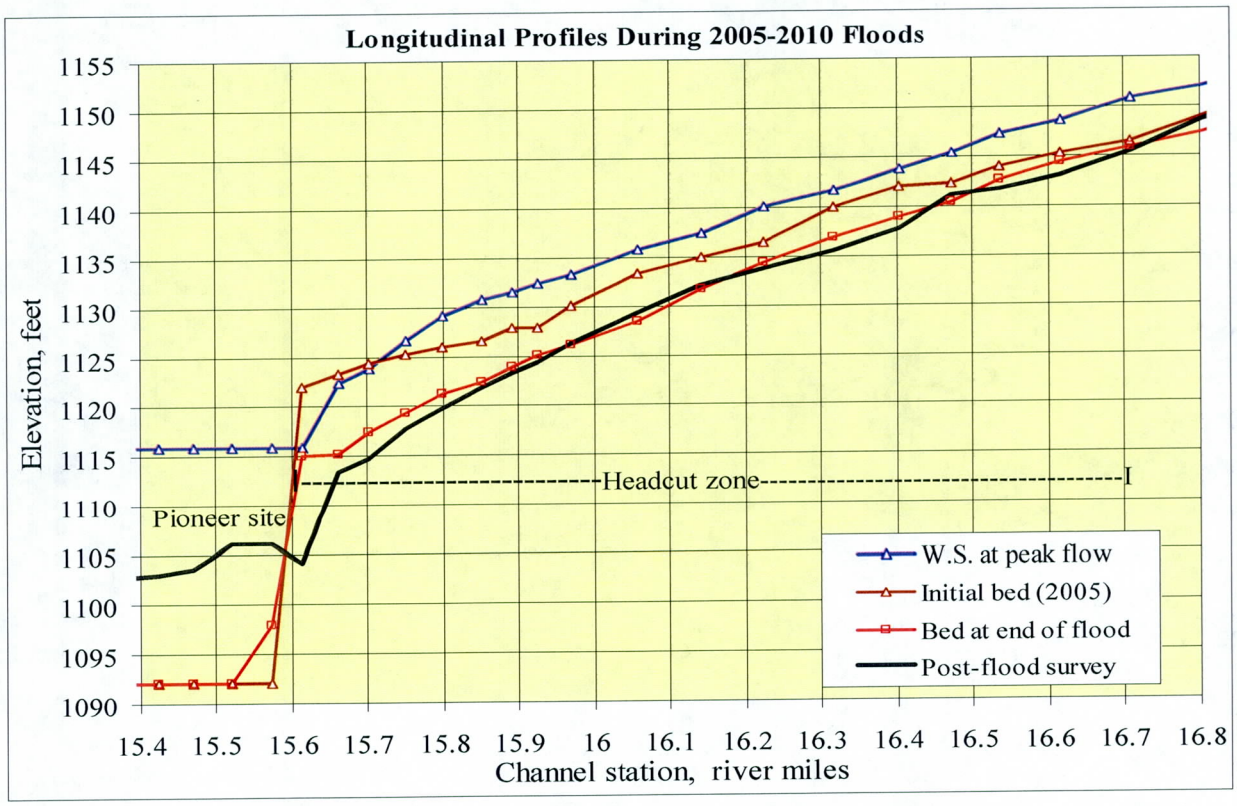

Figure 11. Water-surface and channel bed profiles for channel reach upstream of Pioneer site

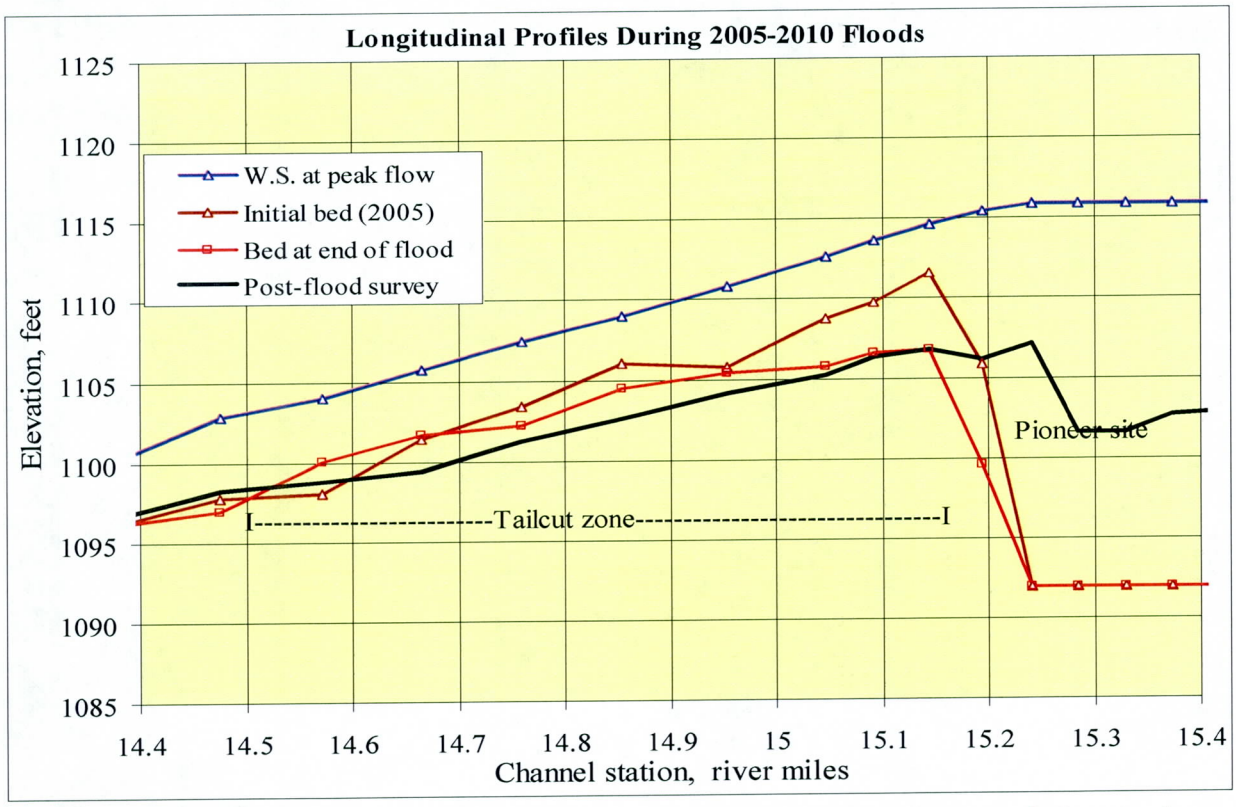

Figure 12. Water-surface and channel bed profiles for channel downstream of Pioneer site

The simulated changes in cross-sectional geometry of the channel based on the Engelund-Hansen formula due to headcut are compared with the surveyed results shown in Figure 13. The comparison is made based on those channel cross sections near the sand pit where channel geometric changes are primarily attributed to the effects of headcut or tailcut. For those cross sections away from the pit, the changes in channel geometry are also affected by several other factors such as the tributary inflows and braided channels. Because of the broad floodplain and braided channel pattern, it is sometimes difficult to identify the effective flow area during the 2010 flood. In other words, identification of the effective flow area in the broad floodplain can be somewhat inaccurate.

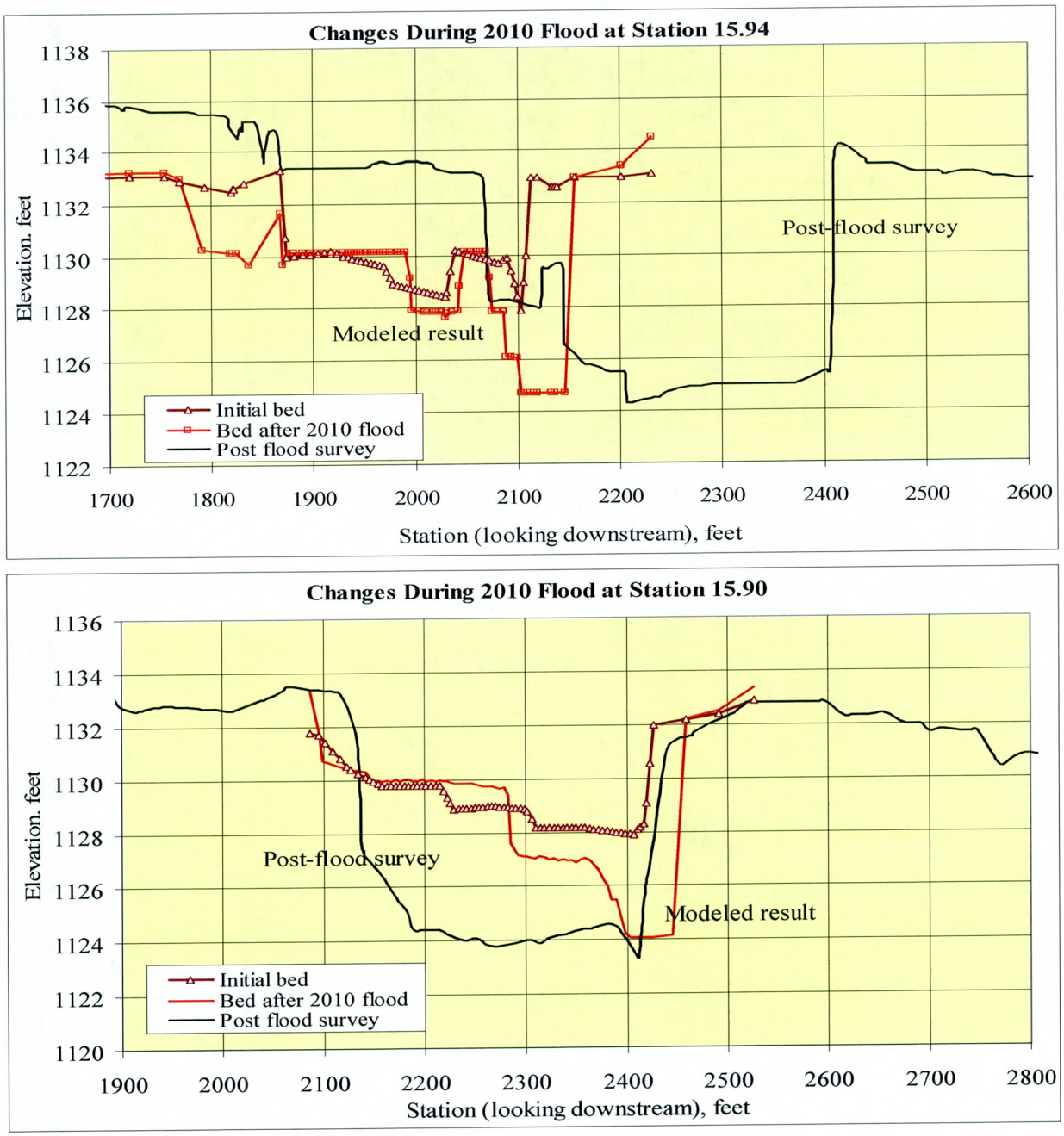

Figure 13. Simulated and surveyed channel cross sections after the 2010 flood

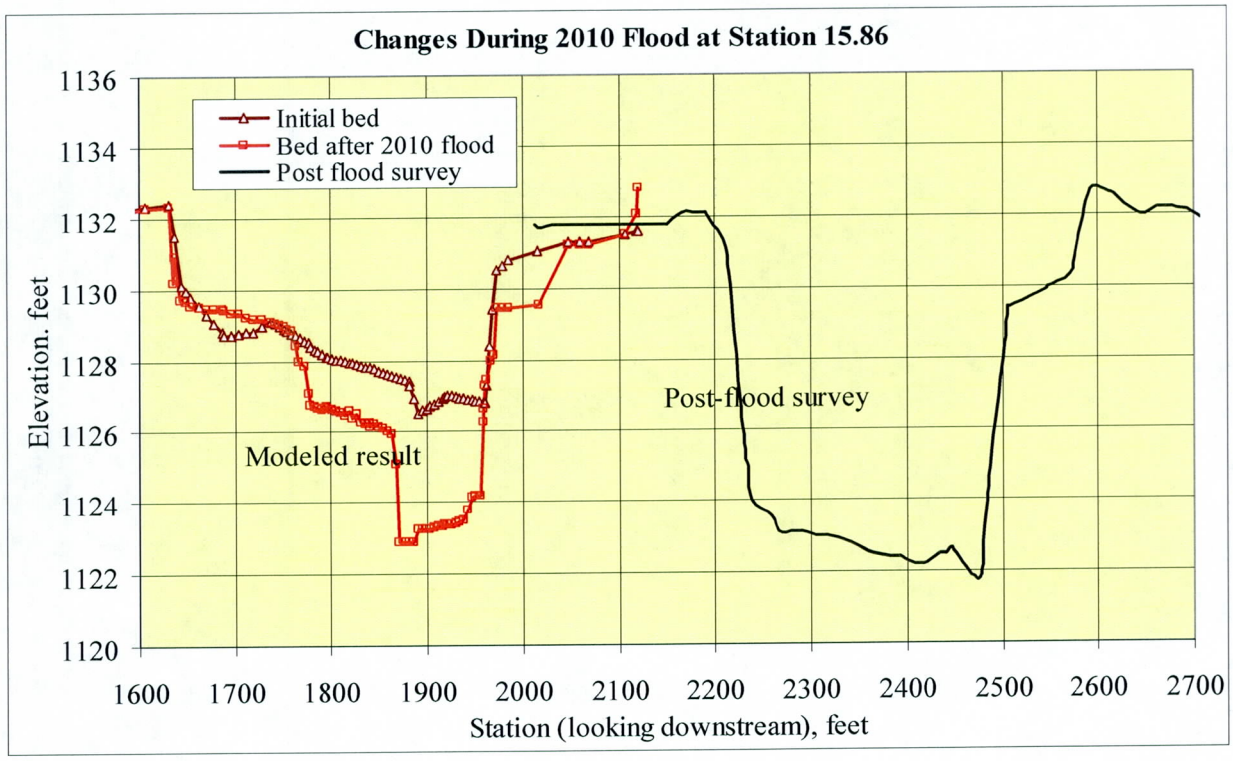

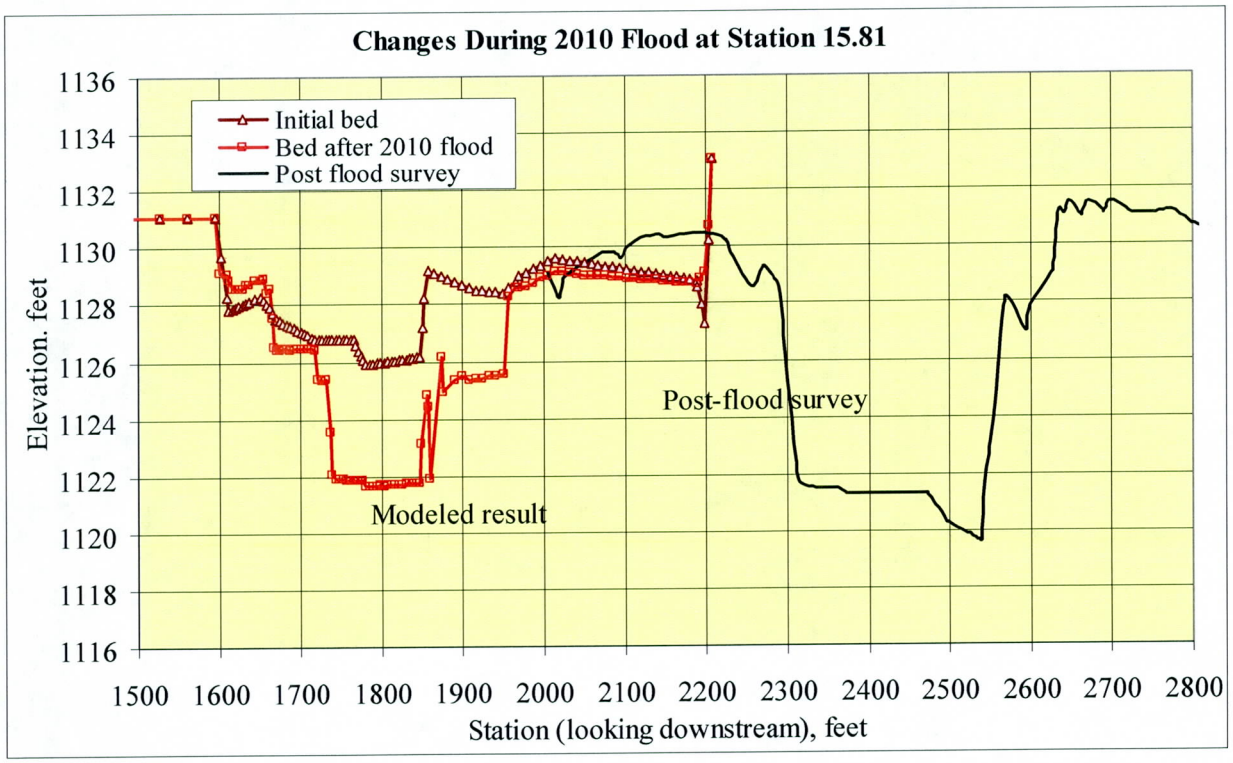

Figure 13(continued). Simulated and surveyed channel cross sections after the 2010 flood

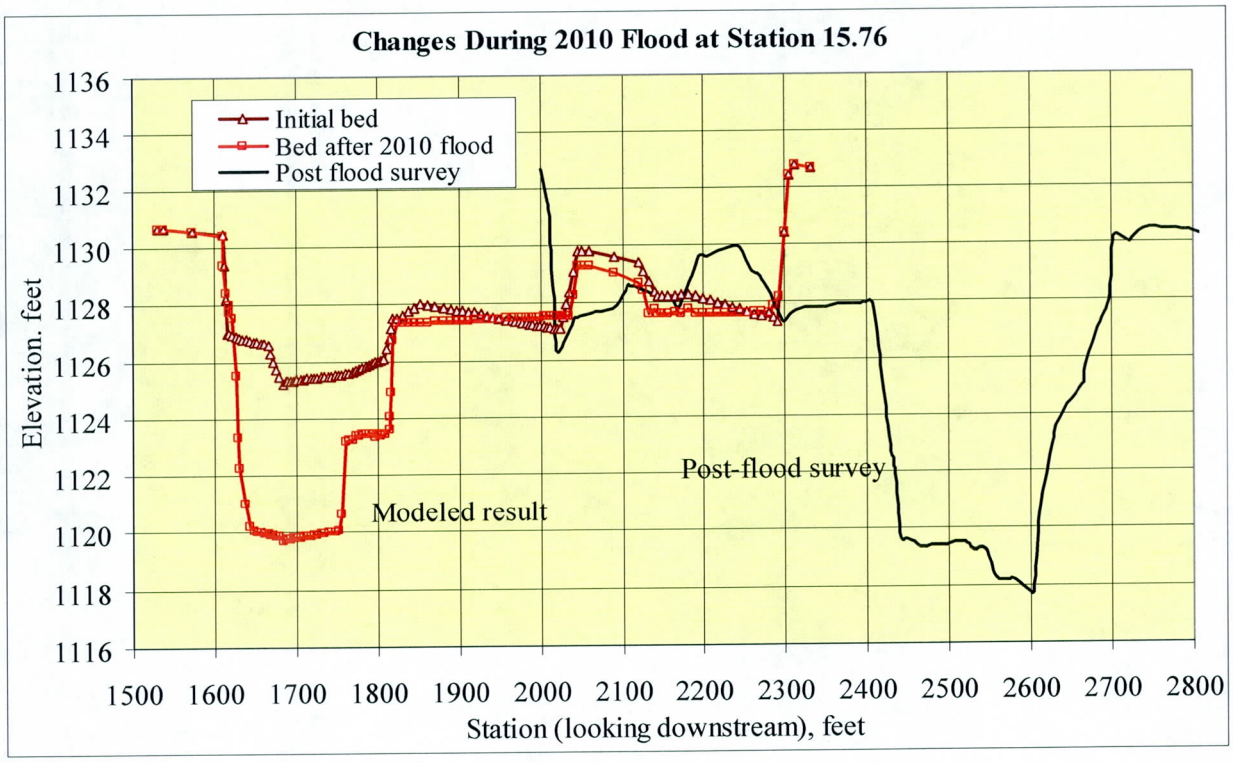

Figure 13(continued). Simulated and surveyed channel cross sections after the 2010 flood

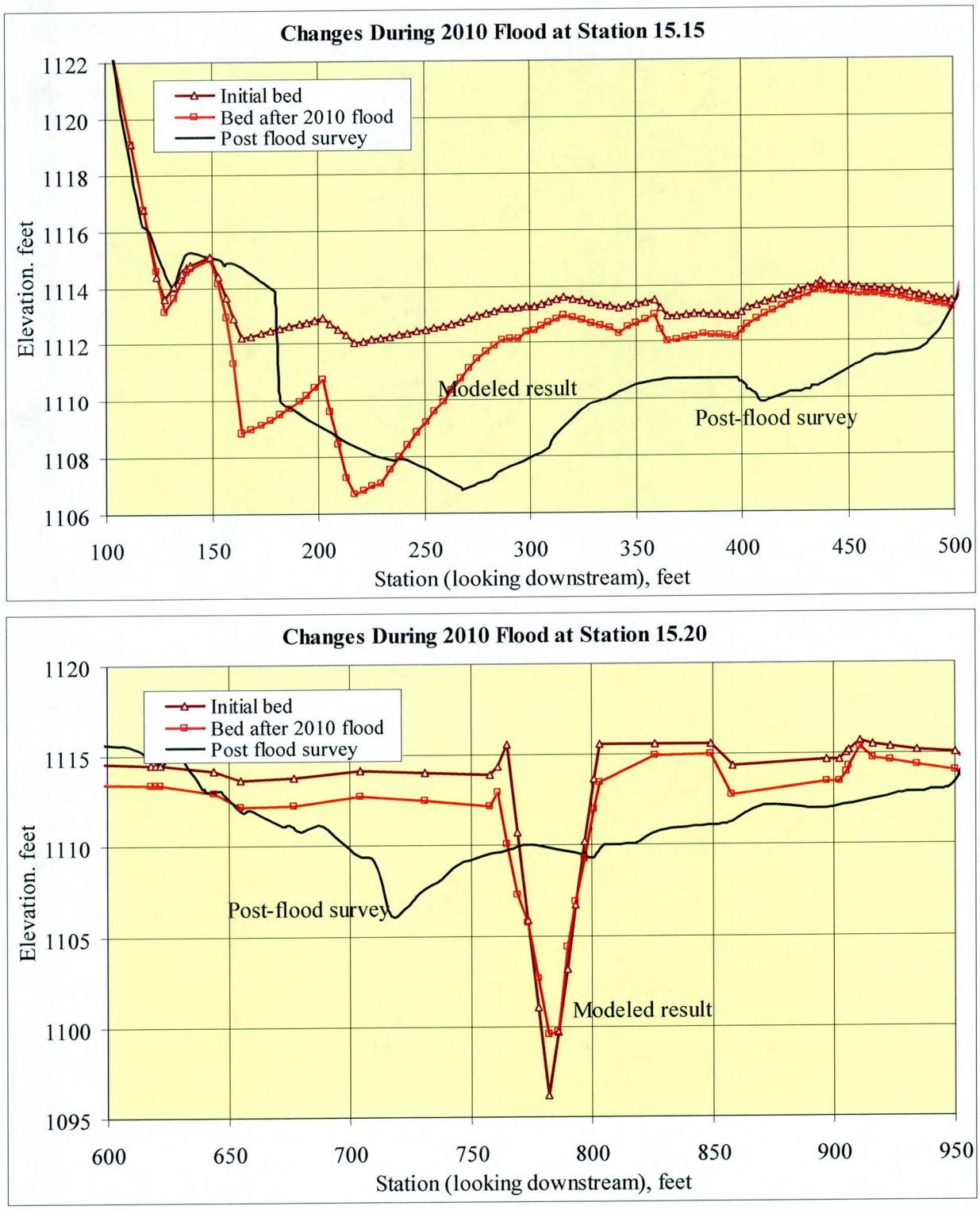

Figure 14. Simulated and surveyed channel cross sections after the 2010 flood

Simulated River Channel Changes near the Cemex and Hanson Mining Sites — Sand and gravel mining has been going on in the Hassayampa River near the Cemex and Hanson mining sites for decades. The new mining activities included in the current study are those that occurred in the effective flow area of the river channel for the time period from 2005 to 2010. There were also mining activities before this time period. In addition, deep mining at the Hanson site has created mining pits outside the effective flow area. These deep pits are separated from the main channel by a berm; therefore, they did not affect channel changes during the floods. However, other mining pits in the effective flow area of the channel had effects on headcut and tailcut changes in the river channel.

The results generated from modeling of the 2010 flood are presented in this section. Simulated waters surface profile and channel bed changes during the 2005-2010 floods using the Engelund-Hansen formula are shown in Figure 15. The uneven channel bed profiles during the time period reflect the effects of instream mining. The Cemex and Hanson mining pits, in comparison to the Pioneer mining pit, are much shallower in depth; therefore, the headcut and tailcut induced by these pits are less pronounced than those near the Pioneer site. The channel reach upstream of the Cemex site is simulated to undergo sediment deposition and channel bed aggradation during the 2010 floods. For this reason, the Cemex pit did not induce headcut along this channel reach during the 2010 flood.

Channel changes along the reach between the Cemex site and the Hanson site were caused by both mining and scour during floods. The effects of these two factors on channel changes can not be separated; therefore, no attempt is made to determine the scour depth due to headcut/tailcut.

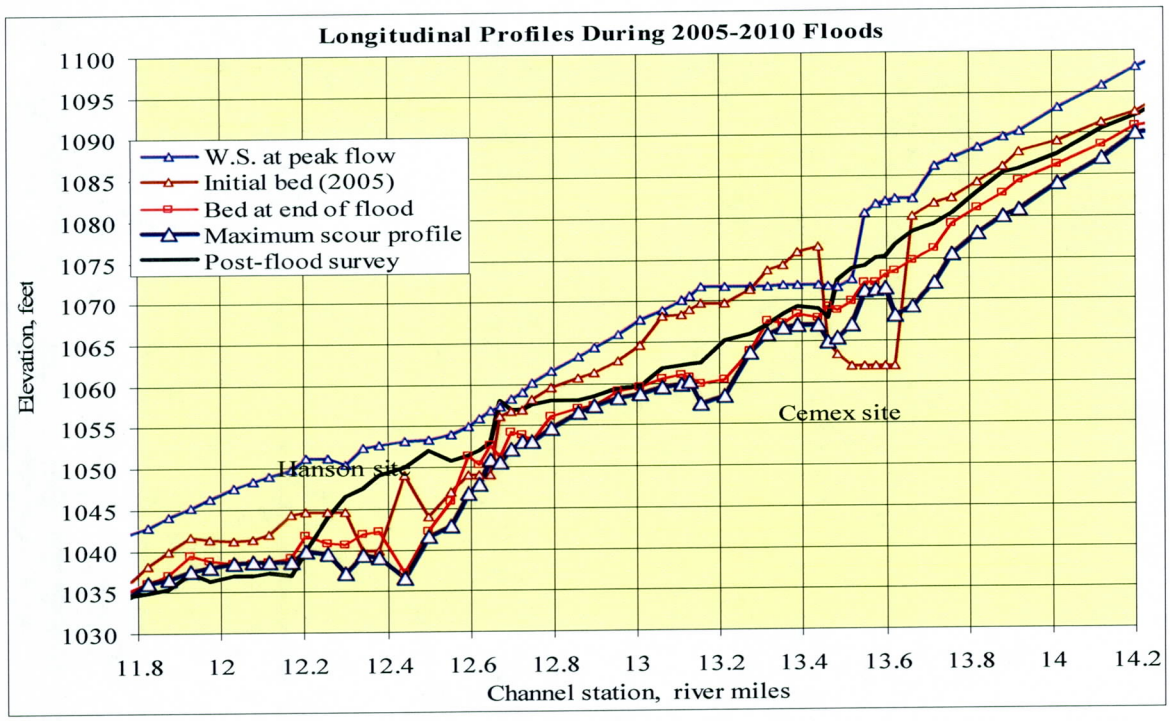

Figure 15. Water-surface and channel bed profiles for the channel reaches near the Cemex and Hanson mining sites simulated using 2010 flood and Engelund-Hansen formula

Channel bed elevations for those cross sections affected by headcut/tailcut are listed in Table 4 below. In the table, the pre-flood thalweg elevation is the minimum bed elevation based on the pre-2005-flood topographic survey. The post-flood elevation from topographic survey is the minimum bed elevation from the topographic survey after the 2010 flood. The post-flood thalweg elevation from modeling is the simulated minimum bed elevation after the 2010 flood. The minimum bed elevation from modeling is the lowest bed elevation reached by scour during the entire simulation period.

Table 4. Scour depths due to headcut/tailcut based on 2010 flood

Location	Pre-flood thalweg elevation (feet)	Post-flood thalweg elevation from topographic mapping (feet)	Post-flood thalweg elevation from modeling (feet)	Minimum bed elevation from modeling (feet)	Scour depth from topographic mapping (feet)	Scour depth from modeling (at the end of flood simulation) (feet)	Maximum scour depth from modeling during the flood (feet)
Headcut above Pioneer pit							
15.67	1123.3	1113.4	1115.2	1113.0	9.9	8.1	10.3
15.71	1124.4	1114.8	1117.4	1116.7	9.6	7.0	7.7
15.76	1125.2	1117.7	1119.3	1119.1	7.5	5.9	6.1
15.81	1125.9	1119.7	1121.2	1120.7	6.2	4.7	5.2
15.86	1126.5	1121.8	1122.5	1122.1	4.7	4.0	4.4
15.90	1127.9	T 1123.3	1123.9	1122.3	4.6	4.0	5.6
15.94	1127.9	1124.3	1125.1	1122.7	3.8	2.8	5.2
15.98	1130.9	1126.3	1126.1	1123.3	4.6	4.8	7.6
16.07	1133.4	1129.4	1128.4	1128.3	4.0	5.0	5.1
16.15	1135.0	1132.2	1131.7	1130.6	2.8	3.3	4.4
16.24	1136.4	1133.8	1134.3	1134.2	2.6	2.1	2.2
16.33	1139.9	1135.6	1136.9	1136.0	4.3	3.0	3.6
16.42	1142.0	1137.8	1139.0	1137.0	4.2	3.0	5.0

16.48	1142.3	1141.1	1140.4	1138.5	1.2	1.9	3.8
16.55	1144.0	1141.7	1142.6	1142.2	2.3	1.4	1.8
16.63	1145.3	1143.0	1144.3	1143.8	2.3	1.0	1.5
16.72	1146.5	1145.4	1145.9	1145.1	1.1	0.6	1.4
16.82	1148.9	1148.7	1147.3	1146.7	0.2	1.6	2.2
16.91	1151.5	1150.6	1149.6	1148.9	0.9	1.9	2.6
17.02	1155.5	1151.9	1152.1.	1150.2	3.6	3.4	5.3
17.11	1155.6	1154.4	1154.2	1153.3	1.2	1.4	2.3
17.20	1156.8	1155.6	1156.0	1155.9	0.8	0.8	0.9
17.29	1159.0	1157.5	1159.2	1157.8	1.5	-0.2	1.2
17.38	1160.7	1159.8	1160.4	1159.9	0.9	0.3	0.8
Tailcut below Pioneer pit							
14.67	1101.8	1099.4	1101.7	1100.9	2.4	0.1	0.9
14.77	1103.9	1101.2	1102.2	1102.1	2.7	1.7	2.8
14.86	1104.7	1102.6	1104.5	1103.7	2.1	0.2	1.0
14.96	1106.9	1104.1	1105.4	1105.4	2.8	1.5	1.5
15.06	1109.5	1105.2	1105.8	1105.8	4.3	3.7	3.7
15.10	1110.7	1106.3	1106.6	1106.5	4.3	4.1	4.2
15.15	1112.0	1106.8	1106.7	1106.7	5.2	5.3	5.3
15.20	1113.7	1106.1	1099.6	1096.2	3.6	14.1	17.5

Headcut developed along the channel reach upstream of the Pioneer site, the headcut zone may be estimated from Figure 11 and the calculated scour depths listed in Table 4. The headcut zone as estimated is from the Pioneer pit at section 15.67 to section 16.72 for a total channel length of about 1 mile. The API for the headcut scour depth is computed using the simulated and the surveyed scour depths in Table 4 as follows.

$$\text{API} = (3.0 + 2.6 + 0 + 1.4 + 1.2 + 1.0 + 1.0 + 0.9 + 0.2 + 0.2 + 0.4 + 1.3 + 0.8 + 1.3 + 0.6 + 1.5 + 0.5)/17 = 1.11 \text{ feet}$$

For the channel reach downstream of the Pioneer site, the tailcut zone may be estimated from Figure 12 and the scour depths listed in Table 4. The tailcut zone as estimated is from the downstream edge of the Pioneer pit at section 15.15 down to section 14.77 for a total channel length of about 0.6 mile. The API for tailcut scour depth is computed using the simulated and the surveyed scour depths in Table 4 as follows.

$$\text{API} = (1.2 + 1.9 + 1.4 + 0.7 + 0.2 + 0.0)/6 = 0.90 \text{ feet}$$

The computed Performance Indices for scour depths due to headcut/tailcut based on 2010 flood modeling are summarized in Table 5 below.

Table 5. Computed Performance Indices for scour depths due to headcut/tailcut based on 2010 flood modeling

Case	Absolute Performance Index
Headcut depth above Pioneer pit	1.05 feet
Tailcut depth below Pioneer pit	1.02 feet

V. FLUVIAL-12 MODELING OF BOTH 2005 AND 2010 FLOOD EVENTS (for February 11-12, 2005 events and January 20-21, 2010 event modeling)

Two steps were taken in modeling the February 11-12, 2005 event and January 20-21, 2010 event. The first step is to incorporate mining pits into the LHWMP-Phase I topographic data. R2D incorporated the mining pits configuration from the GIS Arcview shape file into the topographic data and provided Chang Consultants the HEC-RAS cross-sections. Chang Consultants used these cross-sections to develop a Fluvial-12 model with Engelund-Hansen transport equation. All other parameters used in FLUVIAL-12 are consistent with the same parameters from R2D's HEC-6T and HEC-RAS sediment transport models (February 11-12, 2005 flow hydrograph, sediment inflow, time step for inflow hydrograph, sediment discharge rating curve, …etc.).

After the Fluvial-12 modeling of the 2005 flood, the original cross-section data were changed by Fluvial-12 at the end of the simulation due to river channel changes. Chang Consultants converted the output simulated by FLUVIAL-12 for the 2005 event into the input data for the 2010 flood event.

Chang Consultants modeled the January 20-21, 2010 event based on the end-of-simulation cross-section data after the 2005 event. The cross-section data were then revised by

incorporating the pit configuration prior to the January 2010 event. The Pioneer Pit has an area of 23 acres with a depth of 28-30 ft, Cemex Pit has an area of 45 acres with a depth of 10 ft, and Hanson Pit has an area of 22 acres with a depth of 10 ft. Chang Consultants modified the end-of-simulation cross-sections based on the pit configuration prior to the January 2010 event. Chang Consultants then used these cross-sections to develop a Fluvial-12 model with Engelund-Hansen transport equation. All other parameters were based on the same parameters from R2D's HEC-6T and HEC-RAS sediment transport models (January 2010 flow hydrograph, sediment inflow, time step for inflow hydrograph, sediment discharge rating curve, time step for computation, upstream and downstream boundary conditions,...etc.). R2D submitted a brief memo about the modeling parameters and assumptions to FCDMC and Chang Consultants for review. Chang Consultants then used the same parameters and assumptions.

For the purpose of model calibration, the modeling results on headcut/tailcut are documented and compared with the new 2010 topographic data. Calibration has been performed so that the modeling results would match the new 2010 topographic data as closely as possible. The morphologic parameters for headcut/tailcut include the headcut/tailcut channel length, depth, width, and cross-sectional area. In order to achieve the best correlation in calibration, the hydraulic and sediment parameters are adjusted such that the performance index is as small as possible.

The selection of the sediment transport formula can make a significant difference on the modeled results. The Engelund-Hansen formula for sediment transport was used in previous studies of the Hassayampa River for predicting scour and lateral migration of the river channel. Good correlation of modeled results with field data was obtained. For the present study, two sediment transport formulas are used and the respective results generated by them are evaluated to assess their applicability to the Hassayampa River. Yang's sediment transport equation has also been selected and used in addition to Engelund-Hansen as a separate comparison.

The bank erodibility factor (BEF) is the parameter that governs the rate of bank erosion. Its value will be selected based on the geotechnical data for the bed material. For this calibration study, the BEF value that provides the best correlation of simulated and surveyed results was selected. This value was varied in the modeling runs to select the most appropriate value and this value was determined to be 1.0, through several trial runs. This BEF value means that the bank of the headcut/tailcut channel is as erodible as the channel bed for the Hassayampa River. In addition to the sediment transport formulas and the bank erodibility factor, other hydraulic parameters for calibration include Manning's n coefficient and other parameters associated with sediment transport modeling such as sediment inflow hydrograph and boundary conditions. The n value of 0.026 was finally selected through trial runs.

Simulation of Headcut/Tailcut — Channel changes due to headcut/tailcut during the 2005-2010 floods near the Pioneer pit were simulated following the procedures described previously. The simulation includes the effects of pre-2005 mining sites included in the 2005 channel bed topography; it also includes the new mining sites existed prior to the 2010 flood.

In order to simulate the headcut/tailcut using the Engelund-Hansen formula, the following FLUVIAL-12 files were created and executed:

HASSA-EH05.FLU: This is the FLUVIAL-12 input file for the 2005 channel data and the Engelund-Hansen formula

HASSA-EH05.OUT: This is the output file produced by HASSA-EH05.FLU executed for 2005 flood

HASSA-EH10.FLU: This is the FLUVIAL-12 input file using the output channel data from HASSA-EH05.OUT plus the mining site data just before 2010 flood

HASSA-EH10.OUT: This is the FLUVIAL-12 output file produced by HASSA-EH10.FLU using the Engelund-Hansen formula and the 2010 flood

The following files were created and executed using the Yang formula:

HASSA-Y05.FLU: This is the FLUVIAL-12 input file for 2005 channel data and the Yang formula

HASSA-Y05.OUT: This is the output file produced by HASSA-Y05.FLU executed for 2005 flood

HASSA-Y10.FLU: This is the FLUVIAL-12 input file using the output channel data from HASSA-Y05.OUT plus the mining site data just before 2010 flood

HASSA-Y10.OUT: This is the FLUVIAL-12 output file produced by HASSA-Y10.FLU using the Yang formula and the 2010 flood.

VI. HEADCUT AND TAILCUT NEAR PIONEER MINING SITE

The results generated from modeling with calibration are presented in this section. Simulated water-surface and channel bed profile changes in the headcut/tailcut regions near the Pioneer pit generated by the Yang formula are shown in Figure 16; those by the Engelund-Hansen formula are shown in Figures 17 and 18. Each figure include the channel bed profiles before the 2005 flood and after the 2010 flood together with the surveyed channel-bed profile after the 2010 flood. The post-flood channel bed generated using the Yang formula has on uneven profile not supported by the post-flood survey. Model calibration using the Yang formula failed. All other results as presented in this section are based on the Engelund-Hansen formula.

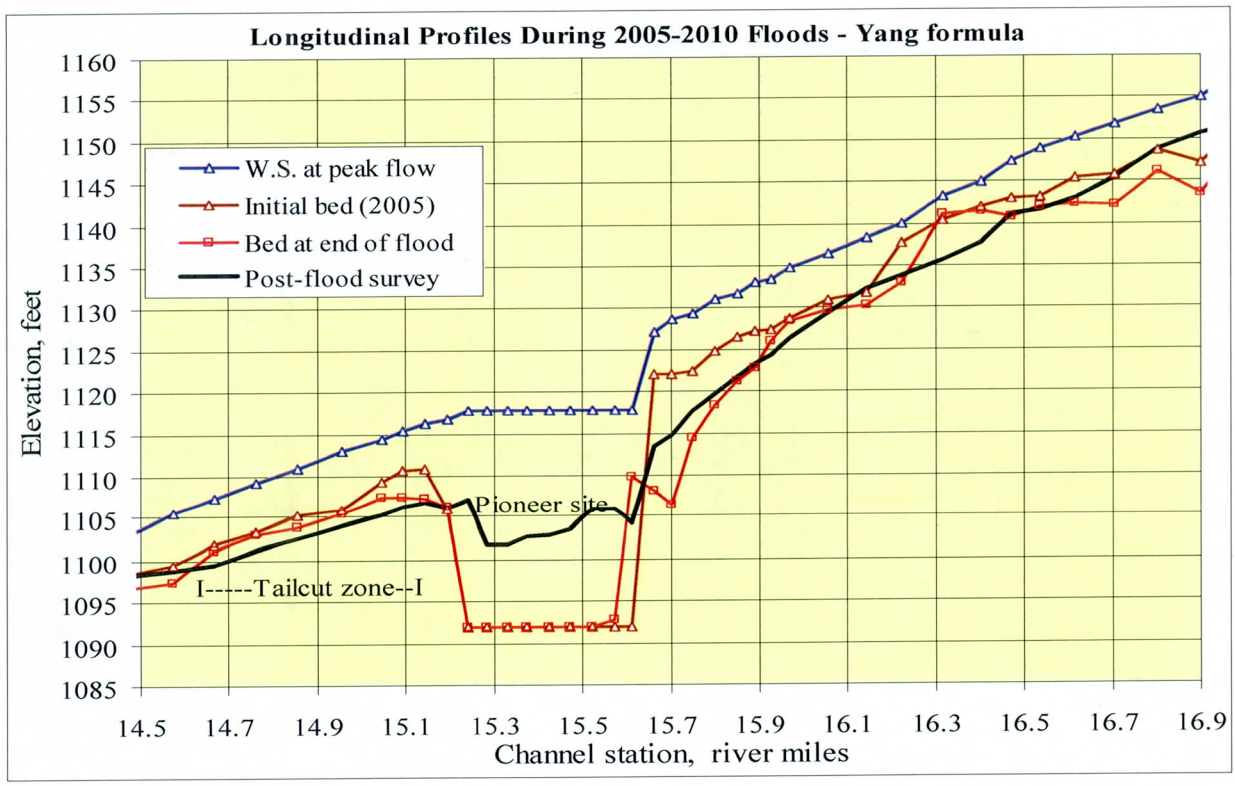

Figure 16. Simulated water-surface and channel bed profile changes near Pioneer pit using 2005 and 2010 floods and Yang formula

Channel changes due to headcut developed upstream of the Pioneer pit. Simulated water-surface profile and channel bed profile changes due to headcut during the 2005-2010 floods are shown in Figure 18, together with the surveyed channel bed profile after the floods. Channel changes due to tailcut developed downstream of the Pioneer pit. Simulated water-surface profile and channel bed profile changes due to tailcut during the 2005-2010 floods are shown in Figure 19, together with the surveyed channel bed profile after the floods. The results shown are also generated by the Engelund-Hansen formula.

The simulated changes in cross-sectional geometry of the channel due to headcut are compared with the surveyed results shown in Figure 20. The comparison is made based on those channel cross sections near the sand pit where channel geometric changes are primarily attributed to the effects of headcut or tailcut. For those cross sections away from the pit, the changes in channel geometry are also affected by several other factors such as the tributary inflows and braided channels. Because of the broad floodplain and braided channel pattern, it is sometimes difficult to identify the effective flow area during the 2005-2010 floods. In other words, identification of the effective flow area in the broad floodplain can be somewhat inaccurate. The simulated changes in channel geometry due to tailcut are compared with the surveyed results shown in Figure 21. The comparison is made based on those channel cross sections near the sand pit where channel geometric changes are primarily attributed to the effects of tailcut. For those cross sections away from the pit, the changes in channel geometry are also affected by several other factors such as the tributary inflows and braided channels. Because of the broad floodplain and braided channel pattern, it is sometimes difficult to identify the

effective flow area during the 2005-2010 floods. In other words, identification of the effective flow area in the broad floodplain with the braided channels can be somewhat inaccurate.

It should be pointed out that the changes in channel cross sections due to tailcut along the channel reach downstream of the Pioneer pit were affected by the tributary inflows from Jackrabbit Wash. As shown in Figure 3, the braided channels of Jackrabbit Wash join the Hassayampa River from the northwest and they approach the main river at a sharp angle. The tributary channels have important effects on the morphology of the main channel. In this case, the channel formed during tailcut became wider as the tributary channels joined in from the west side.

The simulated changes in channel cross sections due to tailcut are shown in Figure 21 for sections 15.15 and 15.20. For both sections, the simulated channel geometries due to tailcut are small in width, as is typical for gulley formation. However, the surveyed channel cross sections are much larger in width. Such large widths are closely related to the lateral inflow from Jackrabbit Wash. The effects of lateral inflow on channel morphology at this location were not simulated in modeling.

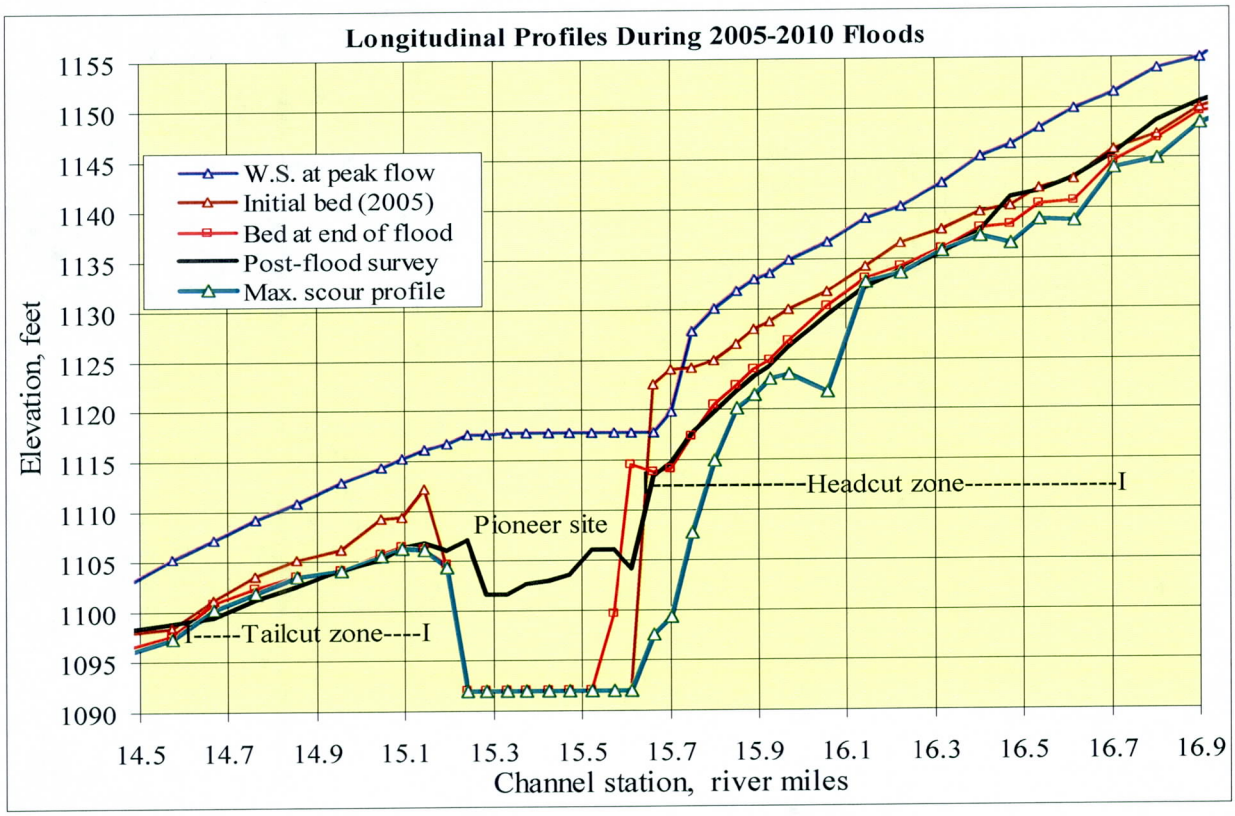

Figure 17. Simulated water-surface and channel bed profile changes near Pioneer pit using 2005 and 2010 floods and Engelund-Hansen formula

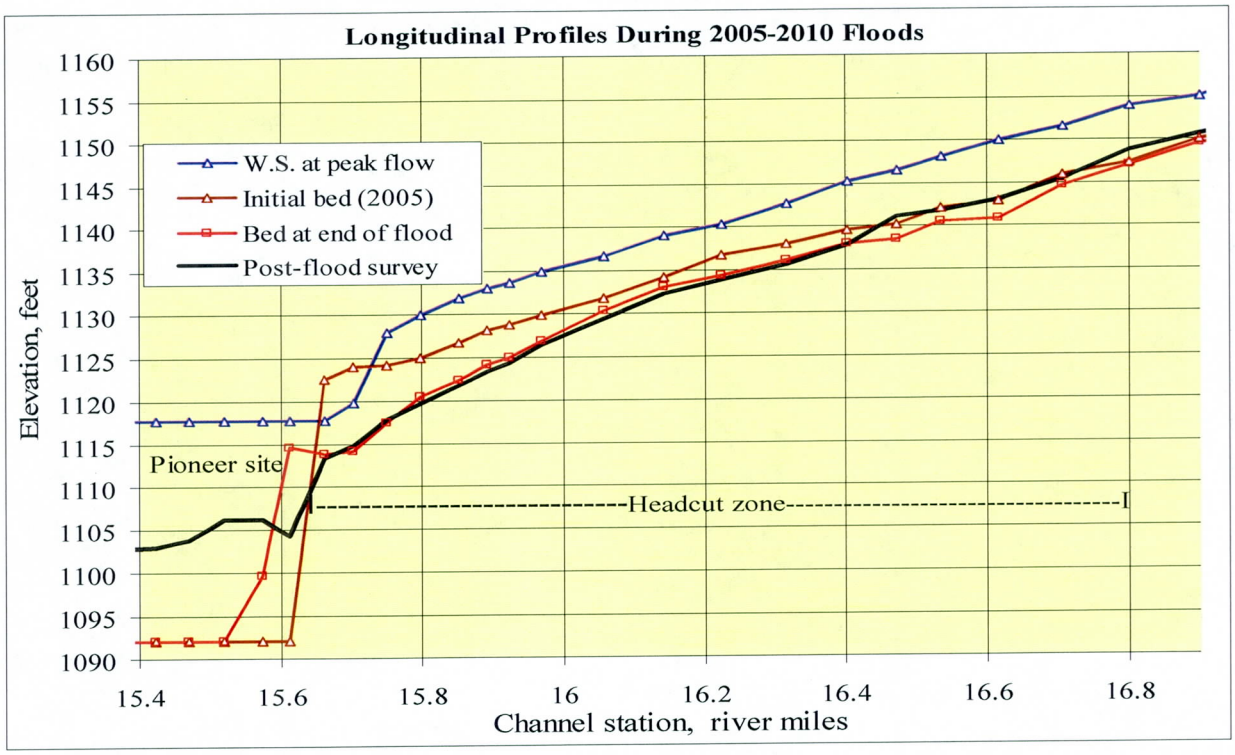

Figure 18. Simulated water-surface and channel bed profile changes upstream of Pioneer pit using 2005 and 2010 floods and Engelund-Hansen formula

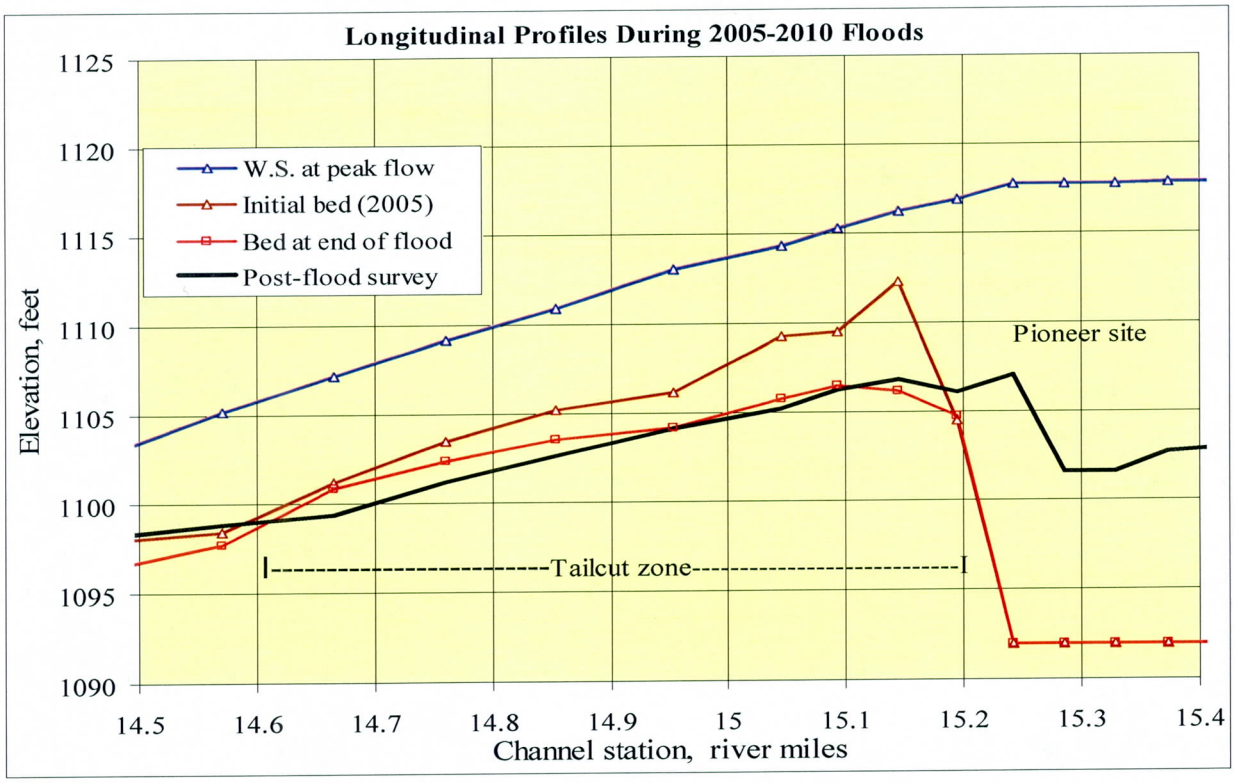

Figure 19. Simulated water-surface and channel bed profile changes downstream of Pioneer pit using 2005 and 2010 floods and Engelund-Hansen formula

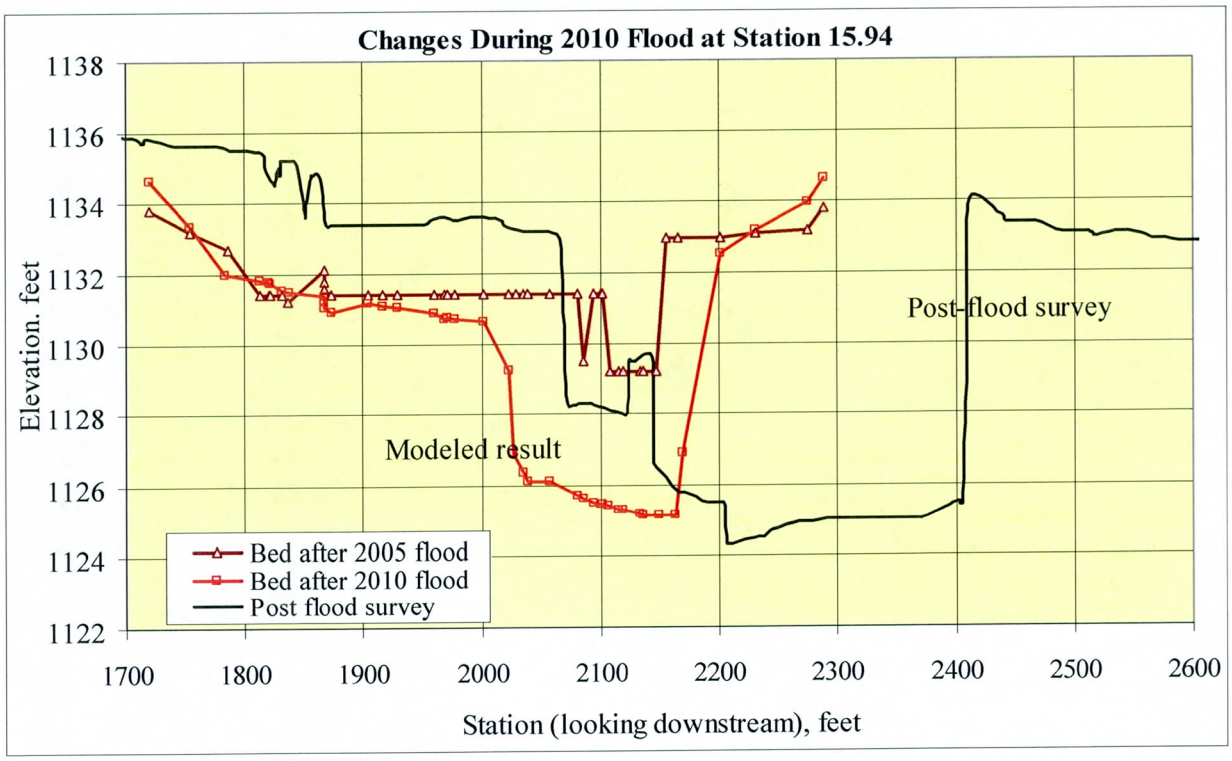

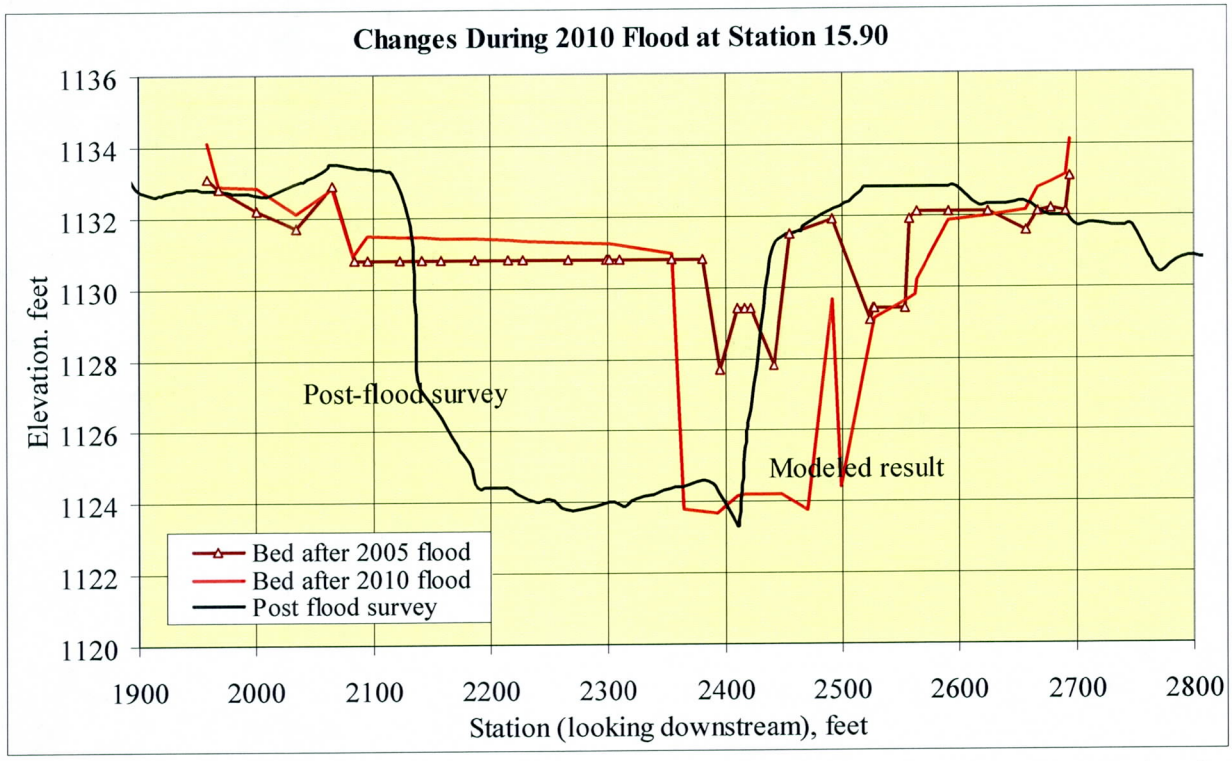

Figure 20. Simulated and surveyed cross-sectional changes due to headcut near Pioneer pit using Engelund-Hansen formula

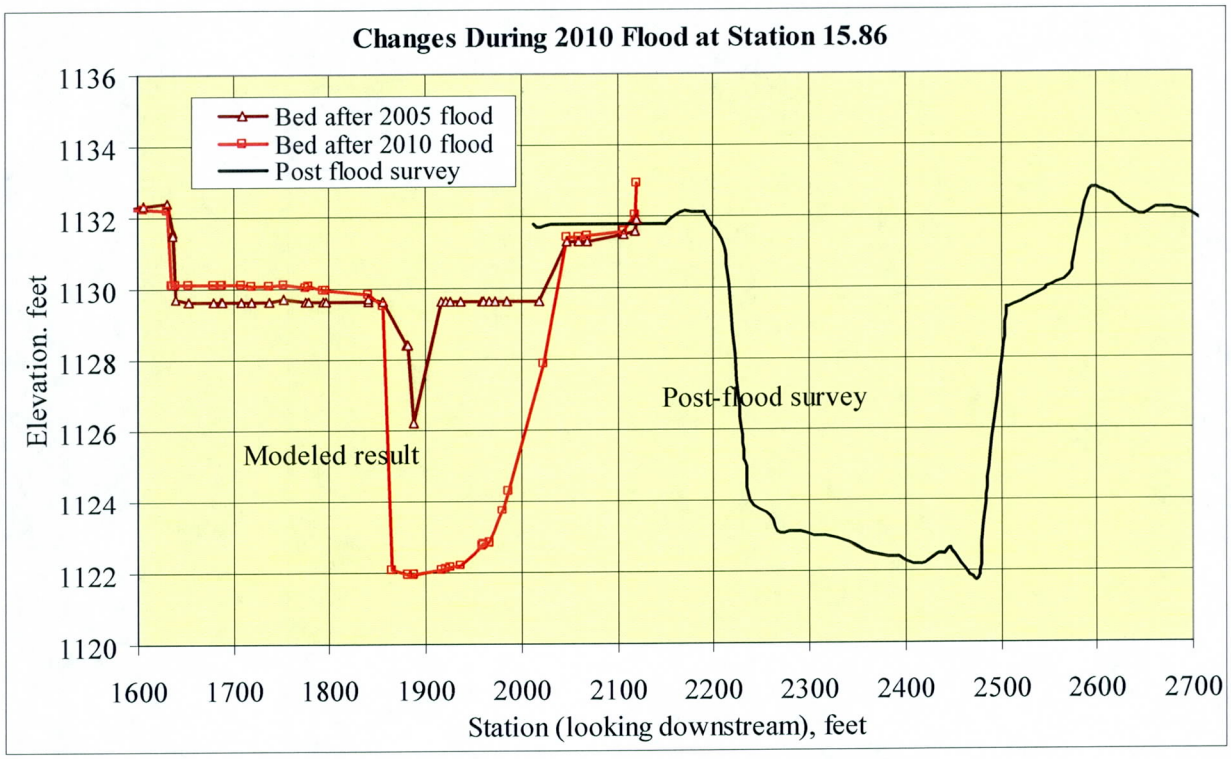

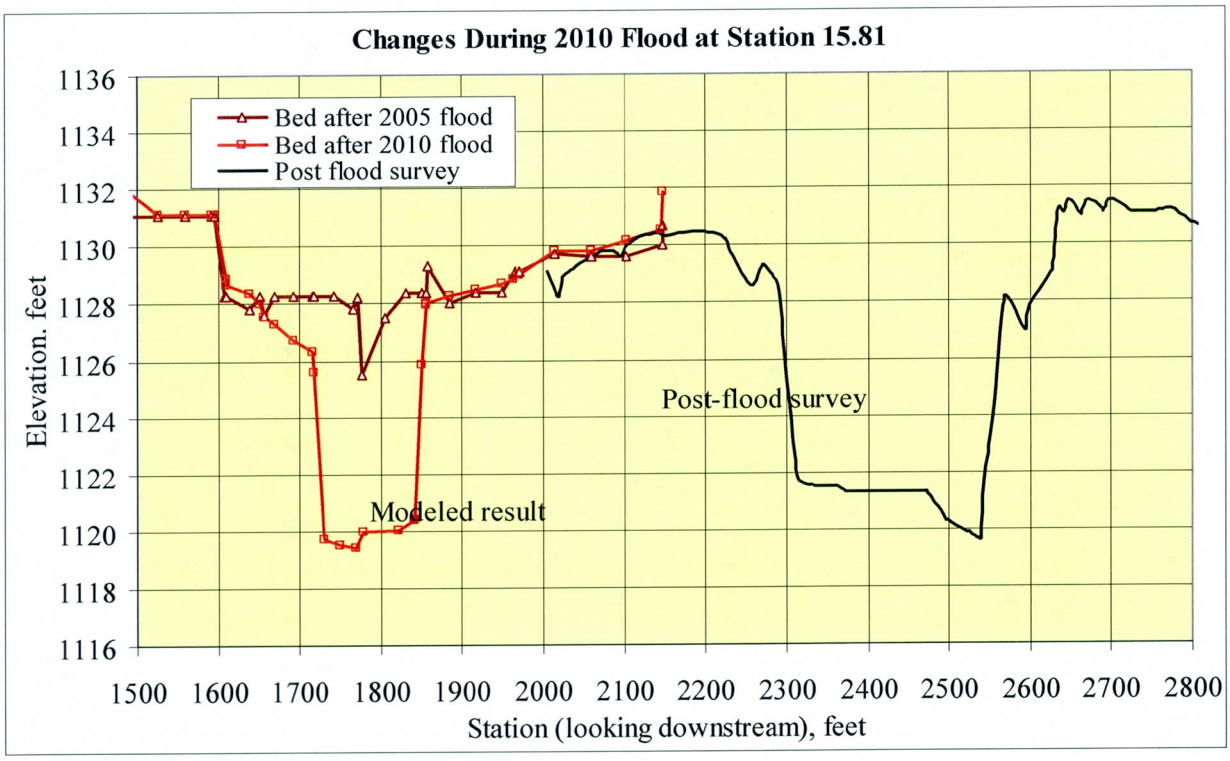

Figure 20(continued). Simulated and surveyed cross-sectional changes due to headcut near Pioneer pit using Engelund-Hansen formula

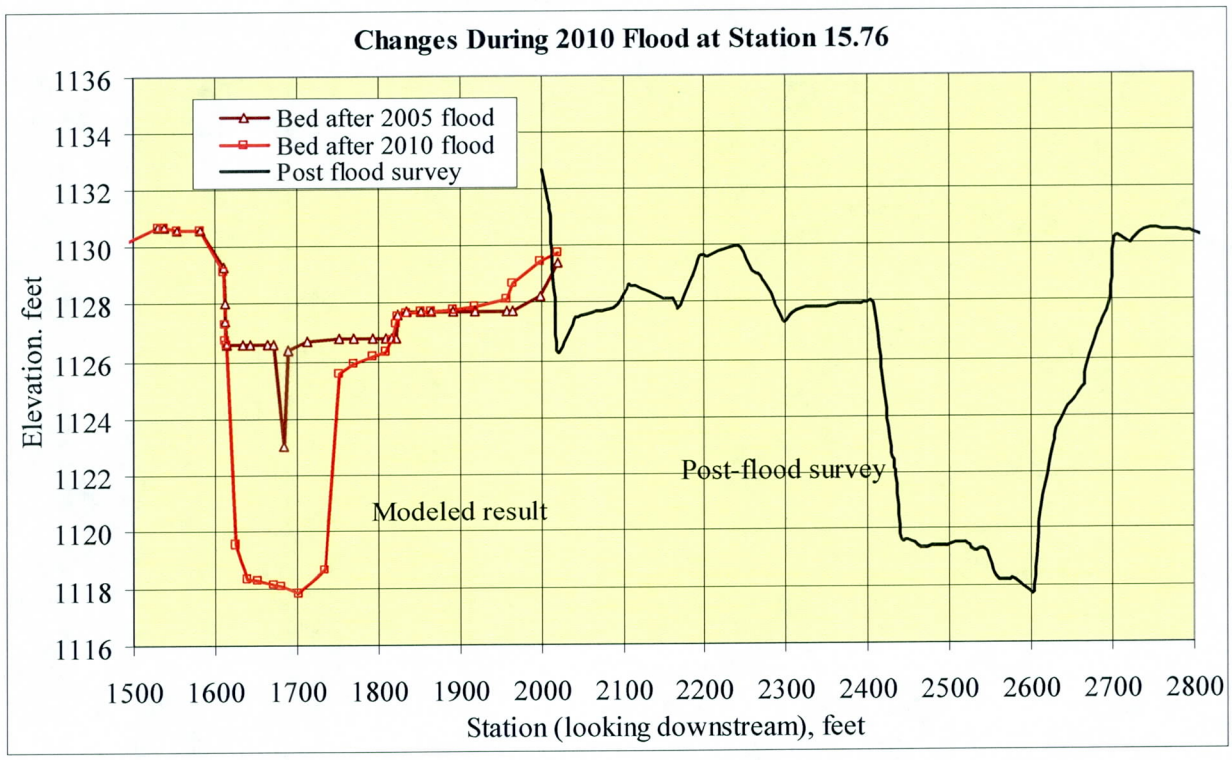

Figure 20 (continued). Simulated and surveyed cross-sectional changes due to headcut near Pioneer pit using Engelund-Hansen formula

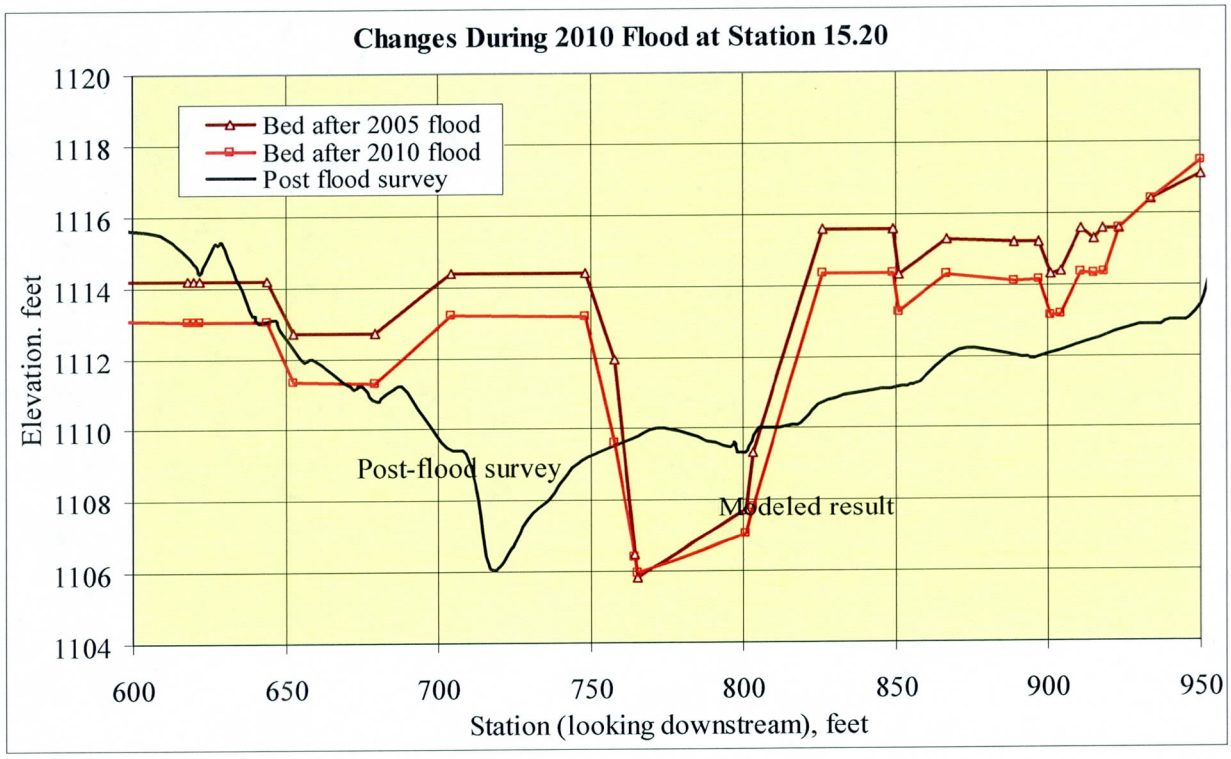

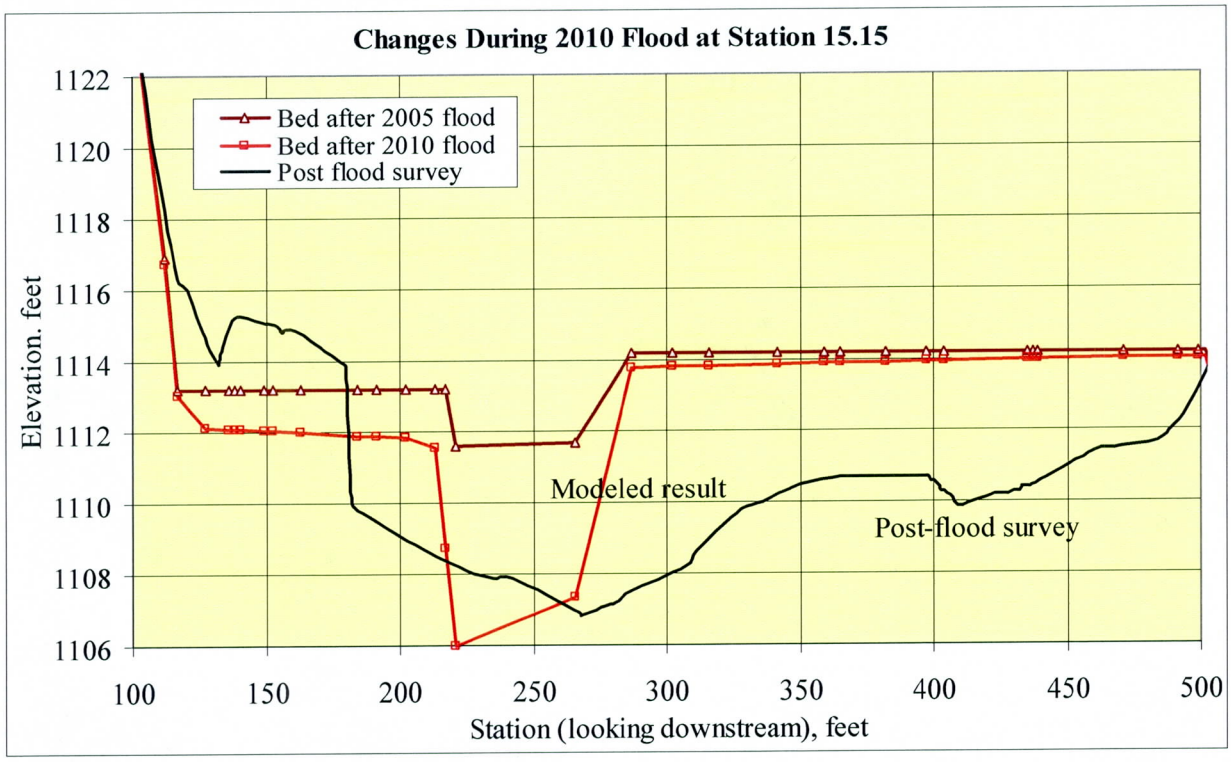

Figure 21. Simulated and surveyed cross-sectional changes due to tailcut near Pioneer pit using Engelund-Hansen formula

The simulated and surveyed results for headcut/tailcut are summarized in Table 6. The table lists the thalweg elevations at those cross sections affected by headcut/tailcut before the 2005 flood and after the 2010 flood; it also includes the thalweg elevations of cross sections from the post-flood topographic survey and the maximum scour depths of the channel bed. The scour depth is measured from the pre-flood thalweg elevation to the post-flood thalweg elevation. The maximum scour depth is measured from the pre-flood thalweg elevation to the minimum bed elevation, which is the lowest bed elevation reached by scour during the entire simulation period. The model keeps track of the channel bed profile for the entire flood period. The minimum bed elevations reached by scour are recorded in a separate file TZMIN.DAT.

Table 6. Scour depths due to headcut/tailcut for calibration case

Location	Pre-flood thalweg elevation (feet)	Post-flood thalweg elevation from topographic mapping (feet)	Post-flood thalweg elevation from modeling (feet)	Minimum bed elevation from modeling (feet)	Scour depth from topographic mapping (feet)	Scour depth from modeling (at the end of flood simulation) (feet)	Maximum scour depth from modeling during the flood (feet)
Headcut above Pioneer pit							
15.67	1123.3	1113.4	1113.3	1097.7	9.9	10.0	25.6
15.71	1124.4	1114.8	1115.5	1099.5	8.6	7.9	24.9
15.76	1125.2	1117.7	1117.9	1107.8	7.5	7.3	17.4
15.81	1125.9	1119.7	1119.4	1115.1	6.2	6.5	10.8
15.86	1126.5	1121.8	1121.9	1120.2	4.7	4.4	6.3
15.90	1127.9	T 1123.3	1123.7	1121.5	4.6	4.2	6.4
15.94	1127.9	1124.3	1125.1	1123.2	3.6	4.8	4.7
15.98	1130.9	1126.3	1127.1	1123.6	4.6	3.8	7.3
16.07	1133.4	1129.4	1130.3	1121.8	4.0	3.1	11.6
16.15	1135.0	1132.2	1133.1	1132.8	2.8	1.9	2.2
16.24	1136.4	1133.8	1134.2	1133.6	2.6	2.2	2.8
16.33	1139.9	1135.6	1135.9	1135.9	4.3	4.0	4.0

16.42	1142.0	1137.8	1138.0	1137.3	4.2	4.0	4.7
16.48	1142.3	1141.1	1138.4	1136.6	1.2	3.9	5.7
16.55	1144.0	1141.7	1140.4	1138.9	2.3	3.6	5.1
16.63	1145.3	1143.0	1140.8	1138.8	2.3	4.5	6.5
16.72	1146.5	1145.4	1144.6	1144.1	1.1	1.9	2.4
16.82	1148.9	1148.7	1147.0	1145.0	0.2	1.9	3.9
16.91	1151.5	1150.6	1149.5	1148.5	0.9	2.0	3.0
17.02	1155.5	1151.9	1150.2	1149.9	3.6	5.3	5.6
17.11	1155.6	1154.4	1155.3	1153.3	1.2	0.3	2.3
17.20	1156.8	1155.6	1156.0	1155.0	0.8	0.8	1.8
17.29	1159.0	1157.5	1157.7	1156.2	1.5	1.3	2.8
17.38	1160.7	1159.8	1160.6	1160.5	0.9	0.1	0.2
Tailcut below Pioneer pit							
14.49	1097.8	1098.2	1096.4	1096.1	-0.4	1.4	1.7
14.58	1098.1	1098.8	1097.7	1097.4	-0.6	0.4	0.7
14.67	1101.4	1099.4	1100.8	1100.3	2.0	0.6	1.1
14.77	1103.4	1101.2	1102.4	1101.9	2.2	1.0	1.5
14.86	1106.0	1102.6	1103.5	1103.5	3.4	2.5	2.5
14.96	1105.8	1104.1	1104.2	1104.1	1.7	1.6	1.7
15.06	1108.8	1105.2	1105.8	1105.6	3.6	3.0	3.2
15.10	1111.6	1106.3	1106.5	1106.4	5.3	5.1	5.2
15.15	1111.6	1106.8	1106.2	1106.2	4.8	5.4	5.4
15.20	1105.8	1106.1	1104.8	1104.5	-0.3	1.0	1.3

Headcut developed along the channel reach upstream of Pioneer pit. The headcut reach as estimated is from section 15.67 at the upstream edge of the mining pit to section 16.72 for a total channel length of about 1 mile. The performance index API for the scour depth is computed using the simulated and the surveyed scour depths in Table 6. The performance index is used to assess the correlation of simulated results on headcut with the measurement.

For headcut depth, the average deviation of the simulated scour depths from the measured scour depths for the cross sections listed in Table 6 is given below. The API as calculated represents the deviation of the simulated depth from the surveyed depth for headcut.

API = (0.1 + 0.7 + 0.2 + 0.3 + 0.3 + 0.4 + 1.2 + 0.8 + 0.9
+ 0.9 + 0.4 + 0.3 + 0.2 + 2.7 + 1.3 + 2.2 + 0.7 + 1.7 +0.8/19
= 0.85 foot

The tailcut reach downstream of the Pioneer as estimated is from section 15.20 at the downstream edge of the mining pit down to section 14.60, for a total channel length of about 0.60 mile. The value of API for the scour depth is computed using the simulated and the surveyed scour depths in Table 6 as follows.

API = (0 + 1.4 + 1.2 + 0.9 + 0.5 + 0.1 + 0.6 + 0.2 + 0.4 + 0.3)/10
= 0.56 foot

Calculated performance indices for the modeling study with calibration are summarized as listed in Table 7 below.

Table 7. Computed Performance Indices for scour depths due to headcut/tailcut with calibration

Case	Absolute Performance Index
Headcut depth above Pioneer pit	0.85 foot
Tailcut depth below Pioneer pit	0.56 foot

VII. COMPARISON OF MODELING RESULTS FOR ONE FLOOD AND TWO FLOODS

There are two modeling approaches for the study. The first approach is simply to model the January 20-21, 2010 event using 2002 topographic data as the basis and using the pit configuration to modify the topographic data. The pit configuration is estimated for the condition prior to the January 20-21, 2010 event. For the second case, both 2005 and 2010 floods were used. For both cases, calibration studies were performed.

The performance index API represents the deviation of the simulated value from the surveyed value for headcut/tailcut. To assess the modeling results for two approaches, the computed API's for the scour depths are compared as summarized in Table 8 below.

Table 8. Comparison of Absolute Performance Indices with calibration

Cases	Performance Index API	
	Based on 2010 flood only	Based on 2005 and 2010 events
Headcut depth above Pioneer pit	1.05 feet	0.85 foot
Tailcut depth below Pioneer pit	1.02 feet	0.56 foot

The comparison presented in the above table shows that the correlations of simulated and measured headcut/tailcut depths near the Pioneer pit are generally good. The modeling results from both flood events have better correlations with measurement than the case of one flood event. This is expected since the scour depths developed during both floods.

The performance indices presented in the report are based on channel bed scour. In addition to the scour depth, simulated changes in cross-sectional profiles for the two cases are also presented in the report. The simulated cross-sectional changed based on both the 2005 and 2010 floods are similar to the surveyed cross sectional profiles. However the cross-sectional profiles based on the 2010 flood only are not as well correlated with the surveyed results. In summary, model study using both the 2005 and 2010 floods has improved the correlation with measurement.

Discussion of Study Results — Certain sources for the discrepancy between the simulated and measured results can be cited. Channel morphology associated with headcut/tailcut is normally characterized by the formation of narrow and deep gullies. However, the channels formed by headcut/tailcut for this case are generally wider and larger in cross-sectional area than a typical gulley. The discrepancies are attributed to several factors. An important factor is the fact that the Hassayampa River has a broad floodplain with a highly braided channel pattern. Because of the multiple channel branches, headcut/tailcut changes induced by the mining pit are also affected by the presence of other channel branches. The tributary inflow from Jackrabbit Wash has significant effects on channel morphology downstream of the Pioneer pit, as the large width is closely related to the lateral inflow from Jackrabbit Wash. The effects of lateral inflow on the channel morphology at this location were not simulated in modeling.

VIII. SUMMARY OF COMPUTER FILES USED IN THE STUDY

Table 9 given below has been created to summarize the computer files used in the study and their respective parameters. The table lists all the parameters selected in model calibration.

Table 9. Summary of computer files and paramters

File name	Type of file	Sediment formula used	Roughness coefficient	Flood(s) used	Bank erodibilit y factor
HASSA-CUT.FLU	Input	Yang or Engelund-Hansen	From R2D	2010 flood	0.5
HASSA-CUTEH0.OUT	Output	Engelund-Hansen	From R2D	2010 flood	0.5
HASSA-CUTY.OUT	Output	Yang	From R2D	2010 flood	0.5
HASSA-CUTEH.FLU	Input	Engelund-Hansen	0.026	2010 flood	1.0
HASSA-CUTEH.OUT	Output	Engelund-Hansen	0.026	2010 flood	1.0
HASSA-Y05.FLU	Input	Yang	0.026	2005 flood	1.0
HASSA-Y10.FLU*	Input	Yang	0.026	2010 flood	1.0
HASSA-Y05.OUT	Output	Yang	0.026	2005 flood	1.0
HASSA-Y10.OUT*	Output	Yang	0.026	2010 flood	1.0
HASSA-EH5.FLU	Input	Engelund-Hansen	0.026	2005 flood	1.0
HASSA-EH10.FLU*	Input	Engelund-Hansen	0.026	2010 flood	1.0
HASSA-EH5.OUT	Output	Engelund-Hansen	0.026	2005 flood	1.0
HASSA-EH10.OUT*	Output	Engelund-Hansen	0.026	2010 flood	1.0

* Channel geometry output from the 2005 flood is used as the input geometry to get the cumulative effects of 2005 and 2010 floods

REFERENCES

JE Fuller Hydrology and Geomorphology, Inc., 2006. Lower Hassayampa River Watercourse Master Plan, River Behavior Report.

JE Fuller Hydrology and Geomorphology, Inc., 2007. Updated HEC-6 Model (dated May 2007) for Lower Hassayampa River Watercourse Master Plan, River Behavior Report.

Waskowsky, R., 11/22/2010. Data Collection and Modeling Approach for Selected River Mechanics Tasks of Phase II of the Lower Hassayampa Watercourse Master Plan, Memo, Submitted to Theresa Pinto of FCDMC, CC to Bing Zhao of FCDMC.

APPENDIX A. INPUT/OUTPUT DESCRIPTIONS FOR FLUVIAL-12

I. INPUT DESCRIPTION

The basic data requirements for a modeling study include (1) topographic maps of the river reach from the downstream end to the upstream end of study, (2) digitized data for cross sections in the HEC-2 format with cross-sectional locations shown on the accompanying topographic maps, (3) flow records or flood hydrographs and their variations along the study stream reach, it any, and (4) size distributions of sediment samples along the study reach. Additional data are required for special features of a study river reach.

The HEC-2 format for input data is used in all versions of the FLUVIAL model. Data records for HEC-2 pertaining to cross-sectional geometry (X1 and GR), job title (T1, T2, and T3), and end of job (EJ), are used in the FLUVIAL model. If a HEC-2 data file is available, it is not necessary to delete the unused records except that the information they contain are not used in the computation. For the purpose of water- and sediment-routing, additional data pertaining to sediment characteristics, flood hydrograph, etc., are required and supplied by other data records. Sequential arrangement of data records are given in the following.

Records	**Description of Record Type**
T1,T2,T3	Title Records
C	General Use Record
G1	General Use Record
G2	General Use Records for Hydrographs
G3	General Use Record
G4	General Use Record for Selected Cross-Sectional Output
G5	General Use Record
G6	General Use Record for Selecting Times for Summary Output
G7	General Use Record for Specifying Erosion Resistant Bed Layer
GS	General Use Records for Initial Sediment Compositions
GB	General Use Records for Time Variation of Base-Level
GQ	General Use Records for Stage-Discharge Relation of Downstream Section
GI	General Use Records for Time Variation of Sediment Inflow
X1	Cross-Sectional Record
XF	Record for Specifying Special Features of a Cross Section
GR	Record for Ground Profile of a Cross Section

SB	Record for Special Bridge Routine
BT	Record for Bridge Deck Definition
EJ	End of Job Record

Variable locations for each input record are shown by the field number. Each record has an input format of (A2, F6.0, and 9F8.0). Field 0 occupying columns 1 and 2 is reserved for the required record identification characters. Field 1 occupies columns 3 to 8; Fields 2 to 10 occupy 8 columns each. The data records are tabulated and described in the following.

T1, T2, T3 Records - These three records are title records that are required for each job.

Field	Variable	Value	Description
0	IA	T1	Record identification characters
1-10	None		Numbers and alphabetic characters for title

C Record – This is an optional record used to skip a number of lines following the C record.

Field	Variable	Value	Description
0	IA	G4	Record identification characters
1	SKIP	+	Number of lines to be skipped

G1 Record - This record is required for each job, used to enter the general parameters listed below. This record is placed right after the T1, T2, and T3 records.

Field	Variable	Value	Description
0	IA	G1	Record identification characters
1	TYME	+	Starting time of computation on the hydrograph, in hours
2	ETIME	+	Ending time of computation on the hydrograph, in hours
3	DTMAX	+	Maximum time increment at allowed, in seconds
4	ISED	1	Select Graf's sediment transport equation.
		2	Select Yang's unit stream power equation. The sediment size is between 0.063 and 10 mm.
		3	Select Engelund-Hansen sediment equation.
		4	Select Parker gravel equation.
		5	Select Ackers-White sediment equation.
		6	Select Meyer-Peter Muller equation for bed load.
5	BEF	+	Bank erodibility factor for the study reach. This value is used for each section unless otherwise specified in Field 9 of the XF and 1 may be used.
6	IUC	0	English units are used in input and output.
		1	Metric units are used in input and output.

7	CNN	+	Manning's *n* value for the study reach. This value is used for a section unless otherwise specified in Field 4 of the XF record. If bed roughness is computed based upon alluvial bedforms as specified in Field 5 of the G3 record, only an approximate *n* value needs to be entered here.
8	PTM1	+	First time point in hours on the hydrograph at which summary output and complete cross-sectional output are requested. It is usually the peak time, but it may be left blank if no output is requested.
9	PTM2	+	Second time point on the hydrograph in hours at which summary usually the time just before the end of the simulation. This field may be left blank if no output is needed.
10	KPF	+	Frequency of printing summary output, in number of time steps.

G2 Records - These records are required for each job, used to define the flow hydrograph(s) in the channel reach. The first one (or two) G2 records are used to define the spatial variation in water discharge along the reach; the succeeding ones are employed to define the time variation(s) of the discharge. Up to 10 hydrographs, with a maximum of 120 points for each, are currently dimensioned. See section II for tributaries. These records are placed after the G1 record.

Field	Variable	Value	Description
First G2			
0	IA	G2	Record identification characters
1	IHP1	+	Number of last cross section using the first (downstream most) hydrograph. The number of section is counted from downstream to upstream with the downstream section number being one. See also section II.
2	NP1	+	Number of points connected by straight segments used to define
3	IHP2	+	Number of last section using the second hydrograph if any. Otherwise leave it blank.
4	NP2	+	Number of points used to define the second hydrograph if any. Otherwise leave it blank.
5	IHP3	+	Number of last section using the third hydrograph if any. Otherwise leave it blank.
6	NP3	+	Number of points used to define the third hydrograph if any. Otherwise leave it blank.

7	IHP4	+	Number of last section using the fourth hydrograph if any. Otherwise leave it blank.
8	NP4	+	Number of points used to define the fourth hydrograph if any. Otherwise leave it blank.
9	IHP5	+	Number of last section using the fifth hydrograph if any. Otherwise leave it blank.
10	NP5	+	Number of points used to define the fifth hydrograph if any. Otherwise leave it blank.

Second G2: Note that this record is used only if more than 5 hydrographs are used for the job. It is necessary to place a negative sign in front of NP5 located in the 10th field of the first G2 record as a means to specify that more than 5 hydrographs are used.

0	IA	G2	Record identification characters
1	IHP6	+	Number of last cross section using the sixth hydrograph if any. Otherwise leave it blank.
2	NP6	+	Number of points connected by straight segments used to define
3	IHP7	+	Number of last section using the seventh hydrograph if any. Otherwise leave it blank.
4	NP7	+	Number of points used to define the seventh hydrograph
5	IHP8	+	Number of last section using the eighth hydrograph if any. Otherwise leave it blank.
6	NP8	+	Number of points used to define the eighth hydrograph
7	IHP9	+	Number of last section using the ninth hydrograph if any. Otherwise leave it blank.
8	NP9	+	Number of points used to define the ninth hydrograph
9	IHP10	+	Number of last section using the tenth hydrograph if any. Otherwise leave it blank.
10	NP10	+	Number of points used to define the tenth hydrograph

Succeeding G2 Record(s)

1	Q11, Q21 Q31	+	Discharge coordinate of point 1 for each hydrograph, in ft^3/sec or m^3/sec
2	TM11,TM21	+	Time coordinate of point 1 for each hydrograph, in hours

	TM31		
3	Q12, Q22 Q32	+	Discharge coordinate of point 2 for each hydrograph, in cfs or cms
4	TM12,TM22 TM32	+	Time coordinate of point 2 for each hydrograph, in hours

Continue with additional discharge and time coordinates. Note that time coordinates must be in increasing order.

G3 Record - This record is used to define required and optional river channel features for a job as listed below. This record is placed after the G2 records.

Field	Variable	Value	Description
0	IA	G3	Record identification characters
1	S11	+	Slope of the downstream section, required for a job
2	BSP	0	One-on-one slope for rigid bank or bank protection
		+	Slope of bank protection in BSP horizontal units on 1 vertical unit. for all cross sections unless otherwise specified in Field 8 of the XF record for a section.
3	DSOP	0	Downstream slope is allowed to vary during simulation.
		1	Downstream slope is fixed at S11 given in Field 1.
4	TEMP	0	Water temperature is 15°C.
		+	Water temperature in degrees Celsius
5	ICNN	0	Manning's n defined in Field 7 of the G1 record or those in Field 4 of the XF records are used.
		1	Brownlie's formula for alluvial bed roughness is used to calculate Manning's n in the simulation.
6	TDZAMA	0	Thickness of erodible bed layer is 100 ft (30.5 m).
		+	Thickness of erodible bed layer in ft or m. This value is applied to
7	SPGV	0	Specific gravity of sediment is 2.65.
		+	Specific gravity of sediment
8	KGS	0	The number of size fractions for bed material is 5.
		+	The number of size fractions for bed material. It maximum value is 8.
9	PHI	0	The angle of repose for bed material is 36°.
		+	Angle of repose for bed material

G4 Record - This is an optional record used to select cross sections (up to 4) to be included at each summary output. Each cross section is identified by its number which is counted from the downstream section. This record also contains other options; it is placed after the G3 record.

Field	Variable	Value	Description
0	IA	G4	Record identification characters
1	IPLI1	+	Number of cross section
		10000	All cross sections included in each summary output
2	IPLT2	+	Number of cross section
3	IPLT3	+	Number of cross section
4	IPLT4	+	Number of cross section
5	IEXCAV	+	A positive integer indicates number of cross section where sand/gravel excavation occurs.
6	GIFAC	+	A non-zero constant is used to modify sediment inflow at the upstream section.
7	PZMIN	0	Minimum bed profile during simulation run is not requested.
		1	Output file entitled TZMIN for minimum bed profile is requested.
10	REXCAV	+	A non-zero value specifies rate of sand/gravel excavation at Section IEXCAV.

G5 Record - This is an optional record used to specify miscellaneous options, including unsteady-flow routing for the job based upon the dynamic wave, bend flow characteristics. If the unsteady flow option is not used, the water-surface profile for each time step is computed using the standard-step method. When the unsteady flow option is used, the downstream water-surface elevation must be specified using the GB records.

Field	Variable	Value	Description
0	IA	G5	Record identification characters
1	DT	0	The first time step is 100 seconds.
		+	Size of the first time step in seconds.
2	IROUT	0	Unsteady water routing is not used; water-surface profiles are computed using standard-step method.
		1	Unsteady water-routing based upon the dynamic wave is used to

			compute stages and water discharges at all cross sections for each
3	PQSS	0	No output of gradation of sediment load
		3	Gradation of sediment load is included in output in 1,000 ppm by weight.
5	TSED	0	Rate of tributary sediment inflow is 1 times the discharge ratio.
		+	Rate of tributary sediment inflow is TSED times the discharge ratio.
6	PTV	0	No output of transverse distribution of depth-averaged velocity
		1	Transverse distribution of depth-averaged velocity is printed. The velocity distribution is for bends with fully developed transverse flow.
10	DYMAX	0	No GR points are inserted for cross sections.
		+	Maximum value of spacing between adjacent points at a cross

G6 Record - This is an optional record used to select time points for summary output. Up to 30 time points may be specified. The printing frequency (KPF) in Field 10 of the G1 Record may be suppressed by using a large number such as 9999.

Field	Variable	Value	Description
First G6 Record			
0	IA	G6	Record identification characters
1	NKPS	+	Number of time points
Succeeding G6 Record(s)			
0	IA	G6	Record identification characters
1	SPTM(1)	+	First time point, in hours
2	SPTM(2)	+	Second time point, in hours

Continue with additional time points.

G7 Record - This is an optional record used to specify erosion resistant bed layer, such as a caliche layer, that has a lower rate of erosion.

Field	Variable	Value	Description
First G7 Record			
0	IA	G7	Record identification characters
1	KG7	+	Number of time points used to define the known erosion rate in

			relation to flow velocity
2	THICK	+	Thickness of erosion resistant layer, in feet

Succeeding G7 Record(s)

0	IA	G7	Record identification characters
1	ERATE(1)	+	Erosion rate, in feet per hour
2	G7V(2)	+	Velocity, in feet per second

Continue with additional time points.

GS Record - At least two GS records are required for each job, used to specify initial bed-material compositions in the channel at the downstream and upstream cross sections. The first GS record is for the downstream section; it should be placed before the first X1 record and after the G4 record, if any. The second GS record is for the upstream section; it should be placed after all cross-sectional data and just before the EJ record. Additional GS records may be inserted between two cross sections within the stream reach, with the total number of GS records not to exceed 15. Each GS record specifies the sediment composition at the cross section located before the record. From upstream to downstream, exponential decay in sediment size is assumed for the initial distribution. Sediment composition at each section is represented by five size fractions.

Field	Variable	Value	Description
0	IA	GS	Record identification characters
1	DFF	+	Geometric mean diameter of the smallest size fraction in mm
2	PC	+	Fraction of bed material in this size range

Continue with other DFF's and PC's.

GB Records - These optional records are used to define time variation of stage (water-surface elevation) at a cross section. The first set of GB records is placed before all cross section records (X1); it specifies the downstream stage. When the GB option is used, it supersedes other methods for determining the downstream stage. Other sets of GB records may be placed in other parts of the data set; each specifies the time variation of stage for the cross section immediately following the GB records.

Field	Variable	Value	Description
First GB Record			
0	IA	GB	Record identification characters
1	KBL	+	Number of points used to define base-level changes

Succeeding GB Record(s)

0	IA	GB	Record identification characters
1	BSLL(1)	+	Base level of point 1, in ft or m
2	TMBL(1)	+	Time coordinate of point 1, in hours
3	BSLL(2)	+	Base level of point 2, in ft or m
4	TMBL(2)	+	Time coordinate of point 2, in hours

Continue with additional elevations and time coordinates, in the increasing order of time.

GQ Records - These optional records are used to define stage-discharge relation at the downstream section. The GQ input data may not used together with the GB records.

Field	Variable	Value	Description
First GQ Record			
0	IA	GQ	Record identification characters
1	KQL	+	Number of points used to define base-level changes
Succeeding GQ Record(s)			
0	IA	GQ	Record identification characters
1	BSLL(1)	+	Base level of point 1, in ft or m
2	TMQ(1)	+	Discharge of point 1, in cfs or cms
3	BSLL(2)	+	Base level of point 2, in ft or m
4	TMQ(2)	+	Discharge of point 2, in cfs or cms

Continue with additional elevations and discharges, in the increasing order of discharge.

GI Records - These optional records are used to define time variation of sediment discharge entering the study reach through the upstream cross section. The GI input data, if included, will supersede other methods for determining sediment inflow. The sediment inflow is classified into the two following cases: (1) specified inflow at the upstream section, such as by a rating curve; and (2) sediment feeding, such as from a dambreach or a sediment feeder. These two cases are distinguished by DXU in Field 2 of this record. For the first case, sediment discharge at the upstream section is computed using size fractions of bed-material at the section, but for the second case, the size fractions of feeding material need to be specified using the PCU values in

this record. The upstream section does not change in geometry for the first case but it may undergo scour or fill for the second case.

Field	Variable	Value	Description
First GI Record			
0	IA	GI	Record identification characters
1	KGI	+	Number of points used to define time variation of sediment inflow.
2	DXU	+ or 0	Channel distance measured from the upstream section to the and KGI signify case 2, for which PCU values are required.
3-10	PCU	+	Size fractions of inflow material. The number of size fractions is given in Field 8 of the G3 record and the sizes for the fractions are given in the second GS record.
Succeeding GI Record(s)			
0	IA	GI	Record identification characters
1	QSU(1)	+	Sediment discharge of point 1, in cubic ft or m (net volume) per second
2	TMGI(1)	+	Time coordinate of point 1, in hours
3	QSO(2)	+	Sediment discharge of point 2
4	TMGI(2)	+	Time coordinate of point 2.

Continue with additional sediment discharges and time coordinates, in the increasing order of time coordinates.

X1 Record - This record is required for each cross section (175 cross sections can be used for the study reach); it is used to specify the cross-sectional geometry and program options applicable to that cross-section. Cross sections are arranged in sequential order starting from downstream.

Field	Variable	Value	Description
0	IA	X1	Record identification characters
1	SECNO	+	Original section number from the map
2	NP	+	Total number of stations or points on the next GR records for
7	DX	+	Length of reach between current cross section and the next down-

			stream section along the thalweg, in feet or meters
8	YFAC	0	Cross-section stations are not modified by the factor YFAC.
		+	Factor by which all cross-section stations are multiplied to increase or decrease area. It also multiplies YC1, YC2 and CPC in the XF record, and applies to the CI record.
9	PXSECE	0	Vertical or Z coordinate of GR points are not modified.
		±	Constant by which all cross-section elevations are raised or lowered
10	NODA	0	Cross section is subject to change.
		1	Cross section is not subject to change.

XF Record - This is an optional record used to specify special features of a cross section.

Field	Variable	Value	Description
0	IA	XF	Record identification characters
1	YC1	0	Regular erodible left bank
		+	Station of rigid left bank in ft or m, to the left of which channel dinates in GR records but not the first Y coordinate.
2	YC2	0	Regular erodible right bank
	+		Station of rigid right bank, to the right of which channel is non-erodible. Note: This station is located at toe of rigid bank; its value must be equal to one of the Y coordinates in GR records but not the last Y coordinate.
3	RAD	0	Straight channel with zero curvature
		+	Radius of curvature at channel centerline in ft or m. Center of radius is on same side of channel where the station (Y-coordinate) starts.
		-	Radius of curvature at channel centerline in ft or m. Center of radius is on opposite side of zero station. Note: RAD is used only if concave bank is rigid and so specified using the XF record. RAD produces a transverse bed scour due to curvature.
4	CN	0	Roughness of this section is the same as that given in Field 7 of the G1 record.
		+	Manning's *n* value for this section
5	CPC	0	Center of thalweg coincides with channel invert at this section.
		+	Station (Y-coordinate) of the thalweg in ft or m
6	IRC	0	Regular erodible cross section

		1	Rigid or nonerodible cross section such as drop structure or road crossing. There is no limit on the total number of such cross sections.
8	BSP	0	Slope of bank protection is the same as that given in Field 2 of the G3 record.
		+	Slope of bank protection at this section in BSP horizontal units
		5	Slope of rigid bank is defined by the GR coordinates.
9	BEFX	0	Bank erodibility factor is defined in Field 5 of the G1 record.
		+	A value between 0.1 and 1.0 for BEFX specifies the bank erodibility factor at this section.
	RWD	+	RWD is the width of bank protection of a small channel in the specified by a value greater than 1 (ft or m) in this field. When RWD is used, BEFX is not specified.
10	TDZAM	0	Erodible bed layer at this section is defined by TDZAMA in Field
		+	Thickness of erodible bed layer in ft or m. Only one decimal place is allowed for this number.
	ENEB	±	Elevation of non-erodible bed, used to define the crest elevation of a grade-control structure which may be above or below the existing channel bed. In order to distinguish it from TDZAM, ENEB must have the value of 1 at the second decimal place. For example, the ENEB value of 365 should be inputted as 365.01 and the ENEB value of -5.2 should be inputted as -5.21. When ENEB is specified, it supersedes TDZAM and TDZAMA

CI Record - This is an optional record used to specify channel improvement options due to excavation or fill. The excavation option modifies the cross-sectional geometry by trapezoidal excavation. Those points lower than the excavation level are not filled. The fill option modifies the cross-sectional geometry by raising the bed elevations to a prescribed level. Those points higher than the fill level are not lowered. Excavation and fill can not be used at the same time. This record should be placed after the X1 and XF records but before the GR records. The variable ADDVOL in Field 10 of this record is used to keep track of the total volume of excavation or fill along a channel reach. ADDVOL specifies the initial volume of fill or excavation. A value greater or less than 0.1 needs to be entered in this field to keep track of the total volume of fill or excavation until another ADDVOL is defined.

Field	Variable	Value	Description
0	IA	G5	Record identification characters
1	CLSTA	+	Station of the centerline of the trapezoidal excavation, expressed according to the stations in the GR records, in feet or meter.
2	CELCH	+	Elevation of channel invert for trapezoidal channel, in feet or meters.

4	XLSS	+	Side slope of trapezoidal excavation, in XLSS horizontal units for 1 vertical unit.
5	ELFIL	+	Fill elevation on channel bed, in feet or meters.
6	BW	+	Bed width of trapezoidal channel, in feet or meters. This width is measured along the cross section line; therefore, a larger value should be used if a section is skewed.
10	ADDVOL	0	Volume of excavation or fill, if any, is added to the total volume already defined.
		+	Initial volume of fill on channel bed, in cubic feet or cubic meters.
		-	Initial volume of excavation from channel bed, in cubic feet or meters.

GR Record - This record specifies the elevation and station of each point for a digitized cross section; it is required for each X1 record.

Field	Variable	Value	Description
0	IA	GR	Record identification characters
1	Z1	"	Elevation of point 1, in ft or m. It may be positive or negative.
2	Y1	"	Station of point 1, in ft or m
3	Z2	"	Elevation of point 2, in ft or m
4	Y2	"	Station of point 2, in ft or m

Continue with additional GR records using up to 79 points to describe the cross section. Stations should be in increasing order.

SB Record - This special bridge record is used to specify data in the special bridge routine. This record is used together with the BT and GR records for bridge hydraulics. This record is placed between cross sections that are upstream and downstream of the bridge.

Field	Variable	Value	Description
0	IA	SB	Record identification characters
1	XK	+	Pier shape coefficient for pier loss
2	XKOR	+	Total loss coefficient for orifice flow through bridge opening
3	COFQ	+	Discharge coefficient for weir flow overtopping bridge roadway

4	IB	+	Bridge index, starting with 1 from downstream toward upstream
5	BWC	+	Bottom width of bridge opening including any obstruction
6	BWP	0	No obstruction (pier) in the bridge
		i	Total width of obstruction (piers)
7	BAREA	+	Net area of bridge opening below the low chord in square feet
9	ELLC	+	Elevation of horizontal low chord for the bridge
10	ELTRD	+	Elevation of horizontal top-of-roadway for the bridge

BT Record - This record is used to compute conveyance in the bridge section. The BT data defines the top-of -roadway and the low chord profiles of bridge. The program uses the BT, SB and GR data to distinguish and to compute low flow, orifice flow and weir flow.

Field	Variable	Value	Description
0	IA	BT	Record identification characters
1	NRD	+	Number of points defining the bridge roadway and bridge low chord to be read on the BT records
2	RDST(1)	+	Roadway station corresponding to RDEL(1) and XLCEL(1)
3	RDEL(1)	+	Top of roadway elevation at station RDST(1)
4	XLCEL(1)	+	Low chord elevation at station RDST(1)
5	RDST(2)	+	Roadway station corresponding to RDEL(2) and XLCEL(2)
6	RDEL(2)	+	Top of roadway elevation at station RDST(2)
7	XLCEL(2)	+	Low chord elevation at station RDST(2)

Continue with additional sets of RDST, RDEL, and XLCEL.

EJ Record - This record is required following the last cross section for each job. Each group of records beginning with the T1 record is considered as a job.

Field	Variable	Value	Description
0	IA	EJ	Record identification characters

1-10 Not used

II. OUTPUT DESCRIPTION

Output of the model include initial bed-material compositions, time and spatial variations of the water-surface profile, channel width, flow depth, water discharge, velocity, energy gradient, median sediment size, and bed-material discharge. In addition, cross-sectional profiles are printed at different time intervals.

Symbols used in the output are generally descriptive, some of them are defined below:

SECTION	Cross section
TIME	Time on the hydrograph
DT	Size of the time step or Δt in sec
W.S.ELEV	Water-surface elevation in ft or m
WIDTH	Surface width of channel flow in ft or m
DEPTH	Depth of flow measured from channel invert to water surface in ft or m
Q	Discharge of flow in cfs or cms
V	Mean velocity of a cross-section in fps or mps
SLOPE	Energy gradient
D50	Median size or d_{50} of sediment load in mm
QS	Bed-material discharge for all size fractions in cfs or cms
FR	Froude number at a cross section
N	Manning's roughness coefficient
SED.YIELD	Bulk volume or weight of sediment having passed a cross section since beginning of simulation, in cubic yards or tons.
WSEL	Water-surface elevation, in ft or m
Z	Vertical coordinate (elevation) of a point on channel boundary at a cross-section, in ft or m
Y	Horizontal coordinate (station) of a point on channel boundary at a cross-section, in ft or m
DZ	Change in elevation during the current time step, in ft or m
TDZ	Total or accumulated change in elevation, in ft or m.